STRAIN MAPPING IN TEETH WITH VARIABLE REMAINING TOOTH STRUCTURE

Mai M. Alhamdan

A dissertation submitted to University College London in accordance with the requirements of the degree of Doctor of Philosophy in the Department of Restorative Dentistry, Prosthodontic Unit, Faculty of Medical Sciences.

2020

Department of Restorative Dentistry, Prosthodontic Unit

UCL Eastman Dental Institute

256 Grays Inn Road

London WC1X 8LD

AUTHOR'S DECLARATION

I, Mai Alhamdan, confirm that all the work presented in this thesis is my own. Where information has been derived from other sources, I confirm that this has been indicated in the thesis. Work submitted for journal publication is included at the rear of this work in the appendices.

Signed……

Date……

Mai Alhamdan

ABSTRACT

Problem: The effect of remaining tooth structure on strain in compromised teeth is not fully understood. Different remaining tooth quantities may affect stress and strain concentration within the remaining structure and potentially the longevity of the related restoration.

Objectives: The aim of this project was to map and evaluate tooth strain levels at different stages and areas of structural tooth loss created by dental preparation (simulating caries created lesions) or soft drink demineralisation (simulating external acid erosion lesions), before and after restoration, and to evaluate and compare different strain measurement techniques: strain gauges (SG), the surface displacement field measured using digital image correlation (DIC), electronic speckle pattern interferometry (ESPI), and finite element analysis (FEA). In addition, testing teeth affected by erosion required testing and verifying different acid demineralisation protocols.

Material and methods: Part I: Enamel samples (sound, polished) were subjected to extended 25 hours (hr) soft drink immersion protocols (accelerated, prolonged) with different salivary protection conditions (no saliva, artificial saliva, and natural saliva) to compare enamel surface loss. Moreover, enamel surface loss of extended erosion periods simulating different levels of clinical erosion lesions was calculated by different imaging methodologies. Microscopic analysis was performed to compare subsurface changes of early and extended erosion protocols. Part II: Strain under static loading was compared in teeth with different stages of unrestored occlusal and buccal accelerated soft drink demineralisation

lesions and after restoration using different techniques (strain gauges, electronic speckle pattern interferometry, and finite element analysis). Part III: Strain under static loading was compared in prepared teeth with different remaining tooth dimensions and different restorations using strain gauges and digital image correlation techniques.

Results: Part I: No statistical significance was detected in enamel thickness loss between sound and polished enamel samples in the accelerated erosion groups under all salivary conditions or between early and extended erosion groups tested. Part II: All testing methodologies measured an increased strain reading after 1 day in occlusal erosion group followed by gradual decrease, while, continuous increase in strain was observed with buccal erosion progression. For both groups, all restorative materials used were able to restore strain close to pre-treatment level. However, strain distribution pattern was more favourable in ceramic and gold occlusal onlays than composite onlays. Part III: for both strain gauges and digital image correlation, remaining tooth height ≥ 3 mm and width of 1 to 1.5 mm of the remaining tooth structure had a positive effect on strain. Tooth compositions of enamel and dentine resisted strain better than dentine counterparts at all dimensions. Both core restorations (with and without cuspal coverage) were found to support the remaining tooth structure and reduce strain. However, only cuspal coverage recorded significantly lower strain than their unrestored counterparts.

Conclusion: Restorations bonded to advanced erosion induced lesions restored strain levels to pre-treatment condition and produced a more favourable strain distribution pattern highlighting the role of adhesion in reducing strain. Remaining

tooth structure suffers less strain under loading when enamel is part of the structure and when the minimum dimension of 3 mm in height and 1.5 mm in width is preserved. Bonding of core restoration or cusp coverage aids in reducing strain under loading. All strain measuring methodologies were comparable, where similar strain behaviour was recorded. Remineralisation of enamel and dentine is effective in the management of initial erosion.

RESEARCH IMPACT STATEMENT

The human oral environment is involved with the first stages of digestion. Tooth structure, diet, oral flora, and saliva are interrelated physically and chemically in one integrated system that contributes to health and in some circumstances to disease. Human diets have changed over the years to include less abrasive foods and more sugars and acids; in particular carbonated drinks, sports drinks, and fruit juices, leading to imbalance within the oral environment complex. The high consumption of these foods explains the two common dental diseases; caries and acid erosion. Teeth that are heavily affected by these conditions may lose a considerable amount of their structure. Under loading, the remaining tooth structure suffers concentration of stresses and strain which may ultimately lead to tooth fracture or loss. Some studies have suggested that stress and strain levels in teeth were directly related to the amount of tooth structure loss.

Reports have shown that about 60% of all operative dental workload is related to placement and replacement of restorations. Therefore, management of compromised teeth should ensure the achievement of proper cavity design and the best restorative material selection. Ideally, the final restoration should restore the lost tissue to its original shape and strain condition.

This research focused on testing strain under loading in different operator generated remaining tooth dimensions; simulating different stages of tooth structure loss after caries or external acid erosion. Strain testing under loading was achieved within the physiological limit for human teeth before and after

preparation and after the application of different restorations whilst utilizing different conventional and new strain measuring methodologies. Results were compared to evaluate strain at all stages, test the potential restoration of strain to sound condition levels, and to verify the different strain measuring techniques applied and conclusions about the most favourable remaining tooth dimensions could be drawn. The application of multiple testing methodologies allows comparison and verification of results, collaboration between different scientific fields, and exchange of experience between dental researchers and experts from other specialties.

Various soft drink demineralisation protocols were tested and compared to decide the best protocol to apply for advanced erosion lesion creation. Soft drink erosion tests gained a deeper insight into their impact on dental tissues to diet and in turn provided dentists with data for patient education and to raise public awareness. This would include evidence about damage caused by high carbonated drink consumption and recommendations of optimal toothpaste type and application method.

This is an *in vitro* study which has limitations. However, it can be used as a baseline for future *in vivo* studies in the same area. In addition, the research findings and recommendations should give guidance to dentists through clinical management of compromised teeth, starting from prevention to the operative decision of the amount of remaining tooth structure to preserve and the most favourable restoration design and material to apply.

ACKNOWLEDGEMENTS

I would like first to sincerely express thanks and gratitude to my academic supervisors Prof Ailbhe McDonald and Prof Jonathan Knowles for their guidance, instructions and support throughout the project.

I appreciate the support I always had from my colleagues at the Prosthodontic unit and Biomaterial and Tissue Engineering Department at Eastman Dental Institute, with special thanks for Drs Graham Palmer, George Georgiou, and Nicky Mordan, whose instruction and unflagging support were indispensable. To all my fellow PhD students for constructive advice and support, and more importantly, their genuine friendship.

I would like to thank my sponsor, Saudi Arabian Cultural Bureau and King Saud University for giving the opportunity and the funding towards my studies.

Special thanks are reserved for my family and children, who despite all the stressful events, managed to draw a smile on my face and push me through the way.

Last but not least, to my loving husband whom without his warming care and support, this journey would never be possible and who will no doubt be happy to have a return to normality.

CONTENTS

TABLE OF FIGURES

LIST OF TABLES

TABLE OF ABBREVIATIONS

Abbreviation	*Definition*
µCT	Micro Computerized Tomography
2D	Two-Dimensional
3D	Three-Dimensional
ANOVA	Analysis of Variance
BC	Before Christ
BC	Direct Buccal Composite Onlay
BEWE	Basic Erosive Wear Examination
BG	Bonded Gold Onlay
CCD	Charge-Coupled Device
CEJ	Cemento-Enamel Junction
CLSM	Confocal Laser Scanning Microscopy
CT	Computerised Tomography
DEJ	Dentino-Enamel Junction
DIC	Digital Image Correlation
ENDO	Endodontic Access
ESPI	Electronic Speckle Pattern Interferometry
ε	Strain
FEA	Finite Element Analysis
GERD	Gastro-Esophageal Regurgitation Disorder
HAP	Hydroxyapatite
Hr	Hour/s
IPS	IPS e.max Press Ceramic Onlay
min	Minute/s
MO	Mesio-Occlusal
MOD	Mesio-Occluso-Distal
NBG	Non-Bonded Gold Onlay
O	Occlusal
OC	Direct Occlusal Composite Onlay
OCT	Optical Coherence Tomography
PAAS	Polished enamel surface/ Accelerated erosion protocol/ Artificial Saliva
PANS	Polished enamel surface/ Accelerated erosion protocol/ No Saliva
PASP	Polished enamel surface/ Accelerated erosion protocol/ Natural Salivary Pellicle
PESP	Polished enamel surface/ Early erosion protocol/ Natural Salivary Pellicle
PPSP	Polished enamel surface/ Prolonged erosion protocol/ Natural Salivary Pellicle
PZT	Piezoelectric Translator
RIDL	Resin Infiltrated Dentin Layer
SANS	Sound enamel surface/ Accelerated erosion protocol/ No Saliva
SD	Standard Deviation
Sec	Second/s
SEM	Scanning Electron Microscope/Microscopy
SG	Strain Gauge
TA	Titratable Acidity
TRI	Tooth Restorability Index
TWI	Tooth Wear Index
USG	Ultrasonography
VDO	Vertical Dimension of Occlusion

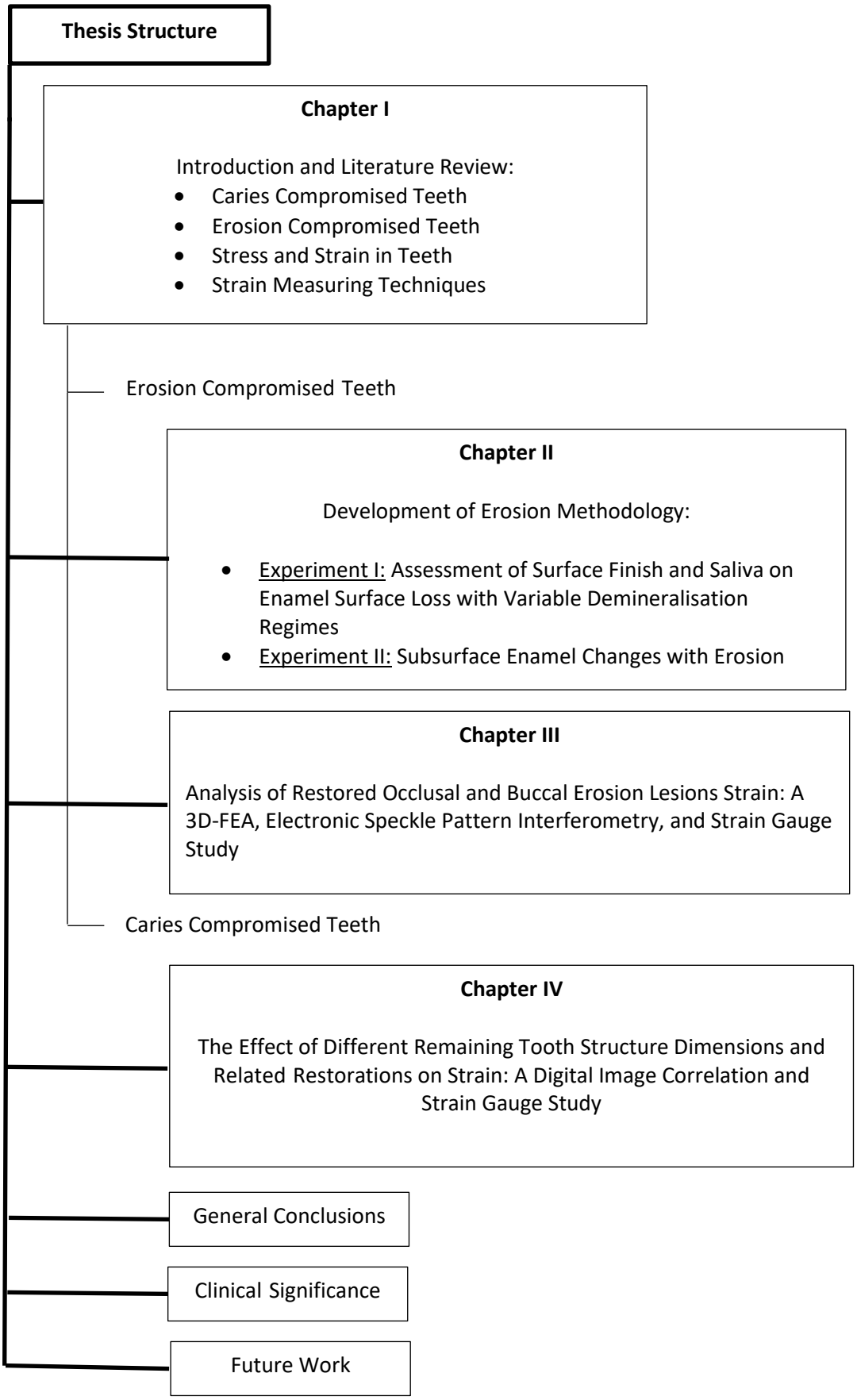
Thesis Structure
Chapter I
Introduction and Literature Review:
Caries Compromised Teeth
Erosion Compromised Teeth
Stress and Strain in Teeth
Strain Measuring Techniques
Erosion Compromised Teeth
Chapter II
Development of Erosion Methodology:
Experiment I: Assessment of Surface Finish and Saliva on Enamel Surface Loss with Variable Demineralisation Regimes
Experiment II: Subsurface Enamel Changes with Erosion
Chapter III
Analysis of Restored Occlusal and Buccal Erosion Lesions Strain: A 3D-FEA, Electronic Speckle Pattern Interferometry, and Strain Gauge Study
Caries Compromised Teeth
Chapter IV
The Effect of Different Remaining Tooth Structure Dimensions and Related Restorations on Strain: A Digital Image Correlation and Strain Gauge Study
General Conclusions
Clinical Significance
Future Work

CHAPTER 1

INTRODUCTION

1.1 Historic Background:

Tooth wear and dental pathology date back in history to antiquity. Investigation of archaeological sites in China and Germany unearthed human remains with preserved teeth from the Bronze and Iron Age. Variable levels and distributions of dental caries and tooth wear were observed. In general, heavy wear affected both posterior and anterior teeth in all specimens (Liu et al., 2010, Meng et al., 2011, Nicklisch et al., 2016). Their findings are used as a tool to assess the lifestyle, diet, and food-preparation techniques in the past. Also, CT scans of the Egyptian Djedmaatesankh mummy, a Theban woman from the 22nd Dynasty (~9th Century BC), showed extensive dental disease including missing teeth, severe attrition, caries, and periodontal disease. Most of the remaining teeth exhibit exposure of their dental pulps with some afflicted by periapical lesions. Some of those lesions could have contributed to a large secondarily infected radicular cyst that displaced the maxillary antrum and enlarged the maxilla. Djedmaatesankh's widespread dental infection probably caused her considerable pain, malaise and personal distress, and possibly caused her death. (Melcher et al., 1997).

By the middle of the seventeenth century in France, sufferers from toothache typically followed several courses to deal with dental pain. They could purchase a medicine that promised the cure. If the pain became too severe to tolerate, self-assisted tooth-drawer extraction was performed; or, finally, they could seek the services of a surgeon to end the ordeal. The surgeon's role was largely forgotten, although teeth operations had long been an integral part of his practice. The main

route was extraction, but occasionally the surgeon would perform tasks as cleaning of teeth, removal of decay, and fixing loose teeth using particular tools specially designed for these operations. By the final decade of the seventeenth century, the possession and knowledge of how to use these instruments, was firmly established as a basic (although relatively small) part of the surgeon's practice (King, 2017).

The early decades of the eighteenth century saw the appearance of a completely new type of practitioner who for some would present a final option: the *dentiste*. The practice of the *dentiste*, although not extensive, was focused on teeth. That included relief of pain, reshaping and straightening of misplaced teeth and even replacement of missing teeth. This new aspect of practice represented a radical change from what had gone before and was all built on sound surgical foundations, leading the *dentiste* to occupy a respected position within the society in general and the medical world in particular (King, 2017).

Eighteenth century Archaeological excavations have shown poor dental health amongst London populations at that time. At least 96% of the oldest adults (56+ years) were affected by dental caries. This could be attributed to the wide accessibility of refined sugars and finely milled carbohydrates. Archaeological evidence from this era showed dental innovation with the discovery of a full high quality French style porcelain denture belonging to Archbishop Arthur Richard Dillon (1721-1806). There was evidence of prolonged use and wear, not only for cosmetic or speech functions but also for mastication. This was discovered during archaeological investigation of St Pancras Old Church burial ground, London, in advance of construction of new London terminus for the Channel Tunnel Rail Link.

The dentures showed adoption of new materials and methods of manufacture. They reflect an era of significant social and economic change of the French society (Powers, 2006).

The first book on Dentistry (The operator for the teeth) written in English was by Charles Allen's in 1685. But Pierre Fauchard's laid dentistry's solid foundation in 1728 with his book Le chirurgien dentiste ou traité des dents (The surgeon dentist or treatise on the teeth), a collection of dental knowledge backed up by many medical contributors (Baron, 1999, Spielman, 2007). Fauchard is widely acclaimed as the 'Father of Modern Dentistry'. In his book, he included many techniques radical for practice of that time, as seating of patients for dental procedures, while the conventional way was laying the patient on the floor. He was also among those who dismissed worms as causative agents of dental decay, and introduced the term 'dental caries'. Many of Fauchard's observations and advice are valuable and still relevant to modern dental practice (Lynch et al., 2006). During the 19th century, the first school of dentistry was founded in Baltimore, USA followed by the spread of dental schools and faculties around the world defining dentistry as a recognized medical profession. In 1826, Amalgam was first used when Traveau described a "silver paste" filling material produced by mixing the silver coins with mercury (Bharti et al., 2010). For pain control, inhalational with nitrous oxide, ether, ethyl chloride and chloroform were mostly used as dental anaesthetics since mid-19th century. It was not before 1884 that the first successful application of local anaesthetic solution occurred in dentistry, when Dr William Halsted conducted the first block of the mandibular nerve with 4% cocaine hydrochloride (Calatayud, 2003, Gopakumar and Gopakumar, 2011).

In 1931, Drummond-Jackson introduced intravenous anaesthetics as hexobarbitone and pioneered its use in dental practice (Gopakumar and Gopakumar, 2011). In 1903, Dr Charles Land patented the first porcelain crown. His invention applied fired porcelains for inlays, onlays, and crowns (McLaren and Whiteman, 2010).

Studies of the effect of saliva on tooth enamel in reference to its hardening and softening started by the early 1900s (Head, 1912, Lambrou et al., 1981, Rao et al., 2017). Investigations of compounds that limit tooth bulk tissue loss started by the mid- 20th century.

Progressive changes in life style and diet affected the prevalence of dental disease. The change from a high fibre diet and the rise in refined sugar consumption since the 18th century with the introduction of sweetened drinks in the recent years are all associated with caries. The situation continues today and is further complicated with new pathologies such as acid erosion. That brings new challenges to the dental profession, to raise awareness and find new solutions to limit the problem, replace the lost, and protect what exists.

One of the main objectives of modern dentistry is prevention of disease, restoration of lost structure and preservation of what's existing. However, a major challenge in everyday dental practice is the success rate, time to adequate clinical function, expenses, and any complications that may occur (Doyle et al., 2006, Angeletaki et al., 2016). The decision to restore a tooth, the selection of the restorative materials and their production expenses should be weighed against the patient's financial status without compromising the success rate and longevity

criteria especially when restoring severely compromised teeth (after caries or acid erosion) where the remaining tooth structure is limited.

1.2 Literature Review:

Tooth fracture is a frequent restorative problem. A tooth's ability to resist fracture can be the result of a combination of clinical factors, including quality, quantity and age of remaining tooth structure (Soares et al., 2008b), cavity preparation, choice of restorative material (Soares et al., 2006, Soares et al., 2008b) and tooth loading. Caries, erosion, attrition and trauma commonly remove tooth structure that in turn decreases the fracture resistance of the tooth and affect stress distribution within the tooth. Stresses within tooth structure in combination with strength properties are important to fracture resistance (Khera et al., 1990, Bassir et al., 2013b). Teeth with different levels of reduced tooth structure related to caries and acid erosion will be studied and analysed in this research work.

Tooth stresses generation is complicated by the non-homogeneous nature of tooth structure and the irregularity of its contours. Tooth structure is composed of different materials with widely varying properties. These include enamel, dentine, pulp, cementum and supporting tissues of periodontium, and bone. Together with the large variations in both the magnitude and direction of chewing forces, the problem is further complicated (Rubin et al., 1983).

Load application to an object causes stress concentration and structural

strain. The ultrastructural integrity of the body is not affected when this occurs within the elastic limit. However, stress concentration beyond this limit may result in crack formation and propagation which will eventually cause fracture and structural failure (Rees et al., 1994, Soares et al., 2008a). The elastic modulus reflects the direct linear relation between stress and strain. Understanding this mechanical property is fundamental to understanding relationships between materials and their biomechanical behaviour (Rees et al., 1994).

1.2.1 Caries Compromised Teeth:

1.2.1.1 Strain in Sound vs Restored Teeth:

(Magne and Belser, 2002) assessed the stress distribution in sound unrestored molars under different occlusal load configurations and concluded that even unrestored teeth suffer from strain under loading. The position of the tooth structure loaded had an influence, as functional cusps were generally more protected under compressive stresses than non-functional cusps, which exhibited more tensile stresses. This also showed that vertical loading of teeth did not generate harmful concentrations of stress compared to lateral loading. This agrees with the findings by (Palamara et al., 2002) that oblique loading on the buccal cusp led to higher strains oriented approximately 35-40º from the long axis of the tooth. Regardless of loading direction and location, the marginal ridges and proximal contact areas were sites of low strain.

(Magne and Belser, 2002) also observed that high stress levels were related to the shape of the loaded structure. Higher strain values were recorded during non-working movement in the central groove of vertically loaded molars, denoting that concave areas tend to concentrate stresses more than convex areas. This confirmed the results of (Magne et al., 1999) who experimented on anterior teeth and concluded that convex surfaces with thick enamel raise less concentrated stresses than concave areas, which tend to concentrate stresses.

Many studies have confirmed that stress concentration and strain values were directly influenced by the quantity of the tooth structure lost (Magne, 2007, Soares et al., 2008a, Soares et al., 2008b).

As the fracture resistance of restored teeth is lower than sound teeth, the dental practitioner is challenged by the design of the cavity preparation (Mondelli et al., 1980, 2007, Pereira et al., 2013). One study showed that 92% of fractured teeth had previously undergone restoration (Gher et al., 1987).

The presence of wide and/or deep restorations may be considered the highest risk of tooth fracture (Valdivia et al., 2012), and cavity preparation typically exaggerates the height of the remaining cusps rendering them unsupported. When unsupported cusps are loaded they may deflect, rotate or fracture (Soares et al., 2008b, Boaro et al., 2013, Pereira et al., 2013). While fracture may not always occur, the tooth-restoration interface may open with deflection or torsion of a weakened cusp. This may subsequently result in marginal leakage, secondary caries formation, and possibly tooth fracture.

1.2.1.2 Anatomical Position of Caries-Compromised Teeth (Anterior vs Posterior):

Posterior teeth anatomy, with cusps and fossae, predisposes them to deflection of cusps under stress (Bassett et al., 1964), the form and height of the cusps influence the direction of stress.

To reduce tooth fracture, it appears to be important to maintain the marginal ridge integrity (Wendt Jr et al., 1987, Reeh et al., 1989b, Magne, 2007, Mondelli et al., 2007, Roperto et al., 2019). In intact teeth, strength is gained from marginal ridges forming a continuous band of tooth structure. Mondelli et al. (1980) also reported that the impact of the width of the isthmus in a cavity preparation was less with Class I than with Class II preparations. The reason behind this was probably the marginal ridge preservation in the Class I preparation. He concluded that a narrower isthmus would increase the fracture resistance of a prepared tooth.

Bassir et al. (2013b) showed that the fracture resistance of sound teeth was significantly reduced with Mesio-Occlusal (MO) and Mesio-Occluso-Distal (MOD) cavity preparations. When non-destructive occlusal loading was applied, (Pereira et al., 2013) observed that MOD cavities presented significantly higher values of strain than MO, occlusal (O), or intact teeth. However, to reduce restorative failure, some authors recommended that cavity preparations should have a combination of a narrow occlusal outline and a shallow pulpal floor (Nadal, 1962, Osborne et al., 1972, Mondelli et al., 1980, Blaser et al., 1983). Blaser et al. (1983)

studied the fracture potential of teeth with MOD cavities, prepared with different internal dimensions. They concluded that the isthmus width did not considerably weaken the teeth as long as a shallow pulpal depth was maintained.

The behaviour of anterior teeth must be differentiated from the behaviour of posterior teeth (Reeh et al., 1989b, Magne and Oganesyan, 2009, Bassir et al., 2013a). Posterior teeth demonstrated dramatic reduction in crown stiffness with MOD preparation, which confirms that the loss of marginal ridge integrity is the most important contribution to the loss of tooth strength. While, stress distribution within an incisor was not significantly affected when the tooth material was removed proximally, whereas, a significant increase in flexibility occurred when tooth material was removed facially and palatally in incisors tested against multiple successive restorative procedures (Magne and Douglas, 2000, Magne and Tan, 2008).

1.2.1.3 Quantification of Remaining Tooth Structure:

1.2.1.3.1 Remaining Tooth Dimensions (Width vs Height):

In order to assess the remaining tooth structure, both remaining wall width and height should be examined. In the literature, few studies have assessed the amount of residual tooth structure in vital teeth. Residual dentine thickness in vital posterior teeth after all-ceramic crown preparation has been reported. The mean residual dentine thickness between the axial wall and pulp chamber in posterior teeth varied between 0.47 and 0.7mm (Polansky et al., 2000). Another study by

(Seow et al., 2005) reported the thickness of remaining dentine on a maxillary second premolar following various preparations for a metal-ceramic or all-ceramic crown. The thinnest section of remaining tooth structure was the palatal wall with only 0.8mm and <0.3 mm remaining, respectively.

To further look into studies of remaining tooth structure related to severely compromised teeth, one should consider the literature discussing the restoration of endodontically compromised teeth (Jotkowitz and Samet, 2010). This can be attributed to the fact that non-vital teeth frequently lack tooth structure (Kurer, 1991).

Many *in vitro* studies on endodontically treated teeth have examined the effect of the preserved coronal dentine height on the success of the final restoration. They appear to agree that maintenance of a height of at least 2mm of coronal dentine has a favourable effect (Sorensen and Engelman, 1990, Libman and Nicholls, 1995, Bandlish et al., 2006, Veríssimo et al., 2014).

(AL-Omiri and AL-Wahadni, 2006) carried out an *in vitro* study to investigate the effect of different heights of remaining coronal dentine on the fracture resistance of teeth restored with composite cores. In their results, although statistically insignificant, higher fracture resistance was witnessed with higher retained dentine height. They also noticed that the fracture pattern was related to the amount of retained dentine only when < 2 mm high.

It has been also recommended that preserving a 2mm of coronal dentine thickness would improve resistance to fracture (Sorensen and Engelman, 1990,

Assif et al., 1993, Ferrari et al., 2000, Murphy et al., 2009).

1.2.1.3.2 The Ferrule Effect:

One of the foundations of the restoration of the endodontic treated tooth is the incorporation of the concept of 'ferrule'. 'The ferrule effect' is often used to express the amount of remaining sound dentine above the finish line. In fact, it is not the remaining tooth structure that constitutes 'the ferrule effect' but rather the actual bracing of the complete crown over the tooth structure, with a positive strengthening influence protecting the remaining structure against fracture (Ng et al., 2006, Pereira et al., 2006, Jotkowitz and Samet, 2010, Lima et al., 2010, Dejak and Młotkowski, 2013, Ausiello et al., 2017).

It is common for only a partial ferrule to remain after crown preparation. Various studies have demonstrated the positive influences of a uniform full ferrule over a partial ferrule that varies in different parts of the tooth (Morgano and Brackett, 1999, Tan et al., 2005, Arunpraditkul et al., 2009, Jotkowitz and Samet, 2010). However, the literature suggests that a non-uniform ferrule, although not as ideal as a full 360°, 2mm ferrule, is still superior to no ferrule at all and has value in providing fracture resistance. Arunpraditkul et al. (2009) compared endodontically treated teeth with four walls to those with three walls and studied the effect of the site of the missing coronal wall on teeth fracture resistance. They concluded that teeth with four walls of remaining coronal dentine had significantly higher fracture resistance than teeth with only three walls. Although the site of the missing coronal wall did not significantly affect the fracture resistance of

endodontically treated teeth, it was noticed that teeth without a buccal wall were the least resistant to fracture among the tested groups. While, the least effect on fracture strength was observed with teeth without a proximal wall. However, different observations regarding the location of the remaining coronal structure were found in anterior teeth. The results of (Ng et al., 2006) suggest that the presence of a palatal axial wall is as effective as a 360-degree circumferential axial wall in providing fracture resistance.

Similar finding were reported by (Al-Wahadni and Gutteridge, 2002), who demonstrated that retained coronal buccal dentine had a significant effect in improving the fracture resistance of posterior teeth restored with partial dowel and cores when compared to teeth without retained coronal dentine.

1.2.1.4 Clinical Evaluation of Remaining Tooth structure:

Clinical evaluation of the remaining coronal dentine is essential in the restorative decision making. A tooth restorability index (TRI) was devised to allow mapping of remaining tooth structure (McDonald and Setchell, 2005, Bandlish et al., 2006). This index allows prediction of tooth restorability by allocating a numerical value to tooth sections summing to a total value for the whole tooth. After all existing restorations and unsupported tooth structure have been removed; each tooth was divided into equal sextants: two proximal, two buccal and two lingual areas. A scoring system of 0–3 was allocated to each coronal

dentine sextant (0=none, 1=inadequate, 2=questionable, 3=adequate) contributing to retention and resistance forms. Thus, a maximum score of 18 could be given for each tooth.

In their *in vivo* investigation to assess the remaining coronal tooth structure in teeth prepared for complete and partial coverage restorations, Murphy et al. (2009) used 3D scanning and a TRI to assess teeth preparations for full and partial coverage restorations. They found there was a strong correlation between mean TRI and scanned volume of tooth structure. They also confirmed that partial coverage preparations removed less tooth structure than full coverage when provided for the same teeth and this varied substantially depending on the tooth anatomy.

Evaluation of remaining tooth structure should focus on both the quantity of the remaining tooth structure and the available restorative options. With different amounts of remaining tooth structure, different types of restorations are recommended. In situations of minimal or no retention, adhesive restorations have a major advantage of bonding to both enamel and dentine (van Dijken, 1999). Bonding to enamel is stable over time, but *in vivo* (Breschi et al., 2008, Liu et al., 2011) and *in vitro* (De Munck et al., 2005) studies have revealed the limited durability of resin-dentine bonds (Marchesi et al., 2013). Although most currently used dental adhesive systems show favourable immediate results reflected in good retention and sealing, dentine bonded interfaces may not withstand ageing and may show long-term degradation (Van Meerbeek, 2003, Frassetto et al., 2016). While, clinical trials evaluating adhesive systems have found dramatically variable bonding qualities between tested materials (van Dijken, 2000). Also,

Marchesi et al. (2014) evaluated the bond strength of a multimode-adhesive system to dentine and stability after ageing. Their results showed no differences between groups at baseline. While, after 1 year of storage, only Scotchbond Universal applied in the self-etch mode and Prime&Bond NT showed higher strength compared to the other groups. Given that the dentine- adhesive bond varies among different conditions and it deteriorates with time, reliance purely on adhesion may not be ideal and investment in studying remaining tooth structure is still considered important to long-term outcomes.

1.2.2 Erosion Compromised Teeth:

Erosion of dental tissues refers to the irreversible chemical and chemical-mechanical processes that involve dissolution of dental hard tissues by acids with no inclusion of any bacterial action (Zipkin and McClure, 1949, Barbour and Rees, 2004, Hemingway et al., 2006, Poggio et al., 2013, Batista et al., 2016). It is considered an important factor for tooth wear besides attrition, abrasion and mastication (Lussi and Hellwig, 2001). A variety of extrinsic and intrinsic factors may cause erosion. Acids intrinsic in origin include hydrochloric acid due to regurgitation of the gastric contents in gastrointestinal refluxes or recurrent vomiting as part of eating disorders in anorexia nervosa or bulimia (Hellström, 1977, Järvinen et al., 1988), or extrinsic as excessive consumption of acidic beverages, foods and medication as well as professional prolonged exposure to acidic environments (Cate, 1968, Levine, 1973).

The problem of erosion is growing in dental health in the recent years affecting up to 80% of adults and about 50% of children (Jaeggi and Lussi, 2006, Rakhmatullina et al., 2011). Some occupational groups show high prevalence of dental erosion and subsequent tooth sensitivity. Those include winemakers, sports people, and individuals with medical conditions including asthma, diabetes, and alcoholism (Sivasithamparam et al., 2003, Amaechi and Higham, 2005, Manton et al., 2010).

Since the mid-1990s, and with the decline in dental caries in many industrially developed countries, research interest in dental erosion and its role in tooth wear increased considerably (Tantbirojn et al., 2008). Early studies on human tooth wear were based on teeth from archeologically obtained skulls. While, later studies examined contemporary adult populations (Johansson et al., 2012). Due to the coarse nature of diet, the earliest form of tooth wear was found mainly on occlusal, incisal and proximal surfaces, whereas modern erosive tooth wear has additional characteristics that include the buccal and palatal/lingual surfaces (Johansson et al., 2012).

In the UK, many studies have covered the prevalence of tooth erosion in children, adolescents and adults (Jaeggi and Lussi, 2014). Prevalence studies of tooth erosion in the UK began in 1993 with the *National Survey of Children's Dental Health*, and subsequently they have varied from reports of small convenience samples and local population studies, to national surveys (Dugmore and Rock, 2004) . The age of the children examined has varied from 1.5 to 18 years. Examination of incisors and molars of 1,753 12-year-old children showed a prevalence of tooth erosion of 59.7%, with 2.7% exhibiting exposed dentine.

Convenience samples of 129 children (aged 11–13 years) in 125 children in the UK were examined. The prevalence data showed that 37% of the UK children had dental erosion (Vargas-Ferreira et al., 2010). Milosevic et al. (1994) examined a total of 1,035 children (mean age 14 years) in 10 schools in Liverpool, UK and found that 305 of them had tooth wear lesions with involvement of dentine, mainly incisally; 8% also exhibited exposed dentine on occlusal and/or palatal surfaces; the occlusal surfaces of the first mandibular molars and the palatal aspects of the maxillary incisors were mainly affected. Al-Dlaigan et al. (2001) established the prevalence of erosion in a cluster random sample of 418 teenagers (aged 14 years, 209 girls, 209 boys) in Birmingham, UK. They found that 48% of the children had erosion within enamel, 51% had erosion within enamel with possible slight involvement of dentine and 1% had erosion with advanced involvement of dentine. Reviewing the data from the national dental surveys of young people in the UK, a trend towards a higher prevalence of erosion in children aged between 3.5 and 4.5 years was found. Overall, the prevalence data from cross-sectional national studies indicated that erosion increased with age of children and adolescents over time (Nunn et al., 2003, Jaeggi and Lussi, 2014). Tooth wear is a relatively common condition in adults, and its prevalence increases with age (Bartlett and Dugmore, 2008, Li and Bernabé, 2016).

Quality of life is affected by the oral condition of subjects. Few studies have formally assessed the impact of tooth wear on people's quality of life (Sanders et al., 2009, Maida et al., 2013, Shen et al., 2013, Li and Bernabé, 2016, Toole et al., 2018). One study reported that quality of life with severe erosive tooth wear was equivalent to that of being edentulous (Papagianni et al., 2013). Patients with a worn dentition often complain of tooth sensitivity associated with dentine

exposure; dental pain due to involvement of the pulp; poor aesthetics owing to shortened clinical crown and loss of vertical dimension; and/or functional impairment for difficulties with chewing due to occlusal alterations and dental tissue loss (El Wazani et al., 2012, Olley et al., 2015). Sociodemographic factors are also closely related to both quality of life tooth wear (Bartlett et al., 2013, Jaeggi and Lussi, 2014); they may confound the association between tooth wear and quality of life.

Management of tooth wear requires early diagnosis and assessment of the severity of the condition followed by treatment planning. Restorations include direct restorations, indirect restorations, or orthodontic treatment can be considered. All these measures even the most conservative are costly and require constant maintenance and may have uncontrolled sequelae (Bernardon et al., 2002). Financial constraints can often restrict these options and limit the choice pathways that can be offered (Sethi, 2016).

1.2.2.1 Stages of erosion lesion development:

Erosive tooth wear can progress with time and cause continuous irritation exposing deeper dental tissues and developing severe lesions that need extensive and costly dental care. Consequences of the long- and short- term erosion are marked with severe and debilitating tooth sensitivity (Mahoney and Kilpatrick, 2003, West, 2006, Manton et al., 2010). This is not the only concern,

as severe cases with considerate bulk loss may compromise the tooth resistance to load and functional stresses and eventually increase the potential loss of teeth.

Erosion mainly involves enamel; the outermost layer of the tooth with its typical high mineral content and prismatic structure (Mahoney et al., 2004, Wang et al., 2014). Remineralisation of the lesion is still possible at the initial stage of the process when decalcification has occurred only below the surface and the lesion is still covered by an intact enamel surface (Dawes, 2003, de Alencar et al., 2014). In this case, the subsurface lesion provides an appropriate matrix for crystal growth when calcium and phosphate ions pass from the surrounding through the salivary pellicle and surface enamel. However, removal of the softened enamel by abrasive forces reduces the lesion's liability to recover because of absence of suitable matrix for crystal growth (Dawes, 2003, Huysmans et al., 2011, Poggio et al., 2013, de Alencar et al., 2014).

Erosion does not only affect the enamel of the tooth but can extend deeper into dentine. If that happens, it causes hypersensitivity or even in severe cases exposing the pulp and even leading to tooth fracture (Addy et al., 1987, Harley, 1999, Wongkhantee et al., 2006). Not only erosion is responsible for tooth wear. In most clinical cases, it acts in synergy with abrasion and attrition. Although several tribological mechanisms exist, the most common mechanisms in tooth wear may be explained by two-body abrasion (typically attrition) or three-body abrasion (typically erosion and abrasion) with an acidic or abrasive medium interaction, respectively (Mair, 1992, Johansson et al., 2012).

Dental hard tissue is composed of a combination of tissues including enamel and dentine with different compositions related to these structures. Enamel is a composite material consisting of both a mineral and an organic phase. The mineral phase is predominant (95–96 wt.%) and consists primarily of large hexagonal hydroxyapatite (HAP) crystals composed of calcium (Ca^{2+}), phosphate (PO_4^{3-}), hydroxide (OH^-), fluoride (F^-), carbonate (CO_3^{2-}) and sodium (Na^+) ions [22]. It is represented by the simplified chemical formula: $Ca_{10-x}\ Na_x\ (PO_4)_{6-y}\ (CO_3)_z(OH)_{2-u}F_u$ (Staines et al., 1981, Cuy et al., 2002, Chun et al., 2014, Shellis et al., 2014, Carvalho and Lussi, 2020). These crystals are arranged to form millions of hexagonal-prism-shaped enamel rods with the diameter of 3–5 μm (1/100th the hair thickness). Enamel contains almost no water and therefore is considered the hardest tissue in the human body. Fluoride mineral concentration is the highest at the outermost enamel layer (Hallsworth and Weatherell, 1969, Carvalho and Lussi, 2015). Enamel minerals (calcium concentration) and density decrease toward the dentino-enamel junction (DEJ) (Robinson et al., 1971, Carvalho and Lussi, 2015). While, the carbonate and magnesium concentrations increase (Weatherell et al., 1974, Carvalho and Lussi, 2015).

Enamel has a shiny surface and comes in variable colours ranging from light yellow to grey. Enamel is the outermost layer of the crown of the tooth extending from the gum upwards covering dentine with variable thicknesses and densities. The thickest and hardest enamel is located at cusps and biting edges. Enamel of primary teeth is different from permanent teeth being less hard and having about half the thickness (Gašperšič, 1995, Chun et al., 2014). Unfortunately, enamel never regenerates once eroded or abraded as the ameloblasts have been lost

(Cuy et al., 2002, Chun et al., 2014). Dentine is different to enamel, with lower apatite content (45– 50 wt. %) with a much smaller crystalline size, and a higher organic matter (30– 35 wt. %) mostly made out of type 1 collagen. In dentine, hydroxyapatite occurs within the tubules fibrils (intrafibrillar mineral) and between fibrils (extrafibrillar mineral) (Bertassoni et al., 2010, Poggio et al., 2013). These characteristics render dentine more susceptible to acidic dissolution than enamel (Tillberg et al., 2008, Vaderhobli, 2011, Chun et al., 2014). Dentine formation initiated by odontoblasts, which are located as a single cell layer around the pulp chamber. Odontoblasts are connected to the calcium ions of dentine by channels within the dentinal tubules (Marshall Jr et al., 1997, Ten, 1998, Chun et al., 2014). Those are responsible of delivering pain, pressure, and temperature change to the nerves in the dentinal tubules (Murray et al., 2003, Arana-Chavez and Massa, 2004, Chun et al., 2014).

1.2.2.2 Erosion and soft drinks:

The erosive role of food and drink on teeth has been documented over the years. The earliest citing of erosion were reported by (Darby, 1892) and (Miller, 1907). It has been traditionally believed that acidity (measured pH) is an accurate indicator of the erosive potential of a food or drink, where the lower the food pH, the greater the erosive potential (Meurman and Ten Gate, 1996, Cairns et al., 2002, Kim and Jin, 2019). However, other chemical factors are equally important as pH in determining the erosive potential of food and drink. These include

titratable acidity (TA), buffering capacity, viscosity, and mineral content (calcium, phosphate, and fluoride) (Lussi et al., 1993, Wongkhantee et al., 2006, Batista et al., 2016, Carvalho and Lussi, 2020). Titratable acidity- sometimes also termed neutralisable acidity, is defined as the total volume of alkali (typically 0.1 molar sodium hydroxide) required to raise the pH of a standardised volume of a solution (typically 25 ml) to neutral pH (pH 7) (Grenby et al., 1989, Min et al., 2011, Chadwick, 2019, Kim and Jin, 2019, Carvalho and Lussi, 2020). In other words, titratable acidity is related to the persistency of an acidic environment in the oral cavity (Grobler and Van der Horst, 1982, Grenby et al., 1989, Min et al., 2011). Baseline pH values are only indicators of the initial hydrogen ion concentration but not of the presence of undissociated acid. Thus, it is now widely accepted that the titratable acidity could be a more accurate measure of the total acid content of a drink, and may be a more realistic means of predicting erosive potential (Grobler and Van der Horst, 1982, Cairns et al., 2002, Kim and Jin, 2019). Products with a combination of mineral undersaturation (especially Ca^{2+} concentration), low pH, and high titratable acidity have a great erosive potential (Lussi et al., 2012b, Lussi and Carvalho, 2015, Carvalho and Lussi, 2020)

Carbonated soft drinks contain additional carbonic acid which makes them potentially more erosive than non-carbonated beverages (West et al., 2003). Cola is one of the most popular acidic drinks with pH of 2.74, the lowest among tested food and drinks, and TA of 9.52 mmol/l ± 0.81 standard deviation (SD) (Chadwick, 2019). Its erosive effect on teeth is well documented, causing the highest change in the tooth surface hardness (West et al., 2000, Wongkhantee et al., 2006, Wang et al., 2014).

The basic composition of a carbonated drink consists of water, sugar, flavour enhancers and carbon dioxide. Flavour enhancers can include caffeine and aspartame. Organic acids (commonly citric acid) are the major constituent of soft beverages. Preservatives such as phosphoric acid, are added particularly in colas preventing deterioration through microbiological spoilage. Furthermore, acids are also used to offset the sweetness of sugar and complement the flavour by improving the sharpness of the drink (West et al., 2000, Laurance-Young, 2012).

Acids are capable of reducing the local pH on the teeth surface, thereby causing mineral dissolution. For citric acid, this process is explained by calcium ions being chelated by citrate anions, decreasing the amount of free calcium ions available for remineralisation in both saliva and at the enamel surface, thereby favouring demineralisation (Featherstone and Lussi, 2006, Manton et al., 2010)

The critical pH is the pH value at which a solution is saturated with respect to a particular mineral, and the concept of critical pH applies only to solutions that are in contact with a particular mineral such as tooth enamel and dentine (Dawes, 2003). The pH of 5.5 was suggested to be the critical pH at which hydroxyapatite dissolves, and teeth are vulnerable to decalcification in acid media as they are composed of *calcium-deficient carbonated hydroxyapatite* (Featherstone and Lussi, 2006, Wongkhantee et al., 2006, Borjian et al., 2010, Li et al., 2014). Others considered pH 4.5 critical for erosive demineralisation (Meurman et al., 1987, Millward et al., 1997, Ganss et al., 2007). Repeated exposure to acidic drinks leads to sustained low intraoral pH below the critical pH (5.5) and allows the development of decalcification lesions (Featherstone and Lussi, 2006). However, recent studies advocate the importance of not judging the erosive potential of

products only by their pH, for there is no “critical pH” related to erosion (Carvalho and Lussi, 2020). Furthermore, the erosive potential of a solution is dependent on calcium and phosphate concentrations (Dawes, 2003, Carvalho and Lussi, 2020).

Other factors have been reported to be related to the erosive potential and extent of acidic drinks, such as, temperature and method of consumption (frequency, duration) (Amaechi et al., 1999a, West et al., 2000, Johansson et al., 2004, Wongkhantee et al., 2006, Manton et al., 2010). It has been also observed that there is a relation between the temperature of the drink and pH. The pH of all beverages significantly increased when the temperature was reduced from 37°C to 4°C (Barbour et al., 2006, Manton et al., 2010).

1.2.2.3 Changes to acidic food consumption:

Through the decades, lifestyles and food habits have changed. Both the amount and the frequency of consumption of acidic foods and drinks were affected by this change. In the USA, soft drink consumption increased by 300% over 20 years and the serving size increased by almost triple the amount between the 1950s and the 1990s and more was expected onwards in the future (Cavadini et al., 2000, Lussi, 2006). This change considerably increased the potential of erosion for all age groups including children and adolescents (Lussi, 2006, Manton et al., 2010). A higher prevalence was reported among children aged between 3 ½ and 4 ½ years consuming soft drinks on most days compared with

toddlers consuming less (Nunn et al., 2003). In another UK study on subjects examined at the age 12 years old and 2 years after, recorded presence of enamel and dentinal lesions (5%, 2% respectively) that noticeably progressed over 2 years period (13%, 9%). Also, 12% of the children who demonstrated no evidence of erosion developed the condition over the subsequent 2 years (Dugmore and Rock, 2003).

Acidic drink consumption behaviour plays a major role in dental health. The extent of erosion has been shown to be significantly affected by the manner of exposure to acidic food and drinks, including frequency of consumption, duration of exposure, and temperature of the drink (Amaechi et al., 1999a, Wongkhantee et al., 2006). Excessive consumption of carbonated drinks was related to clinically encountered dental erosion (Cheng et al., 2009a, Wang et al., 2014), characterized with obviously decreased enamel hardness (Tantbirojn et al., 2008, Wang et al., 2014). The habit of consumption of carbonated drinks is already popular among youngsters and is unfortunately carried over into adulthood (Wongkhantee et al., 2006). Public awareness campaigns have been waged regarding the risk of dental disease related to sugar products consumption. However, awareness on dental erosion, another common cause of tooth surface destruction, is not enough.

1.2.2.4 Diagnosis and Grading of Dental Erosion:

Different clinical scales and indices have been developed to facilitate examination, diagnosis, grading, and monitoring of dental erosion. However, studies are difficult to interpret and compare due to lack of standardization in terminology and the large number of indices developed. Some erosion indices even record lesions on an aetiological basis, yet none has universal acceptance (Bardsley, 2008).

Due to lack of fixed intra-oral reference points and accessibility, it is difficult to accurately monitor the change on natural tooth surfaces and the progression of erosive tooth wear inside the oral cavity. Moreover, most of the devices used for detection of surface and subsurface changes are designed to perform on specially prepared specimens. Therefore, *in vitro* and *in situ* studies are mostly applied to investigate alterations of dental hard tissues (Attin, 2006).

The literature is rich with methods than can be broadly divided into quantitative and qualitative in nature. Quantitative methods rely on objective measurements and are more sensitive and reliable to perform under controlled settings as on a model or in the laboratory. While, Qualitative methods, such as mild, moderate or severe, usually rely on subjective descriptions of the affected tooth surface and are more appropriate for a clinical intra-oral examination, where data collection is often carried out in a setting lacking sophisticated equipment. However, both methodologies utilise grading or scoring systems to identify progression of a condition (Bardsley, 2008).

Early indices relied mainly on qualitative descriptive terms. The earliest index documented by (Broca, 1879) was the foundation for the development of further indices. It graded occlusal wear at horizontal or oblique patterns without including the aetiology.

Another early developed index is Restarski et al. (1945). Their index was a six-point grading system to evaluate the severity of the lingual surface erosive destruction observed in rat and puppy molars. However, concerns were raised regarding reproducibility. Higher accuracy was introduced by (Xhonga and Valdmanis, 1983), who quantitatively divided erosions into four levels utilizing periodontal probe measurements. They further classified erosion by morphological descriptions (wedge, saucer, groove, atypical).

In 1982, the FDI DDE index for enamel defects was developed. This was an example of an ideal basic structure index that allowed for the rise of more expanded categories to serve epidemiological research purposes (Bartlett et al., 2008).

Upon the first and the most frequently reported indices is the Smith and Knight (1984). They developed the Tooth Wear Index (TWI) which classifies tooth wear at 4 sites per tooth (Buccal, cervical, lingual, and occluso-incisal) on a 5- point scale of all present teeth scored for wear, irrespective of the wear aetiology (Bardsley, 2008, Fares et al., 2009). The index notifies changes to enamel as a single grade, whereas records depth changes into dentine with 3 grades. The reason behind this was that the aim of the index, as most early indices, was to assess the need for operative intervention which is more applicable to dentine at

severe levels of involvement (Fares et al., 2009). However, this overlooks the changes in enamel restricting its use in interventional studies for erosion prevention where the short term changes mainly occur in enamel.

Lussi et al. (1991) developed an index modified from Linkosalo and Markkanen (1985), who utilised a qualitative index to categorize lesions as erosive with four grades of severity extending into dentine. Their index has been widely used by European researchers to score all teeth except the third molars.

In 2008, the Basic Erosive Wear Examination (BEWE) scoring system was introduced by Bartlett et al. (2008). This index was designed to provide a simple scoring system using the diagnostic criteria of all existing indices, to ultimately transfer their results into one score sum. The BEWE measures not only the severity of the condition but can also be transferred into risk levels that act as a guide towards management.

The BEWE records the most severely affected surface in a sextant. The four level score grades the lesion according to severity of wear from (0) no surface loss, (1) initial loss of enamel surface texture, (2) distinct defect including dentine (< 50% of the surface area), or (3) defect including dentine (>50% of the surface area). The highest score is recorded on the examined surface (Buccal/facial, occlusal, and lingual/palatal).

In 2009, (Fares et al.) developed “The Exact Tooth Wear Index” which is a modification to (Smith and Knight, 1984). In their index, tooth wear was graded separately for enamel and dentine using 5- and 6-point scales, respectively. All affected surfaces were reported, irrespective of the aetiology of wear. Following

the basic protocol described by Smith and Knight (1984), dentine exposure was scored using the colour of the exposed lesion to represent depth.

In our research, erosion lesions with different extension levels were created to try to resemble different clinically existing lesions. Erosion created lesions should resemble clinical initial lesion, and lesions extending into 1/3rd, 2/3rd, and all the enamel surface. Therefore, a quantitative index with coinciding extension levels for both enamel and dentine was required. The exact tooth wear index by (Fares et al., 2009) fit the criteria and therefore was applied (**Table 1**).

Table 1: Exact Tooth Wear Index:

Exact Tooth Wear Index for Enamel	Exact Tooth Wear Index for Dentine
0 No tooth wear: no enamel loss features or change in contour	0 No dentinal tooth wear: no dentine loss
1 Loss of enamel affecting < 10% of the scored surface	1 Loss of dentine affecting < 10% of the scored surface
2 Enamel loss affecting between 10% and 1/3rd of the scored surface	2 Dentine loss affecting between 10% and 1/3rd of the scored surface
3 Enamel loss affecting ≥ 1/3rd but < 2/3rd of the scored surface	3 Dentine loss affecting ≥ 1/3rd but < 2/3rd of the scored surface
4 Enamel loss affecting two thirds or more of the scored surface	4 Dentine loss affecting ≥ 2/3rd of the scored surface, without pulpal exposure
	5 Secondary dentine exposure or pulpal exposure

1.2.2.4.1 The Role of Saliva in Remineralisation (Natural and Artificial):

In the oral environment exists a constant dynamic process of tooth structure demineralisation and remineralisation (de Alencar et al., 2014). Saliva minimizes the acid effects by its buffering qualities and acid dilution (Hannig and Hannig, 2014, Hara and Zero, 2014). It is recognised as a biological factor that plays an important role in remineralisation. Its protective qualities include salivary clearance, buffering capacity, and level of saturation with minerals (Edgar et al., 1994, Walsh, 2009). Saliva assumes repairing initial enamel lesions as it contains calcium, phosphate and fluoride that can modify the erosive process (Imfeld, 1996b, de Alencar et al., 2014). Deposition of minerals onto the porous erosive layer seems to be involved in the process of remineralisation rather than crystal regrowth (Tantbirojn et al., 2008, de Alencar et al., 2014). In addition, stimulation of salivary flow rate can enhance the remineralising effect of saliva by increasing the bicarbonate buffer and salivary mineral content, which in turn facilitates mineral redisposition onto the enamel surface (Dawes, 1969, de Alencar et al., 2014). Ideally, salivary effects should be replicated by using saliva substitutes in *in vitro* experiments. Artificial saliva is an oversaturated solution with respect to enamel and has long been used and proved to exert a remineralisation effect on softened enamel *in vitro* by saturation of enamel surface (Amaechi and Higham, 2001a, Eisenburger et al., 2001a, Devlin et al., 2006, Torres et al., 2010, Aykut-Yetkiner et al., 2014, Lussi et al., 2014).

The early stage of erosion is characterized by enamel softening and reversible acidic demineralisation. However, if the acidic environment persists, further

enamel dissolution occurs, resulting in gradual irreversible thickness loss (Barbour et al., 2006, Poggio et al., 2013).

For remineralisation, other important components of saliva are its proteins (as glycoproteins and phosphoproteins). When glycoproteins are adsorbed onto the tooth surface, they form a protective pellicle layer, whereas, phosphoproteins are responsible for regulating the calcium saturation of the saliva. In conditions of acid attack, salivary pellicle is known to form a protective barrier against acid penetration, by that reduces enamel mineral loss. Moreover, the early glycoproteins pellicle promotes remineralisation by attracting calcium ions (Hannig et al., 2004, Wiegand et al., 2008). Previous *in vitro* studies have shown that the efficacy of pellicle layer protection is affected by the degree of its maturation (Zahradnik et al., 1978, Hannig, 2002). However, some *in vitro* studies investigated the inhibitory effect of *in vitro* formed pellicle on enamel demineralisation, and observed partial inhibition of demineralisation with short-term pellicle layer formation of 3 min (Hannig et al., 2004). Moreover, no distinct structural differences were observed on eroded enamel surfaces, independent of pellicle formation time (3, 60 or 120 min-old pellicles). Amerongen et al. (1987) observed significant inhibition of demineralisation within a 9 min pellicle formation time. While, maximum enamel surface protection was achieved as early as 60 min of pellicle formation time.

1.2.2.5 Methods for Assessment and Measurement of Dental Erosion:

No one method of erosion assessment is suitable for different stages of the lesion. Many factors determine the potential applicability and limitations of existing methods in characterizing erosion, including: the specimen surface condition (natural or flat), the nature of the lesion included in the study (erosion or erosion plus abrasion), the experimental model type (*in vitro*, *in situ*, or *in vivo*), need for longitudinal measurements (use of destructive or non-destructive methods), and the type of required outcome (qualitative or quantitative data).

Different methodological approaches have been used to assess dental erosion according to the pattern of interest; namely loss or softening of dental hard tissues. A couple of the most established techniques have been implemented in this research including Scanning Electron Microscope (SEM), Surface Microhardness Measurement (SMH), surface profilometry, Confocal Laser Scanning Microscopy (CLSM), Micro Computerized Tomography (µCT), Optical Coherence Tomography (OCT), and Fourier Transform Raman Spectroscopy (FT- Raman) and many more. Techniques applied in our research only were discussed in this chapter.

Enamel and dentine behave differently to acid erosion (Lussi et al., 2011). Because of high mineral content in enamel, erosion is manifested initially as partial surface demineralisation followed by softening and increased roughness. While, dentine composed of less mineral and more organic material, and mineral loss initially starts between the peri- and intertubular dentine, followed by loss of

peritubular dentine and widening of the dentinal tubules and finally intertubular dentine demineralisation and exposure of the organic matrix (Meurman et al., 1991, Kinney et al., 1996, Schlueter et al., 2011). Due to these histological differences, methods suitable for assessment of enamel are not necessarily suitable for dentine.

As a general approach, profilometry was found to be the most commonly applied quantitative method to for both enamel and dentine assessment in *in vitro*, *in situ* and *in vivo* models, followed by surface hardness methods to evaluate enamel and microradiography for dentine. While, the most commonly applied qualitative method to study erosion in both tissues was scanning electron microscopy (SEM).

1.2.2.5.1 Scanning Electron Microscopy (SEM):

Scanning Electron Microscopy qualitatively estimates surface alterations after erosive attacks. SEM imaging can be performed on both polished and unpolished after gold or carbon coating. SEM investigations have been applied to evaluate eroded enamel and dentine surfaces after acid attacks (Oshiro et al., 2007, Poggio et al., 2013). It was also applied to evaluate the salivary acquired pellicle and its efficacy to protect underlying enamel surface from acidic dissolution (Meurman and Frank, 1991b, Hannig, 2002, Hannig et al., 2004), or to demonstrate surface deposits precipitates resulting from mineral deposition with different remineralising agents (Poggio et al., 2013). However, SEM technique

does not provide as detailed information about surface alterations of eroded samples as energy dispersive X-ray spectroscopy that could be coupled with SEM to analyse elemental distribution in the top few micrometres of a sample surface. This is achieved by an electron beam that hits the surface and leads to excitement of surface atoms resulting in X-rays emission. This process may provide information about element distribution, such as calcium, phosphate and carbon with a concentration of about 1 wt. %.

1.2.2.5.2 Surface Profilometry:

A surface profilometer (surfometer) can determine both the irreversible loss of dental hard tissue and surface roughness. It quantifies dental tissue loss in relation to reference area (non-treated) (Attin, 2006, Field et al., 2010, Schlueter et al., 2011). Profilometry is able to generate two- or three-dimensional profiles of the scanned specimen surface. Either a laser beam or a contact stylus (metal or diamond) can be used to scan specimens. A complete map of the specimen surface can be generated with the scan (Attin, 2006). However, laser scanning is preferred over the stylus scanning for erosion samples as the outermost layer of the lesion is very fragile and easy to damage by the stylus movement (Ren et al., 2009) which may lead to overestimation of early erosion lesion depth. Furthermore, the laser beam generates higher resolution scans compared to the contact stylus. Profilometers are able to produce precise measurements with low variations with either irregular or polished surfaces (Attin, 2006). However, flat

specimens are preferred for maximum sensitivity and accuracy (Hara and Zero, 2008). To calculate differences in height (thickness loss) between treated and untreated surfaces, two scans are obtained with a common reference point. Differences between these two scans are determined using a specific software (Venables et al., 2005, Attin, 2006). In this case, correct repositioning of the sample in the profilometer for the two readings is extremely important. Profilometry method is applicable for both direct testing of samples or indirect measurements of intra-oral erosion lesion via replicas.

1.2.2.5.3 Confocal Laser Scanning Microscopy:

CLSM is non-destructive microscopic tomography technique mainly developed for cell biology that allows exploration of cells and their internal structures. This technique is capable of generating high-resolution images, allowing 3D reconstructions of optical scan layers in specimens. In translucent objects such as teeth, it potentially provides insight into internal structure of the enamel lesions and allows visualization of subsurface microstructure that are not otherwise obtainable with other imaging tools. The principle behind it is based on using confocal apertures to eliminate stray light from out-of-focus planes. Images are obtained by scanning the region of interest with a spot-size light source (laser) then collecting the light reflected from the in-focus plane. Tomographic features allow in depth imaging of a series of consecutive images in either *x-y* or *z* optical planes. The CLSM technique was first applied in dentistry by Watson (Watson,

1990a, Watson, 1990b, Watson, 1991, Watson, 1994, Watson, 1997, Watson et al., 2008, Watson et al., 2014) to visualize unsectioned tooth restoration interfaces. It is used in reflection mode to produce images of enamel down to about 100μm from subsurface regions (Duschner, 1995, Øgaard et al., 1996). However, new generation microscopes allow deeper penetration of around 150–200μm below the surface (White et al., 2002, Attin, 2006).

This imaging technique excludes artefacts induced by sample preparation (drying, cutting, and coating) necessary for other techniques as SEM and can assess different types of tooth samples including unpolished and wet. However, polished tooth samples are mostly used for CLSM. The lateral and axial resolution of the confocal microscope is the function of the laser light wavelength and the numerical aperture of the objective lens.

CLSM operates in the following manner: illumination, achieved by a gas type monochromatic laser (e.g. Ar/Kr or He/Ar) which is focused within a fluorescent specimen into a small focal volume by an objective lens. Specific wavelengths of the laser beam can be filtered (usually 488 nm) to allow laser focusing on the focal plane. The emitted fluorescent light in combination with some reflected laser light is then recollected by a detector and objective lenses. Computer software is used to combine images from a sequence of focal planes to generate 2D or 3D images. The focal plane of illumination is equal to the focal plane of detection, which makes them confocal.

For dental erosion studies, CLSM allows histotomographic qualitative assessment of mineral dissolution and hard tissue loss, as light reflection and

scattering in tooth samples are greatly influenced by micro-histological changes within the sample (Zentner and Duschner, 1996, Duschner et al., 2000, Lussi and Hellwig, 2001, Attin, 2006). However, information about the degree of demineralisation is limited by this technique. Thus, to obtain a clearer view, CLSM is often combined with other methods as analysis of mineral loss, surface microhardness, or others.

Although CLSM is mostly applied to obtain qualitative information, quantitative values of erosion softening depth and tissue loss can also be obtained. However, its' application in dentine erosion studies warrants further investigation (Heurich et al., 2010, Schlueter et al., 2011).

1.2.2.5.4 Optical Coherence Tomography (OCT):

Optical coherence tomography (OCT) is a valuable non-invasive optical technique that is considered one of the most promising methods of assessing the surface characteristics of enamel *in vitro* and *in vivo* (Wilder-Smith et al., 2009, Machoy et al., 2017). It is a unique development in relation to X-ray dependant diagnostics exposing patients to unnecessary radiation. OCT is suitable for intraoral scans of both hard tissue (enamel, dentine) (Hsieh et al., 2013, Chew et al., 2014, Lee et al., 2016) and soft tissues (gingival margin, periodontal pockets and attachments) (Otis et al., 2000, Chun-Te Ko et al., 2005, Fernandes et al., 2016, Machoy et al., 2017).

The OCT method uses near-infrared light to generate subsurface cross-sectional images of enamel samples by measuring backscattered light magnitude and echo time delay (Huang et al., 1991, Wilder-Smith et al., 2009, Schlueter et al., 2011, Lee et al., 2016, Machoy et al., 2017). Moreover, information about enamel thickness is provided by the generated images. Imaging of depths up to 3 mm can be obtained, which is ideally suitable for assessing the whole enamel thickness including DEJ. The resulting images (B-scans) are two-dimensional (2D) in the (X-Z) axes. OCT generates multiple sequential B-scans in the Y-axis creating a stack of images that can be reconstructed into a three-dimensional (3D) image of the sample (Al Azri et al., 2016, Machoy et al., 2017). OCT technique is comparable to ultrasonography (USG). As OCT depends on the faster light than sound transmission characteristic for USG, it generates much higher image resolution. However, it allows limited tissue penetration compared to USG (2 mm vs 10 mm) respectively (Machoy et al., 2017).

In dentistry, OCT has been applied since 1998 (Colston et al., 1998) in caries research (Fried et al., 2002, Chun-Te Ko et al., 2005, Manesh et al., 2009, Kang et al., 2010, Machoy et al., 2017), optical properties of enamel prism and dentinal tubules (Hariri et al., 2012, Machoy et al., 2017), enamel erosion (Park et al., 2013, Machoy et al., 2017), demineralisation and remineralisation of enamel and dentine (Kang et al., 2012, Chew et al., 2014, Machoy et al., 2017), detection of enamel defects and cracks (Nakajima et al., 2012, Lee et al., 2016, Machoy et al., 2017), assessment of restorations adaptation and leakage, evaluation of prosthetic work including structural defects and microleakage without the need to remove the restoration (Sinescu et al., 2008, Sumi et al., 2011, Machoy et al.,

2017), evaluation of the salivary pellicle (Baek et al., 2009, Machoy et al., 2017), and application in maxillofacial surgery to separate normal and dysplastic lesion structures (Adegun et al., 2012, Adegun et al., 2013, Machoy et al., 2017).

In erosion, demineralised enamel is more porous compared to sound enamel, resulting in change to its optical properties, and hence reflected light intensity change showing as qualitative results which can also be quantified (Popescu et al., 2008, Huysmans et al., 2011). Quantitative measurements of the backscattered light intensity at the scanned surface, provides information about surface porosity and the depth of penetration of the scanned area, penetration is reduced when scattering occurs. Recent years have witnessed rapid development in OCT in terms of image resolution enhancement, image contrast enhancement, image acquisition time reduction, and tissue penetration (Huysmans et al., 2011). These developments have made OCT one of the most powerful diagnostic tools in experimental and clinical fields.

1.2.2.5.5 X-ray Microcomputed Tomography (Micro-CT):

The early 1970s witnessed the development of x-ray computed tomography (CT) imaging. Since then, the diagnostic tool has advanced and has been applied extensively in medicine and later on in dentistry. X-ray computed tomography (CT) is a non-destructive X-ray method producing images of thin slices with constant thickness. Images are captured from multiple angles and then reconstructed into a 3D maps with spatial distributions corresponding to different

attenuating material densities within the scanned object (Hounsfield, 1973, Swain and Xue, 2009). In contrast, conventional radiography is limited to producing 2D images of the attenuated material in the X-ray path. X-ray micro-computed tomography (Micro-CT or μCT) was introduced in the 1980s with a much higher resolution. They usually produce images composed of voxels (volume elements) in the range of 5-50 μm (Kuhn et al., 1990).

Micro-CT is designed for mineralized tissue examination (bone, teeth, and ceramics). However, its application can extend to soft tissues. And since the procedure is non-destructive, repeated sample examination is possible. The use of micro-CT in conjunction with finite element Analysis (FEA) has become of great interest in recent years. Where micro-CT scans multi-layered and small objects (bone, teeth, dental implants and restorations) to generate a more precise model replica to be used for FEA meshing. Micro-CT of a tooth generates a segmented model into enamel, dentine, and pulp based on different grey levels related to different mineralization level of structure components. After that, unique material properties are assigned to each component segment together with boundary conditions to simulate stress/strain in the tested structure (Magne, 2007, Swain and Xue, 2009).

Micro-CT could be also applied for assessment of structural loss after degradation, precisely locating material loss (Hollister et al., 2005). This gives the advantage of characterizing mineral densities in sound enamel and dentine and tooth tissue loss related to demineralisation with dental caries and erosion (Swain and Xue, 2009, Hamba et al., 2011).

1.2.3 Stress and Strain in Teeth:

Biomechanical studies in medical material sciences are critical to understand how living tissues interact with external forces in their environment. These studies require implementation of particular research techniques. Strain is defined as the geometric deformation within the material under loading. The relationship between stress (intervals of loading) and strain (the amount of deformation) is unique for each material and reveal many properties of the material. Strain is expressed as the ratio between the length change and original length, and is calculated according to the following equation:

$$\varepsilon = \frac{L - L_{\circ}}{L_{\circ}} = \frac{\Delta L}{L_{\circ}}$$

Where $L_{\circ}$: original length; L: current length; ΔL: length change.

According to above equations, compressive strain and tensile strain are negative and positive values, respectively (de Medeiros et al., 2019, Chun et al., 2014).

Different methodologies have been recruited to assess stresses and record strain in teeth but no single technique could meet all the requirements to display the involved physiological interactions. Development of computer systems has enabled complex analytical systems as finite element analysis (FEA). However, traditional techniques including strain gauge measurements and photoelastic analysis are still applied.(Karl et al., 2009).

In vitro investigations include either destructive or non-destructive tests. Destructive tests include load-to-failure tests. While, some common non-destructive methodologies include strain gauge method, photoelastic stress

analysis. High accuracy, whole-field strain measurements can be also achieved by optical techniques such as digital holography, Electronic Speckle Pattern Interferometry (ESPI), and Digital Image Correlation (DIC). Optical techniques allow contact-free measurements with special advantage in cases of specimen fabrication challenges, as the necessity of maintaining hydration or geometric limitations of available tissue samples. While traditional “load-point” experiments provide an insight into surface strain and reveal some biomechanical issues, a complex modelling tool is required to assess the stress distribution within the complexity of a tooth structure under load. The most commonly used is finite element analysis (FEA) method. The use of a combination of one or two methods is important to validate results and provides the potential for major advances in this area.

1.2.4 Strain Measuring Techniques:

1.2.4.1 Strain Gauges:

The gold standard of material strain and stress analysis is the electric resistance wire strain gauges. Gauges have been used for many decades in dental research (Meredith and Setchell, 1997, Jantarat et al., 2001, Soares et al., 2008a, Karl et al., 2009, Yang et al., 2011, Valdivia et al., 2012, Veríssimo et al., 2014, Machado et al., 2017, Vianna et al., 2018, Robinson et al., 2019, Roperto et al., 2019). The gauge consists of a coil of conducting material integrated on a

plastic backing film. The gauge is attached to the surface of the object by means of an adhesive. The gauge measures the electrical resistance of the coil conductor. This merely depends on its cross-sectional area which is altered under tensile or compressive stresses, resulting in a different electric resistance. This current is transferred and measured using a Wheatstone bridge configuration within the strain measurement amplifier. Data gained from strain gauges are quantitative and can be used as a basis for other methodologies calculation and validation. Strain gauges have the disadvantage of having a small size which is considered a common source of error limiting strain reading to a precise area which may not cover the region of interest. Additionally, strain gauge performs measurements of external surface deformation, without reflecting internal surface deformations. Moreover, strain gauge signals are affected by temperature changes, therefore, the temperature sequence should be controlled and monitored (Karl et al., 2009, Machado et al., 2017).

1.2.4.2 Electronic Speckle Pattern Interferometry (ESPI):

(Electronic Speckle Pattern Interferometry) is a branch of coherent optics. It is a well-established precise optical technique that relies on the properties of laser beams. ESPI is often used to study displacement (dislocation) distribution associated with the superficial deformation of an object in a mechanical system due to stresses, loads or vibrations with no direct contact (Vannoni and Molesini, 2005, Monteiro et al., 2010). Displacement measurement is based on the

alteration of the optical path that light follows. Alteration in optical path is due to the mechanical roughness in the surface (Campos et al., 2014). Classical interferometry includes a number of developments used in a wide range of industrial applications, as holography, moiré and speckle techniques (Creath et al., 1993).

Speckle interferometry takes advantage of the behaviour of rough surfaces as it relies on the changes in the specimen surface to produce the distinctive speckle patterns (Creath et al., 1993, Huntley, 1998, Saleem et al., 2003). When a laser beam illuminates a non-polished surface, the reflected light on a screen appears like a random pattern of bright and dark spots “speckle”. This is a result of the coherence of the laser source. (Vannoni and Molesini, 2005).

Interferometry is a subject that is known with phase differences (Moore and Tyrer, 1995, Huntley, 1998, Saleem et al., 2003). These phase differences are typically generated from variation in intensity of coherent light sources such as lasers detected by devices such as charge-coupled device (CCD) cameras. Deformation of the material is translated as changes in the observed speckle pattern due to the superposition of two beams of light and is used to measure the displacements and strains at its surface.

Phase shifting uniquely determines the phase measurement. Phase shifting is introduced between the interfering beams, enabling phase extraction by measuring fringes. Phase shifting could be introduced as a function of time (temporal phase shifting) or of position in the image (spatial phase shifting). Temporal phase shifting is achieved by a mirror controlled by a piezoelectric

translator (PZT). Loading the sample results in alteration of the path and phase differences. Therefore, this technique allows measurement of the surface deformation related phase changes in relation to the reference state. On the other hand, for spatial phase shifting, a single distribution is sampled at discrete points in the image (Creath et al., 1993, Campos et al., 2014).

There are several advantages of this technique that favours its use for measuring displacement and strain distributions in teeth. The method is non-contact and does not require modification of the specimen surface by preparation or grating. Also, far higher strains can be detected than was previously accessible (Saleem et al., 2003). Some concerns in the application of interferometric techniques include the complex surface preparation required to achieve proper reflection. Hydrated sample surface interferes with laser reflection and hence phase map formation (Niu et al., 2000, Zhang and Arola, 2004). This poses a challenge when working with biological tissues that require evaluation to be conducted without dehydration. Although the concept is quite simple, additional concerns as sensitivity to vibration and the need for photographic film processing make it difficult to develop applications outside the laboratories. (Rastogi, 1993, Vannoni and Molesini, 2005, Erf, 2012).

1.2.4.2.1 ESPI Configurations- Out of Plane Displacement Measurement:

Out-of-plane displacement is displacement along the viewing direction. To obtain out-of-plane measurement, a “reference beam”; an expanded beam

derived from the laser beam, is added to the image of the object formed on the video camera through a beam splitter. Another beam “object beam” is directed towards the object to form a “speckle” viewed by the camera. The amplitude of the light at any point in the image is the sum of the light from both the object “object beam” and the “reference beam”. The distance travelled by the object beam changes as the object moves in the direction of viewing and therefore the amplitude of the combined beams changes. Subtracting the second speckle pattern “deformed” from the first “undeformed” generates fringes that represent contours of displacement (**Figure 1.1**).

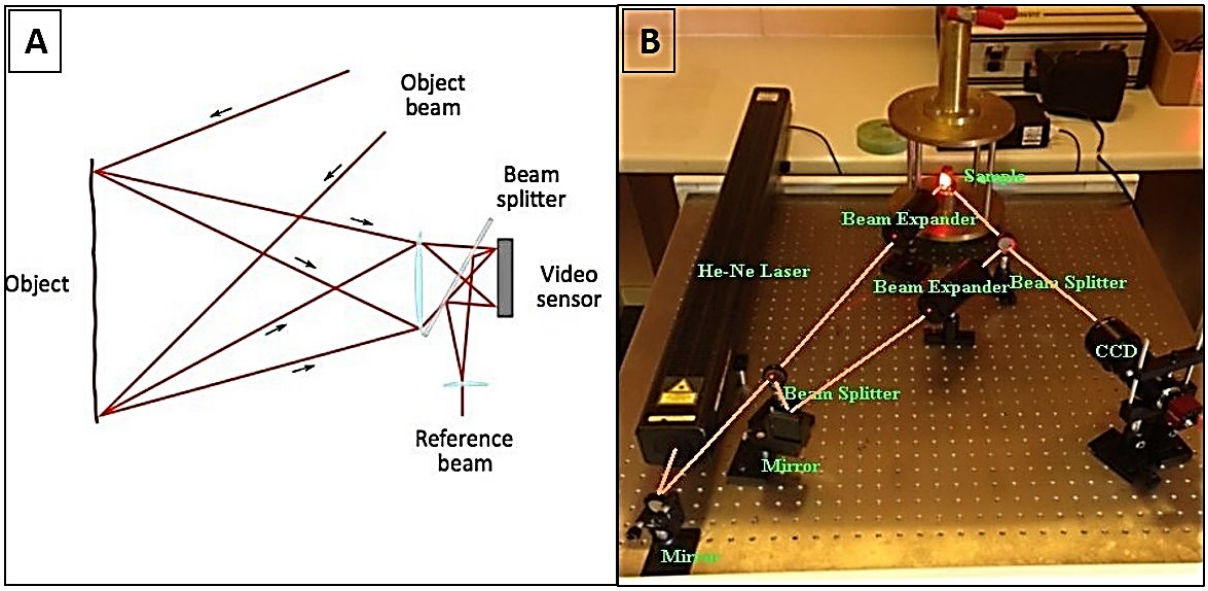

Figure 1.1: ESPI set-up for out-of-plane displacement measurement. (A) Diagram, (B) author’s set-up.

1.2.4.2.2 ESPI Configurations- In-plane Displacement Measurement:

In-plane movement of an object is movement in the vertical direction. To study in-plane movements of a physical system, the object surface is illuminated by two

laser beams expanded from the diode with a beam splitter. The laser beams are mutually coherent with equivalent states of polarization. Plane mirrors are used to reflect the two beams on the object surface at two opposite but equal angles ϑ to the normal forming a speckled image (**Figure 1.2**).

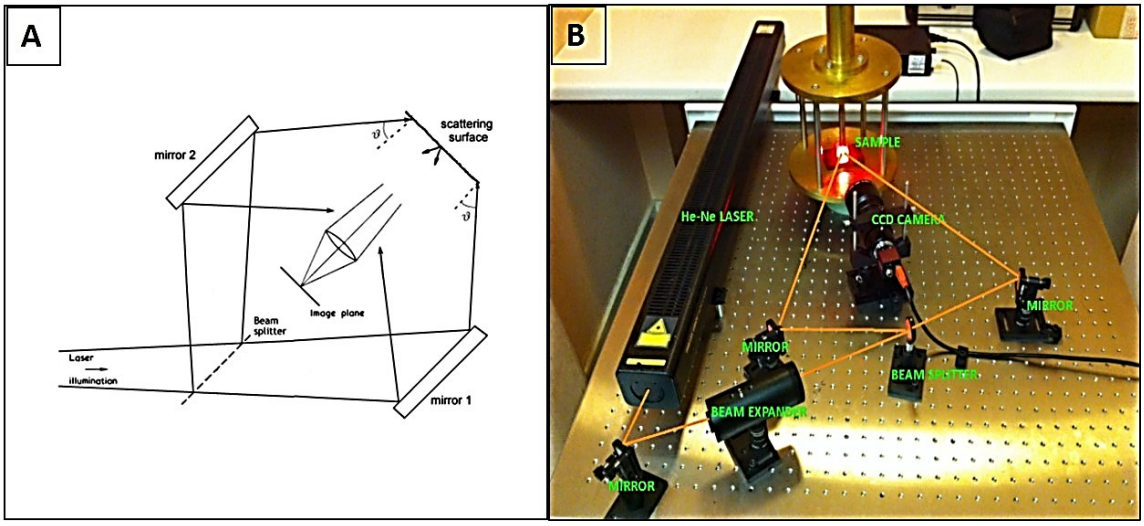

Figure 1.2: ESPI set-up for in-plane displacement measurement, (A) Diagram (Courtesy of Vannoni and Molesini 2005), (B) author's set-up.

1.2.4.2.3 ESPI Data Processing:

For both in-plane and out-of-plane arrangements, the image of the undeformed test surface is captured and stored in electronic memory. A fringe pattern can then be obtained by subtracting "undeformed" image from subsequent live images of the deforming surface, mapping contours of phase difference

between wavefronts (**Figure 1.3**) (Moore and Tyrer, 1996, Vannoni and Molesini, 2005).

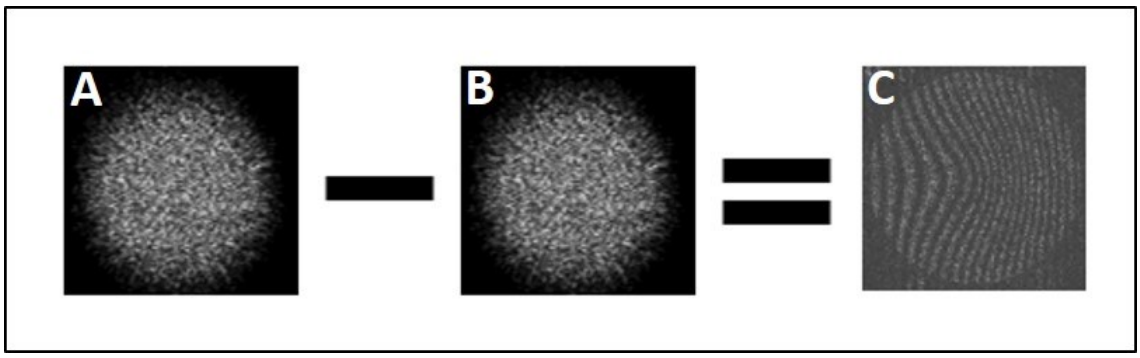

Figure 1.3: Subtraction of the image of the illuminated test surface of the deformed sample (with loading) (B), from the undeformed (before loading) (A) to produce the Interferogram fringe phase map (C).

Once the speckle interferograms are obtained, qualitative and quantitative interpretation can be made. The data consists of the location of the fringes and their sequential ordering number. Numbering can proceed from left to right and fringe location can be associated with fringe centres. Recently, computer softwares were developed to process photos consisting the central figure of the structure under investigation. The result is a file with (*x, y, z*) format on each line, where *x, y* represent the spatial coordinates of the sampled points, while, *z* represents the displacement, given by the fringe number multiplied by the scaling factor (for example, $\lambda/2$) (Vannoni and Molesini, 2004, Vannoni and Molesini, 2005). Finally, we can write software to read this file and fit the data to an appropriate function. It includes a colour scale that serves to analyse the results, with each colour corresponding to a certain percentage of strain obtained during loading (Tanasic et al., 2012).

1.2.4.3 Digital Image Correlation (DIC):

Digital Image Correlation or currently called white light speckle photography is an innovative non-contact optical technique for measuring strain and displacement, with common application in experimental mechanics. However, its application in dentistry is rather limited. In dentistry, DIC is usually focused on strain with restorative material shrinkage and *in vitro* implant, prostheses, and supporting bone loading (Kovacic et al., 2019, Mitrović et al., 2019). The DIC method originated at the University of South Carolina in the early 1980s and has been widely used in displacement, strain and flow measurements in recent years (MORITA et al., 2007, Li et al., 2009, Tiossi et al., 2012, Li et al., 2013, Tanasic, 2017). The optical process in DIC to obtain correlation between signals is replaced by digital procedures. Traditional optical techniques require numerical functions to obtain phases resulting in the process of phase unwrapping. What characterizes DIC is that the process of fringe unwrapping is bypassed as displacements are directly obtained by point movement paths (Sciammarella and Sciammarella, 2012). DIC is relatively simple to use, accurate, cost effective, and less technique sensitive compared to other techniques such as speckle interferometry with the potential to be applied outside of the lab (McCormick and Lord, 2010). DIC has been commonly used to document plastic deformation of materials as it is capable of quantifying large strains (>50%) (Wattrisse et al., 2001, Zhang and Arola, 2004). Yet, application of DIC for evaluation of biological materials is rather limited.

DIC developed as a technique to measure displacement using artificially generated random patterns simulating actual speckles (Peters and Ranson, 1982, Sutton et al., 1988, Sciammarella and Sciammarella, 2012). One way to obtain a random surface speckle pattern that generates a good signal to noise ratio is to have either black spots sprayed on a light/white background, or white spots on a dark/black background. Compared to speckle photography carried out with actual speckles, artificial speckles do not suffer from problems experienced by actual speckles due to the motion of the surfaces (Sciammarella and Sciammarella, 2012). Also, good illumination is always required, for that a white light source can provide the illumination.

Images can be obtained through a variety of sources including conventional CCD cameras, digital cameras, macroscopes, or microscopes (McCormick and Lord, 2010). The procedure to decode displacement is by comparing information of two recorded images of the specimen, one recorded before deformation and another after deformation. By that, two speckle images were recorded and saved in the memory of computer software. A small subset is extracted from these two images. The subset is then enlarged to show the distribution of grey levels (Sciammarella and Sciammarella, 2012, Zhang and Arola, 2004). Each point on the surface is unique and the distribution in light intensity can be described by the grayscale matrix $F(x,y)$. After deformation of the object, each point on the surface (x,y) is assumed to exist at a new location (x^*,y^*) (**Figure 1.4**). By finding the position of the light intensity distribution $F^*(x^*,y^*)$ that most closely resembles the original distribution $F(x,y)$, the in-plane surface displacement can be determined

(Zhang and Arola, 2004). The position with maximum correlation coefficient (C) is calculated to obtain the location of $F^*(x^*,y^*)$ according to the following equation

$$C = \frac{\langle FF^* \rangle - \langle F \rangle \langle F^* \rangle}{[\langle (F-\langle F \rangle)^2 \rangle \langle (F^*-\langle F^* \rangle)^2 \rangle]^{1/2}}$$

Where F and F* represent the grayscale matrices of the subset in the undeformed image at position (x,y) and (x^*,y^*) in the deformed image, respectively. The symbol ‹ & in the Equation indicates the mean value of the elements in the matrix.

The digital cross-correlation between the two subsets is computed and a correlation peak is produced. The amount and direction of local displacement is given from the position of the peak in the sub-set and is measured to the accuracy of the pixel. The height of the peak indicates the degree of correlation. After cross-correlation normalization to the value of 1, values of the peak near 1 will indicate a good correlation. Lower values indicate correlation degradation (Zhang and Arola, 2004, Sciammarella and Sciammarella, 2012).

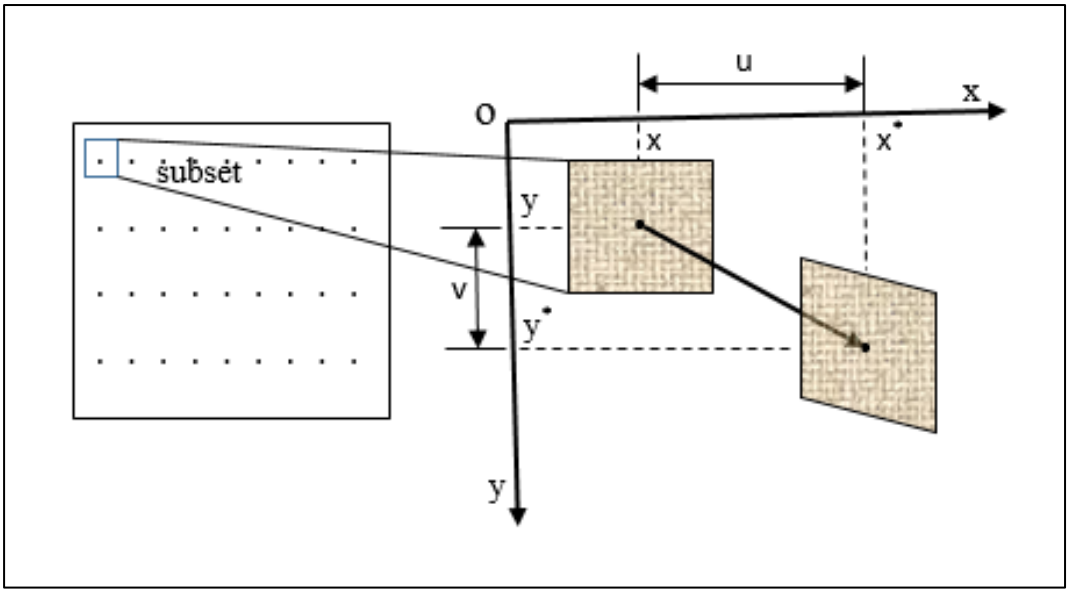

Figure 1.4: Object surface subset point position change with deformation.

Currently, subsequent analysis can be done with specialist software which derives the strain on the surface from displacement field collectives, providing a full-field strain measurement (Li et al., 2009, Tiossi et al., 2012).

As DIC is based on a subset of pixels, the spatial resolution of the obtained results is determined by the ratio of the pixels subset size to the overall size of the region under observation. Conventional DIC only analyses the in-plane displacements. However, using two or more cameras provides information relevant for the extraction of full three-dimensional displacement fields (Roux et al., 2009, Sutton et al., 2000). The out-of-plane displacement can exist but should be limited. This could be established by carefully maximizing the distance between the camera lens and the sample without sacrificing image magnification which affects measurement resolution.

1.2.4.4 Finite Element Analysis (FEA):

Stress- strain analysis of dental structures has gained increasing interest in dentistry in recent years. The main objective of these analyses is to determine weaknesses in the studied structures and work on the improvement of their mechanical strength (Srirekha and Bashetty, 2010). Stress investigations of biological structures offer an insight into their biomechanical properties and can predict their behaviour under loading (Merdji et al., 2013). There are mainly three methods to perform stress analysis: analytical, experimental, and computational (numerical) (Srirekha and Bashetty, 2010, Merdji et al., 2013). Analytical methods are not available for complex dental structures. While, experimental approaches are still widely used where samples are purposely prepared and definitive but these are considered expensive, highly dispersive and time consuming (Ausiello et al., 2001). The numerical method; with the increase in computational power, helps to simulate with a great accuracy the functioning of biological structures. The primary and most applicable computational method for stress analysis today is the finite element analysis (FEA). FEA is a powerful numerical research tool to understand the mechanical behaviour of materials. It provides an insight into the complex mechanical structure of bodies affected by stress fields which is difficult to accomplish otherwise (Ausiello et al., 2001, Romeed et al., 2006, Karl et al., 2009, Merdji et al., 2013, Zeola et al., 2015). FEA has been long used in engineering and industry since the 1960s (Turner, 1956, Zienkiewicz et al., 1977, Rao, 1986, Ameen, 2005, Merdji et al., 2013). It was first developed to solve structural problems in the aerospace industry (Karl et al., 2009, Srirekha and

Bashetty, 2010). Subsequently it has been applied in medical and dental research (Meroueh, 1987, Siegele and Soltesz, 1989, Karl et al., 2009).

In dentistry, the application of FEA is rather recent. The first article on the subject dates back to 1973 and was published by Farah et al. (Farah and Craig, 1975). FEA was mainly focused on studying load transfer between dental implants, their supporting tissues and prostheses (William et al., 1990, DeTolla et al., 2000, Geng et al., 2001, Akça et al., 2002, Karl et al., 2009), and to study strain in teeth enamel, dentine, and related restorations (Thresher and Saito, 1973, Yettram et al., 1976, Magne and Belser, 2002, Palamara et al., 2002, Lertchirakarn et al., 2003, Magne and Tan, 2008, Magne and Oganesyan, 2009). The application of this technique is still relatively small mainly due to (i) the difficulty associated with the modelling of different shapes related to the dental structure to be analysed, (ii) the difficulty in obtaining the mechanical properties and dynamics of the constituent materials of the involved oral structures: enamel, dentine, cementum, pulp, etc., and (iii) the difficulty to predict failure related to complex geometries made of multiple materials (Merdji et al., 2013). Furthermore, there is a complexity associated with an expert running the software. The mathematical description of the structure geometry, loading configuration, material properties, external and internal boundary conditions may also be complex. On the other hand, FEA offers several advantages when compared to laboratory experimental testing. The simulation does not require involvement of human material, the tested variables can be easily changed, and the procedure is highly standardized (Srirekha and Bashetty, 2010).

FEA can minimize the need for experimental testing but cannot replace it. Nowadays, the experimental-numerical method combinations are considered the most comprehensive investigations in restorative dentistry (Tantbirojn et al., 2004, Magne, 2007). The experimental process can be digitally simulated and be available for observation in virtual prototyping with the convenience to change the shape or material properties to obtain the new results (Merdji et al., 2013).

The basic concept of this numerical method is to divide a model of the body of interest, involving complicated geometries for which no simple analytical solution can be applied, into a finite number of elements or small areas where individual deformation (stress, strain, or displacement) can be calculated rather than for the whole large structure. Simultaneously solving deformation of all small elements results in assessment of the deformation of the structure as a whole (DeTolla et al., 2000, Geng et al., 2001, Magne and Belser, 2002, Karl et al., 2009, Magne and Oganesyan, 2009). In contrast to FEA, strain gauges present a single point measurement that may miss critical details and cannot demonstrate strain gradients in anisotropic non-homogenous structures used in biomechanics. Also, the two-dimensional patterns of digital image correlation and electronic speckle pattern interferometry provide only simple in-plane or out-of-plane surface deformation measurements and are extremely sensitive to object movement (Tyson, 2000, Karl et al., 2009).

FEA is usually represented as two- or three- dimensional models. The choice between using 2D or 3D FEA used to investigate complex geometries can only be made with understanding of the advantages and limitations of both approaches. Although two-dimensional FEA is relatively simple and has been

extensively applied in dental research to achieve good element and simulation quality (Magne and Douglas, 1999, Romeed et al., 2006), numerical results of dental structures obtained by this model suffer some shortcomings compared to three dimensional models. As human teeth are irregular in shape and lack symmetry, they cannot be accurately represented by 2D volumes (Rees, 1998, Romeed et al., 2006, Srirekha and Bashetty, 2010). In contrast, new generation 3D models generate optical realistic analysis with detailed anatomical features and computational process. However, older versions of 3D FEA models suffered some disadvantages. They presented coarser meshes that could not represent thin layers as at tooth restoration interfaces, or fine details as preparation margins (Korioth and Versluis, 1997, Magne and Douglas, 1999, Romeed et al., 2006). The application of micro-scale computed tomography scanning technique is one of the new advances in FEA model acquisition that solved the problem and allowed accurate anatomical details of dental structures; such as human teeth and jaws, to be obtained (Rüegsegger et al., 1996, Shimizu et al., 2005, Magne, 2007, Srirekha and Bashetty, 2010).

Properties of the materials involved in the modelled structure including Young's modulus, yield strength, and Poisson's ratio together with the boundary conditions of the virtual object define how an object reacts to certain loading conditions and may greatly influence the resulting stress and strain distributions (DeTolla et al., 2000, Geng et al., 2001, Al-Sukhun et al., 2007, Karl et al., 2009). Material properties can be either isotropic (same properties), or anisotropic (different properties) (Motta et al., 2006, Srirekha and Bashetty, 2010) and FEA can reflect each. All real-life materials are anisotropic, but are simplified into

isotropic or orthotropic (different properties along 3 axes, namely- x, y, and z) (Srirekha and Bashetty, 2010).

Many studies have evaluated the comparability of strain gauge measurements and finite element analysis. Good correlations have been reported between strain gauge and numerical analysis for displacement measurements on dental structures (Al-Sukhun et al., 2007). On the other hand, differences (Akça et al., 2002, Srirekha and Bashetty, 2010) or non-compliance (Lertchirakarn et al., 2003, Srirekha and Bashetty, 2010) between both methods were found by other researchers. However, partial agreement was found by others between the two methodologies (İplikçioğlu et al., 2003, Srirekha and Bashetty, 2010).

1.3 Aim of the study:

Based on the aforementioned literature, caries and acid demineralisation cause tooth tissue loss. Loss of tooth structure within the coronal aspect of the tooth can alter stress distribution within a tooth. It has been well demonstrated that the fracture resistance of the restored teeth is lower than sound teeth. The combined effect of the quantity of the remaining coronal tooth structure together with its dimension recommendations and the most appropriate restoration design and restorative material still need further evaluation. Therefore, the main aim of this research was to map and evaluate tooth strain in teeth with different amounts and areas of remaining tooth structure and tooth surface loss created by dental preparation (simulating caries created lesions) or soft drink demineralisation

(simulating external acid erosion lesions), before and after restoration utilising different techniques: strain gauges (SG), the surface displacement field measured using Digital Image Correlation (DIC), electronic speckle pattern interferometry (ESPI), and finite element analysis (FEA). In addition, testing teeth affected by erosion required testing and verifying different acid demineralisation protocols.

CHAPTER 2

Development of Erosion Methodology

2.1 Introduction- Chapter 2:

Dental literature is replete with studies assessing dental erosion. Studies have covered many aspects, some of them are included in **Table 2**.

Table 2: Literature research topics covered in dental erosion

Research aspects covered	Reference
Understanding early enamel and dentine changes following acid erosion	(Lussi et al., 1993, Imfeld, 1996a, Amaechi and Higham, 2001a, Amaechi and Higham, 2001b, Barbour and Rees, 2004, Amaechi and Higham, 2005, Cheng et al., 2009b, Mann et al., 2014)
Understanding the process of erosion initiation and progression	(Tramini et al., 2000, West et al., 2000, Owens and Kitchens, 2007, Sauro et al., 2008, Thomas et al., 2008, Caneppele et al., 2012, Mylonas et al., 2018)
Erosion prevention	(Hannig, 2002, Cheaib and Lussi, 2011, Wang et al., 2011, Hara and Zero, 2014, Lussi and Hellwig, 2014, Moazzez et al., 2014)
The potential of different external agents on the remineralisation of early enamel erosion lesions	(Ten Cate and Featherstone, 1991, Rees et al., 2007, Lussi et al., 2008, Ten Cate et al., 2008, Lussi, 2009, Poggio et al., 2010, Turssi et al., 2011, Wegehaupt et al., 2012, de Alencar et al., 2014, Hornby et al., 2014, Soares et al., 2016, Cassimiro-Silva et al., 2016)
The potential of different external agents on the remineralisation of early dentine erosion lesions	(Sauro et al., 2011, Zhan et al., 2013, Niu et al., 2014, Poggio et al., 2014b, Toledano et al., 2014, Varanasi et al., 2014)
Imaging and detection techniques available for surface and subsurface lesion assessment	(Silverstone et al., 1975, Dowker et al., 2003, Cheng et al., 2009b, Field et al., 2010, Torres et al., 2010, Rakhmatullina et al., 2011, Schlueter et al., 2011, Poggio et al., 2013, Wang et al., 2014, Koshoji et al., 2015, Cassimiro-Silva et al., 2016)

To the author's knowledge, no previous studies showed interest in studying progressive erosive lesions and their effect on the surface, subsurface, and mechanical qualities of the remaining dental tissues including strain levels in response to loading. This chapter covers research methodology development including, tooth collection and mounting, tooth surface loss assessment using different acid immersion protocols and measurement techniques, and comparison of accelerated versus prolonged immersion protocols in the absence or presence of salivary pellicle to select the most clinically and microscopically suitable protocol to apply in the next experiments. The following text also includes documentation of the extended effect of accelerated erosion on surface loss to produce lesions with variable depths relevant to different clinical stages of erosion. Moreover, it includes a study of the remineralisation potential of five commercially available toothpastes on soft drink eroded dental tissues.

2.2 Human Teeth Collection:

Human molars and premolars were obtained as surgical waste removed as part of routine surgery from patients attending the Department of Oral Surgery at the Eastman Dental Hospital, Grays Inn Road, London, after obtaining written consents from all patients under the national health services research ethics committee (NHS REC) ethical approval no. 11LO/0939. Our NHS REC approved research is in full accordance with the World Medical Association Declaration of Helsinki. Individual plastic containers (Sterilin, UK) were filled with 70% ethanol

(GC) (Sigma-Aldrich Company Ltd. Dorset, England). Patient consent forms were supplied to the clinic (Appendix- A). Collected samples were immediately placed into the ethanol-filled container for a minimum of 48 hr at room temperature in order to minimize the potential risk of pathogenic organisms, e.g.: bacteria, viruses (HIV, Hep B & C) (Laurance-Young, 2012, Li et al., 2016, Calvo-Guirado et al., 2018). Signed informed patient consent forms were received with all collected sample containers. After 48 hr, samples were removed from the ethanol, brush cleaned under soapy water and debrided of any residual soft tissues using #12 scalpel blade and running water. The selection of teeth was based on regular crown anatomy, intact cusps, and lack of wear. Teeth were examined under a polarized light microscope (Olympus BX-50; Olympus America Inc., Centre Valley, Pa) at the magnification of 20x, for evidence of caries and cracks. Any unsuitable samples were disposed of by incineration. The selected samples were randomly allocated to individual containers in order to anonymize them. Samples were finally stored in their containers now filled with 0.2% thymol (BDH, UK) at 4°C to maintain enamel hydration (Jantarat et al., 2001, Palamara et al., 2002, Soares et al., 2008b, Cianconi et al., 2011, Ferla Jde et al., 2013, de Alencar et al., 2014, Poggio et al., 2014a, Santos-Filho et al., 2014, Al Azri et al., 2016) Teeth were vertically or horizontally mounted in clear epoxy resin (Specifix-20; Struers Ltd) as experimentally required. Hard copy consent forms were securely stored in a locked room.

2.3 Vertical and Horizontal Tooth Mounting:

Teeth were removed from the thymol solution, rinsed under soapy water and allowed to dry. For vertical mounting, each tooth was positioned in the centre of a (2.5 cm in height) nylon mounting mould using utility wax (Kemdent, Associated Dental Products Ltd., Purton Swindon, UK). Each root was positioned centrally with the long axis of the tooth aligned parallel to the mould walls (**Figure 2.1**/ a, b). The mould was then poured with epoxy resin used according to the manufacturer's instructions to a level 2.0 mm apical to the cementoenamel junction (CEJ) (Seow et al., 2015). The resin was allowed to set overnight then the mounting ring was opened (**Figure 2.1**/ c). The base of the resin block was machined with water-cooled silicon carbide discs (220-grit) (LaboPol-5; Struers, Copenhagen, Denmark) to expose some of the root structure at the bottom of the base.

For horizontal mounting, each tooth was positioned horizontally in the centre of the mounting mould with the either the buccal or lingual surfaces facing upwards. Special care was taken to completely seal the tooth crown surface facing downwards with silicone putty impression (Express™ STD, Firmer set, Vinyl polysiloxane impression material putty, 3M ESPE, St. Paul, MN, USA) to protect it from contact with mounting resin and preserve the surface if intended for future testing. Cold cure epoxy resin was poured in the mounting ring to cover the tooth and allowed to set (**Figure 2.2**). After demounting, utility wax was removed from the bottom of the sample by a steam cleaner (Triton SLA steam cleaner; BEGO, Bremen, Germany) and the resin blocks were mounted into a

low-speed water cooled microtome (Leica SP1600 saw, Leica Instruments GmbH, Germany) and split into 2 halves (buccal and lingual). For polished surface samples, where a flat enamel surface was required, samples were ground to expose an area measuring about 4mm x 3 mm and finished sequentially with water-cooled silicon carbide discs (500- and 1200-grit). Otherwise, the sound enamel surface was left unprepared. Subsequently, the specimens were cleansed in distilled water in an ultrasonicator (Branson 5800; Branson Ultrasonics, Danbury, CT, USA) for 10 minutes (min) to remove any residues of the polishing procedure and stored in artificial saliva until testing (de Alencar et al., 2014).

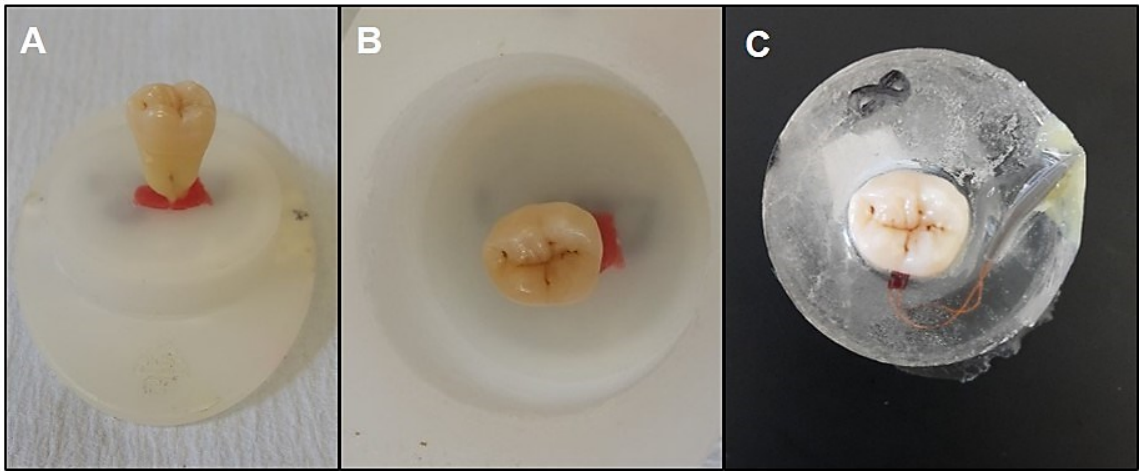

Figure 2.1: Vertical mounting steps. (A) Vertical alignment of tooth in the centre of the mould base, (B) assembly of mould body, and (C) after resin setting and opening of mould.

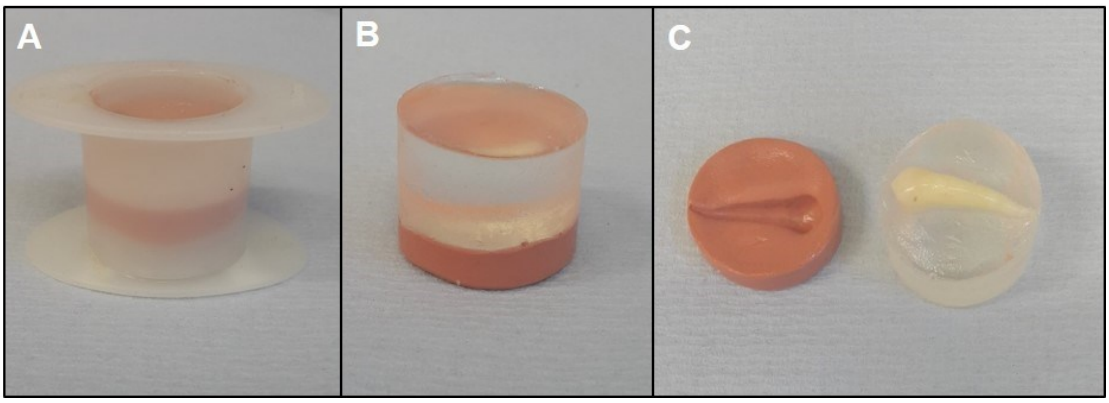

Figure 2.2: Horizontal mounting steps. (A) Horizontal alignment of a tooth over a layer of silicone putty at the mould base- buccal surface facing downwards, followed by resin, (B) assembly after setting and opening of mould, and (C) horizontally mounted tooth after removal of silicone base.

2.4 Artificial Saliva Preparation:

Artificial saliva was prepared in 1000 ml of water solution according to the following composition (g/L): (2.3 Methyl-p-hydroxybenzoate; 0.625 KCl; 0.166 $CaCl_2.2H_2O$; 1.040 $K_2HPO_4.3H_2O$; 0.326 KH_2PO_4; 0.059 $MgCl_2.6H_2O$; 10.00 sodium carboxymethylcellulose) (McKnight Hanes and Whitford, 1992) without sorbitol (Levine et al., 1987), and (Amaechi et al., 1999b, Ionta et al., 2014). All saliva components were powder form products from (Sigma-Aldrich Company Ltd. Dorset, England). Gradual addition of 1M HCL was used to adjust the pH of the artificial saliva to (6.75) using a bench-top pH meter (PH 212 HANNA Instruments).

2.5 Natural Saliva Collection:

The natural saliva collection was carried out daily by one individual. Collection was done early in the morning before any oral hygiene measures or food intake. The saliva donor was non-smoking, had a healthy periodontium with no evidence of any active gingival inflammation, recession or pathological pockets, and had a past caries history with existing fillings but no active new carious or erosion lesions. Salivary flow was stimulated by chewing paraffin wax (Ivoclar Vivadent AG, Schaan, Liechtenstein). Saliva was collected by expectoration for 5 min (Gürsoy et al., 2010, Jayaraj and Ganesan, 2015, Almståhl et al., 2018) and collected in 7 ml bijou containers, each filled in one expectoration. Containers were quickly sealed and retained inside an ice filled beaker in order to prevent the loss of carbon dioxide which would affect the pH of the saliva. Saliva containers were transported in an ice box then clarified by centrifugation (Centrifuge 5810 R; Eppendorf, Germany) at (4,000 rpm/4^{o}C/15 min) (Lussi et al., 2012a). Following centrifugation, the supernatant was filtered sterile using 1 ml per 0.22 µm PES syringe filter (TPP AG, Trasadingen, Switzerland) to remove viable microorganisms (Health and Services, 2004). The pH was then measured and recorded (average PH= 7.2). The final product was divided into 20 ml aliquots and stored immediately at -80^{o}C between experiments. Prior to experimental use, frozen clarified saliva was defrosted at room temperature 24 ±1 ºC (Hall et al., 1999, Amaechi and Higham, 2001a, Austin et al., 2016).

2.6 Sample Size Determination- Erosion Experiments:

The number of human tooth samples available for this study was highly dependent on the number and quality of the clinical material supply of extracted teeth, with the majority being unsuitable for use. For all experiments the sample size was determined after analysis of pilot study results to provide 80% power at the 5% level of significance and review of literature with relevant protocols. For erosion experiments, a range of sample size was considered satisfactory and employed by different relevant studies, ranging from n=5 to n=18 (Amaechi et al., 1999b, Ganss et al., 2000, Eisenburger et al., 2001a, Attin et al., 2003, Kato et al., 2010, White et al., 2010, Laurance-Young, 2012, Wang et al., 2014, Cassimiro-Silva et al., 2016). Ehlen et al. (2008) applied a similar protocol and showed a satisfactory sample size of n=8. Therefore, it appears that our sample size (n=8) agrees well with published work.

2.7 Experiment 1

Assessment of surface finish and saliva on enamel surface loss with variable demineralisation regimes.

2.7.1 Material and Methods- Experiment 1:

2.7.1.1 Sample Preparation:

48 enamel samples were prepared from the mid-coronal portion of the buccal and lingual surfaces of human third molars. 24 sound extracted 3rd molar teeth were collected, cleaned, stored and mounted horizontally in epoxy resin. All resin blocks were then marked and trimmed at 2 sides to create a right angle edge to allow sample reproducible positioning on the working table of the scanning machines where two glass slabs were fixed at right angle to act as a receptacle.

Samples were divided into 5 test groups of 8 samples each (n=40) and 1 control (n=8). The control group received no treatment and samples were stored in artificial saliva at all times. While, test groups were divided according to different combinations of surface treatment criteria including, the surface finish (Sound=S, Polished=P), erosion protocol applied (Accelerated=A, Prolonged=P), and type of saliva used (No Saliva=NS, Artificial Saliva=AS, Natural Salivary pellicle=SP). The test group had the following combinations: [sound enamel surface with an accelerated erosion protocol with no saliva (SANS), polished enamel surface with an accelerated erosion protocol with no saliva (PANS), polished enamel surface with an accelerated erosion protocol with artificial saliva (PAAS), polished enamel surface with an accelerated erosion protocol with natural salivary pellicle (PASP), and polished enamel surface with a prolonged erosion protocol with natural salivary pellicle (PPSP)]. The sound group received no surface preparation.

While, the polished group samples were ground flat and polished. Accelerated erosion protocol means continuous immersion in soft drink solution with or without alternation with any other solution, not following any relevant drink consumption pattern. It includes soft drink solution replacement every 5 hr. While, prolonged erosion protocol mimics the daily consumption pattern of heavy soft drink consumers for a whole year (von Fraunhofer and Rogers, 2004, Ehlen et al., 2008). All tested enamel protocols are summarised in **Table 3**.

Table 3: Enamel erosion protocols:

Group Name	Surface Finish	Erosion Protocol	Storage Medium
Control	Sound	-	Artificial saliva
SANS	Sound	Accelerated (continuous) 25 hr	-
PANS	Polished	Accelerated (continuous) 25 hr	-
PAAS	Polished	Accelerated (intermittent), 5 hr/day for 5 days➔ 25 hr	Artificial saliva
PASP	Polished	Accelerated (intermittent), 5 hr/day for 5 days➔ 25 hr	Natural saliva
PPSP	Polished	Prolonged, 5 cycles of 50 seconds (sec)/day➔ 250 sec/day for 12 months➔ 25 hr	Natural saliva/ artificial saliva

2.7.1.2 Demarcation of the Erosion Window:

The test surface was demarcated into one test area with two control (reference) areas by fixing 2 strips of adhesive cellulose based tape (Scotch®, 3M, UK) (Eisenburger et al., 2001a, Barbour et al., 2006, Lagerweij et al., 2006, White et al., 2010, Austin et al., 2016, O'Toole et al., 2016, Mullan et al., 2018, Mylonas et al., 2018) laid parallel to each other approximately 5 mm apart on tooth test surfaces (sound, polished) (**Figure 2.3**/ A), or covering half the sample (**Figure 2.3**/ B). A commercial resin; nail varnish (Kiko®, Milano), was used to seal by painting in 2 layers around the target erosion site (Larsen, 1973, Larsen, 2001, Kato and Buzalaf, 2012, Rakhmatullina et al., 2013, Souza et al., 2014), at the reference sides of convex enamel surfaces, and some studies applied both adhesive tape and varnish to ensure a seal rendering the surface acid resistant (**Figure 2.3**/ C, D). The erosion window measured about (5 mm x 5 mm). To create a sequential erosion step-like lesion on one sample, nail varnish was painted to protect each step from further erosion. Samples were left to dry for 1 hr then stored in normal saline solution (0.9% NaCl in water, Sigma-Aldrich GmbH, Steinheim, Germany) until testing. Following the acid exposure, the tape was removed and any adhesive left was removed by an ethanol wet cotton pellet (70% solution, Sigma-Aldrich Company Ltd. Dorset, England). While, the removal of the varnish layer was achieved by gentle rubbing with cotton wool dipped in acetone (natural ≥97%, Sigma-Aldrich Company Ltd. Dorset, England) (Rios et al., 2006, Moretto et al., 2010, Danelon et al., 2018).

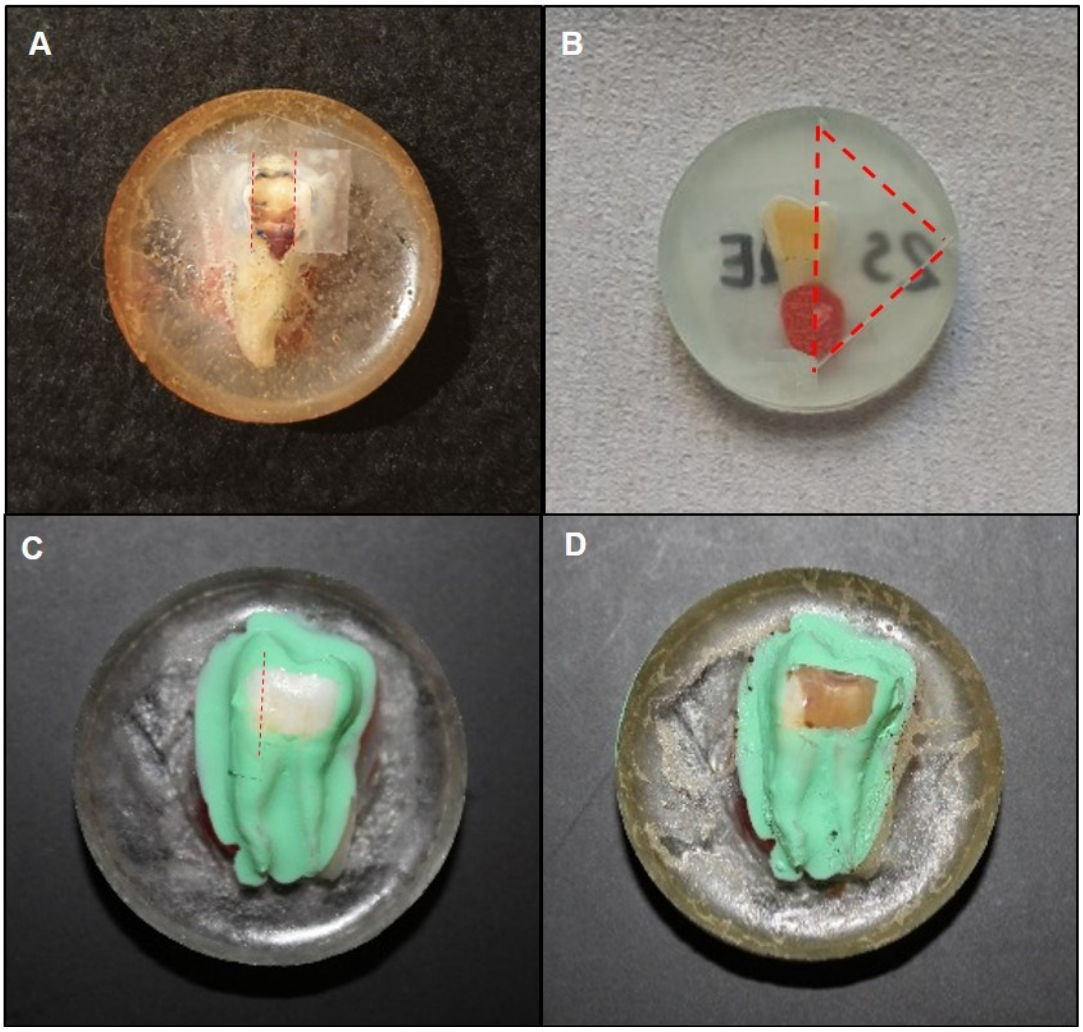

Figure 2.3: Buccal erosion window demarcated on different surfaces of a molar tooth with: (A) adhesive tape on two sides-eroded sample, (B) adhesive tape on one side-polished sample, (C) both adhesive tape and nail varnish-sound surface (pre-erosion), (D) both adhesive tape and nail varnish- acid eroded sound surface (post-erosion). Red dotted line demarcates the boundary of the adhesive tape reference area.

2.7.1.3 Carbonated Drink Immersion Protocols:

2.7.1.3.1 Sound enamel surface/ Accelerated erosion protocol/ No Saliva (SANS):

Samples were immersed in 100 ml carbonated drink (Coca Cola, CC; pH = 2.7; Coca Cola, UK) for 25 hr (1 day) at room temperature under constant agitation on Biometra WT 16 rocking shaker (Biometra, Göttingen, Germany). Cola solution was changed every 5 hr and teeth washed for 30 sec with distilled water

2.7.1.3.2 Polished enamel surface/ Accelerated erosion protocol/ No Saliva (PANS):

Enamel surfaces were ground flat to expose an area measuring around 5 x 5 mm and finished sequentially with water-cooled silicon carbide discs (500- and 1200-grit) (LaboPol-5; Stuers, Copenhagen, Denmark). Polishing followed using rotating polishing cloths wet by diamond sprays (9μm, 3μm, 1μm). Subsequently, the specimens were cleansed in distilled water in an ultrasonicator for 10 min to remove any residues of the polishing procedure. Polished enamel samples received the exact same treatment as the sound samples (SANS).

2.7.1.3.3 Polished enamel surface/ Accelerated erosion protocol/ Artificial Saliva (PAAS):

Samples were immersed in 100 ml Coca Cola at room temperature for 1 hr intervals under agitation alternating with artificial saliva. Samples were rinsed with distilled water for 30 sec after each immersion. 5 hr of cola immersion were achieved per day. Samples were stored in artificial saliva overnight. Experiment was repeated for 5 days to complete the 25 hr cola immersion period.

2.7.1.3.4 Polished enamel surface/ Accelerated erosion protocol/ Natural Salivary Pellicle (PASP):

Before starting the experiment, each group of four samples was placed into 20 ml of natural saliva for 1 hr and gently stirred to initiate pellicle formation on the enamel surface (Faller et al., 2011). Samples were immersed in 100 ml Coca Cola at room temperature for 1 hr intervals under agitation alternating with natural saliva. After each immersion, samples were rinsed with distilled water for 30 sec. Five hr of cola immersion were achieved per day. After the last immersion, samples were stored in artificial saliva overnight. Experiment was repeated for 5 days to complete the 25 hr cola immersion period.

2.7.1.3.5 Polished enamel surface/ Prolonged erosion protocol/ Natural Salivary Pellicle (PPSP):

Before starting the experiment, each group of four samples was placed into 20 ml of natural saliva for 1 hr and gently stirred. Samples were immersed in 100 ml Coca Cola for 5 sec Immersions were repeated for 10 times (total of 50 sec exposure) to create a single erosive cycle (Wongkhantee et al., 2006). Five erosive cycles were completed per day to mimic the oral pattern of acidic drink exposure of 250 sec/day (von Fraunhofer and Rogers, 2004) and follow the four or more daily exposures to acidic drinks by heavy consumers (Lussi and Schaffner, 2000, Lussi et al., 2004b). After each erosive cycle, samples were rinsed with distilled water for 30 sec and stored in natural saliva until the next erosive cycle (in 2 hr intervals). After the last immersion, samples were rinsed and stored in artificial saliva overnight. All steps were done under agitation. To complete 25 hr of immersion, cycles were repeated daily for 12 months. However,

for convenience, weekends were excluded and the experiment was extended for 16 months.

2.7.1.3.6 Extended Accelerated Enamel Immersion Periods:

Extra samples of the (SANS) protocol were prepared and further immersed in cola for 21 days.

2.7.1.4 Measurement of Enamel Surface Loss:

2.7.1.4.1 Laser profilometer:

All enamel 25 hr erosion protocol groups (SANS, PANS, PAAS, PASP, and PPSP) and extensive erosion at (7, 10, and 14 days), were measured with a non-contact laser profilometer (Proscan 1000 scanning laser profilometer, Scantron Industrial Products Ltd., Taunton, England, UK). The instrument used the KL135A displacement probe (z range, 400 μm). The semiconductor laser (λ = 780 nm) had a beam diameter of 12–35 μm and resolution of 0.02 μm. Areas of 4 x 4 mm^2 were measured on each sample at a step size of 10 μm and a vertical resolution of 1 μm. The laser scanned a group of data points on the sample and connected them to create a 3D height map. To measure enamel thickness loss (μm), the data points of two z-range scans of each sample (untreated and treated) were superimposed over the same reference point and subtracted from each other. Scans of representative enamel samples are shown in (**Figure 2.4**).

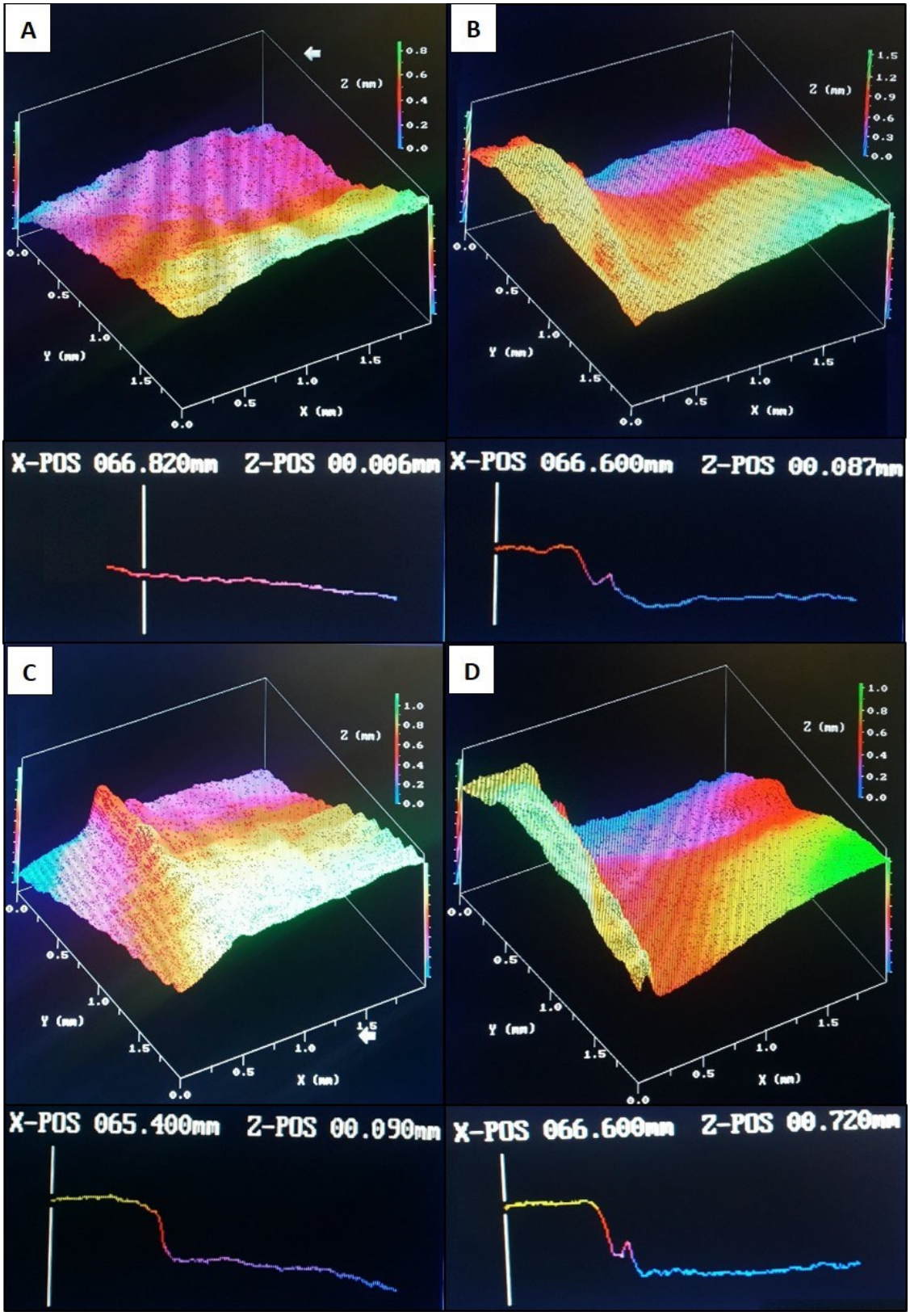
A
Z (mm)
0.8
0.6
0.4
0.2
0.0
Y (mm)
X (mm)
B
Z (mm)
1.5
1.2
0.9
0.6
0.3
0.0
Y (mm)
X (mm)
X-POS 066.820mm Z-POS 00.006mm
X-POS 066.600mm Z-POS 00.087mm
C
Z (mm)
1.0
0.8
0.6
0.4
0.2
0.0
Y (mm)
X (mm)
D
Z (mm)
1.0
0.8
0.6
0.4
0.2
0.0
Y (mm)
X (mm)
X-POS 065.400mm Z-POS 00.090mm
X-POS 066.600mm Z-POS 00.720mm

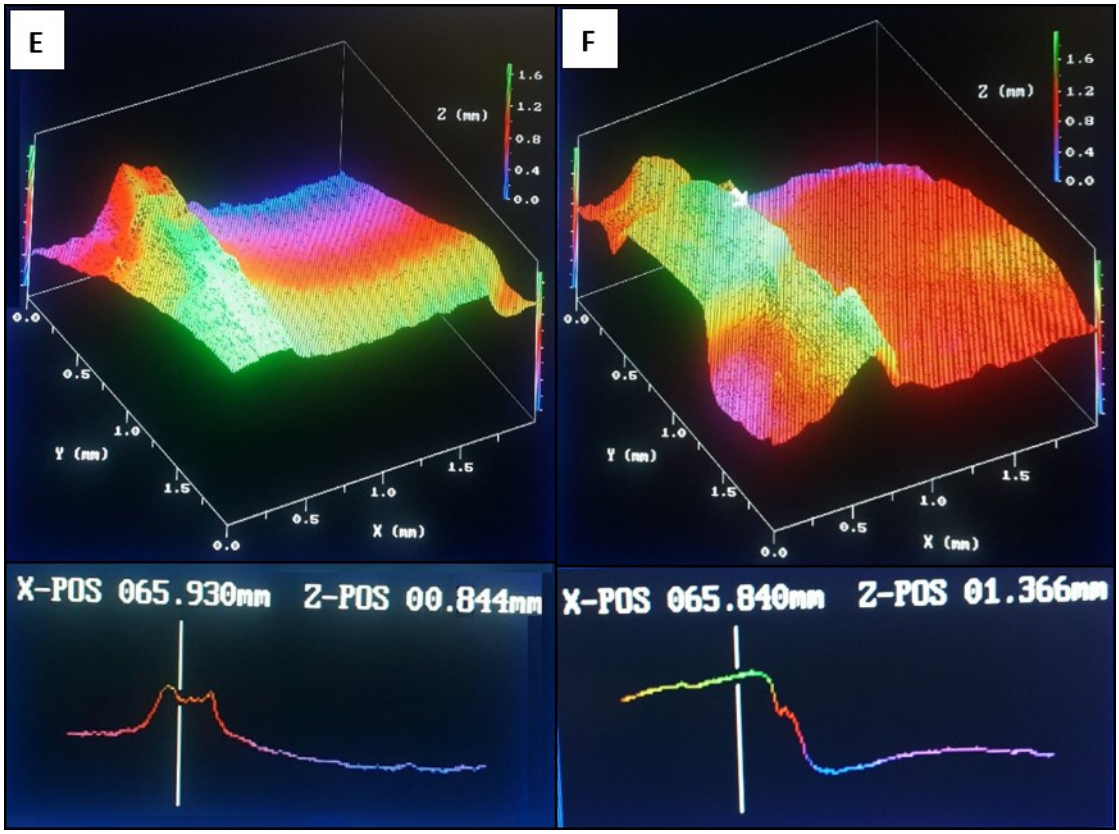

Figure 2.4: Laser profilometry (Proscan 1000) surface scans of erosion samples showing surface profile at z axis and a cross section at the x axis showing the depth of the lesion. (A) Baseline, (B) accelerated 25 hr erosion, (C) prolonged 25 hr erosion over 12 months period, (D) accelerated 7 day erosion, (E) accelerated 10 day erosion, and (F) accelerated 14 day erosion.

2.7.1.4.2 OCT:

After analysis of laser profilometry thickness loss results, further examination was carried out using an optical coherence tomography (OCT) scanner (VivoSight, Michelson Diagnostics, Kent, United Kingdom). OCT is equipped with a class I laser beam (λ=1305 nm). The laser scans an area up to 6 mm x 6 mm with a depth range of 1.2 to 2.0 mm depending on the scanned tissue nature. The images are composed of stacks of vertical scans to the total of 600 frames. 16-bit TIFF images can then be exported from the OCT software to be viewed. OCT scans were made for representative samples of the selected 25 hr erosion protocols (SANS), (PANS), (PPSP) (**Figure 2.5**). OCT scans were also applied for extensive erosion periods at the following points (7, 10, and 14 days) (**Figure 2.6**).

Calculation of the erosion step height representative of the lost enamel thickness in flat samples followed the International Organization for Standardization (ISO) standard; ISO 5435- 1:2000, which utilises 3 relatively flat areas, two reference and one in the depth of the lesion(Mistry et al., 2015, Mylonas et al., 2018). While, in case of sound convex samples, the original surface outline was first drawn by copying the contour of the sound enamel surface before treatment (**Figure 2.6**/ A). A public domain image processing program, ImageJ (LOCI, University of Wisconsin). Was used to calculate the lesion depth in all OCT images where the lesion was divided into 4 sections. In each section, 4 perpendicular equally separated parallel lines were dropped from

the original surface outline to the depth of the lesion (total of 16 lines). The mean of all depth lines was calculated and assigned for the lesion.

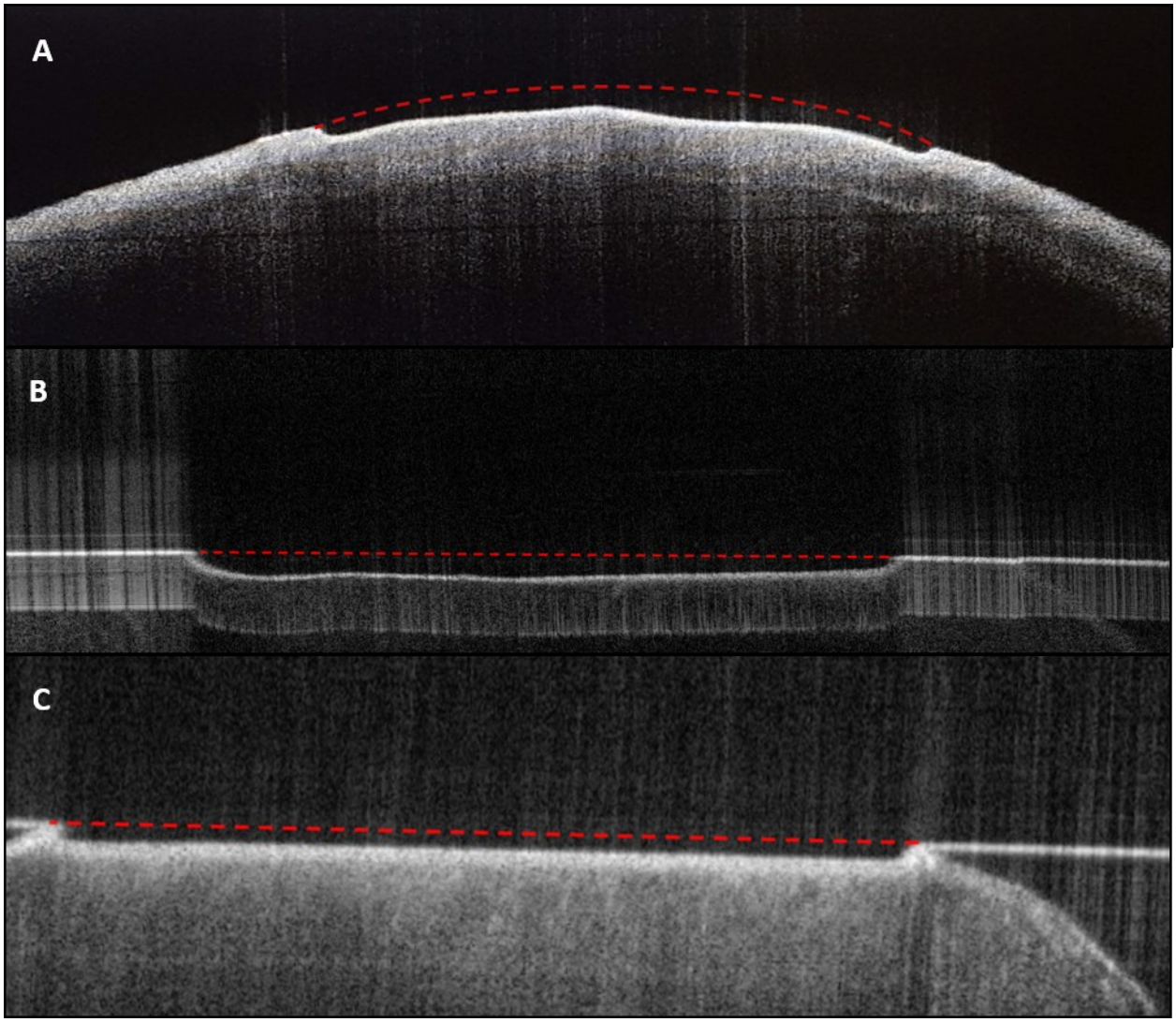

Figure 2.5: OCT scan showing enamel surface loss in accelerated 25 hr (1 day) erosion samples, (A) without saliva on sound enamel surface (SANS), (B) without saliva on flat polished enamel surface (PANS), and (C) with natural saliva over 12 months period on a flat polished enamel surface (PPSP). Red dashed line is the reference untreated surface contour.

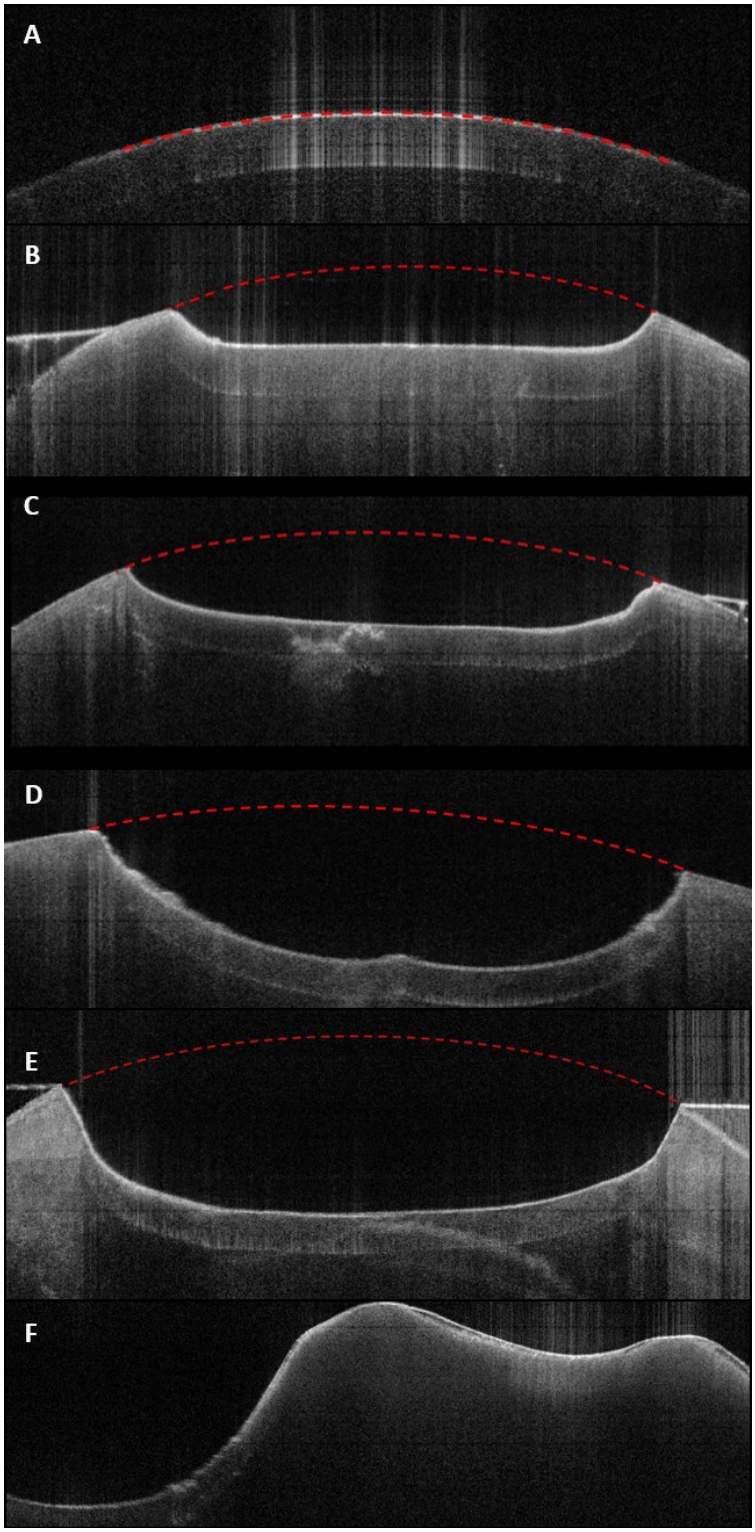

Figure 2.6: OCT scan showing enamel surface loss in accelerated erosion samples on sound enamel surface without saliva (SANS) at different time points. (A) Sound enamel surface (B) 7 days, (C) 10 days, (D) 14 days, and (E) 21 days, (F) 14 days occlusal molar erosion showing dentine cusps with no enamel. Red dashed line is the reference untreated surface contour.

2.7.1.4.3 Light Microscope:

For better viewing of surface thickness loss, sequential erosion lesion steps were prepared over one surface at 1, 7, 10, 14, following the accelerated erosion protocol (SANS) and viewed under a polarized light microscope (magnification 10x) as shown in (**Figure 2.7**).

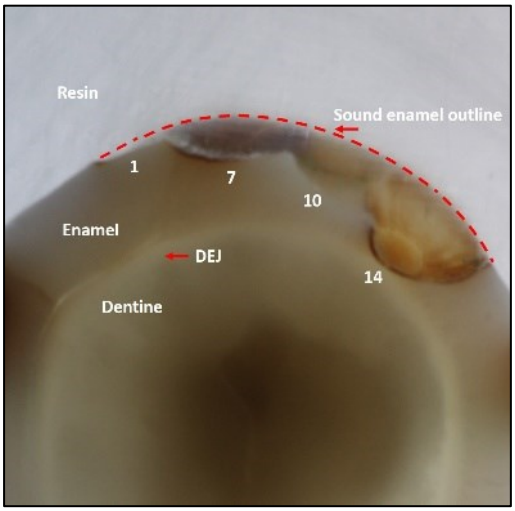

Figure 2.7: A cross-section in a premolar embedded in epoxy resin with a sequential accelerated erosion lesion over the buccal enamel surface. 1= 1 day erosion, 7= 7 day erosion, 10= 10 day erosion, and 14= 14 day erosion. Red dashed line is the reference untreated surface contour.

2.7.1.5 SEM Analysis:

Two representative (SANS) and (PPSP) 25 hr erosion samples were scanned under a scanning electron microscope (SEM; FEI, Eindhoven) (**Figure 2.8**). Two representative samples of the extended erosion periods were selected at the following time points (4, 7, 10, 14, 16, 18, and 21 days) (**Figure 2.9**). Specimens were mounted on aluminium stubs and gold coated. The SEM had an acceleration voltage of 20 kV and images were captured at multiple magnifications.

2.7.2 Results- Experiment 1:

The aim of the experiment was to study the influence of the enamel surface finish (sound, polished) and the presence or absence of saliva together with its type (no saliva, artificial saliva, and natural saliva) on the tooth surface dissolution by acid (Coca Cola) after 25 hr of immersion (accelerated, prolonged) and develop the methodology to be applied for the next experiments to create lesions that simulate different stages of clinical erosion. Data of enamel thickness loss obtained by the laser profilometer were analysed with a one-way Analysis of Variance (ANOVA). Bonferroni post hoc test was applied. Groups were considered statistically different at $\alpha \geq 0.05$.

All test groups were statistically significant to the control but no significance was detected between them. Thickness loss of (89 μm, 91 μm, 87 μm, 86 μm, and 85 μm) was recorded for (SANS, PANS, PAAS, PASP, and PPSP) respectively (**Figure 2.10**).

Three groups were selected for further comparison (SANS, PANS, and PPSP). These groups were selected as (SANS and PANS) are the most suitable for application in upcoming experiments, and (PPSP) represents the clinically relevant protocol. Statistical analysis (2 way ANOVA) of enamel surface loss results was measured by different techniques (OCT and laser profilometry). Both techniques were comparable for all groups with no statistical significance **(Figure 2.11**). Additionally, calculations were made for (SANS) group from representative

light microscope images and their results were comparable to the other techniques (**Figure 2.11**).

Laser interferometry data of extensive accelerated erosion at points (7, 10, and 14) measured (610, 825, and 1310 μm), respectively. Statistical analysis was also applied to extensive erosion results at all selected time points (1, 7, 10, and 14 days) measured by different techniques (OCT, laser profilometry, and light microscope). The results of all techniques were comparable and no statistical significance was recorded (**Figure 2.12**).

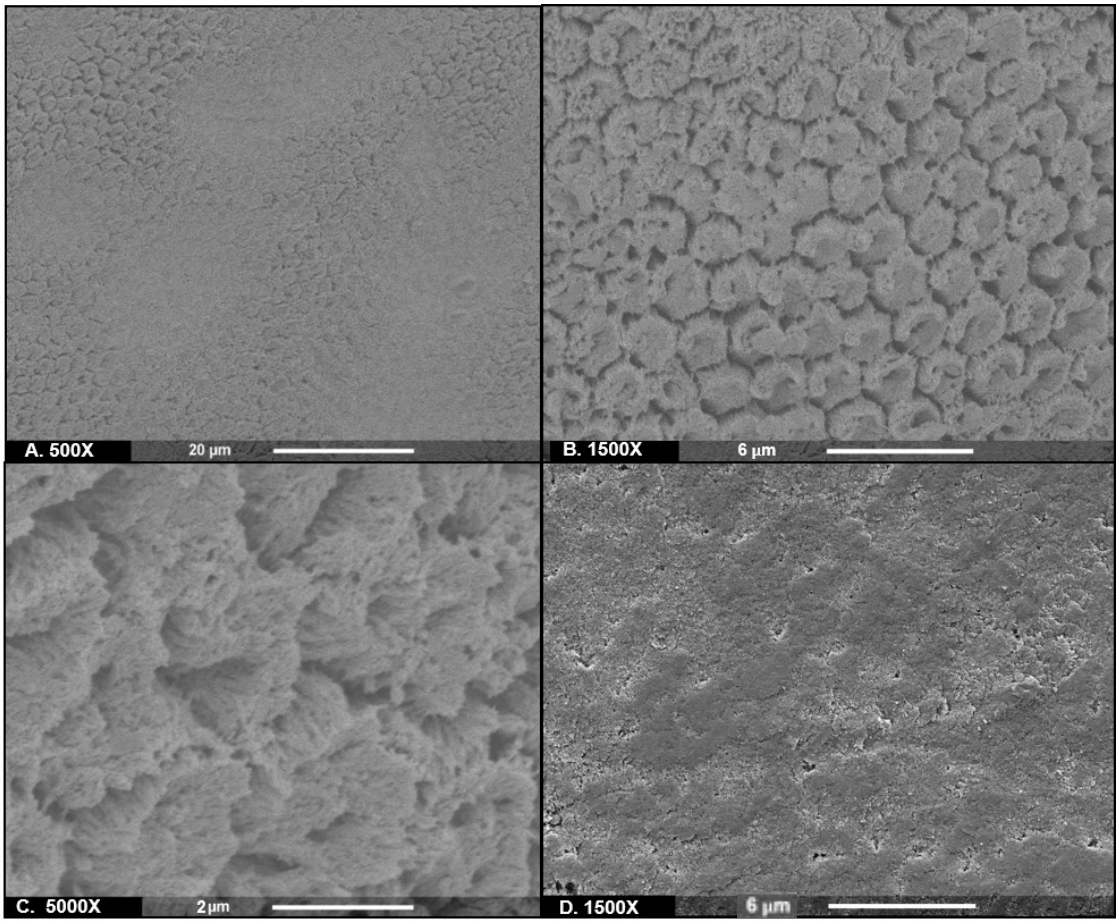

Figure 2.8: SEM images of enamel surface softened by 25 hr cola erosion. (A), (B), and (C) accelerated erosion without saliva (SANS) at different magnifications. (A) 500X, generalized exposed enamel prisms in a honey comb pattern, (B) 1500X, a clear honey-comb pattern and surface deposits, (C) 5000X, thin delicate crystals projecting from the surface of the prisms with different crystal orientation at the boundaries, (D) prolonged 25 hr cola erosion over 12 months showing (PPSP) – 1500X, enamel surface and prisms covered by a uniform continuous layer of amorphous mineral deposits.

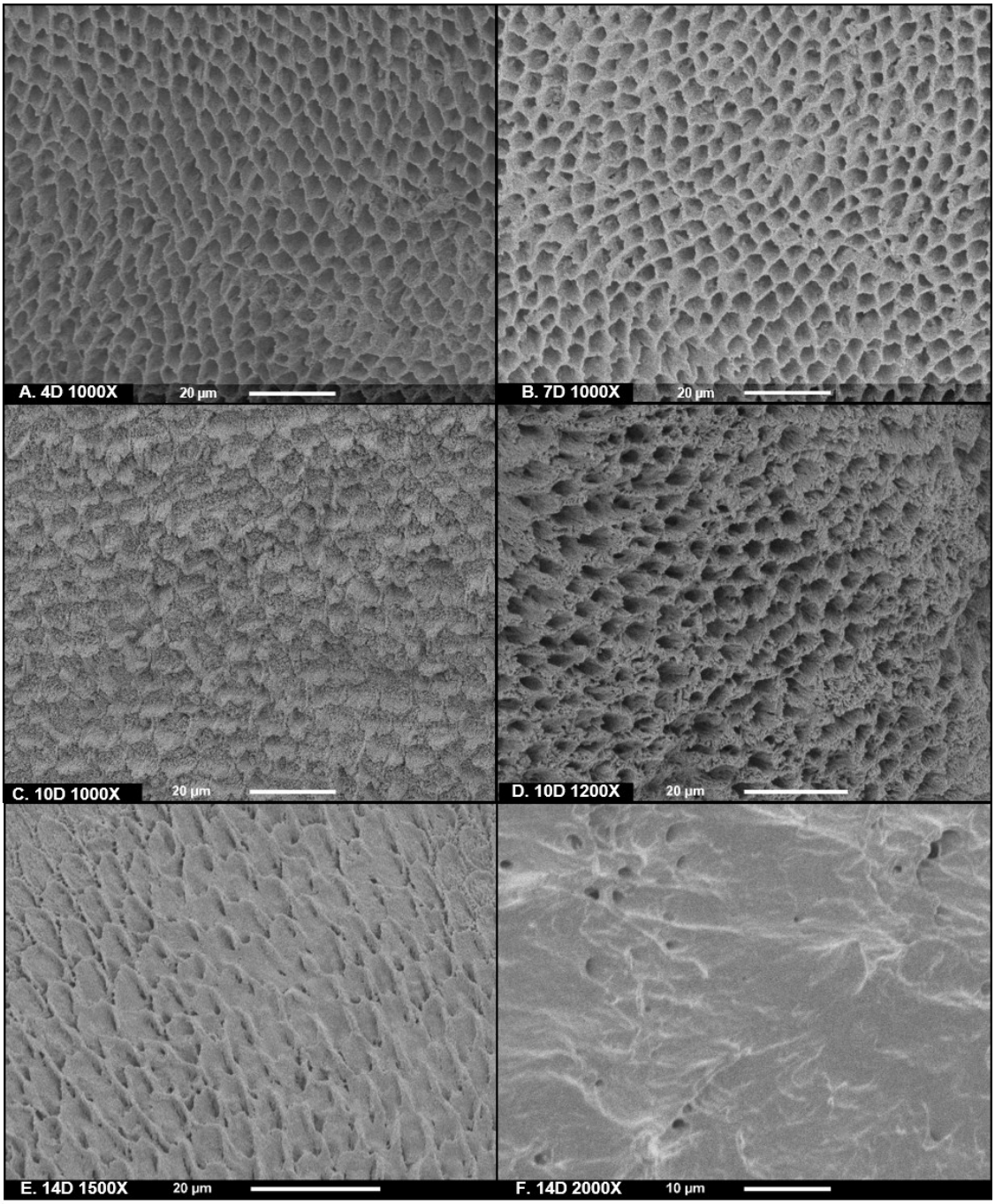
A. 4D 1000X
20 µm
B. 7D 1000X
20 µm
C. 10D 1000X
20 µm
D. 10D 1200X
20 µm
E. 14D 1500X
20 µm
F. 14D 2000X
10 µm

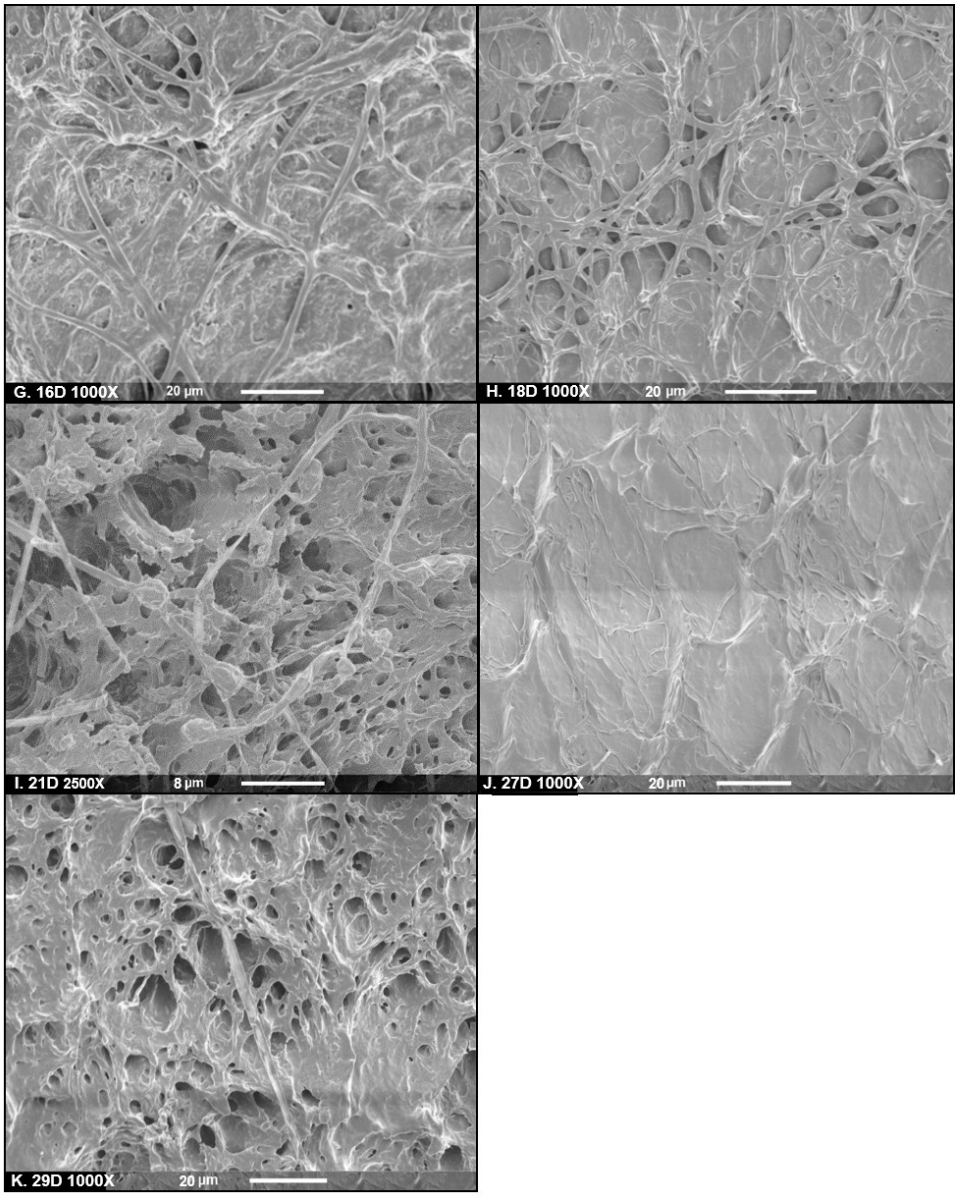

Figure 2.9: SEM images of tooth surface softened by accelerated cola erosion for (A) 4 days - 1000X, (B) 7 days - 1000X. Both showing prominent continuous pseudo-hexagonal network representing enamel prism boundaries with intervening holes (intraprismatic pores) which may have formerly been crystal aggregates. (C) 10 days - 1000X, short enamel prism boundary projections at some areas and (D) 10 days - 1200X, higher enamel prism boundaries at others, (E) 14 days - 1500X, remnants of the enamel prism boundary projections at some areas, (F) 14 days - 2000X, disappearance of enamel prism boundaries and exposed dentine at other areas with some open dentinal tubules, (G, H, I), (G) 16 days - 1000X, (H) 18 days - 1000X, and (I) 21 days- 2500X, all showing different levels of dentine matrix dissolution exposing interwoven distorted collagen matrix. (J) 27 days - 1000X, dissolved collagen matrix, and (K) 29 days - 1000X, unstructured dentine remnants.

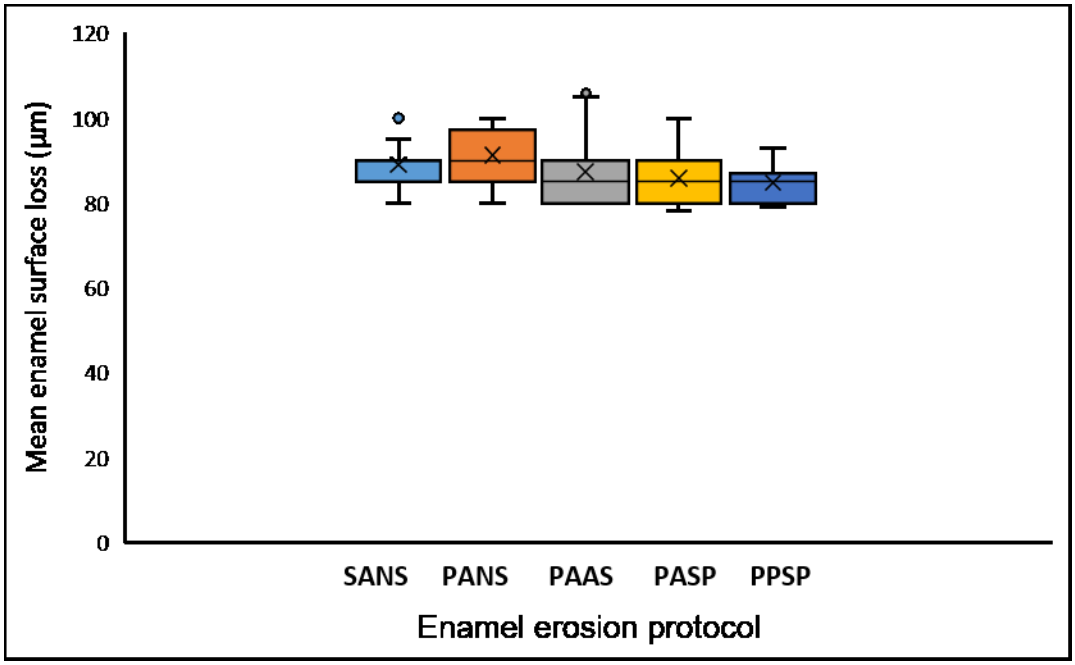

Figure 2.10: Mean ± standard deviation and value range of surface loss of all tested enamel groups after 25 hr cola erosion with different enamel surface finishes, immersion protocols, and saliva conditions (SANS, PANS, PAAS, PASP, and PPSP).

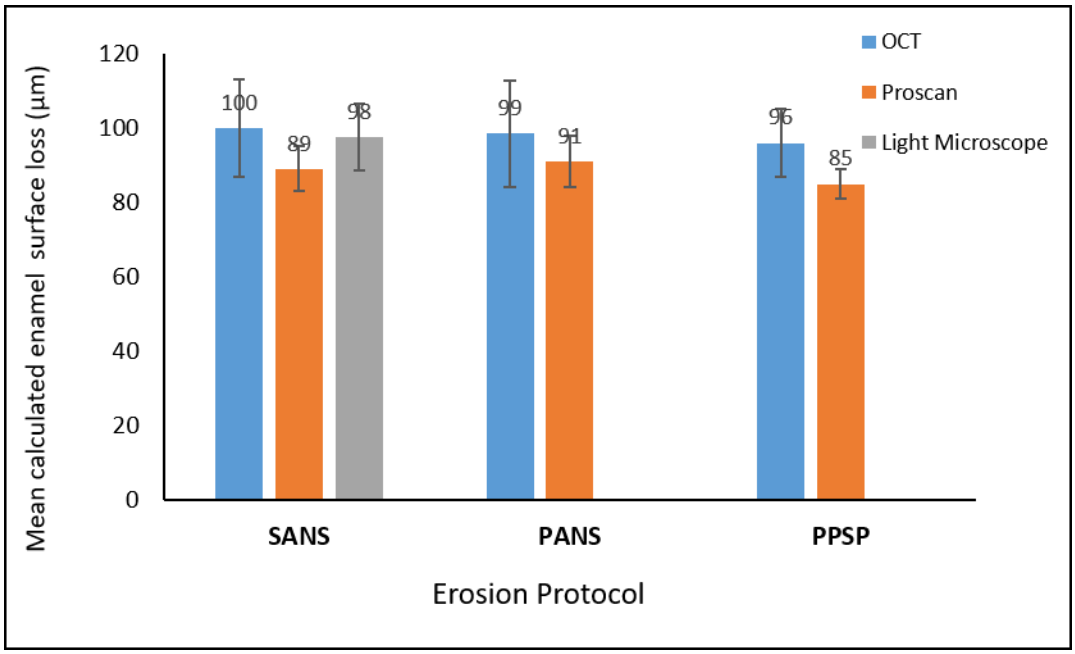

Figure 2.11: Comparison of the mean surface loss (µm) between enamel groups (SANS, PANS, and PPSP) recorded by the laser profilometer (Proscan) and calculated from OCT images. Extra measurements of SANS group were obtained from light microscope images.

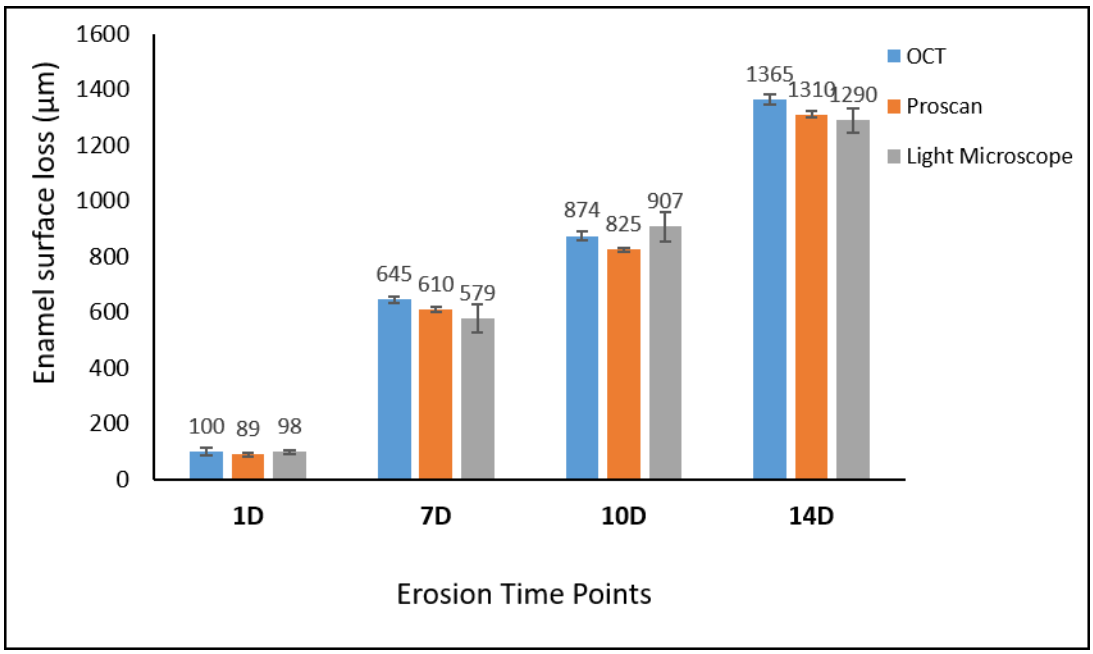

Figure 2.12: Mean ± standard deviation of enamel/ enamel and dentine surface loss with accelerated cola erosion of a sound tooth surface in the absence of saliva (SANS) at different time points calculated from OCT, proscan, and light microscope images. (1D= 1 day erosion, 7D= 7day erosion, 10D=10 day erosion, 14D= 14 day erosion, and 21D= 21 day erosion).

2.7.3 Discussion- Experiment 1:

In this experiment, samples were horizontally mounted and divided randomly into 5 test groups of 8 teeth to receive one of the selected erosion protocols. Regular soft drink (Coca Cola) was chosen over the diet version to carry out the erosive cycles for the current study. Some studies have reported that the potential of 'diet or light' soft drinks to increase caries risk is decreased markedly due to the lack of sugar. However, their erosive potential is similar to that of regular (sugared) drinks (Gurunathan et al., 2012, de Alencar et al., 2014). On the other hand, (Ehlen et al., 2008, Rios et al., 2009) have shown diet cola to be less erosive than the regular one. Ehlen et al. (2008), assessed the effect of sound teeth immersion in cola for 25 hr and the related enamel thickness loss. Their study was the guide to our accelerated immersion protocol with some modifications. This protocol was based on mimicking an annual exposure of enamel to soft drinks with an average daily consumption of 25 ounces of soft drink and mouth residence time of 20 sec before saliva clearance, making a total of 90,000 sec (25 hr) per year (von Fraunhofer and Rogers, 2004, Ehlen et al., 2008). Their experiment was carried out for 350 hr (14 days) equivalent to 14 years of normal beverage consumption, considered a reasonable time period to evaluate enamel erosion effects in young adults (von Fraunhofer and Rogers, 2004, Kitchens and Owens, 2007).

In all soft drink erosion experiments, the beverage and storage solution were kept at room temperature (25°C) (Panich and Poolthong, 2009, Poggio et al., 2017). Samples were eroded in cola drink under constant agitation. Unlike static

baths, agitation action simulates the *in vivo* drink agitation (Ireland et al., 1995, Maupome et al., 1998, Mistry et al., 2015) and increases the rate of replenishment of ions from enamel to the solution by providing a revolving environment, increasing the degree of erosion produced by acidic beverages (Torres et al., 2010, Attin et al., 2012, Shellis et al., 2014, Mistry et al., 2015). This was shown to be true for enamel of both primary and permanent teeth (Maupome et al., 1998, Maupomé et al., 1999, Larsen and Richards, 2002, Torres et al., 2010). In addition, significantly higher enamel surface loss and microhardness change were reported with higher speed shakers (Mistry et al., 2015). 3rd molar buccal enamel test surface was selected for sample production to allow standardization of test surface type. 3rd molars are typically utilised in research owing to their common surgical removal for orthodontic or impaction reasons. Unerupted molars are preferred owing to the constant surface composition and absence of extraneous effects of occlusion on the surface (Hemingway, 2008, Laurance-Young, 2012). In addition, buccal surfaces have been found to be less susceptible to erosion than lingual tooth surfaces (Tucker et al., 1998, Ganss et al., 2000) as enamel properties could vary with variable origins, tooth surfaces and types. However, Carvalho and Lussi (2015) observed no significant differences between these surfaces and explained it by the simultaneous formation of enamel mineral on the buccal, lingual and proximal surfaces of the tooth during the amelogenesis. The differences between enamel surfaces could be attributed to the extent of loss of the fluoride-rich layer by wear (Weatherell et al., 1974). However, the differences in the susceptibility of tooth surfaces to erosion become insignificant after grinding and polishing procedures (Ganss et al., 2000, Carvalho and Lussi, 2015).

Enamel samples with different surface finish (sound, polished), soft drink immersion protocols (accelerated, prolonged), and different saliva protection conditions (no saliva, artificial saliva, and natural salivary pellicle) were tested to compare enamel surface loss with the effect of included variables and choose the most suitable accelerated protocol (SANS, PANS, PAAS, PASP) that compares best with the results of the prolonged protocol (PPSP) that mimics most the clinical situation of heavy soft drink consumption pattern over a period of 12 months. The chosen protocol will be applied for extended periods to create tooth samples with different extensive clinically relevant erosion lesions. These lesions duplicate the amount of lost tooth structure under the effect of erosion but not abrasion which usually work in synergy in the oral cavity. Polished surface samples were preferred over sound ones for dimensional change calculations as they allow precise assessment of the erosively induced lesions by most of the applied methods (profilometry, CLSM, microindentation, OCT, etc.), create clear reference surfaces (Attin, 2006, Mistry et al., 2015), and produce standardized specimens by ensuring removal of natural variations in surface enamel between teeth; which may result in different responses to acid dissolution (Adebayo et al., 2009, Shellis et al., 2011, Poggio et al., 2014b, Carvalho and Lussi, 2015). In addition, polished tooth specimens allowed detection of small surface changes following short acid exposure periods and were sensitive enough to discriminate between different acid exposure times (Mylonas et al., 2018). Thus, polished enamel specimens are appropriate for studies that aim to investigate erosive lesion repair as evaluation of enamel remineralisation agents (Lussi et al., 2004a, O'Toole et al., 2016, O'Toole et al., 2015). Sound enamel surfaces were also tested to allow, as close as possible, the reproduction of the conditions that occur

in the mouth (Torres et al., 2010) and to explore the effect of the outermost enamel surface layer on erosion surface loss results. The outermost enamel layer is often aprismatic and contains considerably higher fluoride concentrations (Hallsworth and Weatherell, 1969, Poggio et al., 2013) rendering it less permeable than the underlying enamel and more resistant to acid dissolution, as a result it may be considered protective (Amaechi et al., 1999a, Torres et al., 2010, Poggio et al., 2013). The enamel barrier method to expose a central window region (about 1/3rd the sample surface), has been widely applied in previous research successfully using PVC taping (O'Toole et al., 2015, Austin et al., 2016, O'Toole et al., 2016, Mullan et al., 2018, Mylonas et al., 2018), or nail varnish painting (Rakhmatullina et al., 2013, Alencar et al., 2017, Alexandria et al., 2017, Santos et al., 2018) without influencing the acid erosion effect on test enamel.

Comparisons were made first to test the effect of enamel surface finish; sound (SANS) vs. polished (PANS), on thickness loss with the accelerated acid erosion protocol in the absence of saliva. Both groups showed comparable results (89 µm, 91 µm), respectively. Earlier studies (Sullivan, 1954, Ganss et al., 2000, Ranjitkar et al., 2009, Poggio et al., 2014b, Carvalho and Lussi, 2015, Lin et al., 2017) suggested that sound natural enamel surfaces were more resistant to erosive challenges than polished surfaces which could be explained by the process of enamel maturation where the outermost layer of enamel acquires higher fluoride (Brudevold et al., 1956, Nakagaki et al., 1987, Carvalho and Lussi, 2015), and therefore becomes more resistant to demineralisation (Meurman and Frank, 1991a, Ganss et al., 2000, Carvalho and Lussi, 2015). However, calculations from Sullivan (1954) (Sullivan, 1954) suggest that this layer is only a

few micrometres thick. This could explain the insignificant surface loss results between sound and polished enamel surfaces in this experiment. This layer may be significant with early (short-duration) erosion and not observed with our protocol of 25 hr acid immersion.

The lost enamel surface thickness in the sound enamel accelerated cola erosion group with no saliva (SANS) after 25 hr immersion (89 μm) was comparable to the results of (Ehlen et al., 2008) (92 μm), who followed the same protocol for 25 hr. Also, all laser interferometer recorded enamel surface loss measurements were not statistically significant between all test groups.

In the literature, the definition of (short-duration) acid erosion has not been specified by one particular acid exposure time or number of cycles. However, typically short-duration exposure lasts for several sec or min but does not exceed 5 min total exposure (Jaeggi and Lussi, 1999, Wiegand et al., 2007a, Voronets et al., 2008, Voronets and Lussi, 2010, Mylonas et al., 2018). (PANS) was selected for further comparison with polished enamel groups with different saliva types (PAAS) & (PASP). No statistical significance was found between groups (PANS, PAAS, and PASP) (91 μm, 87 μm, and 86 μm), respectively. This is in agreement with Batista et al. (2016), who found no significant difference in the surface microhardness between eroded enamel and dentine samples treated with different *in vitro* artificial saliva formulations and both *in vitro* and *in situ* natural saliva. Moreover, Hall et al. (1999), showed that the protective qualities of natural saliva was significantly impared when used outside the oral cavity compared to the *in situ* environment which could be related to pH changes and depletion of

inorganic components by salivary protein breakdown. Finally, comparisons were made to verify the selected experimental groups (SANS & PANS) against the clinically relevant protocol (PPSP), and resulted again in no statistical significance in enamel loss between any of the immersion protocols (89 µm, 91 µm, and 86 µm), respectively. Comparison of all test groups is presented in (**Figure 2.10**).

It was clearly observed from the results above that enamel with different surface preparations, all salivary conditions, and immersion protocols produced lesions with comparable thickness loss. By that, either erosion protocol; of sound or polished enamel with any saliva condition (no saliva, artificial saliva, and natural saliva) at any erosion rate (accelerated, and prolonged), can be applied in the next erosion experiments. Some experiments used polished samples (PANS, PPSP) as it was necessary for some experimental tools to have a flat surface for reference. While, sound surface group (SANS) was selected for testing in other experiments mimicking extensive oral erosion conditions. In addition, all enamel loss measuring techniques gave comparable results confirming their validity for this application.

Accelerated erosion protocol was extended and the following points 1, 7, 10, and 14 days were selected for clinically relevant surface loss **measurement** (**Table 4**) and microscopic analysis. These points were selected for being comparable to some of the clinical grades of erosion described by “The exact tooth index” (**Table 1**) (Fares et al., 2009) (refer to Page 57). These points were implemented in the next experiments to test the effect of enamel loss and dentine exposure on tooth strain.

SEM images of the accelerated erosion group with absence of saliva (SANS) showed the characteristic honey-comb pattern of exposed enamel prisms (**Figure 2.8**/ A, B, & C). While, the prolonged erosion mimicking the oral consumption pattern (PPSP) showed a solid enamel surface with a uniform layer of deposits (**Figure 2.8**/ D). This layer could be explained by surface hardening or stabilization by prolonged immersion in artificial saliva in this protocol. Artificial saliva caused complete surface stabilization after 25 hr remineralisation (Eisenburger et al., 2001a, Eisenburger et al., 2001b). With progression of erosion, a pseudo-hexagonal network predominated, representing boundaries of enamel prisms around intra-prismatic pores. These pores became deeper at 4 and 7 days then started to replenish at 10 to 14 days exposing areas of dentine indicated by a smooth structure with a few open dentinal tubules. With further erosion (16-21 days), the surface showed increasing levels of dentine matrix dissolution exposing interwoven distorted collagen matrix. While, after 29 days only unstructured dentine remnants were remaining.

From SEM images it was confirmed that etched human enamel surfaces exhibited a variety of morphological changes with different resulting etching patterns (Silverstone et al., 1975, Ganss et al., 2000). While, dentine surface etching began in the area of peritubular dentine and resulted in the exposure of organic components and the opening and funnelling of dentinal tubules (Isokawa et al., 1970, Ganss et al., 2000). Morphological surface changes were only analysed at this stage and no subsurface imaging was obtained.

Table 4: Selected Extensive Erosion Time Points and their Related Clinical Picture in Comparison with the "Exact Tooth Wear Index"

Erosion time point	Degree of enamel thickness loss	Relevant clinical scale "The exact tooth wear index" *
1 day	initial erosion of enamel surface	Enamel 1
7 day	"loss of up 1/3rd of the enamel surface"	Enamel 2
10 day	"loss of up to 2/3rd of the enamel surface"	Enamel 3
14 day	complete removal of enamel and exposure of dentine	Dentine1

* (Fares et al., 2009)- refer to (**Table 1**- Page 57)

2.8 Experiment 2

Subsurface enamel changes with erosion

2.8.1 Material and Methods- Experiment 2:

The experiment included 24 horizontally mounted pre-eroded enamel samples divided into 3 groups according to the erosion protocol used (n=8). Groups (PANS) and (PPSP) were extensive erosion samples from experiment 1, (PANS= polished/ 25 hr accelerated erosion/ no saliva), (PPSP= polished/ 25 hr prolonged erosion over 12 months/ salivary pellicle). While, the third group represented relatively early erosion (PESP= polished/ early/ salivary pellicle). (PESP) samples were stored in natural saliva for 1 hr prior to each erosive cycle. Erosion cycles took place twice daily in 100 ml cola drink for 4 intervals of 2 min at 0, 12, 24, 36, 48, and 60 hr under constant agitation resulting in a total of 8 min of demineralisation per cycle (Poggio et al., 2010, de Alencar et al., 2014, Wang et al., 2014), then rinsed with distilled water for 30 sec using a squeeze bottle and stored in artificial saliva until the next erosive cycle begins.

After all erosion cycles were completed, all samples were tested under a scanning laser profilometer to measure enamel surface loss then further prepared to be examined under the CLSM; BioRad Radiance 2100 Confocal Laser Scanning Microscope (Bio-Rad Laboratories Ltd, Hemel Hempstead, Hertfordshire, UK) fitted by LaserSharp2000 v6.0.0.846 (Carl Zeiss Ltd, Cambridge, Cambridgeshire, UK). The current experimental settings included (Olympus 60x; 1.4 numerical aperture (NA), oil immersion objective). A cross-section of all samples was made through the lesions using a water-cooled diamond-edged Accutom 5 rotary saw (Struers, Denmark). The sectioned halves were flipped and re-embedded in epoxy resin as depicted in **Figure 2.13**. The cut

surfaces of both halves were polished with diamond pastes on polishing discs (LaboPol-5; Struers, Copenhagen, Denmark). Subsequently, the specimens were ultrasonicated for 10 min and air dried, followed by submersion in 20 ml of 0.25% ready-to-use Rhodamine B solution (Sigma-Aldrich Company Ltd. Dorset, England) for 60 sec (Banerjee et al., 2011). Confocal images are presented in **Figure 2.14**, **Figure 2.15**.

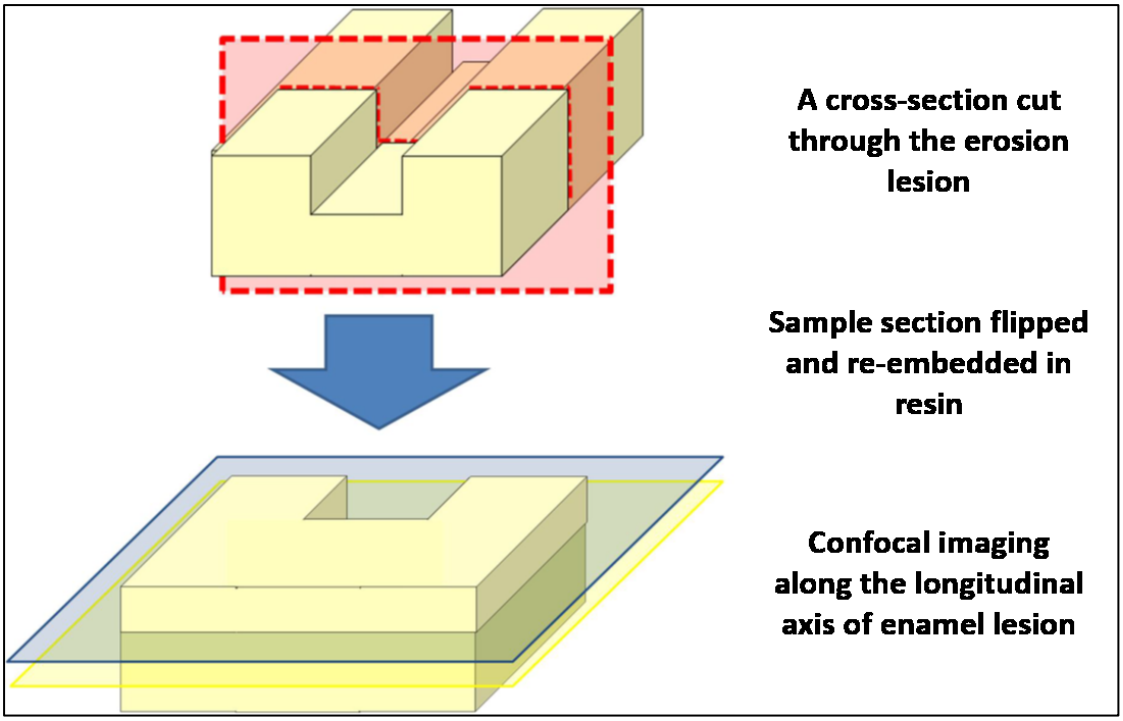

Figure 2.13: A diagram of an erosion sample preparation by cross-sectioning and resin re-embedding for confocal microscope viewing -Courtesy of (Laurance-Young, 2012).

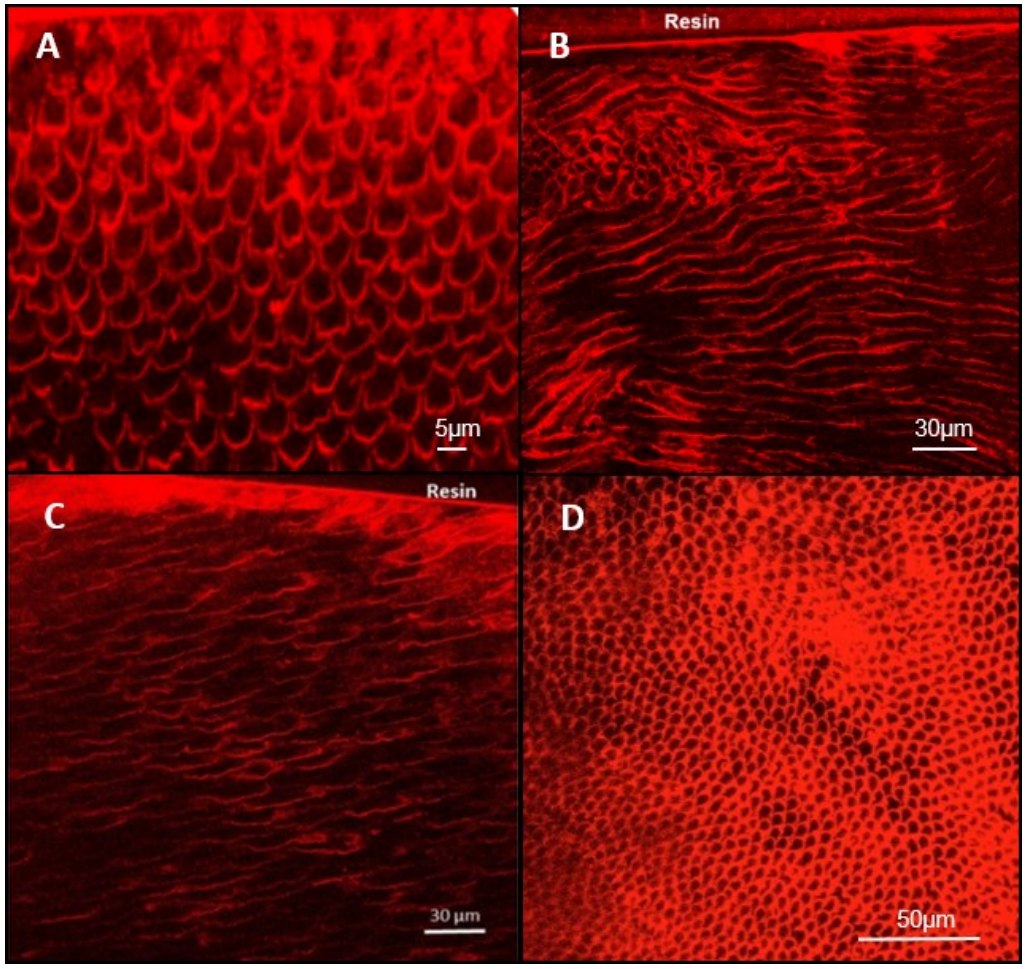

Figure 2.14: Confocal optical section scans of sound enamel specimens, under fluorescent channel and Rhodamine B dye. (A, B, & C) Surface enamel section showing different enamel prism orientation. Resin lies on top of images (D) Mid-thickness enamel section.

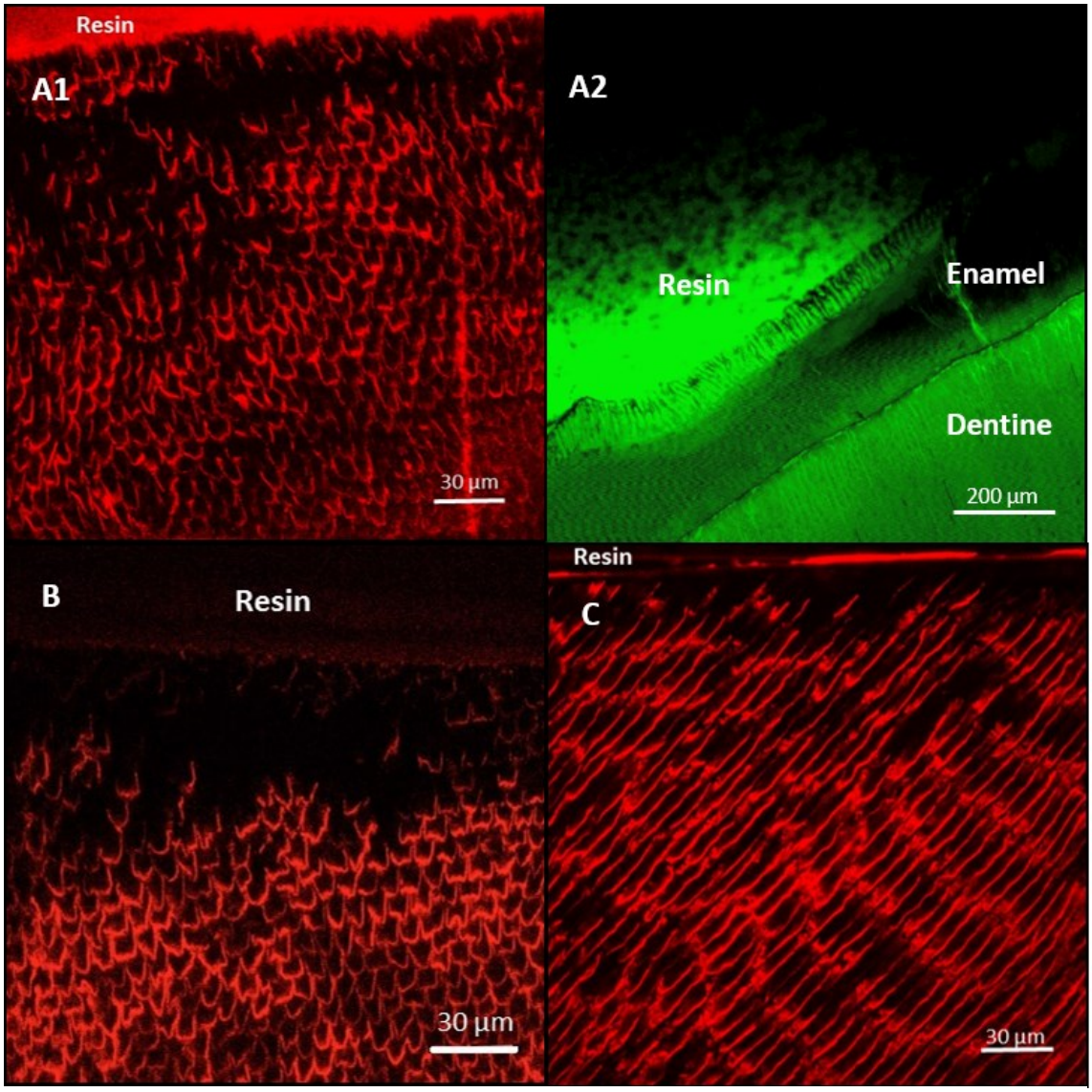

Figure 2.15: Confocal optical section scan of enamel under fluorescent channel and Rhodamine B dye, after different conditions of 25 hr erosion. In all, black punched out cavities are observed directly under the eroded enamel surface presumed to be subsurface enamel lesion. (A1 & A2) accelerated erosion (PANS), (B) prolonged erosion over 12 months (PPSP), and (C) early erosion (PESP).

2.8.2 Results and Discussion- Experiment 2:

The tested protocols were selected for the following reasons: 1- all the selected groups had a polished surface finish. 2- (PANS) was comparable to (SANS) the protocol planned to apply for creation of *in vitro* extensive erosion-like lesions. While, 3- (PPSP) was considered to be representative of a clinically relevant erosion pattern, and 4- (PESP) was the relatively early erosion protocol. The enamel thickness loss and subsurface changes with erosion should be comparable between groups to allow qualitative and quantitative comparisons and verification of the most suitable experimental protocol to create *in vitro* erosion-like lesions. Data of the calculated subsurface softened enamel thicknesses for all group (PANS, PPSP, and PESP) were obtained and analysed using SPSS. One-way ANOVA was employed with post hoc multiple comparisons (Bonferroni) to compare results between groups.

Enamel surface softening process occurs during acid-mediated erosion. Acid penetration into the enamel subsurface occurs after prolonged acidic attack before any superficial enamel bulk is lost (Attin et al., 2003, Shellis et al., 2014, Mylonas et al., 2018). While short acid immersion periods may produce enamel surface changes with minimal subsurface alterations, longer acid immersion periods are required for subsurface changes to occur in enamel (Mullan et al., 2018, Mylonas et al., 2018). For PESP group, the demineralisation cycle included sample immersion in soft drink for 8 min. To stress its demineralising potential of the soft drink, it was replenished every 2 min, to ensure it was carbonated and to

reduce the buffering effect from ions dissolved from the sample surface (Tantbirojn et al., 2008, Poggio et al., 2013).

Samples were immersed in Rhodamine B stain and this leads to emission of red fluorescent signal from the examined lesions under the confocal microscope. This was recorded by applying the appropriate fluorescence excitation and barrier filters (Watson and Boyde, 1991, Sidhu and Watson, 1998, Banerjee et al., 2011). Laser scanning confocal microscope images of all sound and eroded enamel sections were taken in perpendicular position to the cross-sectional surfaces as shown in **Figure 2.13**. The epoxy embedding resin appears at the top rim of the images. In confocal images, red colours stand for highly reflective structures, e.g. organic components and interprismatic structures, as seen clearly in sound enamel images (**Figure 2.14**). However, in some areas the laser beam penetrates but is not scattered so minimum light is reflected and appears as black or dark colours like prism cores. In all erosive protocols tested (PANS, PPSP, and PESP), subsurface enamel erosion lesions were observed as black cavitated (punched out) areas directly below the eroded enamel surface, with loss of reflection of enamel interprismatic arcade shaped regions (honeycomb pattern) when compared to the continuous pattern seen in sound enamel, while, the outer layer was still intact (**Figure 2.15**). These areas are potentially representative of mineral loss leading to loss of prism structures in softened enamel. The pattern of this lesion suggests formation of islands of subsurface softening lesions rather than a uniform softening of the acid exposed surface with a dense reflecting band seen underneath the softened surface. To calculate the subsurface lesion depth, imageJ software was used. Each image was divided into 4 equal longitudinal

segments. The width of each segment was measured and 10 equally separated perpendicular lines were dropped from the surface of enamel to the deepest point of the black cavities representing the lesion. The average of all readings from all 4 sections gave the average reading for each sample (μm). Lesion depth was compared between tested groups.

All groups recorded comparable lesion extension into the body of enamel (PANS= 62 μm ± 24, PPSP= 63.77 μm ± 18, and PESP=63.08 μm ± 28) (**Figure 2.16**). However, the pattern of extension was different between the early protocol and both extensive immersion protocols (accelerated and prolonged). With relatively early erosion (PESP), less branching was observed by the subsurface pitting lesions similar to the observations of Laurance-Young (2012) in samples of enamel eroded with 0.05% phosphoric acid for 600 sec. The author suggested those black cavities to be isolated subsurface softening within the enamel lesion rather than the expected more uniform softening. On the other hand, in both accelerated and prolonged erosion groups in the absence or presence of salivary pellicle (PANS, PPSP), multi-branched lesions were seen with connections between the subsurface cavities creating a wider lesion with similar extension depth. This could be attributed to the effect of the extended and repeated acid immersion periods aiding in the creation of channels between the primary formed lesions.

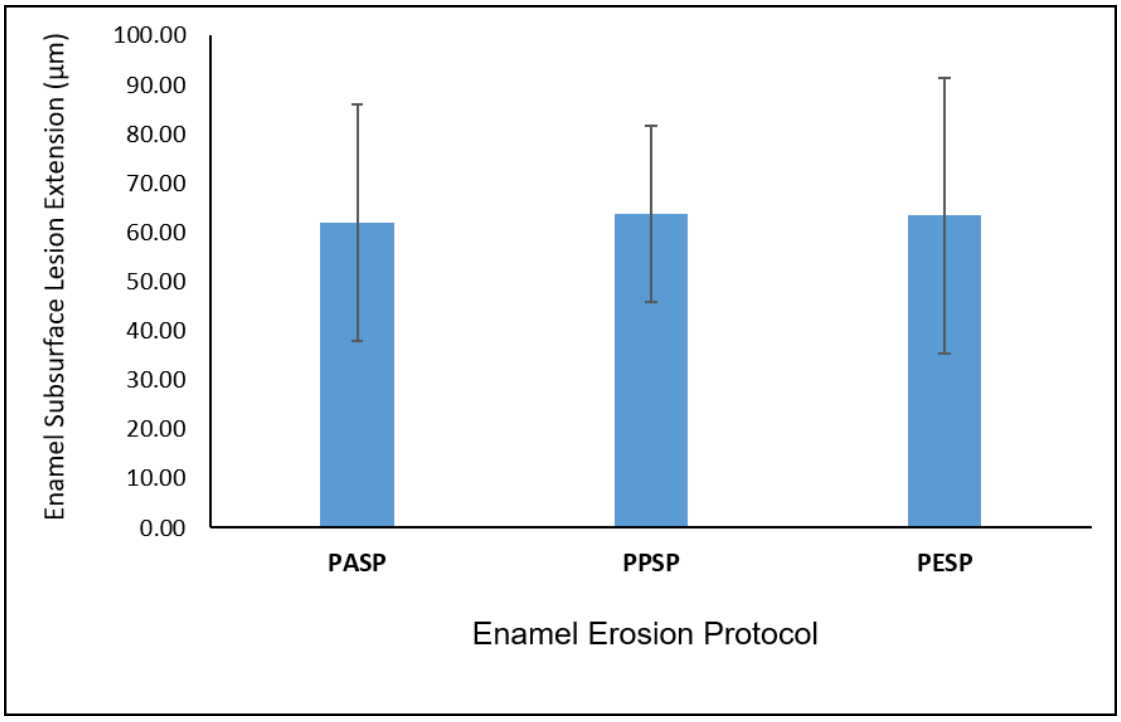

Figure 2.16: Mean ± standard deviation of enamel subsurface lesion extension with different erosion protocols (PANS, PPSP, and PESP) calculated from CLSM images, (*n*= 8).

In the literature, the reported thickness of erosion affected enamel was calculated according to the affected enamel thickness removed with tooth brushing after exposure to different acid concentrations and length of immersion. The thickness varied between 0.2 and 5 µm (Attin et al., 2000, Eisenburger and Addy, 2003, Wiegand et al., 2007b, Voronets and Lussi, 2010), and between 2–4 µm measured by ultrasonication after 2 hr acid exposure [Eisenburger et al., 2000]. While, Eisenburger et al. (2004) who measured the lesion by the extension of resin replicas of subsurface erosion pores found lesions of 9–12 µm below the surface. This is several times greater than the technique based on the affected

layer removal by physical forces. The authors suggested that even this depth was an underestimate as the most demineralised part of the affected layer was deeper and not detectable. They explained that this discrepancy could be accounted for by two factors. Firstly, the low resistance offered by the outer most demineralized part of the softened enamel to the contact profilometer stylus used that may have led to poor registration by the instrument. Secondly, that demineralisation appears to be confined to the prism boundaries at deeper layers of affected enamel offering similar resistance to ultrasonication as sound enamel. By that, the sound/affected enamel interface appears closer to the surface than it actually is. On the other hand, a more recent study by (Paepegaey et al., 2013) with a similar experimental protocol, quantified enamel loss after different acid erosion models using three instruments including CLSM. Citric acid (pH 2.26) and a total acid exposure time of 180 min (7.5 min/cycle) were used. The depth of the softened layer was comparable to our results (63.22 μm). In addition, Amaechi et al. (1999a) observed that 1hr eroded bovine incisors in orange juice produced subsurface enamel demineralisation reaching a depth of 75 μm.

Various *in vitro* erosion models are available in the literature. They have the advantage of excluding complex clinical trials, have low operational cost, and provide rapid efficient results. However, these models have limitations, and cannot replicate intraoral conditions. Human intraoral biological conditions include the presence of saliva consisting of both organic and inorganic compounds, cited to be important to erosion studies (Buzalaf et al., 2012). There is difficulty in saliva collection and storage (Schipper et al., 2007) and compositional changes may occur affecting its protective qualities (Hall et al., 1999, Aykut-Yetkiner et al.,

2014). Therefore, artificial saliva substitutes were developed. Various artificial saliva formulations are available in the literature with little standardization or guidance about the most suitable type to be applied in different erosion protocols (Leung and Darvell, 1997). Selection of a type of artificial saliva is mainly dependant on its previous application by leading research groups (Levine et al., 1987, McKnight Hanes and Whitford, 1992, Amaechi et al., 1999b), or their remineralisation potential compared to control (not remineralised) (Ionta et al., 2014). The artificial saliva formulation prepared for this study is one of the oldest and commonly used formulations (Levine et al., 1987, McKnight Hanes and Whitford, 1992, Amaechi et al., 1999b), with confirmed ability to remineralise erosive lesions (Ionta et al., 2014). In addition, Batista et al. (2016) tested the effect of artificial saliva formulations in the remineralisation of enamel and dentine samples measured by the change in surface microhardness and no significant difference was found between any of the test groups. Mucin was not considered as a component of our prepared saliva as its addition did not affect the remineralisation potential of artificial saliva (Klimek et al., 1982). Meyer-Lueckel et al. (2004) compared erosion in the presence of mucin-containing saliva with mucin-free saliva and also found that both induced a similar subsurface lesion remineralisation. However, (Hara et al., 2008) reported that mucin (a glycoprotein) increased the viscosity of the prepared saliva which may decrease mineral diffusion during remineralisation.

CHAPTER 3

Analysis of Restored Occlusal and Buccal Erosion Lesion Strain with Strain Gauges and 3D-FEA

3.1 Introduction- Chapter 3:

Tooth wear has been attributed to two major mechanisms, mechanical wear (abrasion and attrition) and chemical wear (erosion). It has been confirmed through literature that the prevalence of severe tooth wear increased generally with age (Spijker et al., 2009) with the highest prevalence of cervical lesions reported in 77% of middle-aged group and up to 81% in elderly populations (Jiang et al., 2011, Zi Yun et al., 2015, Duangthip et al., 2017). Cervical erosive lesions are categorized among the non-carious cervical lesions (NCCLs) (Bevenius et al., 1993, Duangthip et al., 2017). Other NCCL categories include abrasion and abfraction (Grippo, 1991, Duangthip et al., 2017). Cervical lesions mainly affect buccal aspects lower teeth and palatal surfaces of maxillary teeth (Smith et al., 2008, Zeola et al., 2015) and mostly occur in teeth with occlusal attrition or erosion (Khan et al., 1999, Bartlett and Shah, 2006, Benazzi et al., 2011, Wada et al., 2015, Duangthip et al., 2017). While, occlusal erosion lesions are most common on mandibular posterior teeth and incisal edges of anterior teeth. The joint action of occlusal factors of acid erosion and abrasion has been suggested by earlier studies (Lee and Eakle, 1984, Khan et al., 1999, Rees and Hammadeh, 2004, Staninec et al., 2005, Guimarães et al., 2014) in the progressive cyclic process of cervical tissue dissolution. This theory suggests that erosive acids play a role in weakening the enamel and dentine structure in the bucco-cervical region, rendering the area more susceptible to fracture, aiding lesion formation (Romeed et al., 2012).

A major complication in everyday dental practice is failure of dental restorations. Reports have shown that about 60% of all operative dental workload is related to placement and replacement of restorations (Mjor et al., 1990, Angeletaki et al., 2016). Appropriate material selection and manipulation and proper technique may be considered the key factors that lead to restoration success or failure (Lange and Pfeiffer, 2009, Angeletaki et al., 2016). Stress behaviour of the tested material is highly dependent on the load configuration and the physical properties of the material (Morin et al., 1988b, Manhart et al., 1996, Abu-Hassan et al., 2000). Various restorative materials have been involved in the fabrication of occlusal onlays and inlays including gold alloys, composite resins, and ceramics and some were tested in this study.

Both experimental and numerical techniques are common tools for strain assessment. Strain gauges have long been applied in dentistry to record surface strain with great success (Morin et al., 1988a, Versluis et al., 1996, Sim et al., 2001, Soares et al., 2008a, Santos-Filho et al., 2014, Barcelos et al., 2017). While, FEA is an engineering tool for analysis of stresses in complex structures. It has been applied in dentistry to measure stress distribution pattern in different tooth layers and restorations (Srirekha and Bashetty, 2010, Guimarães et al., 2014, Soares et al., 2015, Zeola et al., 2015, Machado et al., 2017). In this study, strain was measured by strain gauges, while, the finite element analysis model calculated the biomechanical behaviour of the human tooth and restorations under static load. FEA uses von Mises stresses to compare the calculated equivalent strain to the yield stress of each material. The analysis was performed on 9 different erosive and restorative steps on a computer tomography based

dental model of a mandibular first molar. The results should be useful in guiding dentists in their restoration of severely eroded teeth (molars) and the best material choice.

The null hypotheses were that:

- Different degrees of erosion and erosion restored with different restorative materials do not influence strain in molar teeth,
- Strain generated following occlusal and buccal erosion, does not produce a different pattern,
- There would be no correlation in strain measured using the three different techniques.

3.2 Material and Methods- Chapter 3:

50 human mandibular 3rd molar teeth were collected, cleansed and mounted vertically in epoxy resin (refer to Page 91, 92). Teeth were selected with similar dimensions, by measuring the buccolingual and mesiodistal width at the height of contour and the cervico-occlusal length in millimetres using a digital calliper (Moore & Wright MC MW110-15DBL 0-150 mm, Sheffield, UK), to verify they were within the following means ± SD: (B-L= 9.2 mm, M-D= 9.8 mm) ± 0.1 SD). Samples were divided into 2 main groups according to the site of the erosive lesion [occlusal (n=40) and buccal (n= 10)]. Occlusal group was divided into 4 further groups according to the restorative material used (n= 10) [bonded gold onlay (BG), non-bonded gold onlay (NBG), bonded IPS e.max® Press onlay (IPS), and bonded direct occlusal composite onlay (OC)]. While, the buccal group was restored with direct buccal composite resin (BC).

3.2.1 Sample size Determination- Strain Experiments:

In the following occlusal loading experiments to study strain in teeth, samples were divided at random into groups of 10 teeth. To determine the sample size, two aspects were considered; review of relevant literature (Soares et al., 2008c, Schlichting et al., 2011, Valdivia et al., 2012, Bassir et al., 2013b, Seow et al., 2015), and analysis of pilot study results to provide 80% power at the 5% level of significance.

3.2.2 Sample Preparation:

3.2.2.1 Occlusal Erosion Samples:

The cervical one third of each tooth was sealed with 2 layers of nail varnish, creating a 3mm band above the CEJ (**Figure 3.1**). Silicone putty impression was used to produce a reference key of the original occlusal anatomy for all samples (**Figure 3.2**), except the direct occlusal composite onlay (OC) group where the occlusal anatomy was recorded using a “suck-down” 0.9mm polymeric sheet (Sof-Tray, Ultradent Products, Inc) vacu-formed by a vacuum former (Ultra-Form; Ultradent) over the samples forming polymeric shell cavities as reference keys (**Figure 3.3**).

Figure 3.1: Mounted molar sample with cervical nail varnish band.

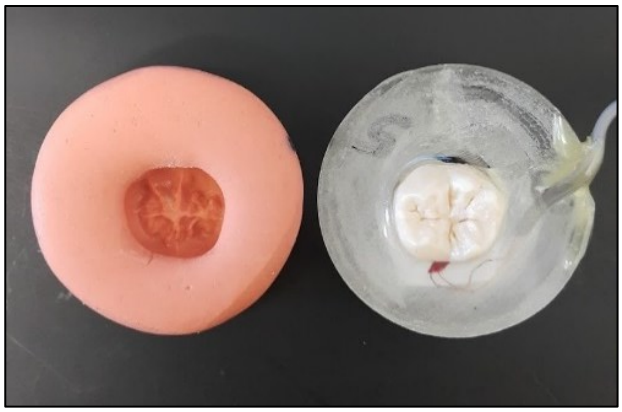

Figure 3.2: Silicone putty reference key duplicating the crown of a sound sample.

Figure 3.3: Plastic vacu-formed polymeric shell duplicating the crown of a sound sample.

3.2.2.2 Buccal Erosion Samples:

A buccal window measuring 10mm x 8mm (width x height) extended occlusally from the CEJ. The lesion was drawn by a pencil with rounded corners to resemble a cervical Cl V lesion. All the crown remaining areas surrounding the lesion were sealed by applying 2 layers of nail varnish (**Figure 3.4**). For each

sample, silicone putty impression of the buccal surface was made to produce a reference key.

Figure 3.4: Sound molar with buccal erosion window created by nail varnish sealing.

3.2.3 Erosive phase:

Samples of both groups underwent an extended 14 day accelerated soft drink erosive protocol (SANS= Sound accelerated erosion with no saliva). Samples were strain tested at baseline, 1 day, 7day, 10 day, and 14 day erosion. The created erosion lesion depths were measured to be (0µm, 100 µm, 600µm, 850µm, and 1300µm), respectively, as measured earlier (**Figure 2.12**). The created occlusal and buccal lesions formation steps are shown in **Figure 3.5**, **Figure 3.6**. Wet cotton pellets were placed on top of the samples to keep them moist in a humidor at room temperature until restoration.

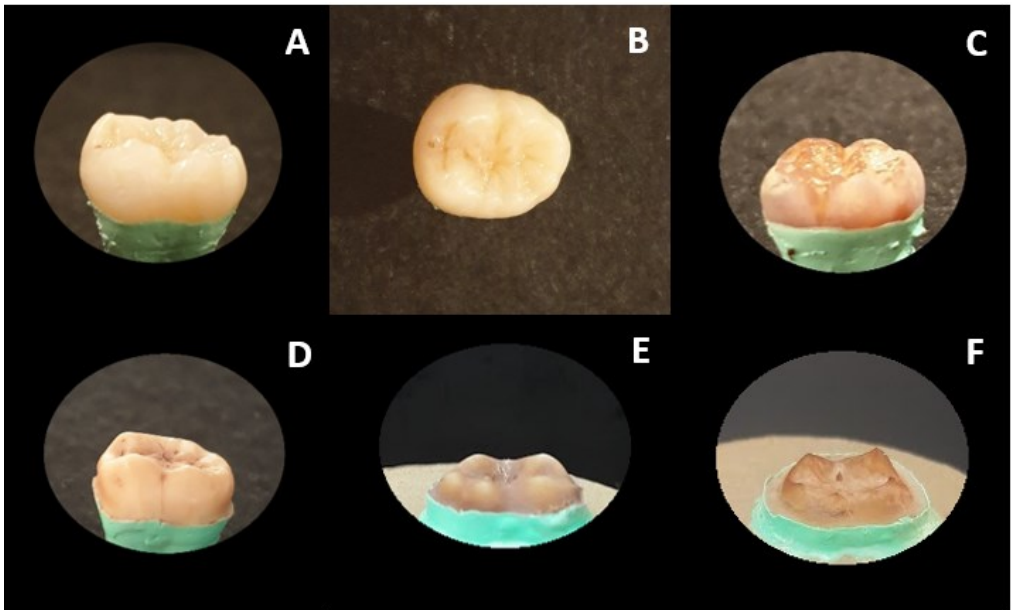

Figure 3.5: Occlusal erosion lesion formation steps. (A) Sound sample- buccal view, (B) sound sample- occlusal view, (C) 1 day erosion, (D) 7 day erosion, (E) 10 day erosion, and (F) 14 day erosion.

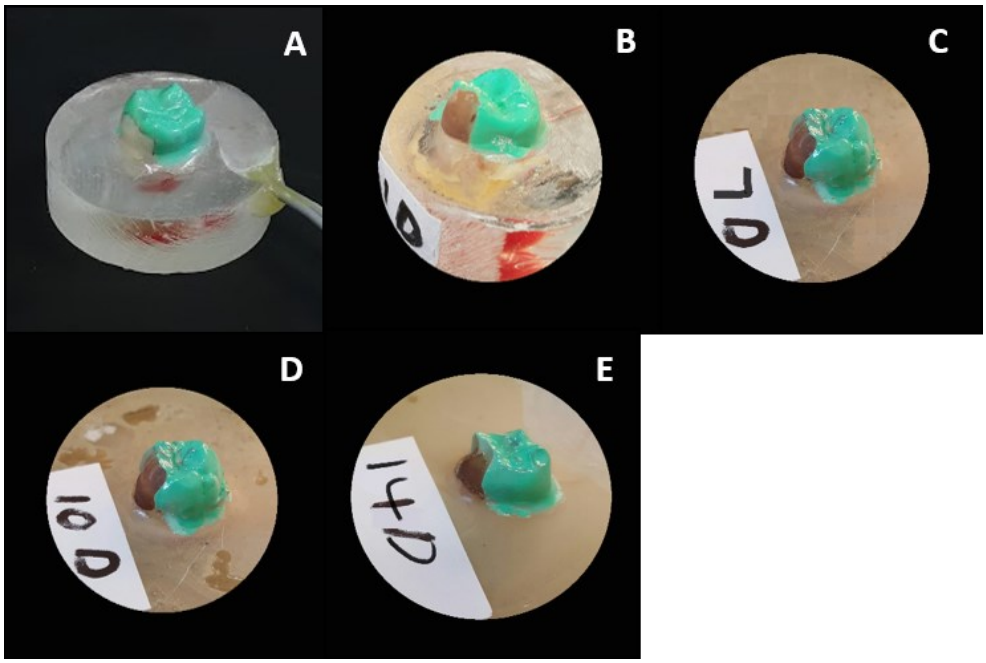

Figure 3.6: Buccal erosion lesion formation steps. (A) Sound sample, (B) 1 day erosion, (C) 7 day erosion, (D) 10 day erosion, and (E) 14 day erosion.

3.2.4 Restorative phase:

3.2.4.1 Occlusal Erosion Samples:

After 14 days of erosion the created lesion on the occlusal surface resembled a full occlusal surface onlay preparation with a circumferential chamfer-like finish line (**Figure 3.7**). The prepared samples of all groups except the direct occlusal composite onlay (OC) were duplicated with a silicone duplicating material (Accusil, Garreco, Germany) (**Figure 3.8**). To create working dies, the silicone moulds were poured in gypsum die stone (Talladium, Inc, California, USA) (**Figure 3.9**). The stone dies were treated with die hardener (Die hardener; Yeti Dentalprodukte GmbH Engen, Germany) and 2 coats of die spacer (colour Spacer red; Yeti Dentalprodukte GmbH, Engen, Germany) in accordance with the manufacturer's recommendations, starting 1.0 mm above the finish line to obtain a cementation space of about 30 µm. Onlay wax build-ups were completed using Inlay casting wax (GEO model wax avantgarde occlusal opaque mint, Henry Schein Europe) guided by the previously generated silicone keys (**Figure 3.10**). Wax patterns were finalized, re-marginated under high magnification (20x), and sprued ready for casting (**Figure 3.11**).

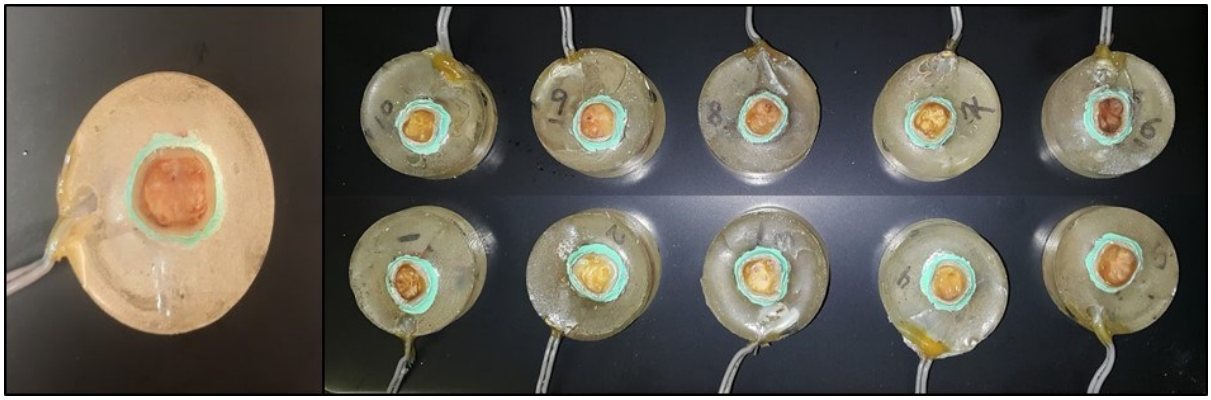

Figure 3.7: Occlusal 14 day erosion lesion (occlusal view) with a chamfer-like finish line.

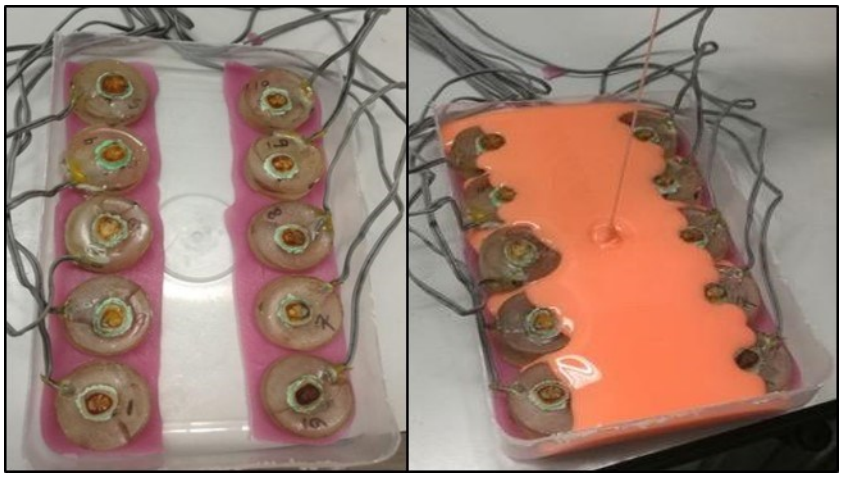

Figure 3.8: Prepared sample duplication.

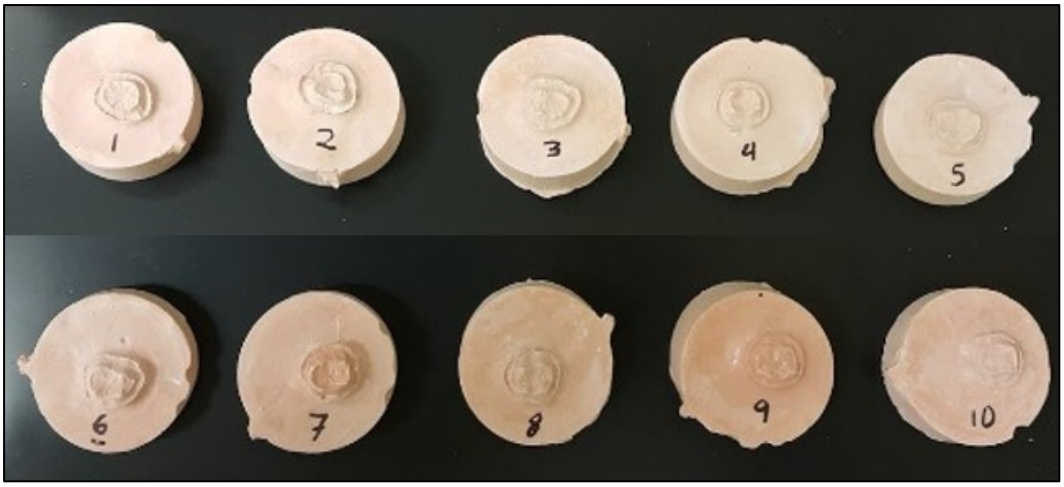

Figure 3.9: Stone dies duplicating prepared samples.

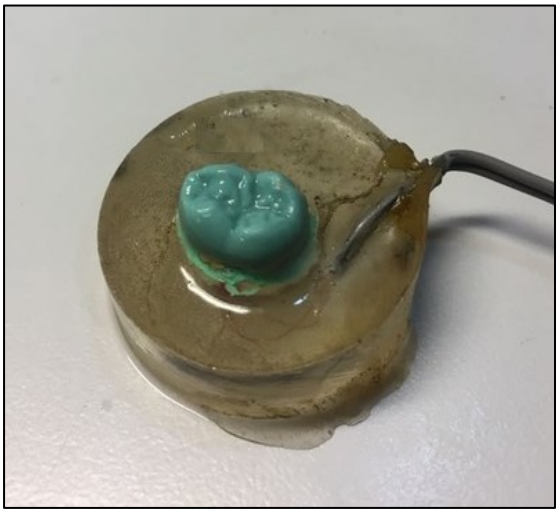

Figure 3.10: Occlusal onlay wax build-up.

Figure 3.11: Sprued occlusal onlay wax patterns.

3.2.4.1.1 Gold Onlays [bonded (BG), non-bonded (NBG)]:

The sprued onlay wax-patterns were attached to the crucible former of the investing ring (**Figure 3.12**). The investing ring was lined with asbestos ring liner to allow expansion of the investment during setting. The sprued wax patterns were sprayed with debubblizer (Debubblizer, Kerr, USA) and allowed to dry before being invested in a vacuum mixed carbon free phosphate bonded investment (Hi-Temp, Whip Mix Corp., Louisville, KY) and left to set. The investment ring was heated up to 900˚C for wax burnout. The preheated casting ring was then placed into a broken-arm centrifugal casting unit (Kerr Centrifico, Kerr Manufacturing Corp., Romulus, MI) where ingots of type III white gold alloy suitable for metal-ceramic restorations (PG-52X; Baker Dental Corp, Lake Zurich) for (NBG) onlays, and type II yellow alloy (Argenco bio light; Baker Dental Corp, Lake Zurich) for (BG) onlays. Gold ingots were heated to the casting temperature of (1450, 1055) ºC for (NBG, BG) respectively, and injected into the created mould. After 2-3 min the casting ring was quenched in warm water. The casting was then divested, cleaned, and desprued. Gold onlays were then finished with stones and polished using Shofu Gold Polishing HP Kit, (Shofu, Japan) and brushed with tripoli and red rouge. The finished castings were checked for fit on their respective stone dies using a fit checker (Occlude, Aerosol Indicator Spray, Pascal Company, Inc., Washington, USA) and adjusted using diamond burs (HP medium round diamond & HP medium round taper diamond) (Brasseler, Savannah, GA, USA). The final gold onlays (**Figure 3.13**) were steam-cleaned to remove the fit checker remnants.

Figure 3.12: The sprued wax patterns of gold onlay (NBG, BG) attached to the crucible former at the base of the investment ring.

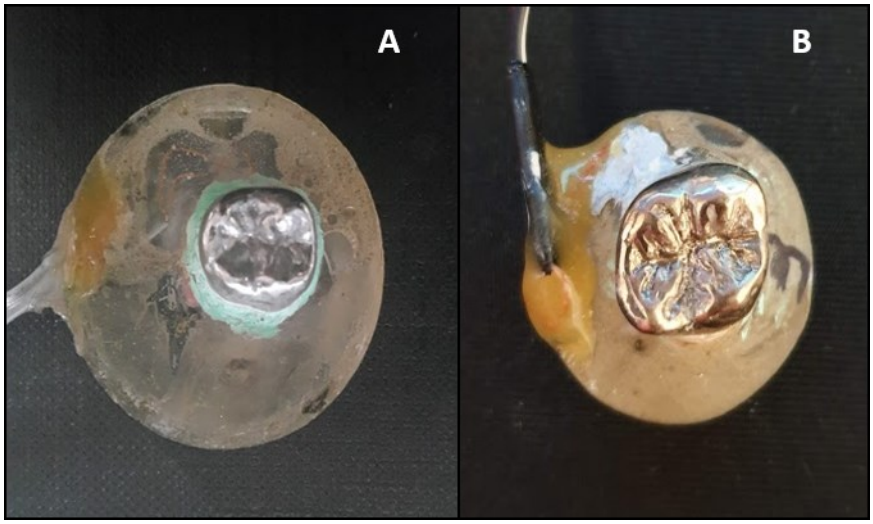

Figure 3.13: Finished and polished gold onlays fitted on their respective samples. (A) Non-bonded white gold and (B) Bonded yellow gold.

3.2.4.1.2 IPS e.max® Press onlays (IPS):

The finished onlay wax patterns were secured into IPS multi-investment ring base. The sprued wax patterns were invested in phosphate-bonded investment (GC MultiPressVest, GC EUROPE). The investment ring was heated up to 750˚C to burn-out the wax. The ceramic ingots (IPS e.max® Press Low Translucency-LT, Shade B1, Ivoclar Vivadent, Schaan, Liechtenstein) were next placed inside the pre-heated investment ring with the preheated pressing plunger and transferred into the pressing oven (Ivoclar Programat EP 3000, Ivoclar Vivadent, Schaan, Liechtenstein) at 915˚C to complete the ceramic pressing process. The pressed ceramic restorations were then divested, cleaned, and desprued. Ceramic onlays were then finished with diamond finishing burs (Composhape, Intensiv, Viganello-Lugano, Switzerland) and polished with rubber wheels and discs using a slow speed motor (Brasseler ceramic polish kit, Savannah, GA, USA). The finished onlays were checked for fit on their respective stone dies using a silicone pressure indicator paste (Fit Checker, GC, Japan) and adjusted using diamond burs. Onlays were then steam-cleaned and air-dried ready for cementation (**Figure 3.14**).

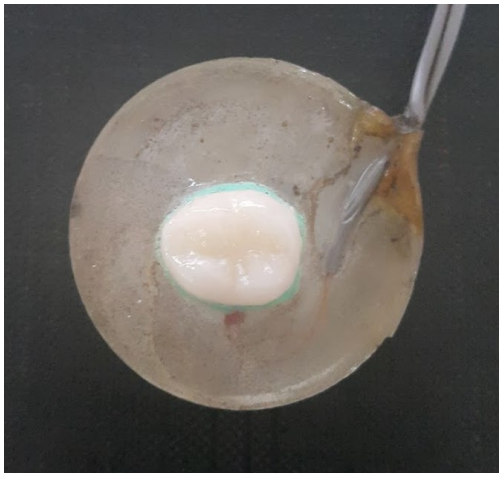

Figure 3.14: A finished and polished IPS empress onlay fitted on its respective sample.

3.2.4.1.3 Direct Occlusal Composite Onlays (OC):

All samples were further prepared to receive composite resin restorations according to the manufacturer's instructions for 2 step dental bonding. Samples were polished with prophy brushes and rubber cups with pumice in preparation for bonding. Samples were rinsed and dried then acid-etched (total etch technique of the entire cavity surface including enamel and dentine) using 32% phosphoric acid gel (Scotchbond™ Universal Etchant, 3M ESPE, St. Paul, MN, USA) for 15 sec. The cavities were then rinsed thoroughly for 20 sec and dried with water-free and oil-free air for 10 sec without over-drying. A bonding agent (Scotchbond™ Universal Adhesive, 3M ESPE, St. Paul, MN, USA) was applied and rubbed in gently for 20 sec, air dried for approximately 5 sec to evaporate the solvent, then light cured for 10 sec with a LED curing gun (wavelength range: 450-470 nm, intensity from 1100 mW/cm^2 to peak of 1330 mW/cm^2, Demi Plus, Kerr, USA). Composite resin (Filtek™ Z250, Shade B2, 3M ESPE, St. Paul, MN, USA). Build-

up of the 1st 2mm layer of composite material over the entire occlusal surface was achieved and light-cured for 40 sec. Subsequent layers were built incrementally and shaped by adapting the previously fabricated plastic key over the tooth (**Figure 3.15**). Excess composite was allowed to flow through a venting hole prepared on the top of the plastic keys and light-cured duplicating the original occlusal anatomy. The plastic mould was then stripped off and composite resin onlay was finished and polished (**Figure 3.16**).

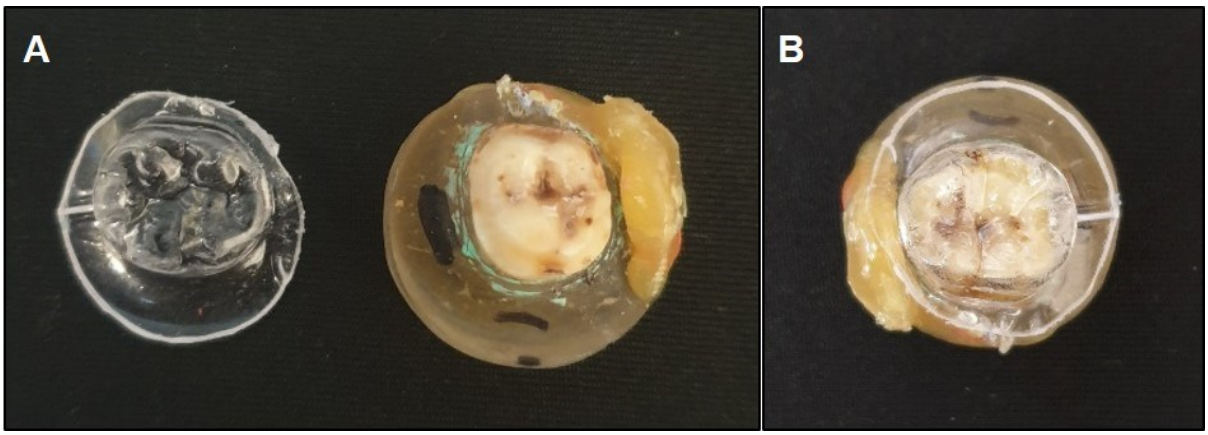

Figure 3.15: Composite build up guiding apparatus. (A) Plastic shell reference key and eroded sample, (B) plastic shell reference key adapted over sample for guided occlusal composite build-up.

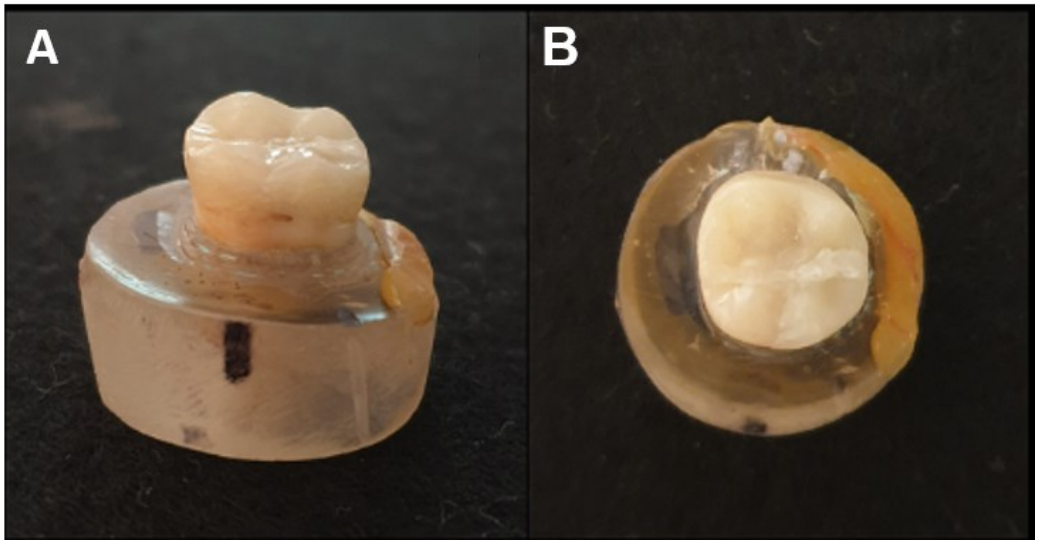

Figure 3.16: Finished and polished occlusal composite build-up. (A) Buccal view, (B) occlusal view.

3.2.4.2 Buccal erosion samples:

3.2.4.2.1 Direct Buccal Composite (BC):

The resultant lesion resembled a large Cl V lesion exposing dentine. Samples were polished with prophy brushes and rubber cups with pumice, rinsed, and dried in preparation for bonding. Etching and bonding following the same previously mentioned technique for direct occlusal composite onlay. Incremental composite resin 2mm thick layers were added in until full buccal contour was achieved as indicated by the buccal putty index. The final restoration was finished and polished (**Figure 3.17**).

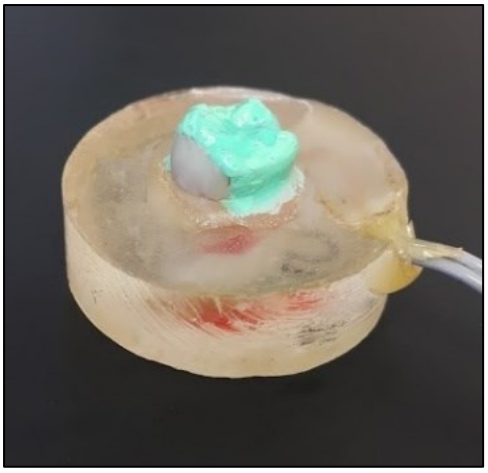

Figure 3.17: Finished and polished direct buccal composite restoration.

3.2.4.3 Onlay Cementation:

PANAVIA 21™ OP (Kuraray Co, Kurashiki, Japan) was used to cement all onlays. Prior to cementation, preparation of both the tooth surface and the intaglio surface of the gold and ceramic onlays took place. However, different treatments were required for different onlay material used.

3.2.4.3.1 Pre-cementation Treatment of Tooth Surface:

All eroded occlusal tooth surface was etched using PANAVIA ETCHING AGENT V (35% phosphoric acid) (PANAVIA 21™ OP, Kuraray Co, Kurashiki, Japan) for 30 sec followed by washing for 10 sec and drying. One drop of each ED PRIMER Liquid A and Liquid B was dispensed into the well of the mixing dish and mixed for three to five sec. The mixture was applied with a small sponge

pledget onto the prepared tooth surface and left for 60 sec. A gentle stream of air was then sprayed to evaporate the volatiles until the surface appeared glossy.

3.2.4.3.2 Pre-cementation Treatment of Gold Onlays:

The intaglio surface of both (NBG) and (BG) gold onlays was sandblasted with 50μm aluminum oxide particles at an air pressure of 4 kg/cm^2 (~60 PSI) for 2-3 sec per cm^2 to achieve a matt finish surface. The onlays were washed in a stream of water for one minute then ultrasonically cleaned for 2-3 min in a neutral detergent solution, before being washed and dried. For (BG) gold onlays, heat treatment took place. The oxidation cycle of 400˚C for 4 min was applied followed by painting the intaglio surface with a metal primer (Alloy Primer, Kuraray, Kurashiki, Japan) to enhance the bond strength of the alloy to the resin cement.

3.2.4.3.3 Pre-cementation Treatment of IPS e.max® Press Onlay:

The restorations were thoroughly rinsed for 30 sec with water spray and dried for 10 sec with water- and oil-free air. A self-etching ceramic primer (Monobond Etch & Prime, Ivoclar Vivadent, Schaan, Liechtenstein) was applied onto the adhesive surface of the restoration using a microbrush, agitated into the surface for 20 sec, and allowed to react for another 40 sec. The surface was then thoroughly rinsed off with water for 20 sec and dried for approximately 10 sec. This ceramic primer is a single-component containing ammonium polyfluoride and

silane to allow etch and silanate glass-ceramic surfaces in one step. Therefore, the need for using hydrofluoric acid etchant is eliminated.

3.2.4.3.4 Preparation of PANAVIA 21™ OP Cement:

Equal amounts of PANAVIA 21 Catalyst and Universal Pastes were dispensed and mixed for 20-30 sec spreading the mix thinly over the mixing pad until a smooth uniform paste resulted. A thin layer of the mixed paste was applied to the adherent surface of the restoration only, being careful to avoid trapping air bubbles. The onlays were seated on their respective teeth and held with static vertical finger pressure of 60N (≈ 6kg) for 3 min measured by a counting bench scale (Cruiser CCT8, Adam's Equipment, UK) placed under the die. Meanwhile, excess cement was removed with a small brush. OXYGUARD II was then applied to all restoration margins with a small brush and left for 3 min until the cement was completely set. Any excess was removed with a sharp probe.

3.2.5 Strain Measurement:

Strain measurements of the eroded teeth in each group were repeated at 0, 1, 7, 10, and 14 days and post restoration application. Strain measurements in all occlusal erosive and restorative steps were tested by two methodologies: strain gauges and finite element analysis (FEA). While, electronic speckle pattern interferometry (ESPI) was applied to occlusal erosive stages only. Buccal erosion group was tested by strain gauges only.

3.2.5.1 Strain Gauge Attachment and Loading Protocol:

One strain gauge (Micro-Measurements Group UK Ltd) attached to copper leads, with a resistance of 120Ω (type C2A-06-062LW-120), and a gauge factor of 2.15 was positioned at the buccal surface of each tooth 1 mm above the CEJ (Machado et al., 2017) (**Figure 3.18**). Care was taken to align the gauges vertically along the long axis of the tooth so that they were parallel to the direction of loading. The enamel surface of each sample was prepared by etching with 37% phosphoric acid (Heraeus, i Bond Etch 35 Gel, Germany) for 30 sec. The surface was washed with water for 20 sec and dried with a stream of air for 10 sec. The backing of each strain gauge was bonded to the prepared buccal wall of molars with a thin layer of cyanoacrylate adhesive (M-Bond 200 Adhesive; Micro-Measurements Group UK Ltd). After the adhesive had set, the gauges were covered with a thin layer of a silicone rubber protective coat against moisture contamination (M-COAT C, Micro-Measurements Group UK Ltd). To guarantee moisture control and stability around strain gauges, a groove was prepared in the resin mounting-block to house the leads of the strain gauge. Another layer of epoxy resin was poured over the site to seal the leads (**Figure 3.18**). The strain gauges were connected to the strain indicator (Vishay Measurements Group, Raleigh, North Carolina) in a half bridge configuration. To complete the bridge and compensate for dimensional changes related to temperature fluctuations due to local environmental alterations or the gauge's electrical resistance, a dummy gauge was mounted on an untreated unloaded tooth under the same environmental conditions. The strain indicator settings were initiated by entering

the gauge resistance and connecting both sample and dummy leads. The bridge circuit was balanced to zero baseline reading and allowed to set for 20 sec before loading began.

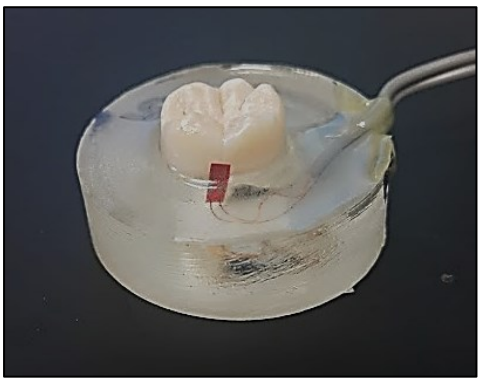

Figure 3.18: Strain gauge attached to the buccal surface of a molar.

For strain measurement, static vertical loading was ramped within physiological limits for the human dentition from 5 N to 130 N and back to 5 N with 25 sec dwells at 50 N, 70 N, 90 N, 110 N, and 130 N. The load was introduced into the central fossa of the molars using a 2.5 mm stainless steel ball bearing. A small pre-load of 5 N was used to hold the experimental setup in place before the test started and after the test ended. Three cycles were completed for each sample to verify results. There was a 30 min delay between testing cycles (Pereira et al., 2013). Central loading was verified at the beginning of each cycle of testing. The resin block containing the specimen was screwed into a servohydraulic testing machine receptacle (Dartec series HC10, Dartec Ltd) with a 1.0 kN load cell. The loading program was initially set in the test machine. Gradual loading and unloading cycles were controlled by the testing machine software (Workshop 96. Dartec HC10; Zwick Ltd). Samples were subjected to

gradual loading and unloading cycles and strain values were recorded at peak load (130N).

3.2.5.2 Setting-up the Electronic Speckle Pattern Interferometry (ESPI) Assembly:

A phase-shifting electronic speckle pattern interferometer was constructed to measure the strain pattern in the occlusal erosion group (**Figure 1.1**, **Figure 3.19**). A 75 mW He–Ne laser beam (wavelength λ = 632.8 nm) (Cl IIIb He-Ne laser, Melles Griot, California) was used as a source of illumination. A polarizing beam-splitter was used to split the beam into two beams. One beam served as a (reference beam) and was directed to the CCD camera (JAI CV-M2, Japan) with 1200x1600 pixels and 10 bits resolution. The other beam was passed through a piezoelectric translator (PZT) (Piezoelectric actuator (Ae0203D04F), Thorlabs Inc, US), (MDT694B Single Channel, Open-Loop Piezo Controller, Thorlabs Inc., US) controlled mirror to enable small path differences to be introduced in a controlled fashion. The resultant beam was used to illuminate the surface of the specimen (object beam). The specimen was secured into a loading apparatus and sprayed with a white matte crack detection spray (Rivelex 200 Rilevatore Bianco, Italy) (**Figure 3.20**). The reflected light from the tooth surface was collected onto the CCD.

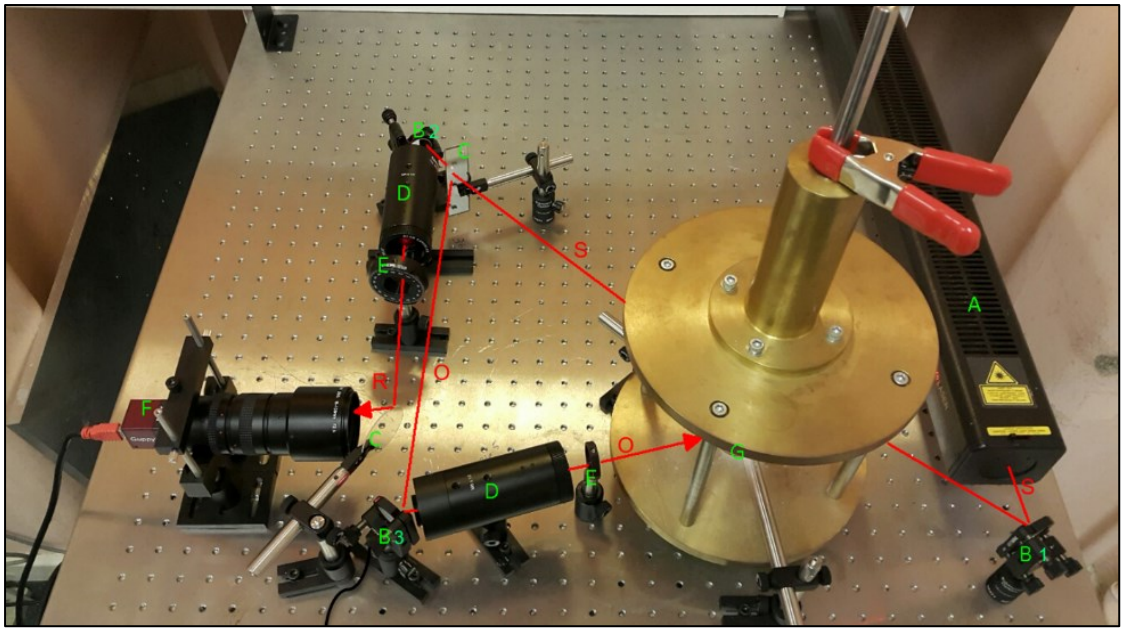

Figure 3.19: Out-of-plane displacement ESPI set-up. (A) He-Ne laser, (B1, B2) mirror, (B3) PZT-controlled mirror, (C) density filter/ beam splitter, (D) beam expander, (E) linear polarizer, (F) CCD camera, (G) sample, (S) source beam, (O) object beam, (R) reference beam.

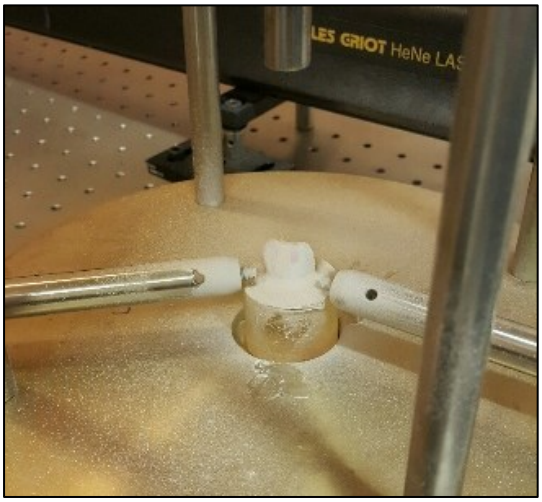

Figure 3.20: Sample surface prepared by matte spray coverage.

Subtracting the live image of the “deformed” tooth surface under loading at 130N from the image of the “undeformed” tooth surface, initially captured and

stored in the electronic memory, resulted in a fringe pattern. This pattern mapped the contours of phase difference between wavefronts (**Figure 1.3**). Matlab v.7 software (Mathworks, Natick, USA) was used to digitally unwrap the resultant phase maps and out-of-plane displacement was calculated.

3.2.5.3 Setting-up FEA:

3.2.5.3.1 FEA Model Generation:

A Skyscan 1172 X-ray high-resolution microtomography (micro-CT) system (Bruker microCT, Kontich, Belgium) was used to perform the scanning at a very high resolution in increments of 23.8 μm. The scan produces 821 Slices along the height direction of the tooth also in the thickness of 23.8 μm. Each slice contains 492 x 557 pixels. In order to obtain a scan that covers the whole tooth, the lower half of the sample was scanned and later stitched to the upper one. However, the resulting data were too detailed for the purposes of this study, so the resulting file resolution had to be reduced by scaling it down by a factor of 4. Essentially, the mean of every 8 pixels was calculated and combined into 1 pixel. The resulting picture had a resolution of 0.1mm for every pixel as well as a slice thickness of 0.1mm (**Figure 3.21**).

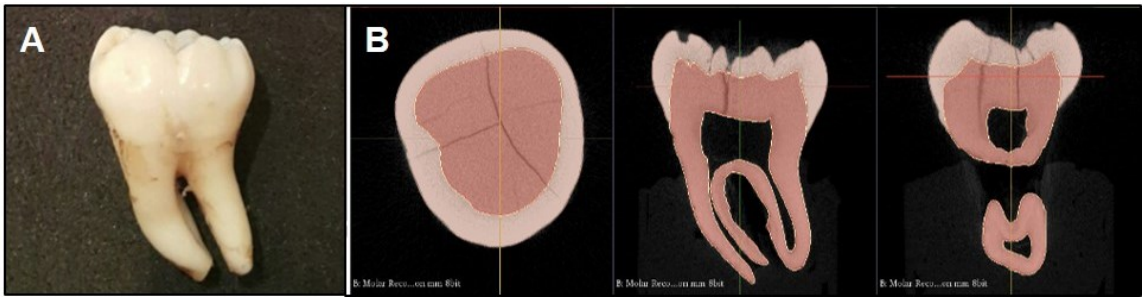

Figure 3.21: Scanning of a sound molar tooth by micro-CT. (A) Sound molar model, and (B) generated micro-CT scans.

3.2.5.3.2 CT to 3D reconstruction:

The CT scanned slices were imported into an interactive image control system (Slicer) to perform the segmentation of different hard tissues of the tooth based on image density thresholding. A 3D object was automatically created, refined, and exported into a stereolithography (STL) file format (**Figure 3.22**). This format captures only triangulated surface shell details and is widely used in 3D models (**Figure 3.23**).

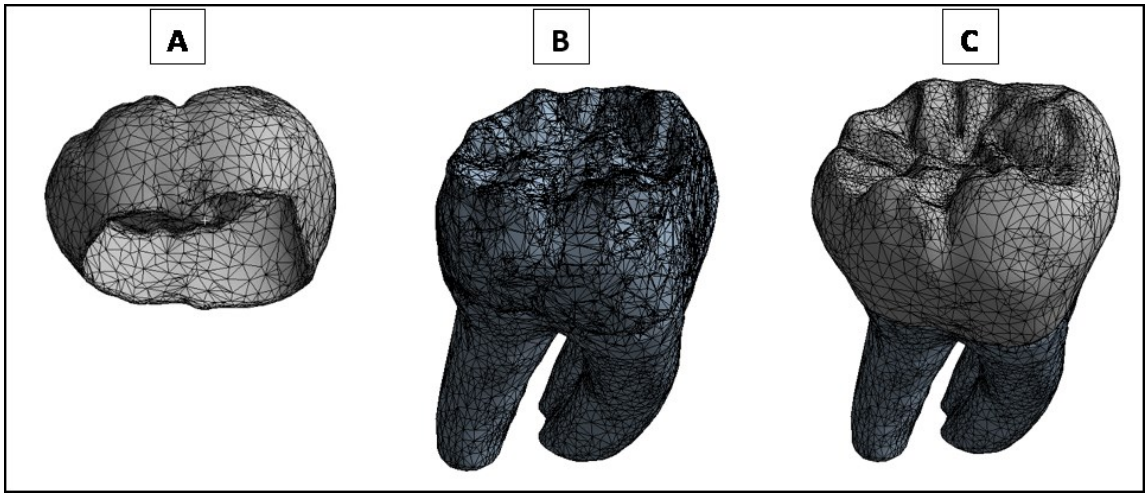

Figure 3.22: FEA model coarse geometry. (A) Enamel, (B) dentine, and (c) full (enamel+ dentine).

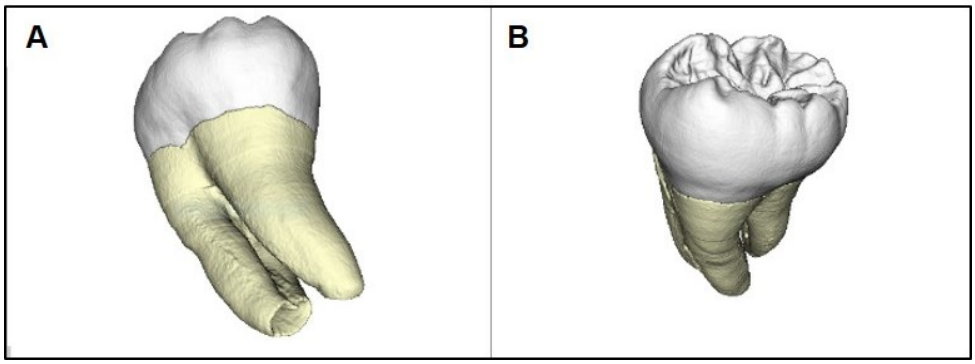

Figure 3.23: Final full FEA model after smoothing (A) apical view, (B) lingual view.

3.2.5.3.3 FEA Testing Set-Up:

After listing the appropriate material properties (**Table 5**), STL files were imported into a **FEA software package**, **ANSYS**™ which converted the shells into solid parts. The scanned sample did not contain the resin base so it was added in the FEA model. The FE model resulted in 183968 elements and 324714 nodes.

The under surface of the resin base and tooth roots were fixed for zero-displacement. The contact surfaces between the dentine and the resin base and between different domains of the tooth were considered to be bonded. The pulp was modelled as an empty cavity as its contents (blood vessels, nerves, connective tissues and cellular elements) are of very low modulus of elasticity (Abu-Hassan et al., 2000). Care was taken to ensure the orientation of the molar was upright as tilt of the model would result in a load at an angle. The orientation was corrected until symmetric strain was observed in the enamel.

A static finite element analysis was adopted in this study to predict the stress distribution generated in the tooth at each erosive and restorative condition. The

sample being analysed was not subject to changes with time such as fatigue. The model was prepared by uniformly slicing the enamel to the thicknesses eroded in the experiment. Multiple surfaces were manually constructed by offsetting the outer surface of the enamel for each erosion thickness. Offsetting involves copying every small triangle on the surface and moving them in a perpendicular direction where they are stitched back together completely to form the new surfaces. Then these surfaces are used to slice the enamel resulting in layers of consistent thickness, representing the erosion. The FEA strain values were also measured on all nodes corresponding to the 2mm x 2 mm surface where the strain gauge was fixed on the laboratory strain gauge test (at the buccal surface 1mm above the CEJ to allow comparisons. A small area was selected manually on the central fossa of the occlusal surface to represent the 2.5 mm ball contact area. The model was then run with a vertical load up to 130N at baseline and recorded for each erosive case (**Figure 3.24**). The 14 day occlusal erosion cavity model was restored to original form with different material properties according to the restoration group represented (**Table 5**). Equivalent stress criterion (von Mises) was used to perform stress distribution analysis.

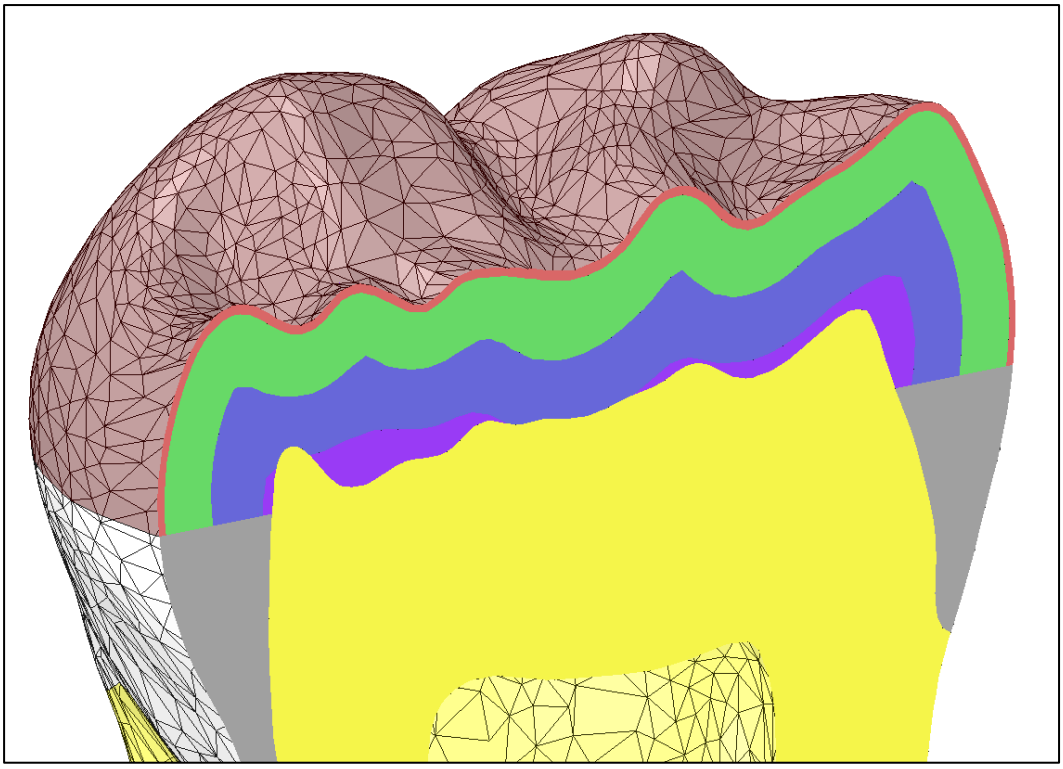

Figure 3.24: Model mid-section showing different eroded thicknesses in enamel. Brown= 1 day erosion (100μm), Brown+ Green= 7 day erosion (600μm), Brown+ Green+ Blue= 10 day erosion (850μm), Brown+ Green +Blue +purple= 14 day erosion (1300μm), Yellow= dentine, Grey= uneroded enamel, and patterned yellow= pulp chamber.

Table 5: Material Properties Used for FEA Model (elastic modulus, Poisson's ratio, and related references)

Material	*(E)* Modulus (GPa)	*(V)* Poisson's Ratio	Reference
Enamel	84.1	0.33	(Craig et al., 1961, Farah et al., 1977)
Dentine	18.6	0.31	(Farah et al., 1977, McGuinness et al., 1991)
Resin base	3.4	0.33	(Qasim et al., 2005)
Composite resin restoration	10.0[a]	0.24[b]	a: (Eldiwany et al., 1993, Magne, 2007) b: (Magne, 2007, Nakayama et al., 1974)
Type II gold alloy (bonded)	83	0.33	(Farah et al., 1989, Romeed et al., 2006)
Type III gold alloy (Non-bonded)	96.6	0.35	(Asmussen et al., 2005)
IPS impress	67.2	0.3	(Abe et al., 2001, Yamanel et al., 2009)
Panavia21 Cement	3	0.35	(Yi and Kelly, 2008)

3.2.6 Results- Chapter 3:

3.2.6.1 Strain Gauge Results:

Mean values and standard deviation of the overall deformation in occlusal and buccal groups were tested for all erosive and restorative phases at the load of 130N (n=10). For all occlusal groups, erosive and restorative data were analysed by SPSS two-way repeated measure ANOVA. Where significant differences were detected, a post-hoc test (Bonferroni) was used. All tests were performed at a 95% confidence level. While for the buccal group, one-way ANOVA and paired t-test were used for comparisons between before and after restorative procedure. Occlusal and buccal strain values at erosive and restorative phases are listed in (**Table *6***).

Occlusal erosive steps showed no significant strain change with loading when compared to the baseline except at 14 days erosion, where strain significantly dropped (**Table *6***), (**Figure 3.25**). However, between erosive stages, significant changes were observed only between 1 day and 7 days, and between 14 and both 1 and 10 days of erosion. As a behaviour pattern, strain showed a slight increase from baseline at 1 day erosion, followed by a decrease at 7 days, no change at 10 days, and a drop at 14 days (**Figure 3.25**). After restoring occlusal samples, all restorative groups were not statistically significantly different from the baseline or from each other with regards to strain. All restorative materials used

for occlusal onlays (NBG, BG, IPS e.max, and composite resin) were able to restore strain to the pre-treatment condition (**Figure 3.26**).

In contrast, a completely different behaviour pattern was observed with buccal erosion samples. All erosive steps recorded significant strain increase from the baseline reading (**Table *6***), (**Figure 3.25**). No significant changes were observed between erosive stages 1 and 7 days or between 10 and 14 days. However, a substantial increase of strain was recorded at 10 days with continued increase at 14 days, rendering strain values at both 10 and 14 days significantly higher than strain at 1 and 7 days (**Figure 3.27**). While, restoring buccal samples resulted in a significantly lower strain than 14 day erosion, producing strain level similar to baseline.

Table 6: Strain Values of Occlusal and Buccal Erosion Groups at All Erosive and Restorative Phases

Treatment/ Restoration	Occlusal groups strain (µstrain)	Buccal group strain (µstrain)
Baseline	207±55	195±56
1D	251±80	221±49
7D	193±70	235±64
10D	217±82	524±129
14D	146±81	533±133
NBG	158±90	-
BG	172±61	-
IPS	172±80	-
OC	168±81	-
BC	-	250±80

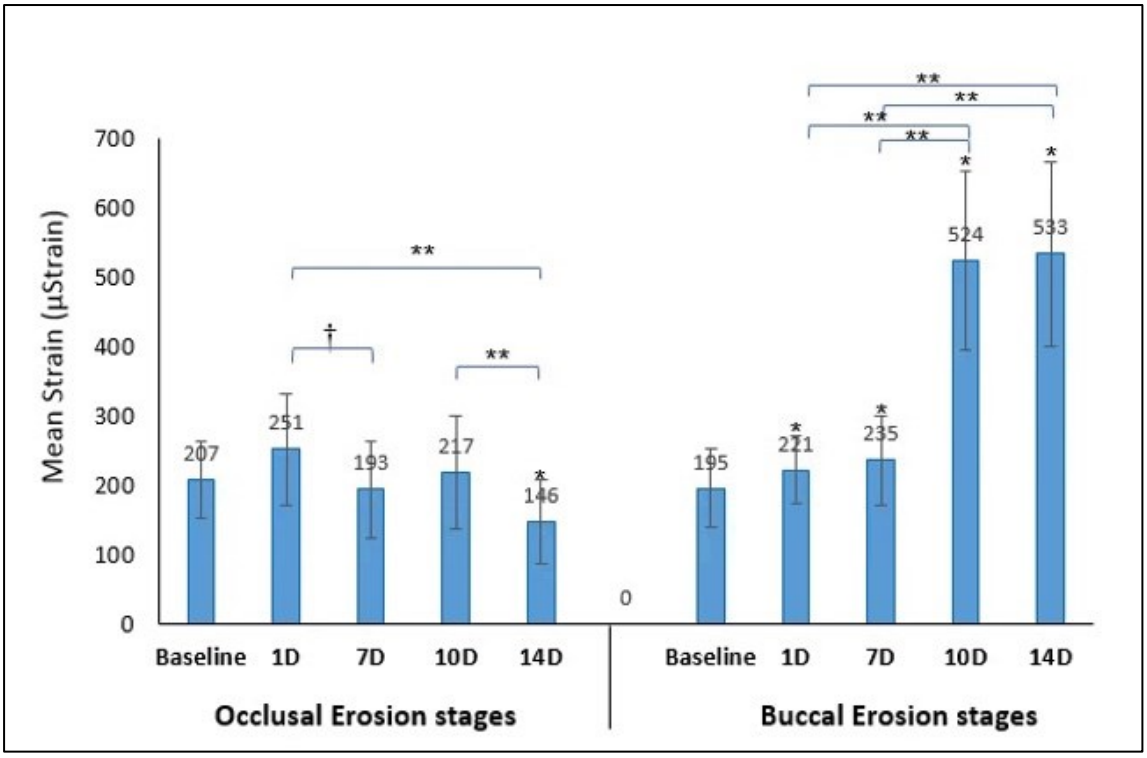

Figure 3.25: Mean strain values ± standard deviation with strain gauge testing for all erosive stages in occlusal and buccal groups. n=10 per group (*p< 0.05 statistical difference with respect to relative baseline), (**p<0.005 statistical difference between erosive groups), (†p<0.05 statistical difference between groups). (Baseline= sound tooth, 1D=1 day erosion, 7D= 7 day erosion, 10D= 10 day erosion, 14D= 14 day erosion).

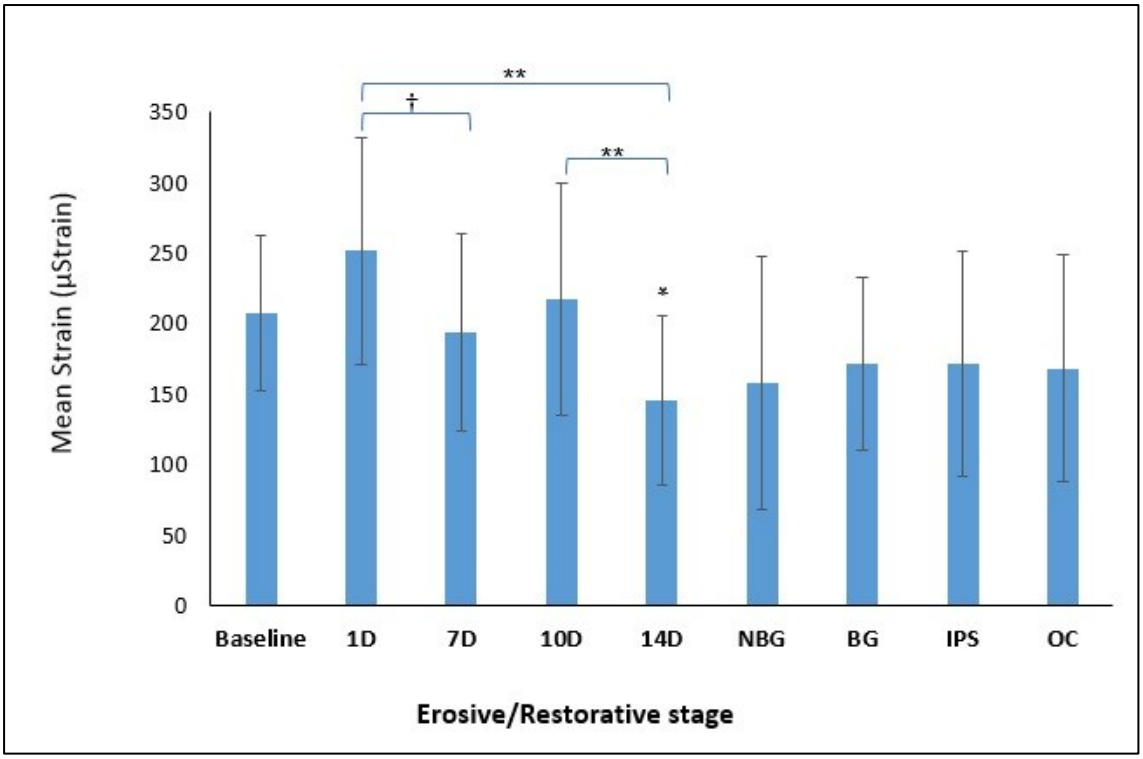

Figure 3.26: Mean strain values ± standard deviation with strain gauge testing of all erosive and restorative stages in occlusal groups. n=10 per group group (*p< 0.05 statistical difference with respect to baseline), (**p<0.005 statistical difference between erosive groups), (†p<0.05 statistical difference between erosive groups). (^p< 0.005 statistical difference between restorative groups). (Baseline= sound tooth, 1D=1 day erosion, 7D= 7 day erosion, 10D= 10 day erosion, 14D= 14 day erosion, NBG= Non-bonded gold onlay, BG= Bonded gold onlay, IPS= IPS e.max onlay, OC= occlusal direct composite onlay).

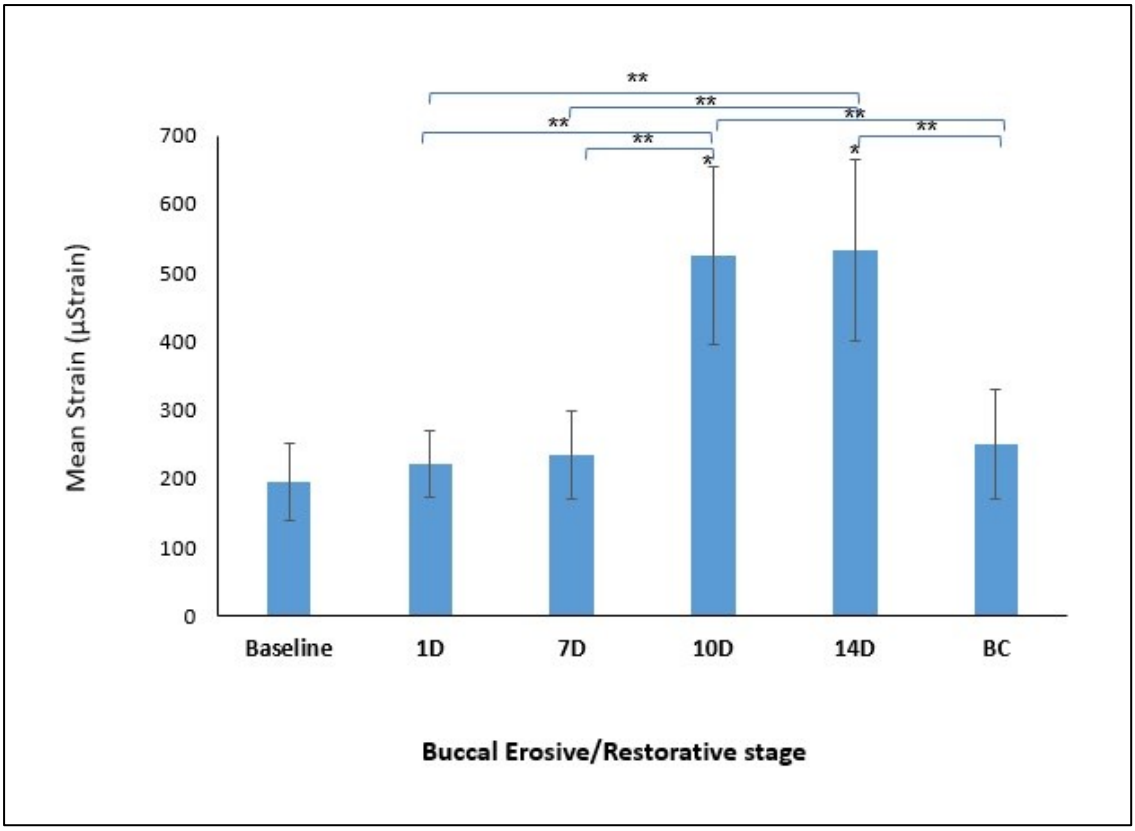

Figure 3.27: Mean strain values ± standard deviation with strain gauge testing of progressive erosive and the final restoration in buccal group. *n=10* per group (*p< 0.005 statistical difference from baseline), (**p<0.005 statistical difference between erosive groups). (Baseline= sound tooth, 1D=1 day erosion, 7D= 7 day erosion, 10D= 10 day erosion, 14D= 14 day erosion, BC= buccal direct composite restoration).

3.2.6.2 ESPI Results:

The deformation induced by loading was imaged on the buccal surface of each sample. The resulting phase maps are shown in (**Figure** (A) **Figure 3.28**, **Figure 3.29**, **Figure 3.30**, **Figure 3.31**, **Figure 3.32**). While the unwrapped phase maps are shown in (**Figure** (B) **Figure 3.28**, **Figure 3.29**, **Figure 3.30**, **Figure 3.31**, **Figure 3.32**), where zones of high strain intensity are represented by red colour, while zones of lower strain are blue. The mean displacement results of all erosion stages are plotted in (**Figure 3.33**).

The occlusal erosion stages tested by ESPI showed similar behaviour to SG results (**Figure 3.26**, **Figure 3.33**). With gradual loading, strain increased gradually at 1, 7, and 10 days then dropped at 14 days of erosion. All erosive phases were significantly higher strain than the baseline except the 14 day erosion. While, between groups, all were not significatly different from each other except the 14 days which was significantly lower strain than at all other times.

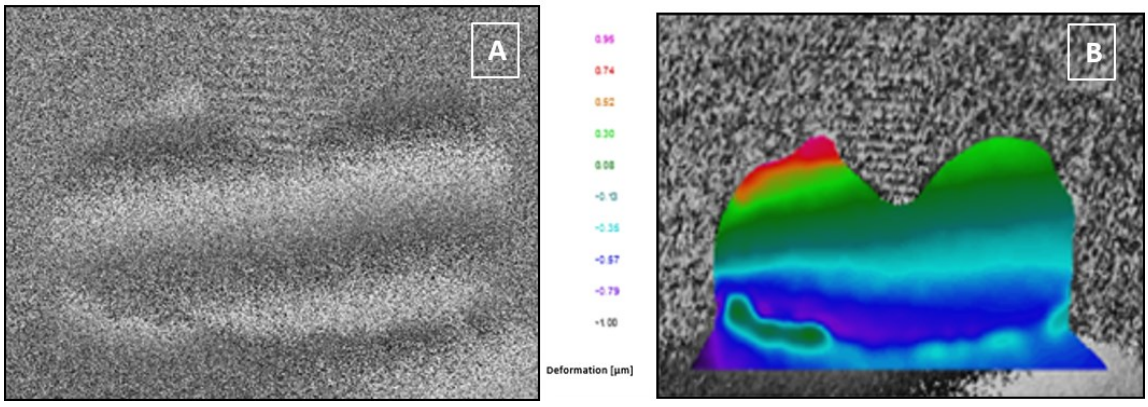

Figure 3.28: Baseline sound molar sample captured by ESPI under loading. (A) Resultant phase map showing wide spaced fringes, (B) heat map of the baseline unwrapped phase map indicating surface strain distribution.

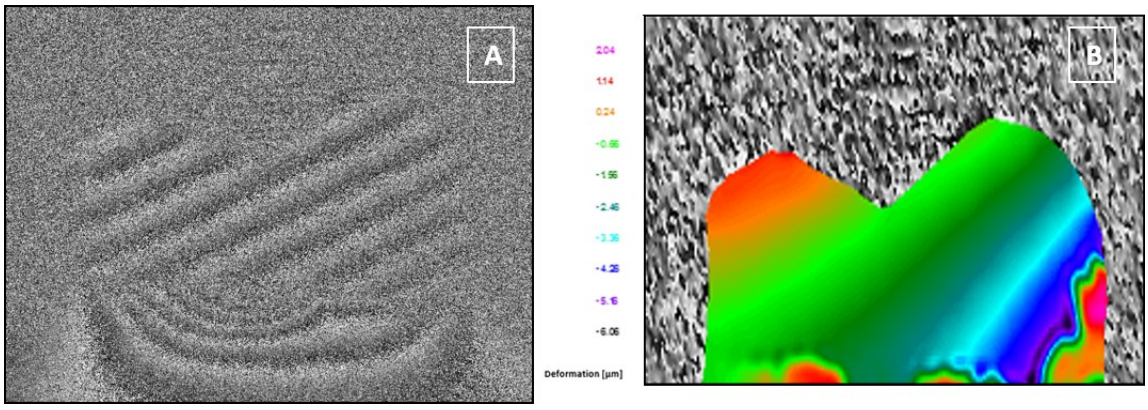

Figure 3.29: 1 Day erosion molar sample captured by ESPI under loading. (A) Resultant phase map showing closer fringes indicating higher strain than the previous stage, (B) heat map of the 1 day erosion unwrapped phase map indicating surface strain distribution.

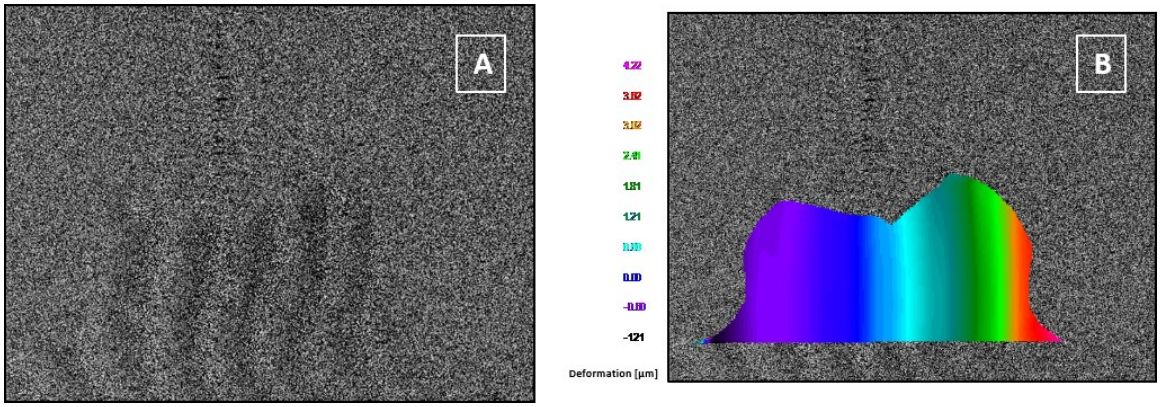

Figure 3.30: 7 Day erosion molar sample captured by ESPI under loading. (A) Resultant phase map showing wider spaced fringes than the previous stage indicating lower strain, (B) heat map of the unwrapped 7 day erosion phase map indicating surface strain distribution.

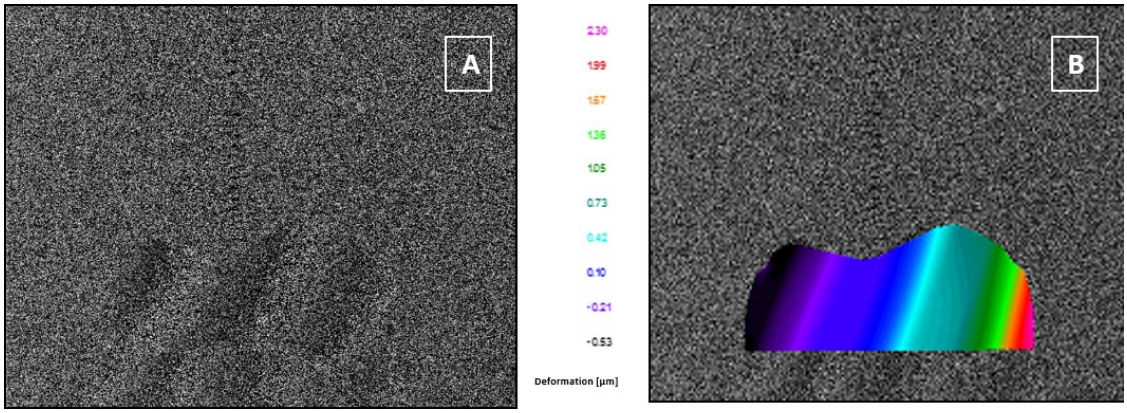

Figure 3.31: 10 Day erosion molar sample captured by ESPI under loading. (A) Resultant phase map showing wider spaced fringes than the previous stage indicating lower strain, (B) heat map of the unwrapped 10 day erosion phase map indicating surface strain distribution.

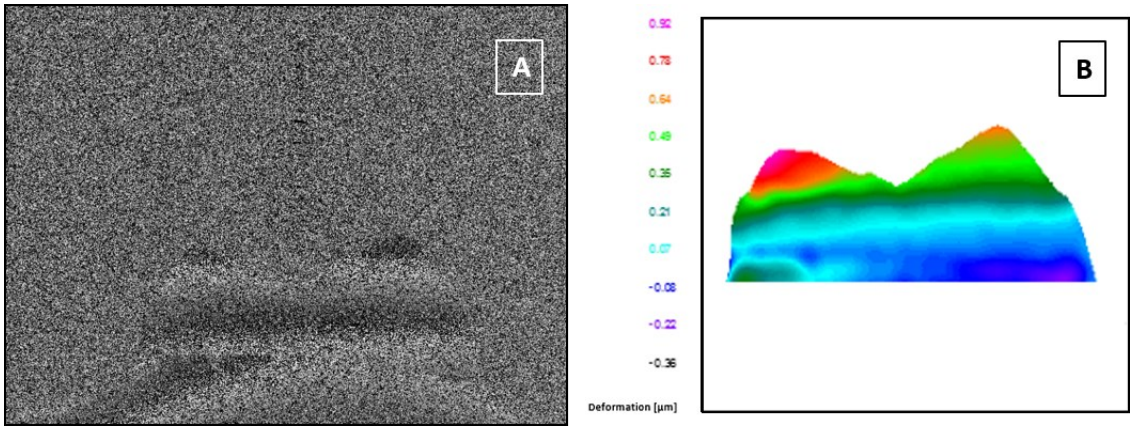

Figure 3.32: 14 Day erosion molar sample captured by ESPI under loading. (A) Resultant phase map showing wider spaced fringes than the previous stage indicating lower strain, (B) heat map of the unwrapped 14 day erosion phase map indicating surface strain distribution.

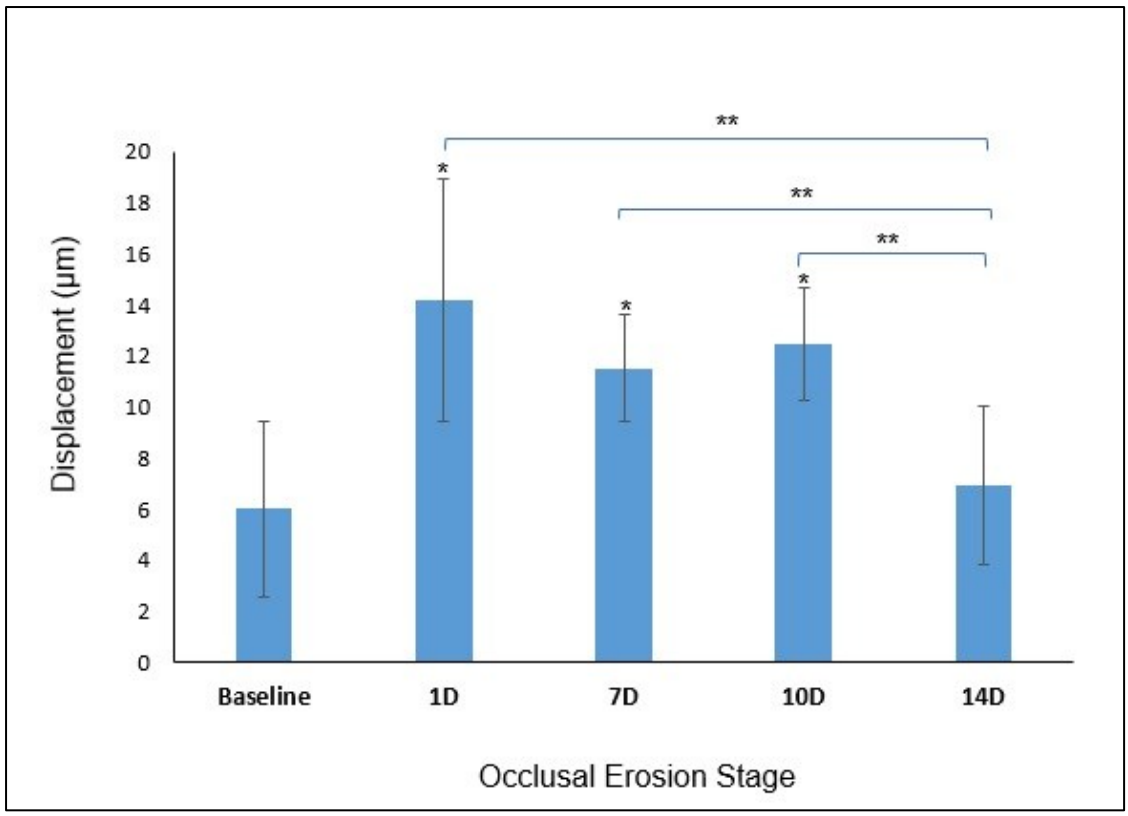

Figure 3.33: Mean displacement values ± standard deviation with ESPI testing for all occlusal erosive stages. *n=10* per group (**p*< 0.001 statistical difference to the baseline), (***p*<0.005 statistical difference between groups). (Baseline= sound tooth, 1D=1 day erosion, 7D= 7 day erosion, 10D= 10 day erosion, 14D= 14 day erosion).

3.2.6.3 FEA Results:

Two sets of data were obtained from the FEA. Von Mises stresses (MPa) show the distribution of strain in enamel and dentine at every erosive-restorative stage (**Figure 3.34**). Strain was also recorded on a virtual strain gauge (μstrain) simulating the position of the experimental gauges at the buccal surface of the crown above the CEJ to verify the experimental results at all erosive-restorative stages (**Figure 3.35**). These results confirmed the efficacy of the applied numerical model. Readings of the virtual strain gauge showed a similar behavioural pattern to the experimental gauges (**Figure 3.26**, **Figure 3.35**).

Internal and external strain distribution pattern can be better observed and understood in FEA loaded case models of all stages presented in (**Figure 3.36**, **Figure 3.37**, **Figure 3.38**, **Figure 3.39**, **Figure 3.40**, **Figure 3.41**, **Figure 3.42**, **Figure 3.43**, **Figure 3.44**).

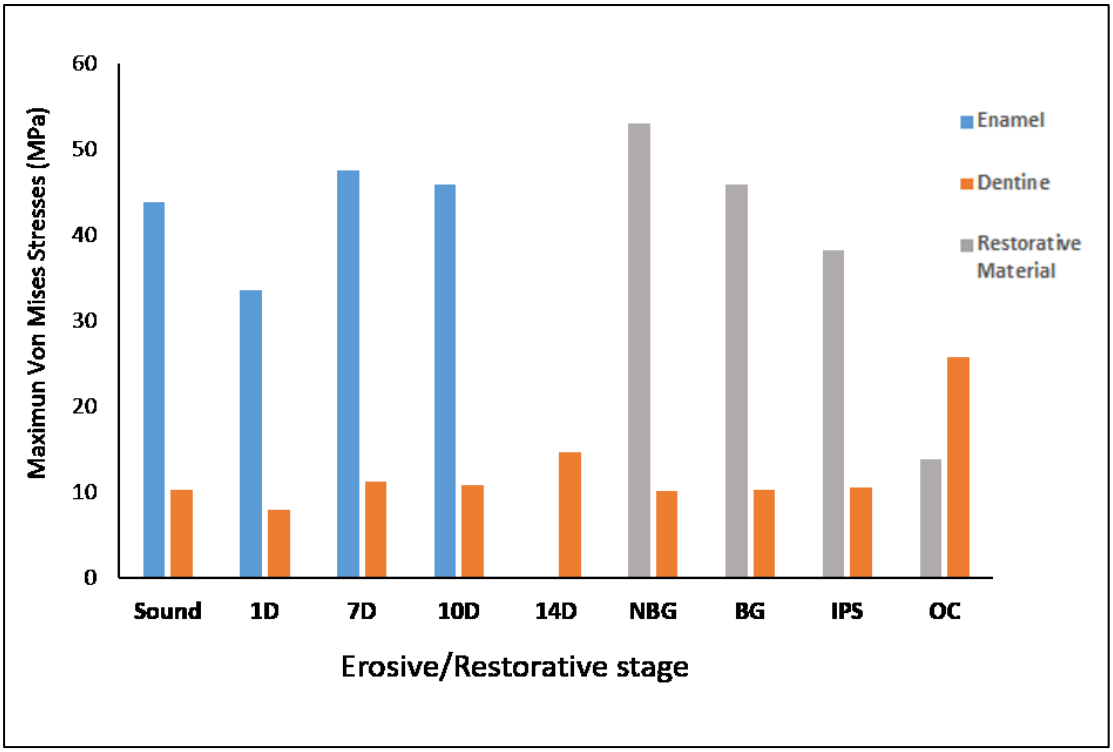

Figure 3.34: Internal von Mises stresses distribution recorded by FEA at different tooth layers and onlay restorations at all occlusal erosive and restorative stages. (Baseline= sound tooth, 1D= 1 day erosion, 7D= 7 day erosion, 10D= 10 day erosion, 14D= 14 day erosion, NBG= Non-bonded gold onlay, BG= Bonded gold onlay, IPS= IPS e.max onlay, OC= occlusal direct composite onlay).

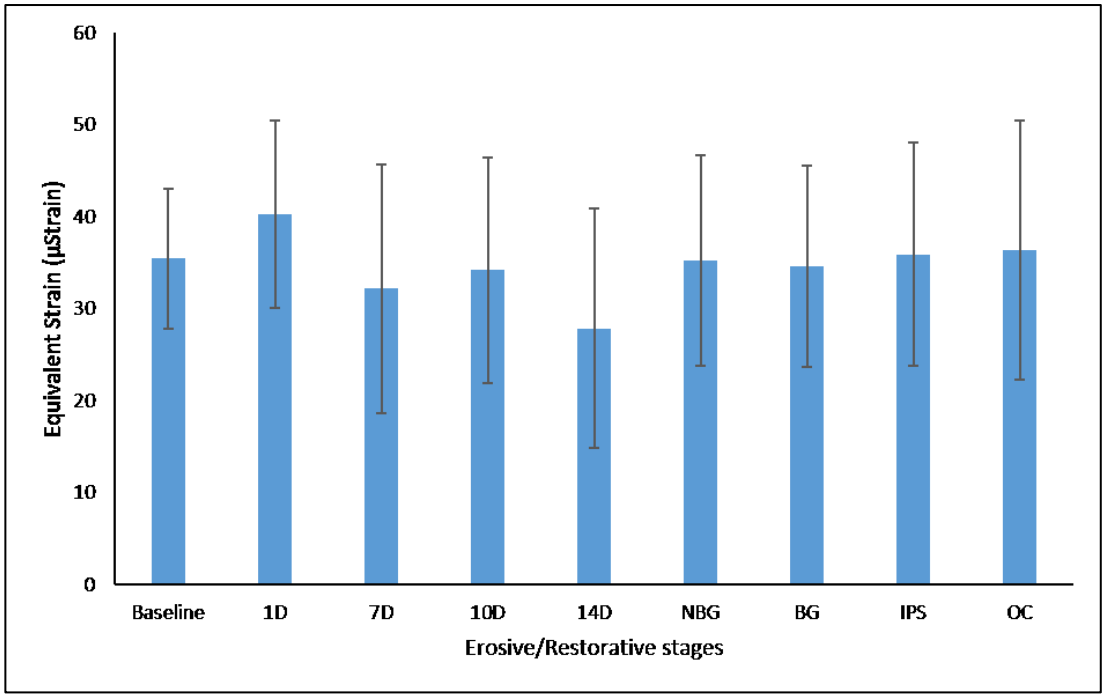

Figure 3.35: Mean equivalent strain values in FEA model for all occlusal erosive/restorative stages recorded at the cervical buccal wall (area simulating experimental strain gauge position). (Baseline= sound tooth, 1D= 1 day erosion, 7D= 7 day erosion, 10D= 10 day erosion, 14D= 14 day erosion, NBG= Non-bonded gold onlay, BG= Bonded gold onlay, IPS= IPS e.max onlay, OC= occlusal direct composite onlay).

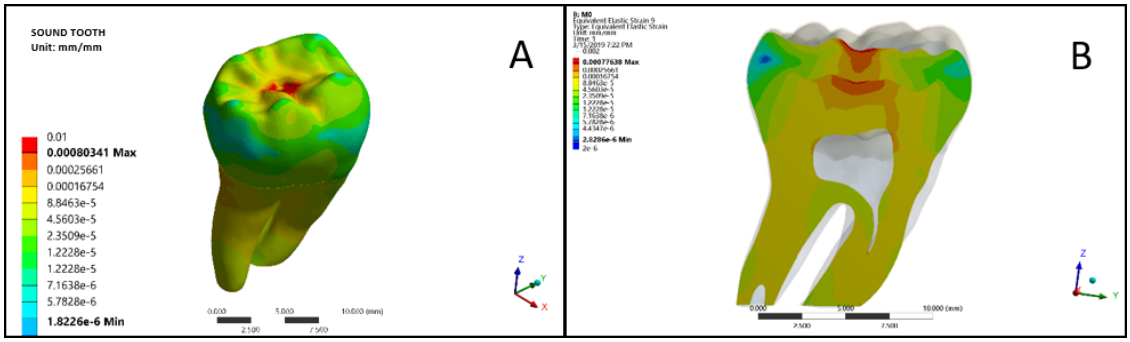

Figure 3.36: Strain distribution areas, maximum, and minimum values in FEA loaded case of a sound molar model. (A) Occluso-buccal view) with central fossa strain concentration and low level at the outer enamel area, (B) midsection view showing medium strain level distributed in enamel and underlying dentine.

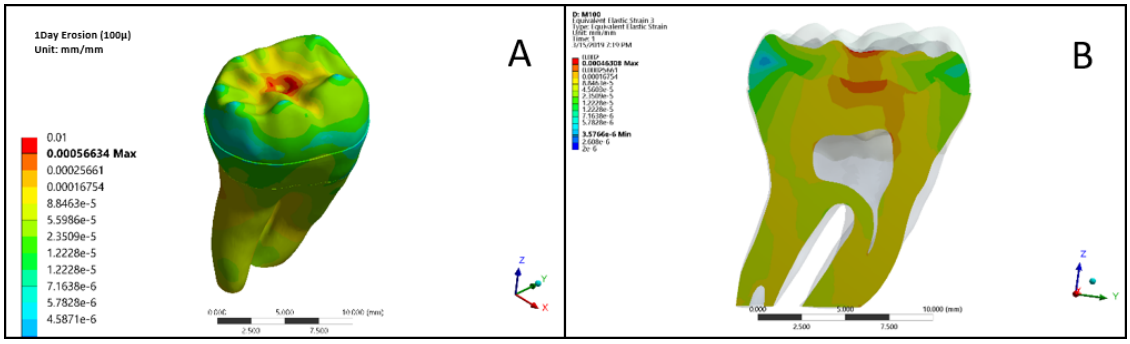

Figure 3.37: Strain distribution areas, maximum, and minimum values in FEA loaded case of 1 day eroded molar model. (A) Occluso-buccal view with a wider central fossa strain concentration area than the sound model with low strain level in the outer enamel layers, (B) midsection view showing lower strain levels than the sound model with similar distribution between enamel and underlying dentine.

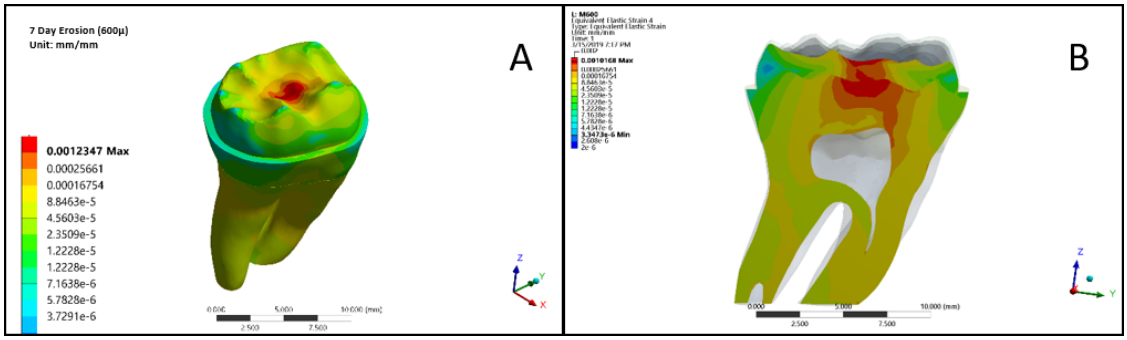

Figure 3.38: Strain distribution areas, maximum, and minimum values in FEA loaded case of 7 day eroded molar model. (A) Occluso-buccal view with a wider central fossa strain concentration area than the preceding model with low strain level in the outer enamel layers, (B) midsection view with a high rise in strain level in both enamel and underlying dentine (in dentine more than enamel).

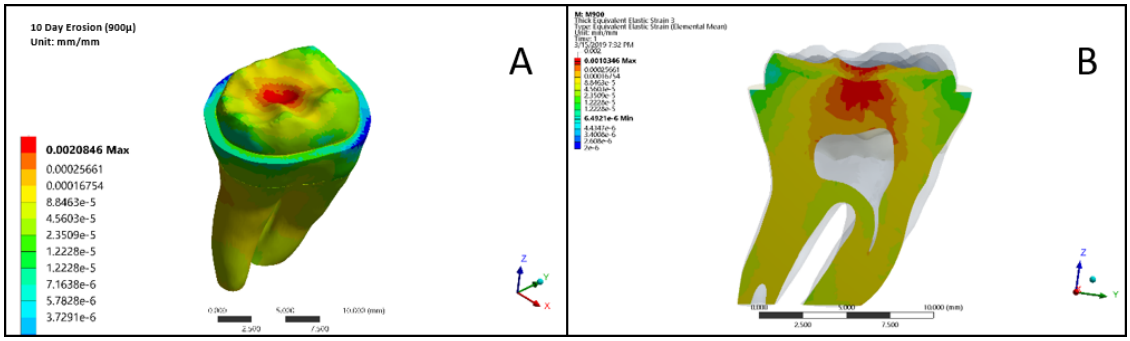

Figure 3.39: Strain distribution areas, maximum, and minimum values in FEA loaded case of 10 day eroded molar model. (A) Occluso-buccal view with a wider central fossa strain concentration area than the preceding model with low strain level in the outer enamel layers, (B) midsection view with further high rise in strain level in both enamel and underlying dentine (in dentine more than enamel).

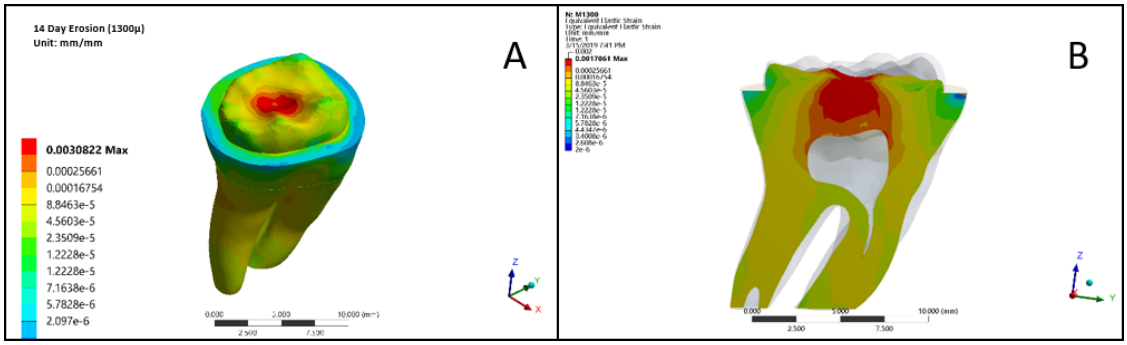

Figure 3.40: Strain distribution areas, maximum, and minimum values in FEA loaded case of 14 day eroded molar model. (A) Occluso-buccal view showing the widest area of concentrated strain of all erosive stages with low strain level in the outer enamel layers, (B) midsection view showing the highest strain levels in dentine among the erosive stages reaching the roof of the pulp chamber.

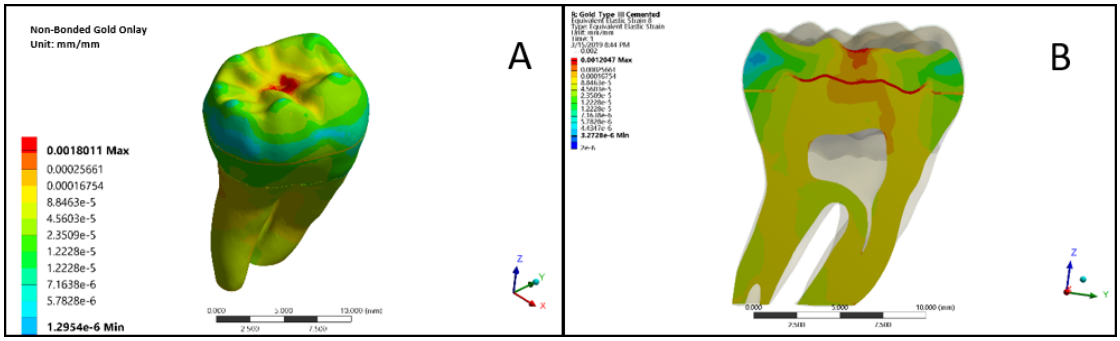

Figure 3.41: Strain distribution areas, maximum, and minimum values in FEA loaded case of non-bonded gold onlay (NBG) restored molar model. (A) Occluso-buccal view, with a confined central area of high strain and low levels in the outer enamel layer, (B) midsection view showing strain concentration in (NBG) onlay and underlying resin cement more than underlying dentine.

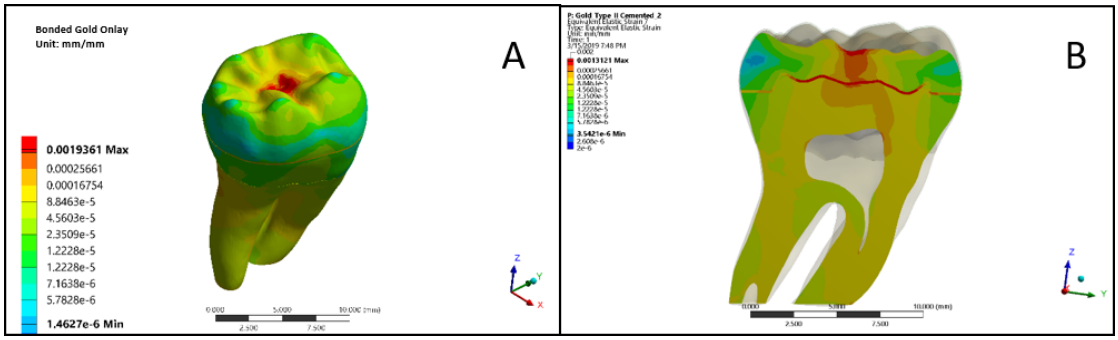

Figure 3.42: Strain distribution areas, maximum, and minimum values in FEA loaded case of bonded gold onlay (BG) restored molar model. (A) Occluso-buccal view, with a confined central area of high strain and low levels in the outer enamel layer, (B) midsection view showing strain concentration in (BG) onlay and underlying resin cement more than underlying dentine.

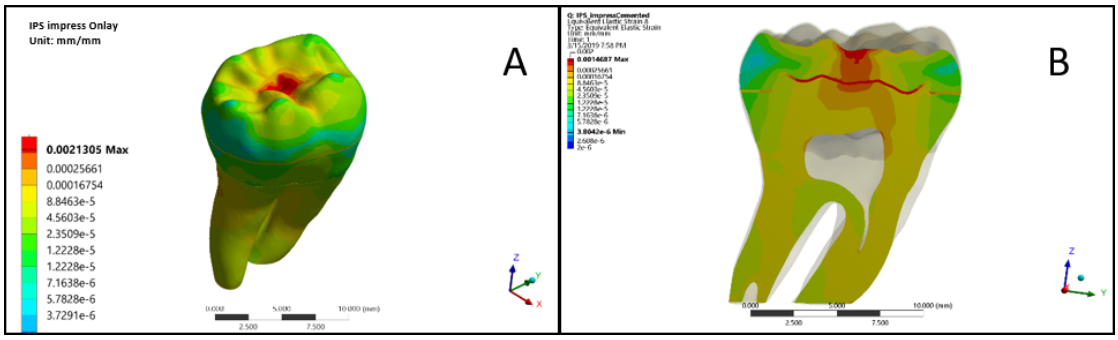

Figure 3.43: Strain distribution areas, maximum, and minimum values in FEA loaded case of IPS empress onlay (IPS) restored molar model. (A) Occluso-buccal view, with a confined central area of high strain and low levels in the outer enamel layer, (B) midsection view showing strain concentration in (IPS) onlay and underlying resin cement with lower levels in dentine.

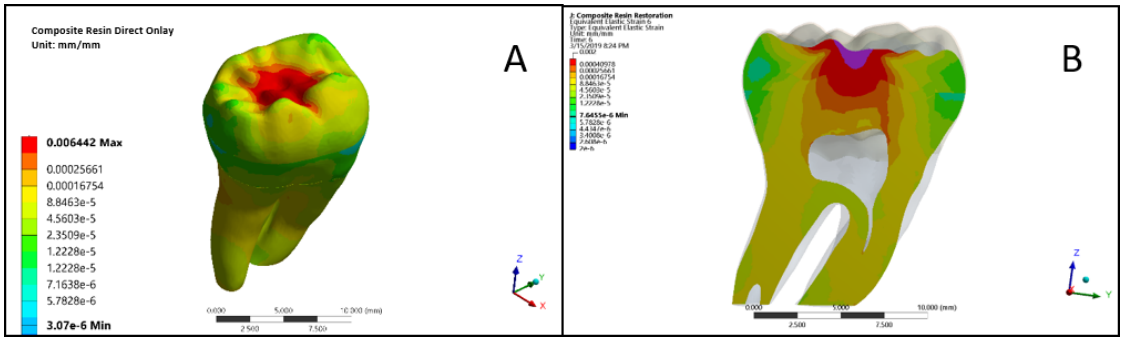

Figure 3.44: Strain distribution areas, maximum, and minimum values in FEA loaded case of direct composite resin onlay (OC) restored molar model. (A) Occluso-buccal view, with a wide high strain area concentrated in the central fossa under the loading point and low levels in the outer enamel layer, (B) midsection view showing the highest strain level concentration under the loading point in composite and underlying dentine.

3.2.7 Discussion- Chapter 3:

The human tooth and its supporting tissues is a complex assembly of different materials with variable mechanical properties. Properties of these elements are reasonably well-known. When a structure is loaded, stress distribution within its components rely on both the shapes of these components and their stiffness. Great difficulties could arise with different stiffness related to the tooth structural model containing enamel, dentine, cementum, and pulp. The modulus of resilience (fracture toughness) of dentine is higher than enamel rendering it better in absorption of impact forces than enamel which is brittle under tension. Although enamel is supported by dentine, which can undergo significant elastic deformation, teeth rarely fracture under normal occlusal forces (Phillips, 1991, Musani and Prabhakar, 2010). Under normal intact tooth conditions, external loads are transferred from enamel into dentine as compression, with only one seventh its magnitude is in the tensile form (Zhou et al., 1989, Musani and Prabhakar, 2010). The large internal tooth structure volume distributes the external loads into lower local stresses. Dentine deformation may occur during this process resulting in tooth flexure. In addition, the DEJ is well-known to be mechanically stable and play an important role in accommodation of mechanical stresses (Kinney et al., 2003, Zaytsev and Panfilov, 2014). On the other hand, a restored tooth tends to distribute stresses differently. Loading the restoration results in complex stresses at the restoration-tooth interface with a significant increase in the tensile stresses. However, when the stresses reach dentine, they will be resolved in a manner similar to the normal tooth condition. Minimal stresses

are borne by the supporting bone, while negligible stresses are borne by the pulp chamber and the root canals.

Variable extrinsic or intrinsic factors are important causes of tooth erosion and affect lesion distribution in the oral cavity. Extrinsic factors include dietary habits; related to high consumption of acidic foods, drinks, or medications, or occupational exposure to acidic environments. While, intrinsic factors include endogenous reflux and recurrent vomiting. In addition, distribution of erosion lesions is to some degree saliva dependent. The association between the protection capacities of saliva against enamel erosion by forming pellicle has been long proven (Zahradnik et al., 1977, Zahradnik et al., 1978, Øgaard et al., 1994, Hara et al., 2006, Lussi et al., 2008, Poggio et al., 2010, Poggio et al., 2013). Properties of the formed pellicle; including thickness and velocity have been shown to affect the salivary protection potential. It appears that dental erosion is inversely correlated with the pellicle thickness which varies between oral sites affecting the distribution of erosion lesions (Amaechi et al., 1999c, Young and Khan, 2002). Mandibular occlusal and buccal oral sites were selected for testing as they are commonly affected by acid erosion. These areas are bathed mostly with thick mucus saliva that lacks the required buffering capacity for acid clearance (Dawes, 1987, Khan et al., 1999, Young and Khan, 2002). Furthermore, the tongue protects lingual surfaces of mandibular teeth but not the occlusal and buccal surfaces in both cases of external acid erosion (soft drink in our situation) and gastro-oesophageal reflux disease (GERD). This supports the effect of the site of contact of the erosive agent, and the protective effect of tooth contact by

anatomical structures in the site-specificity of dental erosion (Amaechi and Higham, 2001b, Amaechi and Higham, 2005).

Numerous studies have attempted to explain the effect of occlusal stresses, morphology, and characteristics on the development and progression of cervical lesions (Khan et al., 1999, Palamara et al., 2000, Rees, 2002, Palamara et al., 2006, Romeed et al., 2012, Guimarães et al., 2014, Duangthip et al., 2017). It is generally accepted that the formation and progression of cervical lesions are multifactorial, including stress as in the case of abfraction, or biocorrosion involving biochemical and electrochemical degradation, and friction or wear (Grippo et al., 2012, Zeola et al., 2015). A strong association was suggested between the occlusal and cervical lesion sites. Acid demineralisation initiates cervical lesions and produces occlusal cupping. Furthermore, when occlusal forces are exerted on a tooth during function and parafunction, stresses will be distributed throughout its structure. These stresses were hypothesized to be the primary aetiology of non-carious cervical lesions (McCoy, 1982, Lee and Eakle, 1984, Grippo, 1991, Palamara et al., 2000, Litonjua et al., 2004, Romeed et al., 2012, Guimarães et al., 2014). However, far too little attention has been paid to the effect of loading on strain level at different stages of occlusal and buccal erosion and surface loss. Knowledge in this area will subsequently affect the management decision and the choice of the best restorative material for these lesions. Although emphasis was placed on occlusal and buccal lesions in this study, their combined effect was not studied.

One of the aspects of restorative dentistry involves the conservation of tooth structure. Restoring compromised teeth should involve removal of decay, existing

defective restorations, and the severely undermined tooth structure, while maintaining the integrity of the rest of the tooth. It is important to observe the mechanical properties of dental tissues and restorative materials when restoring the loss of tooth structure. The ideal material should recover the biomechanical behaviour of the lost structure, resulting in a similar mechanical pattern to sound tooth structures (Dirxen et al., 2013, Soares et al., 2013a, Machado et al., 2017). The extensive occlusal erosion lesions prepared for this study require restorations involving cuspal replacement. In this case the treatment options are direct restorations or indirect onlays or crowns (Hui, 2013). If teeth are either functionally and/or aesthetically unacceptable, indirect restorations may be indicated (Christensen, 2017). Although full crowns are easier to fabricate than onlays (Christensen, 2008), they involve extensive tooth structure removal reaching the gingival level or below causing gingival trauma and inflammation and possibly compromising vitality. In addition, crown cementation may leave foreign material sub-gingival, which in return causes permanent irritation and further inflammation and tissue loss (Ruiz JL, 2011, Ruiz, 2017). On the other hand, onlays, either adhesive or conventional, have proven themselves to be successful for a significant number of years (Heymann et al., 1996, Fabianelli et al., 2006, Magne, 2006, Christensen, 2008, Magne and Knezevic, 2009). They offer cuspal coverage with supragingival margins without the need to extend sub-gingivally to gain retention and they can be adhesively bonded to the tooth structure (Ruiz JL, 2011, Ruiz, 2017). By covering one or more cusps or even all the occlusal surface, onlays result in favourable stress distribution in teeth (Magne and Belser, 2003, Jiang et al., 2010), together with a decreased risk of fracture when compared to inlays (Mondelli et al., 1980, Jiang et al., 2010). Onlay restorations have become

a frequently chosen treatment option that increases the strength and resiliency of the residual tooth structure (Yamanel et al., 2009). Also, the growing popularity of modern production techniques, such as clinical CAD/CAM machines, has encouraged dentists to provide more conservative restorations than in the past (Christensen, 2008). The findings by (Seow et al., 2015) also demonstrated that using an onlay was effective in protecting and splinting the buccal and palatal cusps of the endodontically treated tooth. Moreover, onlays and ultra-thin occlusal veneers have been applied successfully in restoration of severely eroded occlusal surfaces of molars (Magne et al., 2012, Politano et al., 2016, Schlichting et al., 2016). Therefore, onlays were selected as the treatment option for the occlusally created erosion lesions. Different onlay material options and techniques were selected according to the restorative needs including (non-adhesively bonded type III gold, adhesively bonded type II gold, IPS e.max, and direct composite resin). The selection of onlay material to restore the occlusal erosion was intended to cover the most commonly applied materials for extensive or generalized tissue loss affecting the entire occlusal surface (Lambrechts et al., 1996, Schlichting et al., 2011, Chabouis et al., 2013, Oleszek-Listopad et al., 2015, Angeletaki et al., 2016, Politano et al., 2016). Restoration of occlusal surface could prevent reduction of the vertical dimension of occlusion (VDO) or post-eruptive tooth movement that compromise the occlusal restorative space (Schlichting et al., 2016).

Gold alloys were selected for their enduring performance history in dentistry in terms of biological compatibility and functional durability (McLean, 1980). Gold remains the standard when aesthetics are not a factor, particularly for posterior

full and partial coverage restorations (Small, 2006). Gold alloy inlay and onlay restorations have recently gained growing interest. This was primarily stimulated by a group of dentists who strongly believe that these restorations are still the best long-term restorations (Christensen, 2008). However, patient's demand for "natural" aesthetics, guides contemporary dentistry. Patients often reject gold treatment options, as they desire a highly aesthetic restoration that resembles natural tooth structure, even for posterior teeth, (Anusavice, 1989, Angeletaki et al., 2016).

Tooth-coloured restorations including composite resin and ceramic materials are the most popular restorations currently used (Sadowsky, 2006, Jiang et al., 2010). The primary advantages of non-metal restorations are superior aesthetics and cost effectiveness (Stein et al., 2005, Jiang et al., 2010). Composite resin restorative systems can provide minimally invasive rehabilitation of posterior teeth. Composite resin restorations are also characterised by their low elastic modulus, this allows more absorption of functional stresses by deformation (especially when used for onlays) (Brunton et al., 1999, Magne and Knezevic, 2009). Directly or indirectly placed composite materials are among the best alternative non-metallic, tooth-coloured treatments (Spreafico et al., 2005, Angeletaki et al., 2016). Although direct composite resin restorations are expected to wear more than ceramic, it has been proposed that they preserve more of the antagonistic enamel as the composite resins will wear preferentially (Panitvisai and Messer, 1995, Magne and Knezevic, 2009). The elastic modulus values of ceramic veneer materials are close to enamel (Piwowarczyk et al., 2005, Yamanel et al., 2009, Dirxen et al., 2013, Machado et al., 2017). While, composite resins

have mechanical properties similar to dentine as their modulus of elasticity is lower than dentine (Craig and Peyton, 1958, Yamanel et al., 2009, Jiang et al., 2010, Soares et al., 2013a, Zeola et al., 2015, Machado et al., 2017). Their properties (elastic modulus, hardness, and compressive strength) depend mainly on the volume and size of filler particles in the material. Small filler particle and higher volume combination generally leads to improved properties of the composite material (Yamanel et al., 2009). In recent years, both direct and indirect composite resins have improved in terms of their mechanical properties (Leinfelder, 2005, Magne and Knezevic, 2009). Their increased filler content provides improved fracture toughness (Shortall et al., 2001, Magne and Knezevic, 2009). Direct light-cured composite resin restoration was selected as one of the onlay restorative materials in the study as it has great advantages; it permits preservation of tooth structure, it is usually performed in one treatment appointment, and is at relatively low cost. However, it is also associated with polymerization shrinkage and low wear resistance (Feilzer et al., 1987, Barnes et al., 1991, Davidson, 2000, Yamanel et al., 2009, Angeletaki et al., 2016). On the other hand, indirect composite technique involves fabricating the restoration outside the oral cavity, on a virtual or traditional model of the prepared tooth. This overcomes some of the disadvantages of the direct technique, such as polymerization shrinkage (Wassell et al., 1995, Angeletaki et al., 2016). Furthermore, it provides better physical and mechanical properties of the restoration by light or heat post-curing, and achieves ideal occlusal and proximal contouring (Roberson et al., 2002, Duquia et al., 2006, Barone et al., 2008, Yamanel et al., 2009, Angeletaki et al., 2016). However, this technique has some disadvantages as it does not achieve improved clinical longevity when compared

with directly placed composite resin restorations (Wassell et al., 1995, Fennis et al., 2004, da Veiga et al., 2016). It is also more time consuming and requires extra cost and clinical appointments to complete the additional procedures.

When comparing the direct and indirect composite onlay techniques and properties, similar flexural strength, flexural modulus, and hardness were found (Yamanel et al., 2009). Furthermore, results of the systematic review carried out by (Angeletaki et al., 2016) on the long-term clinical performance of direct versus indirect inlay/onlay composite restorations in posterior teeth showed no statistically significant difference between the two restoration techniques. For these reasons, the direct composite onlay technique was selected in this study.

To standardize cementation pressure and achieve a uniform cement thickness for all groups, cementation was carried out under static vertical finger pressure of around 60N. This is based on the recorded average achievable clinician finger pressure (Black and Amoore, 1993, Zortuk et al., 2010).

Lost enamel and dentine in the cervical region of the tooth, such as buccal erosion lesions, are usually restored with adhesive restorations (composite resins) (Kim et al., 2009), flowable resins (Perez, 2010), and glass ionomer cements (Ichim et al., 2007)), regardless of the cause of the lesion. Our material choice was limited to direct composite resin restorations as previous findings of (Machado et al., 2017) indicated that composite resin tested for NCCL was able to restore strain and the biomechanical properties similar to the sound pre-treatment level. Moreover, direct composite material is kind to periodontal tissues if proper restoration finishing and polishing is performed, allowing for a

satisfactory restoration contour and surface polish (Santos et al., 2007). This selection also allowed comparison of the material behaviour in different lesion sites (occlusal and buccal).

Ceramics have been in use in restorative dentistry for many years and is growing in popularity. A part from being highly aesthetic, ceramic restorations maintain a more stable occlusion than composites and possess superior colour stability (Manhart et al., 2001, Roberson et al., 2002, Magne, 2007, Yamanel et al., 2009). However, ceramic restorations suffer their own limitations of having low tensile strength and being brittle (Anderson, 1976, Abu-Hassan et al., 2000, McLaren and Cao, 2009, Zhang et al., 2013). Fortunately, the use of adhesive cements (Grossman, 1989, Van Meerbeek, 2003, Spencer et al., 2010, Marchesi et al., 2014, Weiser and Behr, 2015, Manso and Carvalho, 2017, Ramakrishnaiah et al., 2018, Pan et al., 2019) and different surface treatment techniques (Abu-Hassan et al., 2000, Dejak and Mlotkowski, 2008, Romanini-Junior et al., 2018) can improve these properties. In this connection, IPS e.max® Press, was selected for this study. The IPS e.max was introduced in 2007 to fabricate all-ceramic inlays, onlays, single- and multiple-unit restorations for both anterior and posterior region (Heintze et al., 2011, Tang et al., 2014). IPS e.max® Press is a pressable glass-based system with lithium-disilicate fillers (where the alumino-silicate glass has lithium oxide added). The pressable lithium-disilicate (LS_2) glass-ceramic was first introduced by Ivoclar in 1998 as IPS Empress® II (the predecessor of IPS e.max®) (Della Bona et al., 2004, Piwowarczyk et al., 2005, Ozen et al., 2007, Yamanel et al., 2009, Tang et al., 2014, Alkadi and Ruse, 2016). This material had higher mechanical properties than the lucite-reinforced glass-ceramic (IPS

Empress). However, it had high opacity and had to be used as a core material and always veneered (Tang et al., 2014). IPS e.max combined durability and esthetics which can be directly fabricated as a bulk without veneering (Wolfart et al., 2009, Gehrt et al., 2013, Pieger et al., 2014, Tang et al., 2014). The crystals that form within the lithium-disilicate materials comprise about two thirds of the volume of the glass ceramic. The shape (needle-like) and volume of the crystals contribute to almost double the fracture toughness and flexural strength of this material (Della Bona et al., 2004, McLaren and Cao, 2009).

The IPS e.max material comes in a pressable (e.max Press) and machinable (e.max CAD) forms. Different lithium-disilicate crystal sizes are related to each form (e.max Press- 3 to 6 μm, e.max CAD- 0.2 to 0.1 μm), leading to different flexural strengths (e.max Press- 470 MPa, e.max CAD- 530 MPa) and therefore different applications. Clinical data for single restorations are excellent with this material, especially if it was bonded (Piwowarczyk et al., 2004, McLaren and Cao, 2009). The basic mean survival rate of 96% was calculated for both forms from the values reported by some clinical studies involving IPS e.max® Press based on 3-10 year long studies (Gehrt M, 2012, Kern et al., 2012, Guess et al., 2013).

Both all ceramic and composite onlays rely on chemical bonding for retention in an adhesive preparation, which eliminates the need for residual cuspal outline for mechanical retention (Sinescu et al., 2011). Restoration margin design also affects the restoration material selection and outcomes. As ceramic materials have relatively low tensile strength, the thickness of a restoration is critical (especially at the restoration margins). With the occlusal erosion protocol followed in this study, a rounded external enamel margin (chamfer-like) was formed by

erosion. This design resembles the final overlay preparation with circumferential adhesive ferrule effect for heavily compromised vital teeth (with thin walls, cracked teeth, and endodontically treated molars and premolars) (Magne et al., 2012, Politano et al., 2016, Schlichting et al., 2016). This circumferential design provided good enamel peripherally to which to bond. Isaacs (1987) preferred chamfered occlusal margins. In addition, Abu-Hassan et al. (2000) reported insignificant differences between stresses registered with chamfer and bevel design margins compared to shoulder type when vertical load was applied.

For all restorative materials used in this study, a dentine-bonding agent was used. Consequently the simulation assumed a perfectly bonded interface between the dentine surface and the onlays (Frankenberger et al., 1999). In case of cemented restorations (IPS, BG, and NBG), a space of 120 μm (McLean, 1971, Holmes et al., 1992, Reich et al., 2011) was added to accommodate the cement layer. In the FEA modelling, the fitting surface of all onlays regardless of the material was considered as bonded for the simulation.

Before testing, the resin base of all samples was machined to expose some of the root structure. This was designed in this way so that on loading, only micromotion occurred. Intraoral functional loads vary widely with a reported range from 10 to 431 N (Roberson et al., 2002, Yamanel et al., 2009). Gradual occlusal loads up to 130N were applied to test the effect of load within the physiological limit for human teeth (Kiliaridis et al., 1995, Ranjitkar et al., 2008, Valdivia et al., 2012, Pereira et al., 2013, Soares et al., 2013b). During loading, contact was established between the stainless-steel ball bearing loading tip and the central

fossa of molars. This was reported to facilitate repeatable loading of the specimen (Magne and Knezevic, 2009).

At all testing stages, FEA images show that stresses with vertical load were highest at the central fossa related to the load point at all erosive and restorative stages as found by Abu-Hassan et al. (2000). Only vertical load was applied in this experiment as vertical load orientation normal to the tooth long axis is more evenly distributed to the supporting tissues, avoiding tooth bending and stress concentrations (Lee et al., 2002, Rees et al., 2003, Borcic et al., 2005, Guimarães et al., 2014, Seow et al., 2015). Earlier experiments applied similar protocols of vertical loading (Panitvisai and Messer, 1995, Jantarat et al., 2001, Magne, 2007, Soares et al., 2008a). In addition, The effect of the loading type (vertical, horizontal) on stress distribution has been investigated and compared in the literature (Palamara et al., 2000, Asmussen et al., 2005, Romeed et al., 2006, Yamanel et al., 2009, Jiang et al., 2010, Romeed et al., 2012, Guimarães et al., 2014, Wayne et al., 2014). Vertical load leads mainly to compressive-type interfacial stresses, which can be assumed to minimise potential onlay restoration debonding (Magne and Belser, 2003). Moreover, horizontal load always produced higher concentration of stresses in the cervical region compared to the vertical load (Soares et al., 2015, Zeola et al., 2015).

Strain gauges and FEA (virtual strain gauge on buccal cervical enamel position) (**Figure 3.27**, **Figure 3.36**) gave comparable results at both erosive and restorative stages. They correlated early loss of occlusal enamel (≈ 80-100 μm) with increased measured strain to the baseline. Strain increase may be related to the effect of removing the stiffer aprismatic enamel. However, with further

reduction of enamel thickness; erosion extended over 7 days (≈ 550- 650 μm) and 10 days (750- 850 μm), overall strain in both strain gauge and FEA testing tended to reduce and stabilize with values insignificant to the baseline. Moreover, with total enamel loss and exposure of dentine (≈1250- 1350 μm), strain level further reduced and maintained an insignificant difference to the baseline. Strain reduction could be related to the generalized loss of tooth height and loss of the stiffer enamel layer which may lead to load absorption and dissipation by the more resilient dentine. Also, this could be related to the strain distribution pattern shown by FEA model, where higher strain was transferred into dentine than enamel, which may not be captured by strain gauges attached to the enamel surface. In the literature, mounting strain gauges on tooth surfaces was suggested to be a reliable means of recording relative stress/strain under non-destructive occlusal loading (Reeh et al., 1989b, Lopes et al., 1991, Shor et al., 2003, Seow et al., 2015). However, the record of strain obtained by strain gauges is regional, related to the tested surface and is continuous in time but discontinuous in space, i.e. a gauge captures a measurement at a single point (Moore and Tyrer, 1995).

Both strain gauge and FEA restorative results were comparable to each other and to baseline (**Figure 3.27**, **Figure 3.36**). All tested onlay materials showed favourable strain distribution. Both restoration and adhesive layer alleviated part of the strain from the underlying tooth structure (Çötert et al., 2001, Dalpino et al., 2002, Sagsen and Aslan, 2006, Seow et al., 2015). This is in agreement with earlier studies that suggested that the use of resin luting cements together with dentine adhesive systems was able to strengthen restored tooth units. However, in our study, both bonded and non-bonded gold onlays had similar results

supporting the role of the properties of the restorative material over bonding on the durability of the restoration (De Munck et al., 2005, Breschi et al., 2008, Liu et al., 2011, Marchesi et al., 2013). Conversely, Abu-Hassan et al. (2000) found that the tooth structure suffered more stresses than the restoration when vertical load was applied to onlay restored teeth.

Although similar strain values were recorded with all tested onlay materials, direct composite resin suffered more stresses than gold and ceramic onlays and transferred more stresses to the tooth structure (**Figure 3.35**, **Figure *3.44***). Subsequently, the tooth may suffer a catastrophic fracture or the bond between the tooth and the restoration may be compromised (Mesquita et al., 2006). Yamanel et al. (2009) carried out a 3D finite element analysis study on the effects of different composite resin or ceramic materials on stress distribution in inlay and onlay cavities and had similar findings with respect to composite resin. They explained that the low elastic modulus of the composite resins may have accounted for these results as it allows the transfer of large amount of stresses to the tooth. Our results are consistent with findings of studies comparing the efficacy of ceramic and composite inlays (Fasbinder et al., 2005, Thordrup et al., 2006, Chabouis et al., 2013), onlays (Magne and Belser, 2003), or restorations for endodontically treated teeth (Zhu et al., 2017), where ceramic was favoured over composite resin.

Von Mises stress is “the value used to determine if a given material will yield or fracture”. Von Mises calculates the distortion energy density at a particular point in the system. This also indicates stress distribution within the FEA model upon loading and may also explain the results by strain gauges, where absorption of

stresses internally could decrease the stresses suffered by the external enamel surface, on which strain gauges were attached (**Figure 3.35**, **Figure 3.36**). For example, the 1D erosion showed a slight decrease in the von Mises strain in both internal enamel and dentine layers, which was reflected as increased strain recorded by strain gauges. On the other hand, with progression of erosion (7D, 10D, and 14D), von Mises stresses constantly increased at both tooth layers, while decreased by strain gauges. After restoration with composite resin onlay, both composite resin and underlying dentine suffered high strain. While, other onlay materials; gold and ceramic (BG, NBG and IPS), and bonded cement layer, suffered more strain than the underlying dentine. IPS had the best results followed by BG, NBG, and finally composite resin. Similarly, Magne and Belser (2003) found that ceramic onlays were the most promising solutions to restore severely damaged posterior teeth when compared to composite resin. Moreover, earlier conclusions by Douglas (1985) stated that the strength of composite resin falls off with cavity size increase. While, the opposite was true about ceramic-restored teeth, where the stiffness had increased with increased cavity size.

FEA prediction data are in good agreement with the experimental data, as discussed earlier. This comparison indicates the great accuracy of the numerical model with respect to a very complex simulation of compression test in a human tooth model and confirms the efficacy of strain gauges as a strain testing tool.

Strain behaviour tested by ESPI was comparable to results by strain gauges where strain increased after 1 day of erosion followed by a decrease at 7 and 10 days and reached the lowest at 14 days which was insignificant to baseline. ESPI uses a live stream video system for image acquisition Therefore, it provides data

that are continuous in space and time (Moore and Tyrer, 1996). Out-of-plane displacement records strain related to the imaged surface where phase maps were acquired after subtraction of loaded from unloaded images of the surface. The phase maps consist of parallel fringes that are processed (unwrapped) to calculate displacement. Although ESPI allowed generation of valid data that agreed with strain gauge data, the procedure was ultimately sensitive to vibration and required high expertise and knowledge of involved physical science required for set-up and interpretation of results. Therefore, this technique was limited to testing the erosive stage of the experiment and discontinued for the restorative stage. Difficulties encountered with the ESPI technique were the reason behind exploring other novel methodologies (preferably contact-free optical ones) to measure strain. Searching the literature gave results about the digital image correlation technique (DIC) which was selected and applied for the next strain experiment.

Cervical lesions come in different shapes (wedge, saucer, combination) (Hur et al., 2011, Soares et al., 2015). Although multifactorial in origin, the predominant causal factor was speculated to be key in determining the lesion's final shape (Sognnaes et al., 1972, Lee and Eakle, 1984, Bartlett and Shah, 2006). Saucer-shaped lesions (U-shaped) are thought to be produced by acid erosion (Levitch et al., 1994, Palamara et al., 2006), whereas lesions with sharply defined margins (V-shaped) could be caused by abrasive factors and non-functional occlusal loading (Grippo, 1991, Levitch et al., 1994, Piotrowski et al., 2001, Guimarães et al., 2014). According to our experiment (involving only acid erosion) U-shaped lesions were produced. However, Soares et al. (2015) found that the shape of the

lesion had little effect on the stress distribution pattern, whereas the loading type and the use of composite restorations influenced the biomechanical behaviour of maxillary premolars.

Buccally eroded samples showed different behaviour to loading than occlusal erosion. The results indicate that the size of the lesion greatly influences the magnitude of strain on loading. With erosion progression, strain gradually increased but only after 10 days (2/3rd enamel thickness lost) became significant to baseline and all previous erosion stages. Buccal lesion restoration restored their mechanical properties to become similar to that of sound pre-treatment condition. These results are in agreement with Zeola et al. (2015) who found that the loss of dental structure in the cervical region promoted changes on stress distribution pattern, even lesions as small as (0.5mm) generated high stress concentration in the cervical area. Authors suggested in lower premolars that stress magnitude increased as the cervical lesion depth increased. Additionally, Zeola et al. (2015) and other authors (Soares et al., 2015, Machado et al., 2017) confirmed that the replacement of lost tooth tissue with adhesive restorations recovered biomechanical behaviour that was close to the sound model.

In their study, Zeola et al. (2015) found that despite all other factors (load type, lesion morphology, and restorative material), non-restored models produced the highest stress concentration on the cervical lesion walls. These findings place great emphasis on the need for restoration of cervical lesions even if lesions are arrested and sensitivity is not an issue. Extensive lesions at a later stage of progression maybe arrested but can still pose critical biological and mechanical consequences (like pulpal devitalisation and/or calcification, bone resorption,

tooth mobility and ultimately tooth fracture) if left untreated (Guimarães et al., 2014). Bone loss scenarios (pathological, or physiological with aging) amplifies stress magnitudes in deep lesions due to the increase in bending moments. Treatment planning for non-carious cervical lesions should seek not only to restore the lost tissue (Michael et al., 2009), but also to control all etiological factors involved (Grippo et al., 2012).

Strain testing methodologies applied in this study (strain gauges, ESPI, and FEA) are non-destructive and are useful in analysing the biomechanical behaviour of teeth associated with different levels of tissue loss, different restorative materials, and strain measuring techniques, analysing the relation between stress and strain (Rees et al., 2003, Soares et al., 2013a, Machado et al., 2017). However, all techniques present some limitations. The strain gauge and ESPI measure only deformations related to the external surface. High standard deviations result with these techniques because of the high variability related to human teeth. In addition, ESPI is sensitive to set-up accuracy and environmental vibration which renders it unsuitable for simple strain testing. On the other hand, for FEA, although efforts are made to produce a model close to reality, issues related to bonding and dynamic aspects of restoration and lute shrinkage, cannot always be duplicated. Because of these limitations, combination and correlation of more than one technique was applied to validate results. The tested methodologies showed good inter-correlation and complemented each other facilitating reliable data generation.

In conclusion, it was observed that vertical loading of occlusally eroded lesions resulted in increased strain at the initial erosion stage followed by gradual

decrease with erosion progression. While, strain in buccally eroded molars was directly related to erosion progression. Restoration of both lesions resulted in strain levels similar to sound teeth. All occlusal onlay materials had comparable performance. However, stain patterns favoured ceramic and gold onlays over composite onlays. All applied methodologies gave similar results and are valuable in assessment of strain in teeth. Therefore, all null hypotheses can be rejected.

CHAPTER 4

The Effect of Different Remaining Tooth Structure Dimensions and Related Restorations on Strain: A Digital Image Correlation and Strain Gauge study

4.1 Introduction- Chapter 4:

Evaluation of remaining tooth structure should focus on both the quality/quantity of the remaining tooth structure in order to consider the available restorative options. Moreover, teeth are subject to varying magnitudes and directions of functional and para-functional forces (Ausiello et al., 2004, Yamanel et al., 2009). Restorative procedures influence stress and strain in teeth. With varying amounts of remaining tooth structure, different tooth positions and load directions, different types of restorations are recommended. In this chapter, the effects of different quantities and qualities of remaining tooth structure were tested and compared using two testing methodologies; strain gauges (SG) and digital image correlation (DIC). Additionally, the effect of two restorative options (intracoronal restoration and cuspal coverage) was carried out by SG.

The null hypotheses tested in this study were that:

- There would be no significant difference in strain in teeth with differing structural loss,
- There would be no difference in strain in teeth restored with different designs of restoration (core restoration, cuspal coverage),
- There would be no correlation in strain measured using the two different techniques.

4.2 Material and Methods- Chapter 4:

50 extracted premolars of similar size were selected to measure within the following means ± SD: 8.2 ± 0.1 mm (buccolingual), 6.4 ± 0.1 mm (mesiodistal), and 8.3 ± 0.1 mm (cervico-occlusal). Each tooth was mounted vertically in epoxy resin (refer to Page 91, 92). 10 sound premolars served as control (Control). 40 premolars served as test and each premolar was divided into 2 samples (buccal and lingual walls) (n=80). Samples were divided into 2 subgroups (n=40) according to the composition of the prepared walls. One group was prepared to have both enamel and dentine elements in the remaining walls (E+De), while the other was prepared to remove all enamel and have dentine only (De). Foe each sample, silicone putty impression of the buccal or lingual surface was made to produce a reference key to guide surface reduction. Each group was further divided into 4 sets of dimensions according to the preparation height to width ratio of the 2 remaining cusps (n=10). The dimensions of 1mm and 1.5mm were selected to represent the width for (2:1 and 3:1) height to width ratio generating 4 preparation dimensions (A, B, C, D) as shown in (**Table 7**).

Table 7: Sample Preparation Dimensions

Wall Width	(H:W mm) 2:1	(H:W mm) 3:1
1mm	2:1 (A)	3:1 (B)
1.5mm	3:1.5 (C)	4.5:1.5 (D)

H = Height of prepared wall; W= Width of prepared wall.

4.2.1 Sample Preparation:

Tooth preparation started as an MOD cavity, then cuspal walls were reduced in thickness at both outer and inner aspects following the outer contour of the tooth to the test dimensions (**Table 7**) with a high-speed hand piece and constant water irrigation at 40 ml/min flow rate. A digital calliper was used constantly to check dimensions along 6 approximate points on the prepared wall (mesial, central, and distal points at both the incisal and cervical ends of each prepared wall). For initial preparation the FG 765X Coarse chamfer diamond bur (Kerr Blu White Coarse Diamond Bur, Henry Schein Europe) was used, followed by FG SF2 fine chamfer diamond bur (Kerr Blu White Diamond Bur FG Yellow, Henry Schein Europe) and finally with a tungsten carbide finishing bur (T/C Fine Finish 30 Blade, Henry Schein Europe). The base of each prepared sample wall was considered to be 1 mm above the CEJ. Teeth were lightly prepared as a slice preparation with no finish line cervically. The external walls were cut to be parallel with a maximum wall inclination of 6°-14° on buccal, lingual, and proximal aspects (Johnston et al., 1965, Shillingburg et al., 1997) creating a total occlusal convergence (TOC) of 10°-20° (Goodacre et al., 2001, Rosella et al., 2015). The inclination angles formed was determined by direct viewing of the preparation from all aspects (buccal, lingual and proximal). A dimple (1mm diameter and 0.5 mm depth) was prepared on the top of each wall to allow a point of loading at the centre of the wall (**Figure 4.1**, **Figure 4.2**). All preparations were made by one operator to ensure standardization. Teeth were prepared according to 4 sets of dimensions involving different height to width ratios. The resulting walls followed

the natural convexity of the buccal and palatal tooth surfaces. To standardize preparations, the radius (R) of the convex walls was calculated to have an average value of 3.25mm ±0.15 (SD) according to the following equation:

$$R = \frac{\left(\frac{X}{2}\right)^2 + H^2}{2H}$$

Where X is the mesiodistal width of the convex wall and H is the depth of the convexity.

To keep teeth moist after preparation, a damp cotton pellet soaked in thymol was placed over each tooth. Teeth were kept within a sealed plastic container resting on a thymol moist tissue to act as a humidor and refrigerated until ready for testing.

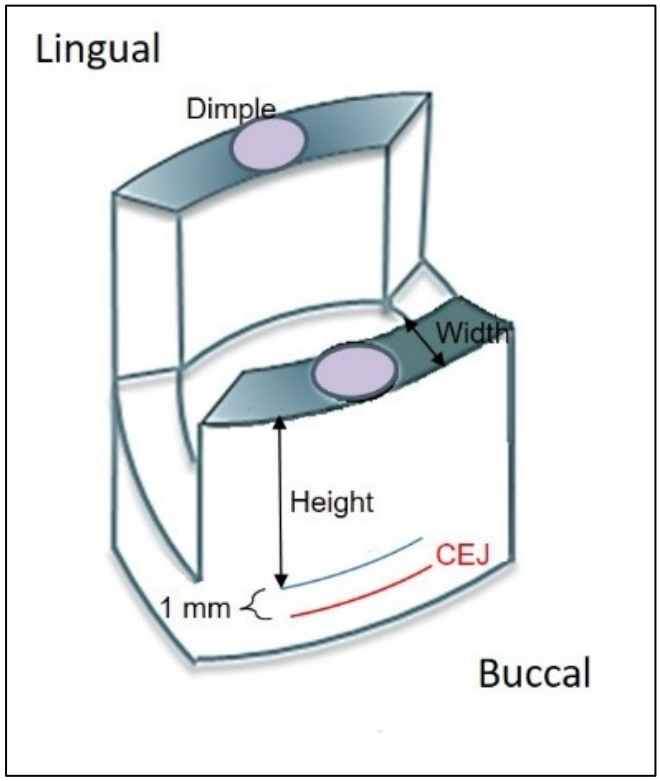

Figure 4.1: A diagram of the prepared tooth.

Figure 4.2: mounted prepared specimen.

4.2.2 Restorative Phase:

To test the effect of tooth restoration on the prepared walls, all samples were prepared to receive 2 types of composite resin core restorations (core1, core2). Samples were polished with pumice, rinsed, dried, and etched. A clear Mylar matrix strip (Henry Schein Europe); fitted in a Universal Tofflemire matrix retainer (Henry Schein Europe), was placed around specimens. Bonding agent was applied followed by composite resin incremental application and light curing. The final restoration was finished and polished (Refer to Page 152-153) for detailed technique).

4.2.2.1 Core restoration (core1):

The direct composite resin core was built up incrementally to fill the prepared cavity in each tooth and end at the level of the prepared sample wall. The dimple at the top of each preparation was preserved to allow future loading (**Figure 4.3**).

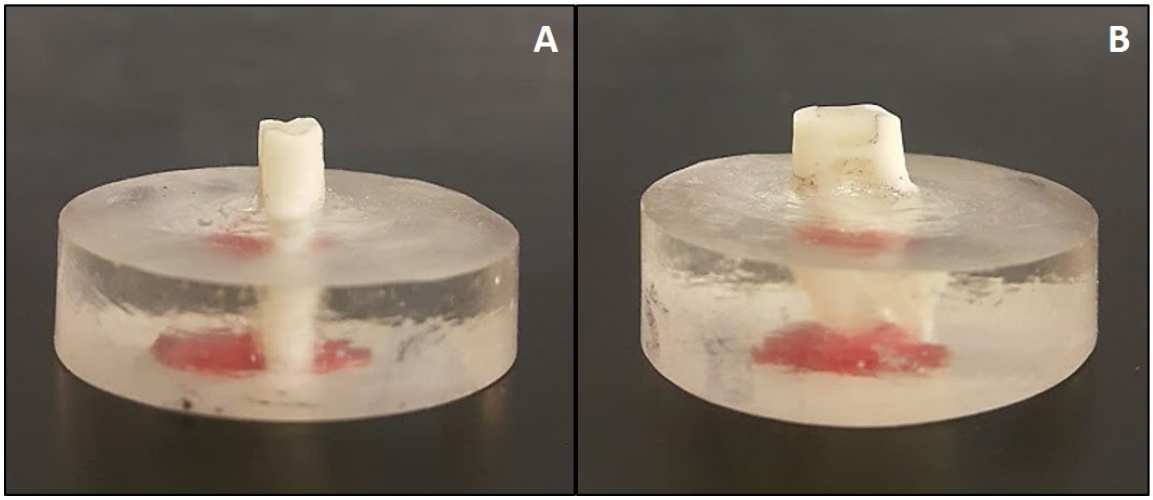

Figure 4.3: Sample with direct composite resin core build-up (core1). A. buccal view, B. proximal view.

4.2.2.2 Core restoration with cuspal coverage effect (core2):

Extra layers of composite with varying thicknesses; according to the prepared wall height, (**Table 8**) were added on top of both (core1) and the prepared sample walls (**Figure 4.4**).

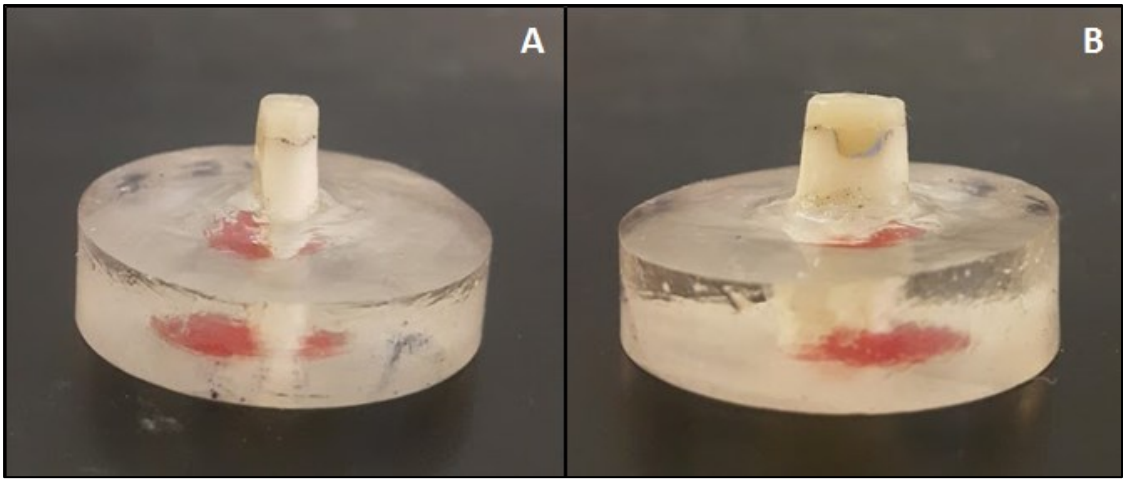

Figure 4.4: Sample with direct composite resin cuspal coverage build-up (core2). A. buccal view, B. proximal view.

Table 8: Composite Restoration Dimensions for (Core2)

Wall Height	Group	Covering Composite Thickness
2mm	(A)	4mm
3mm	(B), (C)	3mm
4.5mm	(D)	1.5mm

4.2.3 Displacement Measurements on Tooth Specimens:

After tooth preparation, (prepared) readings for all specimens were recorded using two different methodologies: Digital Image Correlation (DIC) and strain gauges (SG) under uniaxial compression tests. The load was introduced into the dimple on the top of each specimen using a 2.5 mm ball bearing. Loading was ramped within physiological limits for the human dentition (refer to Page 159). Strain was recorded at 130N for (SG) or calculated for (DIC).

4.2.3.1 Experimental Setup for Strain Gauge Testing:

Strain gauges were attached to the outer surface of the prepared samples (either buccal or lingual according to the prepared wall) (refer to Page 158). Samples were subjected to the same gradual loading and unloading cycles as previously described and strain values were recorded at (130N) the peak load point representative of physiological loading.

4.2.3.2 Experimental Setup for Digital Image Correlation (DIC) Testing:

The specimens in the resin mount were placed in an Instron Electropuls E3000 machine (Instron, Norwood, Massachusetts, USA) which was programed to produce the predetermined loading cycle (refer to page 159). A speckle pattern was painted onto the specimens using a black-ink spray as better quality DIC measurements could be obtained using this patterning method (**Figure 4.5**). The imaged face of the samples was kept dry for the duration of the test. Images were analysed and a displacement field determined.

The speckled buccal/palatal surface of the specimen was imaged using a macro lens of a CCD camera (Imager Intense, LaVision Inc.) that had a field of view of approximately (3mm x 2mm) in a circular area caused by internal vignette of the image, (**Figure 4.5**). At this magnification, this corresponded to approximately 1800 pixels per mm or 1.8 pixels = 1 micrometre. Vertical

displacement was measured in an area directly below the point of indentation on the buccal/ palatal surface of the specimen. Images were captured at peak load (130N) and final unload (5N) and these were used to measure displacement. To calculate the surface strains, the digital image correlation system (StrainMaster, LaVision Inc., Göettingen, Germany) was used. The displacement field was processed in several ways to calculate strain over appropriate fields of view, either a long narrow width representative area or a shorter vertical height where linear strain behaviour was observed. The effect of the dimensions of the specimen under load was incorporated by calculating the bulk modulus from the zone where linear strain behaviour has been measured. Data were averaged over a small width either side of the central line and these were plotted against a vertical position within the specimens. Strain was recorded when it was constant at areas where appreciable linear relationship between displacement and vertical position were observed (**Figure 4.6**).

4.2.4 Results- Chapter 4:

The goal of the analysis was to determine the influence of the three factors involved in this study: tooth composition, dimensions of the remaining tooth structure, and two different restorative options on strain. Also, to compare the data acquired by two techniques: the surface displacement field measured using Digital Image Correlation (DIC) and strain gauges (SG). Two tooth compositions (E+De and De) and four height to width (H:W) dimensions (A=2:1mm, B=3:1mm, C=3:1.5mm, D=4.5:1.5mm) were tested. For (DIC), Data of tested strain under gradual loading and unloading technique were analysed with a 2-way ANOVA. While, for (SG) technique, a 3-way ANOVA was applied where restoration was added as a variable [two restorative stages (a bonded composite resin core (Core1) and a bonded composite resin core with cuspal coverage (Core2)] was completed. Bonferroni post hoc test was applied when significance between tested groups was confirmed. Groups were considered statistically different at $\alpha \geq 0.05$.

4.2.4.1 DIC Results:

A typical image from a measurement is shown in (**Figure 4.5**). Here the position of the loading ball can be seen at the top of the image. The speckle pattern is clearly visible. The area at the bottom of the image is partially embedded in resin and behaved differently under load to the bulk of the specimen.

The area used for the measurement is demarcated as a red box in (**Figure 4.5**). The data were averaged over a small width either side of the centre line and this was plotted against the vertical position within the specimen. For many specimens there were appreciable areas where a linear relationship between displacement and vertical position was observed and the strain was constant within these areas and was recorded. A displacement field, in micrometres is shown as an example in (**Figure 4.6**). This was generated by using the relative movement between two images to measure in-plane displacements of one image against another. The images used for this were fully-loaded with subsequent unloading.

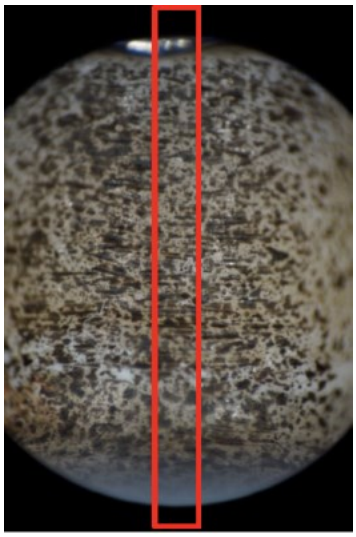

Figure 4.5: A typical image used for displacement field measurement.

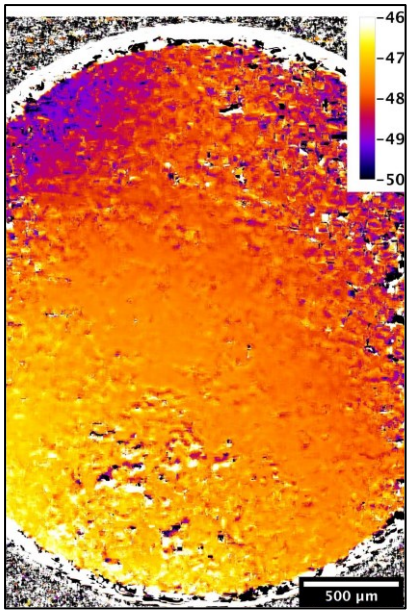

Figure 4.6: A full field displacement measurement using DIC showing movement in the vertical direction, the pixels increase from top to bottom. The scale is in micrometres.

The two-way ANOVA indicated a statistically significant difference in the mean strains between the different preparation dimensions (A, B, C, D) ($p<.05$) but not between the compositions (De, E+De) (**Table 11**). Foe E+De groups, dimension A showed a significantly higher strain than C & D. While, Dimension D showed significantly lower strain than A & B. No significance was detected between dimensions B & C or C & D. Displacement in Control samples was too low to be recorded by the DIC system.

Comparison between the estimated mean strain values and their associated standard deviation for all groups (A, B, C, D) including both Dentine (De) and Enamel+ Dentine (E+De) compositions are shown in (**Figure 4.7**).

Table 9: Tests of Model Effects (DIC)

Source	Type III		
	Wald Chi-Square	Degree of freedom df	Significance
Dimension	27.055	3	*.000*
composition	2.804	1	.094
Dimension * composition	.559	3	.906

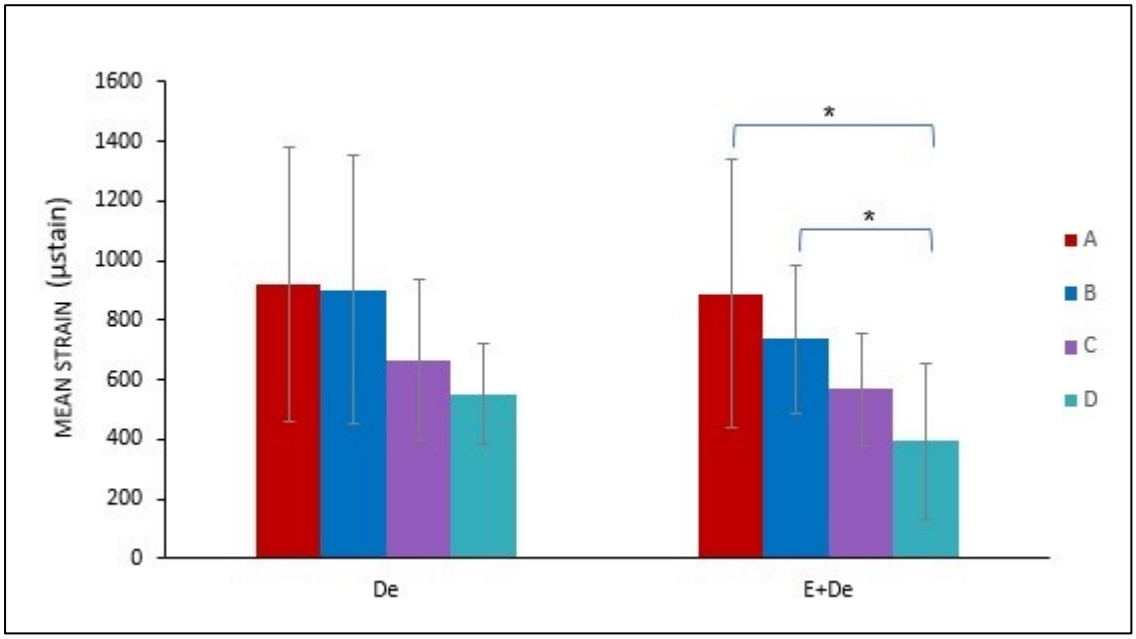

Figure 4.7: The mean strain values for all the groups ± standard deviation with Digital Image Correlation (DIC) testing for both Dentine (De) and Enamel+Dentine (E+De) groups. n=10 per group (*p< 0.05). A, (Height to Width ratio (H:W) = 2:1mm). B, (H:W= 3:1mm), C, (H:W= 3:1.5mm), D, (H:W= 4.5:1.5mm).

4.2.4.2 Strain Gauge Results:

The 3-way ANOVA indicated a statistically significant difference (p<.05) in the mean strains between the different preparation dimensions (A, B, C, D), between the 2 composition groups (De, E+De), and between different restoration stages (prepared, core1, core2 (**Table 10**).

Strain readings for all prepared cavity dimensions in both composition groups (De, E+De) were statistically significantly higher than control. Dimension (A) showed significantly higher strain than all other dimensions. While, dimensions B showed significantly higher strain than D only in (E+De) composition (p<.05).

After restorations, all restored groups (A, B, C, and D) in both compositions (De, E+De) showed significantly higher strain than control. The effect of different restoration design was evaluated for each composition. In Dentine (De) groups, dimension (A) showed significantly higher strain for both core1 and core2 than all other groups (B, C, & D), but no significance was detected from the prepared unrestored group. Strain in dimension (B) with core1 showed no significance from the prepared or core2 groups but was significantly lower than dimension (A) and higher than dimension (D). While strain in dimension (B) with core2 was significantly lower than the prepared group and dimension (A), and higher than dimension (C) and (D). Dimension (C) with core1 showed no significance from prepared or core2 but was significantly lower than dimension (A). While, dimension (C) with core2 was significantly lower than the prepared and dimensions (A) and (B). Dimension (D) with core1 showed significantly lower

strain than dimension (A) and (B) but this was not significantly different to the prepared group or dimension (C). Also, the strain in core1 was significantly higher than that found with core2. While, Dimension (D) with core2 demonstrated significantly lower strain than the prepared group and dimensions (A) and (B) groups.

In (E+De) group, the strain generated in dimension (A) with both core1 and core2 was significantly higher than all other groups (B, C, D). Also the strain associated with core1 was significantly higher than that with core2, and both were significantly lower than the prepared group. Dimension (B) with core1 showed no significance from the prepared or core2 groups strain but was significantly lower than dimension (A) and higher than (D). While, the strain in dimension (B) with core2 was significantly lower than the prepared group and dimension (A) and higher than (C) and (D). Both dimensions (C) and (D) with both core1 and core2 showed only significantly lower strain than dimension (A). However, no significance was detected between core1 and core2 in both groups. Dimension (C) with core2 yielded significantly lower strain than (prepared) groups. Finally, for dimension (D), no significance was detected between core1, core2, or the prepared groups.

The effect of tooth composition on strain in all dimension over all restorative stages revealed the following. Group (A) and (C) showed no significance between restorative types and for all compositions. Group (B), recorded significantly higher strain in (De) than (E+De) for all restorative stages. While, in group (D), significantly higher strain was only recorded between the two compositions in the prepared groups.

The estimated mean strain values and their associated standard deviation for all dimension groups (A, B, C, D) in (De) and (E+De) compositions at all restorative stages (Prepared, core1, core2) are shown in (**Figure 4.8**). While, comparison of the mean strain values within each dimension group at different compositions and restorative levels with (SG) testing is shown in (**Figure 4.9**).

Table 10: Tests of Model Effects in All Groups with Strain as Dependant Variable

Source	Type III		
	Wald Chi-Square	Degree of Freedom (df)	Significance
Dimension	683.029	3	.000
Composition	129.108	1	.000
restoration	173.702	2	.000
Dimension * Composition	28.857	3	.000
Dimension * restoration	22.890	6	.001
Composition * restoration	6.683	2	.035
Dimension * Composition * restoration	11.087	6	.026

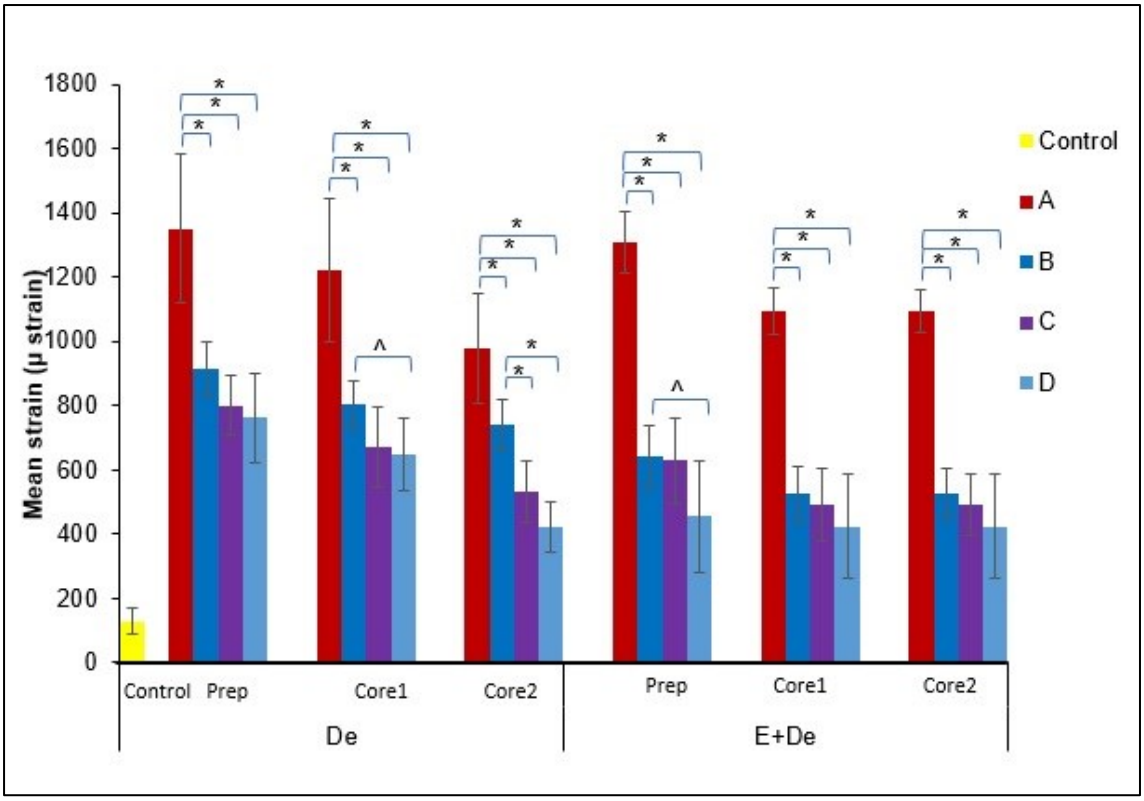

Figure 4.8: Comparison of the mean strain values between different dimensions with the same composition at all restorative stages ± standard deviation with Strain Gauge (SG) testing. *n*=10 per group (*p<0.05 statistical difference between groups), (^p<0.01 statistical difference between groups). De= Dentine, E+De= Enamel+Dentine. A, (Height to Width ratio (H:W) = 2:1mm). B, (H:W= 3:1mm), C, (H:W= 3:1.5mm), D, (H:W= 4.5:1.5mm). Prep= prepared unrestored sample, Core1= intracoronal core composite restoration, Core2= cuspal coverage composite restoration).

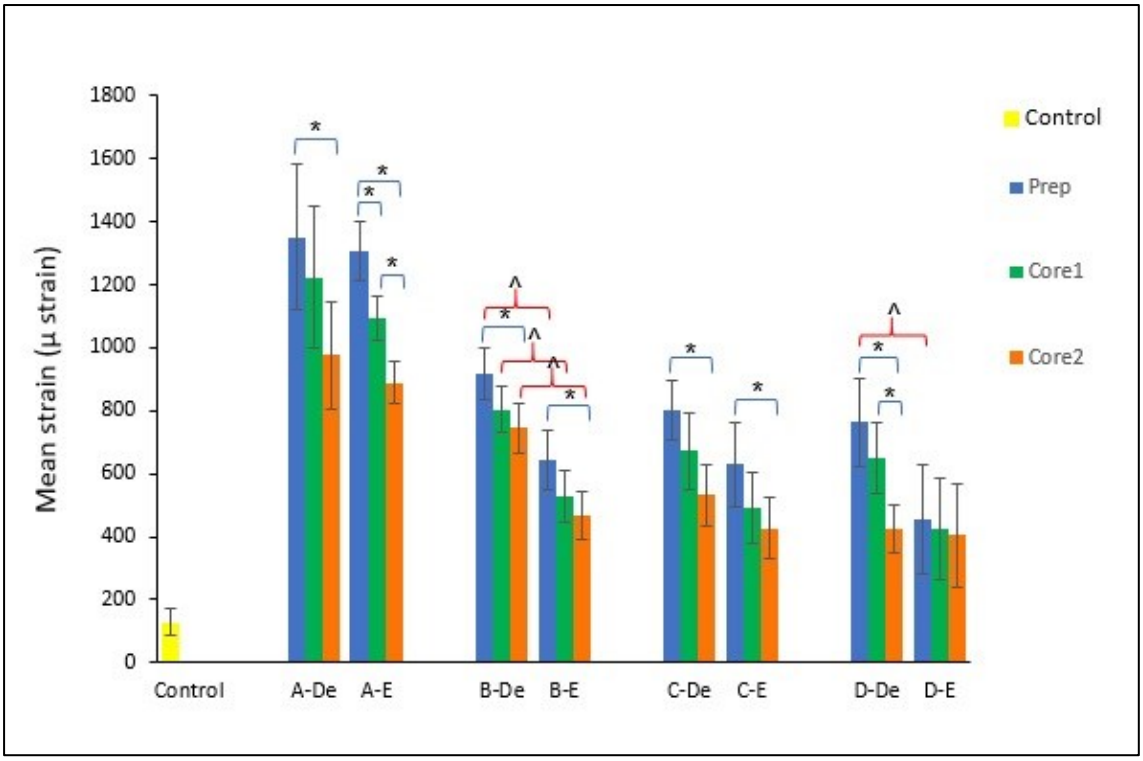

Figure 4.9: Comparison of the mean strain values within each dimension group (with different compositions and restorative levels) ± standard deviation with Strain Gauge (SG) testing. n=10 per group (* $p<0.01$ statistical difference between restorative stages in groups of the same dimension and composition), (^ $p<0.01$ statistical difference between restorative stages in groups of the same dimension and different compositions). De= Dentine, E= Enamel+Dentine. A, (Height to Width ratio (H:W) = 2:1mm). B, (H:W= 3:1mm), C, (H:W= 3:1.5mm), D, (H:W= 4.5:1.5mm). Prep= prepared unrestored sample, Core1= intracoronal core composite restoration, Core2= cuspal coverage composite restoration).

4.2.5 Discussion- Chapter 4:

In the present study, teeth were subjected to gradual non-destructive occlusal loading followed by unloading in order to try to mimic a clinically relevant loading pattern. Different dimensions, qualities of remaining tooth structures and the effect of directly bonding composite core restorations using 2 restoration designs were investigated with no attempt to restore the teeth to their original form. Teeth were prepared according to 4 sets of dimensions involving different height to width ratios. The resulting walls followed the natural convexity of the buccal and palatal tooth surfaces.

DIC is an innovative non-contact optical methodology to measure strain and displacement. It uses the relative movement between two images to measure in-plane displacements. The effect of the size of the tooth specimen under load was incorporated by calculating bulk modulus for each sample from the zone where linear strain behaviour has been recorded. This was done to overcome the inevitable size variations expected to occur between samples although they were carefully hand-prepared but not machined.

Some areas of the DIC displacement field image appear noisy (**Figure 4.5**), this is due to the out of focus areas and spatial variations in the speckle pattern. The central area across the image was chosen to overcome the noise and maximise the area for the measurement that was in focus (**Figure 4.5**). DIC can measure displacements at a resolution down to about 1/20th of a pixel or in this case about 10 nanometres. However, the limitation of the optical system is the

very limited depth of field and areas away from the centre of the image, that are out of focus, are less suitable for DIC measurements. This may explain the failure of the system to detect the very low displacement expressed by control samples and for this reason they were excluded from testing.

Fabrication of indirect restorations usually includes tooth preparation to remove defects and reshape the remaining tooth structure. There is little published data on the optimal thickness of remaining dentine in preparation walls. Different heights of remaining coronal walls (0 to 5mm) and widths (0.5 to 4mm) have been tested in both vital and non-vital teeth (Al-Wahadni and Gutteridge, 2002, Varvara et al., 2007, Marchi et al., 2008, Arunpraditkul et al., 2009, Veríssimo et al., 2014).

Many studies have been carried out to look at coronal dentine height without consideration of width (Al-Wahadni and Gutteridge, 2002, Varvara et al., 2007, Santana et al., 2011, Santos-Filho et al., 2014, Veríssimo et al., 2014, Zhu et al., 2017), root dentine thickness (Lloyd and Palik, 1993, Tjan and Whang, 1985, Marchi et al., 2008), remaining coronal tooth structure location (Ng et al., 2006, Arunpraditkul et al., 2009, Murphy et al., 2009), or a combination of these (Sherfudhin et al., 2011).

The aforementioned studies had different designs, looked at different parameters, and lacked a common standardization with most being carried out *in vitro* and little work being undertaken *in vivo.* So far, however, there have been no controlled studies which define specific recommendations on height to width dimensions and locations of remaining tooth structure to best withstand stresses

and resist fracture. By that, this study is considered the first to evaluate remaining tooth walls with a specified height to width ratio.

Seow (2005) found that following tooth preparation for a ceramic inlay and onlay, the width of 2.0-2.5mm of buccal and palatal tooth structure was remaining. While, following preparation for a metal-ceramic crown, approximately 1.0mm of tooth structure was left buccally, and between 1.6mm-1.8mm palatally. On the other hand, preparation for an all-ceramic crown, using the slightly more aggressive dimensions recommended for ceramics at that time, retained 1.0mm-1.2mm of tooth structure surrounding the endodontic access cavity. The effect of these varying dimensions is unknown.

Another study by Davis et al. (2012) developed a method to measure local dentine thickness using x-ray micro-tomography scans. Scans were made on extracted upper central incisors before and after preparation for metal ceramic crowns. Their results revealed multiple thicknesses of residual dentine along different prepared crown areas ranging between 0.5mm (the thinnest), and 1-1.5mm (the thickest). Following the aforementioned studies and the tooth restorability index as a guide and considering the size of human posterior teeth and the space occupied by the pulp, the thickness of 1mm and 1.5mm were selected to represent the most common range. In order to assess the possible influence of height and width combinations, these dimensions of remaining wall thicknesses were prepared against multiple wall heights to produce the height: width ratios of 2:1 and 3:1.

In our study, tooth preparation was started as an MOD cavity to create buccal and lingual samples in each premolar. To standardize dimensions, the depth of the mesial and distal cavities was positioned 2mm coronal to the CEJ. The height of the buccal and lingual walls (samples) was measured coronal to an imaginary line positioned 1mm above the CEJ (equivalent to the position of the gingival margin) as Bandlish et al. (2006), used the gingival finish line to assess the remaining tooth structure coronal to this level. This was designed in order to prevent pulpal exposure and to simulate a clinical approach to avoid encroaching on the biologic width.

Samples in this study were tested as independent walls of remaining tooth structure without the incorporation of a finish line or investigation of the effect of 'ferrule' if these teeth were restored. The incorporation of the 'ferrule' concept is considered one of the foundations of restoration of vital and endodontic treated teeth. (Ng et al., 2006, Jotkowitz and Samet, 2010).

Destructive mechanical tests can be used in situations of high intensity load application, to determine fracture resistance and analyse tooth behaviour. However, these tests show limitations in obtaining the valuable internal behaviour of the tooth restoration complex. For a more reliable response, a combination of non-destructive methodologies has been implemented (Reeh et al., 1989b, Deng et al., 1995, Soares et al., 2008a). The implementation of non-destructive testing methods allows sequential and repeated measurements on the same tooth. This allows consistency of measurements, takes into consideration the individual differences between teeth, and minimizes the effects of the natural variation between teeth (Jantarat et al., 2001).

Based on these results, the null hypothesis that there would be no significant difference in tooth strain with different structural loss could be rejected. The results of both DIC and strain gauge testing methodologies showed significant difference in strain values between some of the geometries tested (A, B, C, & D). (E+De) group showed generally lower strain values than (De) at all dimensions and all restorative stages (prepared, core1, core2) tested with strain gauges. This is most likely due to the stiffening effect enamel has on dentine albeit its minimal dimension in (E+De) groups when compared to the presence of dentine only in (De) groups. The role of enamel in resisting and dissipating strain may be particularly important to patients who have lost enamel due to attrition, ageing, or trauma. However, significant difference between the two compositions could be detected only when strain gauges were used. This could be attributed to the reliability and accuracy of the strain gauges mounted directly on the tooth structure, in measuring relative stress/strain.

Regarding dimensions, dimension (A) always recorded a significantly higher strain at all restorative stages than all groups (B, C, D) in both tooth composition groups (De and E+De). This may indicate the insufficiency of this dimension in both height and width aspects and therefore, failure in withstanding functional stresses. Moreover; in (De) group, significant results were observed among different restorative stages when dimension (B) was tested. Dimension (B) with (core1) was significantly higher than (D). While, with (core2) it was significant to both (C) and (D). This was not seen in (E+De) groups, suggesting the strengthening effect of enamel and the particular effect of width and not only the height of the remaining tooth structure on its ability to resist stresses.

Since both testing methodologies gave similar result patterns, the null hypothesis that there was no difference in strain measured using 2 techniques can be partially accepted. In both methodologies, group (A) possessing the smallest height and width (2:1mm) showed the highest strain and was significantly different to both groups (C) & (D) (3:1.5mm & 4.5:1.5mm) respectively. These results suggest the importance of the height to width ratio in the preparation, and that by preserving a minimum height of 3 mm and a width between 1-1.5 mm lower strain is achieved.

This study's findings with regards to remaining tooth width agree with the results of (Shahrbaf et al., 2007) who found that fracture resistance of endodontically-treated teeth with composite restoration could be reduced by preserving a mesial marginal ridge thicknesses of 2mm, 1.5mm and 1mm. However, preserving a 0.5mm thickness of the mesial marginal ridge did not provide fracture resistance at the level of intact teeth, yet it conferred higher strength than teeth with no marginal ridge at all.

The results also accord with earlier observations by (AL-Omiri and AL-Wahadni, 2006), who investigated the effect of different heights of remaining coronal dentine on the fracture resistance of root canal treated teeth restored with composite cores. Although results were not statistically significant, greater fracture resistance was achieved with greater retained dentine height. However, the fracture pattern of teeth was not related to the height of retained dentine when the height was >2mm. The positive influence of maintaining 3mm of tooth structure was also confirmed by Al-Wahadni and Gutteridge (2002).

Magne (2007) and (Magne and Oganesyan, 2009) have tested the response of both anterior and posterior teeth under different loading configurations. The authors concluded that progressive loss of tooth substance [MO to MOD to ENDO (Endodontic Access)] produced a progressive loss of cuspal stiffness. They also confirmed that linear axial loading of posterior teeth did not generate harmful concentrations of stress compared to lateral loading. However, the behaviour of posterior teeth must be differentiated from the behaviour of anterior teeth due to shape and occlusal loading patterns. Stress distribution within an incisor was not significantly affected when the tooth material was removed proximally, whereas, a significant increase in stress concentration and flexibility occurred when facial and palatal tooth material was removed (Magne and Douglas, 2000, Magne and Tan, 2008).

Our results are also in agreement with findings of a FEA study to test the influence of remaining tooth structure on stress distribution in endodontically treated maxillary premolars (Zhu et al., 2017). In order to protect the residual tooth structure, the authors recommended a conservative preparation including preservation of coronal tooth structure height (enamel and dentine).

A number of studies suggested that when the biophysical stress and strain in restored teeth were analysed, restorative procedures were found to induce the tooth crown deformation, and that teeth strength could be improved by increasing their resistance to crown deformation (Morin et al., 1988a, Morin et al., 1988b, Magne, 2007, Yamanel et al., 2009). In situations of minimal or no retention, adhesive restorations have a major advantage of bonding to both enamel and dentine (van Dijken, 1999). Bonding to enamel is stable over time, but *in vivo*

(Breschi et al., 2008, Liu et al., 2011) and *in vitro* (De Munck et al., 2005) studies have revealed the limited durability of resin-dentine bonds (Marchesi et al., 2013). Frassetto et al. (2016) carried out a review on the durability of resin-bonded interfaces and their degradation with ageing and concluded that although most currently used dental adhesive systems show favourable immediate results reflected in good retention and sealing, dentine bonded interfaces may not withstand ageing and may show long-term degradation (Van Meerbeek, 2003). Additionally, clinical trials evaluating adhesive systems have found dramatically variable bonding qualities between tested materials (van Dijken, 2000) and substrate (Heymann et al., 1988, Prati et al., 1999). Bonding to ageing teeth had the greatest incidence of retention failure when two dentine bonding systems where tested in conjunction with various materials to restore Class V cervical lesions (Heymann et al., 1988). Similarly, difficulty in bonding to old sclerotic dentine was reported earlier by (Lambrechts, 1987). This could be attributed to ageing dentinal changes that can result in a substrate less receptive to dentinal bonding (Heymann et al., 1988). Prati et al. (1999) evaluated the morphology of the resin tags and the resin infiltrated dentin layer (RIDL) of several bonding systems in young, old and sclerotic dentin. Sclerotic and old dentin showed thinner RIDL, with short resin tags, and fewer lateral branches than normal dentin. Similar results were observed in a more recent study by Lopes (2011), where resin tags in young dentin were larger and more numerous than old dentine. Also, the hybrid layer formed in intertubular old dentin was very thin. Given that the dentine- adhesive bond varies among different condition and it deteriorates with time, reliance purely on adhesion may not be ideal and investment in studying remaining tooth structure is still considered important to long-term outcomes.

Two restoration designs were tested to study the effect of bonding direct restorations to compromised tooth structure. The first stage (core1) included a composite core restoration up to the level of the remaining wall of each sample. While, the second stage (core2) included an added build-up mimicking the effect of cuspal coverage on top of the prepared walls to achieve a total height of 6mm. The original cervico-occlusal height, buccolingual and mesiodistal width dimensions of a sound premolar crown are cited as 8.5mm, 9mm, 7mm, respectively (Fehrenbach and Popowics, 2015). Samples were not restored to the original dimensions as only the height of the crown and not the width was restored. During sample preparation the total axial thickness was reduced by 1-1.5 mm at each wall (total of 2-3 mm; mean of 2.5 mm, from each dimension) leaving a width of 6.5mm buccolingually and 4.5mm mesiodistally. This axial reduction (2.5 mm) was also accounted for in calculating the total crown height. The height had to be modified to be 6mm (8.5 mm - 2.5 mm= 6 mm), to end up with a comparable height to width ratio to a sound premolar.

The results show a decrease in strain with addition of restorations. The lower strain recorded by both core1 and core2 than the prepared group at all dimensions, of both tooth composition groups highlights the advantage of restoration. Cuspal coverage (core2) showed significantly lower strain than the prepared group in almost all dimensions. Additionally; although insignificant, the strain recorded with core1 was always lower than the prepared group. Moreover, core2 always recorded lower strain than core1, but again the values were not statistically significant. This agrees with the findings of (Çötert et al., 2001, Dalpino et al., 2002, Sagsen and Aslan, 2006, Seow et al., 2015) that adhesive systems

had shown the ability to strengthen the restored tooth units. Also, bonding intracoronal restorations was suggested to offer cusp splinting and decrease cuspal flexure, thus strengthening the remaining tooth unit (De Souza et al., 2002, Seow et al., 2015). This was considered particularly important when restoring endodontically treated and extensively compromised posterior teeth (Eakle et al., 1986). However, it should be always borne in mind the unknown length of time that this bond may last. Dentin adhesion is designed to remain in place for decades. However; as a result of hydrolytic breakdown, proteases, decay or fracture, the adhesive interface degrades and fails, and various deterioration times have been reported (Sano, 2006, Opdam et al., 2010, Spencer et al., 2010, Montagner et al., 2018).

Results of restorative stages also emphasize the advantage of cuspal coverage in strengthening the remaining tooth structure. Cuspal coverage restorations have been shown to be superior to intracoronal inlay restorations in terms of protection of the remaining structure against the effect of functional loading and in improvement of the overall success rate of posterior teeth clinically (Sorensen and Martinoff, 1984). In addition, Seow et al. (2015) found that teeth restored with cuspal coverage restorations in the form of full ceramic onlays had stiffness values equal or greater than that of sound teeth. However, the level of stiffness with ceramic inlay restorations in their study was found to be significantly lower than unrestored teeth. Results of core1 and core2 in our study showed a similar behaviour pattern to inlays and onlays in Sorensen and Martinoff (1984) and Seow et al. (2015). Core1 compares to the behaviour of inlays, as recorded strain was not significantly lower than the prepared group. While, core2 behaved

as an onlay with significantly lower strain than the prepared group. Furthermore, the advantages of onlay restorations in terms of cuspal splinting, reducing cuspal flexure and strengthening the remaining structure was confirmed by (Brunton et al., 1999, De Souza et al., 2002, Seow et al., 2015) and that bonded restorations may restore the substantially lost cuspal stiffness after preparation (Reeh et al., 1989a, Shor et al., 2003, Taha et al., 2011, Seow et al., 2015).

The results of core1 and core2 in our study are in agreement with the results by Magne and Belser (2003). In their study, both ceramic and composite resin inlays and onlays were compared under vertical loading. For both materials, more favourable stress pattern was observed with onlays where the majority of the stresses were compressive, while tensile stresses were the majority for inlays, given rounded line angles were provided. The low elastic modulus of composite resin allowed more strain transfer to the underlying tooth structure when compared to ceramics (Magne et al., 1999, Magne and Belser, 2003).

In conclusion, this is an *in vitro* study so it cannot replicate the clinical situation although it was designed to replicate the clinical environment as closely as possible. The preservation of a remaining minimum tooth height of 3 mm and a width of 1-1.5 mm produced lower strain upon loading than 2mm tooth height with the same cusp width. However, 1.5 mm width performed better than 1 mm. Although H:W dimension 3:1 mm performed better than 2:1 mm, the strain reduced further with an increased width (3:1.5 mm). Remaining tooth structure, comprised of both enamel and dentine, resisted strain under load better than dentine only counterparts at all test dimensions when evaluated with strain gauges. The results obtained with strain gauges and DIC showed similar trends.

DIC is a relatively simple optical methodology that allows measurement of strain and displacement without the need for physical attachment to the object. Although no restoration was able to restore strain levels to control, cuspal coverage restoration appears to be more effective than intracoronal restoration in supporting the remaining tooth structure.

General Conclusions

Erosion development methodology experiments confirmed that enamel with different surface preparations, all salivary conditions, and immersion protocols produced lesions with comparable thickness loss. So, either erosion protocol; of sound or polished enamel with any saliva condition (no saliva, artificial saliva, and natural saliva) at any erosion rate (accelerated, and prolonged), were suitable for application to generate different lesions simulating clinical erosion. However, some experiments used polished samples as it was necessary for some experimental tools to have a flat surface for reference. While, sound surfaces were tested in other experiments mimicking extensive oral erosion conditions. In addition, subsurface erosion experiments verified lesion morphology of different immersion protocols (early, accelerated and prolonged) to be comparable in lesion extension. Therefore, for testing convenience and to produce extensive erosion lesions mimicking clinical lesions created over years of heavy soft drink consumption, the accelerated erosion protocol with no saliva was chosen. Lesions with extensions mimicking different clinical erosion stages were selected for testing at 0, 1, 7, 10, and 14 days of continuous erosion.

Strain testing under static vertical loading within the physiological limit for human teeth was carried out on tooth samples with different created levels of structural loss (by acid erosion or tooth preparation). Erosion samples were prepared with different levels of occlusal or buccal soft drink erosion lesions in mandibular molar teeth followed by restorations to full form using onlays. While,

samples with different levels of prepared tooth wall dimensions were created by handpiece preparation mimicking different levels of compromised tooth structure after caries, followed by different composite resin core restorations. Occlusal erosion lesions recorded slightly increased strain readings at the initial enamel loss stage followed by gradual decrease through-out the stages. While, buccal erosion lesions recorded continuous increase in the recorded strain readings through-out all stages to reach its highest at the deepest lesion. Restoration of occlusally eroded molars restored strain levels close to the pre-treatment level with all restorative materials used. However, IPS ceramic and gold onlays resulted in a better strain distribution pattern and conveyed less stresses to the underlying tooth structure unlike composite resin onlays. While, Composite resin was the only restorative material applied for buccally created lesions and was able to restore strain level to pre-treatment condition. FEA and ESPI were applied to test occlusal erosion samples and their results were comparable to strain gauges. However, ESPI showed increased sensitivity to vibration which complicated the testing process.

Strain recorded by different remaining wall dimensions showed that walls with the minimum height of 3mm and width of 1.5mm recorded lower strain levels than smaller dimensions and were not significantly different than bigger dimensions. The same remaining tooth dimensions showed significant reduction in strain when samples were restored with a core only or a core with cuspal coverage restorations. Remaining tooth structure with both enamel and dentine compositions resisted strain under loading better than dentine only counterparts. Both strain gauges and DIC were applied for theses samples and generated

comparable results. Therefore, strain gauges may still be considered the gold standard for localized strain measurement.

Summary

There is a relative paucity of literature relating to guidelines for assessing and managing badly broken down teeth. This body of work is set out to determine the effect of remaining coronal tooth dimensions on internal stain of teeth and the most suitable restorative material to select. Strain under loading was measured in teeth with different dimensions and restoration designs. The conditions that foster reduced strain particularly if strain was restored to levels close to the pre-treatment condition.

Preservation of remaining tooth dimensions with the minimum height of 3mm and width of 1.5mm recorded lower strain levels than smaller dimensions under gradual occlusal loading within the physiological load limit that exists during function. The same remaining tooth dimensions showed significant reduction in strain when samples were restored with a core only or a core with cuspal coverage restorations. Remaining tooth structure with both enamel and dentine compositions resisted strain under loading better than dentine only counterparts. Correlating strain gauge findings with an alternative technique (digital image correlation substantiated results and supported the use of the innovative technique. These showed similar behavior of remaining tooth structure dimensions albeit small changes with altered tooth structure composition when loaded. This is most likely attributed to the strengthening effect of enamel on the remaining structure albeit its minimal thickness.

Soft drink erosion experiments to measure enamel surface/subsurface changes and surface loss were carried out under different immersion protocols; (early, prolonged, and accelerated) and media (no saliva, artificial saliva, and natural saliva), to develop the most appropriate protocol for generation of different levels of external erosion-like lesions (lower molar occlusal or buccal surface). Different experimental techniques were applied and verified (scanning electron microscopy, confocal microscopy, laser profilometry, optical coherence tomography, and light microscopy). All tested protocols showed comparable results. Thus, the accelerated erosion protocol with no saliva was selected. Erosion periods of (1, 7, 10, and 14 days) of continuous acid immersion were selected to represent four clinical stages of acid erosion lesions (initial enamel erosion, 1/3rd enamel thickness loss, 2/3 enamel thickness loss, and total enamel loss). Under loading, strain levels in occlusally eroded molars slightly increased at the initial enamel loss level followed by gradual decrease through-out the stages. Correlating strain gauge findings with alternative techniques (electronic speckle pattern interferometry and finite element analysis) supported the strain gauge results. Restoration of occlusal lesions with onlays of different materials restored strain close to the pretreatment level and showed comparable results. However, favorable strain distribution patterns were observed by FEA with ceramic and gold onlays compared to composite onlays. On the other hand, teeth with buccal erosion lesions behaved differently under loading, where strain gradually increased at the 1st and second stages of erosion followed by a significant increase at the 3rd and fourth stages. However, restoration of buccal lesions with composite restoration restored strain close to the pretreatment level.

Clinical management of tooth surface demineralisation should focus first on early detection and prevention, such as remineralisation, before a restorative approach is applied. Restoration of buccally eroded lesions is essential even at an early stage to prevent excessive stress concentration in teeth under loading.

Clinical Significance

Deformation of teeth under occlusal loading is particularly important to the broken-down tooth. Under loading, stresses concentrate within the remaining tooth structure. Increased loss of tooth structure can affect stress distribution within the tooth, increasing the potential of tooth fracture and the risk of restorative failure or further loss.

Restoration of structurally compromised teeth is essential. Restoration of teeth to full form and function using the best restorative material option are key factors for the success and longevity of the placed restoration. Equally important are the design of the restoration and the role of adhesion in dentistry.

Future Work

- ***Lateral Loading:***

As testing was done in an axial direction along the long axis of the prepared teeth, loading in a lateral direction can represent a more realistic view of both load directions present in the oral cavity.

- ***The use of cyclic loading and chewing simulator:***

A chewing simulator can be used to allow the evaluation of dental restorative systems under clinically relevant conditions. After placement of different coronal restorations, both fracture resistance of the restoration and tooth substructure can be evaluated.

- ***Comparison of sound and root canal treated teeth:***

The study was done on premolar and molar teeth without exposing the pulp tissue and teeth were considered vital. The same testing protocol should be carried out on root canal treated teeth to compare the effect of the lost root dentin/medicaments on the strain pattern.

- ***The use of different preparation designs:***

The effect of different remaining tooth structure locations and distribution can be tested with the combination of different restorative design and material options comparisons.

References

2007. Tooth structure and fracture resistance. *Dental Abstracts,* 52**,** 66-67.

ABE, Y., LAMBRECHTS, P., INOUE, S., BRAEM, M. J., TAKEUCHI, M., VANHERLE, G. & VAN MEERBEEK, B. 2001. Dynamic elastic modulus of 'packable' composites. *Dental materials,* 17**,** 520-525.

ABU-HASSAN, M., ABU-HAMMAD, O. & HARRISON, A. 2000. Stress distribution associated with loaded ceramic onlay restorations with different designs of marginal preparation. An FEA study. *Journal of oral rehabilitation,* 27**,** 294-298.

ADDY, M., ABSI, E. G. & ADAMS, D. 1987. Dentine hypersensitivity. The effects in vitro of acids and dietary substances on root-planed and burred dentine. *Journal of Clinical Periodontology,* 14**,** 274-279.

ADEBAYO, O., BURROW, M. & TYAS, M. 2009. An SEM evaluation of conditioned and bonded enamel following carbamide peroxide bleaching and casein phosphopeptide-amorphous calcium phosphate (CPP-ACP) treatment. *Journal of dentistry,* 37**,** 297-306.

ADEGUN, O., TOMLINS, P., HAGI-PAVLI, E., BADER, D. L. & FORTUNE, F. 2013. Quantitative optical coherence tomography of fluid-filled oral mucosal lesions. *Lasers in medical science,* 28**,** 1249-1255.

ADEGUN, O. K., TOMLINS, P. H., HAGI-PAVLI, E., MCKENZIE, G., PIPER, K., BADER, D. L. & FORTUNE, F. 2012. Quantitative analysis of optical coherence tomography and histopathology images of normal and dysplastic oral mucosal tissues. *Lasers in medical science,* 27**,** 795-804.

AKÇA, K., ÇEHRELI, M. C. & İPLIKÇIOĞLU, H. 2002. A comparison of three-dimensional finite element stress analysis with in vitro strain gauge measurements on dental implants. *International Journal of Prosthodontics,* 15.

AL-DLAIGAN, Y., SHAW, L. & SMITH, A. 2001. Dental erosion in a group of British 14-year-old, school children. Part I: Prevalence and influence of differing socioeconomic backgrounds. *British Dental Journal,* 190**,** 145-149.

AL-OMIRI, M. & AL-WAHADNI, A. 2006. An ex vivo study of the effects of retained coronal dentine on the strength of teeth restored with composite core and

different post and core systems. *International endodontic journal,* 39**,** 890-899.

AL-SUKHUN, J., KELLEWAY, J. & HELENIUS, M. 2007. Development of a three-dimensional finite element model of a human mandible containing endosseous dental implants. I. Mathematical validation and experimental verification. *Journal of Biomedical Materials Research Part A: An Official Journal of The Society for Biomaterials, The Japanese Society for Biomaterials, and The Australian Society for Biomaterials and the Korean Society for Biomaterials,* 80**,** 234-246.

AL-WAHADNI, A. & GUTTERIDGE, D. 2002. An in vitro investigation into the effects of retained coronal dentine on the strength of a tooth restored with a cemented post and partial core restoration. *International endodontic journal,* 35**,** 913-918.

AL AZRI, K., MELITA, L., STRANGE, A., FESTY, F., AL JAWAD, M., COOK, R., PAREKH, S. & BOZEC, L. 2016. Optical coherence tomography use in the diagnosis of enamel defects. *Journal of Biomedical Optics,* 21**,** 036004.

ALENCAR, C. R. B. D., OLIVEIRA, G. C. D., MAGALHAES, A. C., BUZALAF, M. A. R., MACHADO, M. A. D. A. M., HONORIO, H. M. & RIOS, D. 2017. In situ effect of CPP-ACP chewing gum upon erosive enamel loss. *Journal of Applied Oral Science,* 25**,** 258-264.

ALEXANDRIA, A. K., VIEIRA, T. I., PITHON, M. M., DA SILVA FIDALGO, T. K., FONSECA-GONÇALVES, A., VALENÇA, A. M. G., CABRAL, L. M. & MAIA, L. C. 2017. In vitro enamel erosion and abrasion-inhibiting effect of different fluoride varnishes. *Archives of oral biology,* 77**,** 39-43.

ALKADI, L. & RUSE, N. D. 2016. Fracture toughness of two lithium disilicate dental glass ceramics. *The Journal of prosthetic dentistry,* 116**,** 591-596.

ALMSTÅHL, A., FINIZIA, C., CARLÉN, A., FAGERBERG-MOHLIN, B. & ALSTAD, T. 2018. Explorative study on mucosal and major salivary secretion rates, caries and plaque microflora in head and neck cancer patients. *International journal of dental hygiene,* 16**,** 450-458.

AMAECHI, B. & HIGHAM, S. 2001a. In vitro remineralisation of eroded enamel lesions by saliva. *Journal of Dentistry,* 29**,** 371-376.

AMAECHI, B., HIGHAM, S. & EDGAR, W. 1999a. Factors influencing the development of dental erosion in vitro: enamel type, temperature and exposure time. *Journal of Oral Rehabilitation,* 26**,** 624-630.

AMAECHI, B., HIGHAM, S. & EDGAR, W. 1999b. Techniques for the production of dental eroded lesions in vitro. *Journal of oral rehabilitation,* 26**,** 97-102.

AMAECHI, B., HIGHAM, S., EDGAR, W. & MILOSEVIC, A. 1999c. Thickness of acquired salivary pellicle as a determinant of the sites of dental erosion. *Journal of dental research,* 78**,** 1821-1828.

AMAECHI, B. T. & HIGHAM, S. M. 2001b. Eroded enamel lesion remineralization by saliva as a possible factor in the site-specificity of human dental erosion. *Archives of Oral Biology,* 46**,** 697-703.

AMAECHI, B. T. & HIGHAM, S. M. 2005. Dental erosion: possible approaches to prevention and control. *Journal of Dentistry,* 33**,** 243-252.

AMEEN, M. 2005. *Computational elasticity: theory of elasticity and finite and boundary element methods*, Alpha Science Int'l Ltd.

AMERONGEN, N., ODERKERK, C. H. & DRIESSEN, A. A. 1987. Role of Mucins from Human Whole Saliva in the Protection of Tooth Enamel against Demineralization in vitro. *Caries Research,* 21**,** 297-309.

ANDERSON, J. N. 1976. *Applied dental materials*, Blackwell Scientific.

ANGELETAKI, F., GKOGKOS, A., PAPAZOGLOU, E. & KLOUKOS, D. 2016. Direct versus indirect inlay/onlay composite restorations in posterior teeth. A systematic review and meta-analysis. *Journal of dentistry,* 53**,** 12-21.

ANUSAVICE, K. 1989. Criteria for selection of restorative materials: properties versus technique sensitivity. *Quality evaluation of dental restorations: criteria for placement and replacement***,** 15-59.

ARANA-CHAVEZ, V. E. & MASSA, L. F. 2004. Odontoblasts: the cells forming and maintaining dentine. *The international journal of biochemistry & cell biology,* 36**,** 1367-1373.

ARUNPRADITKUL, S., SAENGSANON, S. & PAKVIWAT, W. 2009. Fracture resistance of endodontically treated teeth: three walls versus four walls of remaining coronal tooth structure. *Journal of Prosthodontics,* 18**,** 49-53.

ASMUSSEN, E., PEUTZFELDT, A. & SAHAFI, A. 2005. Finite element analysis of stresses in endodontically treated, dowel-restored teeth. *The Journal of prosthetic dentistry,* 94**,** 321-329.

ASSIF, D., BITENSKI, A., PILO, R. & OREN, E. 1993. Effect of post design on resistance to fracture of endodontically treated teeth with complete crowns. *The Journal of prosthetic dentistry,* 69**,** 36-40.

ATTIN, T. 2006. Methods for assessment of dental erosion. *Dental Erosion.* Karger Publishers.

ATTIN, T., BECKER, K., WIEGAND, A., TAUBOCK, T. T. & WEGEHAUPT, F. J. 2012. Impact of laminar flow velocity of different acids on enamel calcium loss. *Clinical Oral Investigations,* 17**,** 595-600.

ATTIN, T., BUCHALLA, W., GOLLNER, M. & HELLWIG, E. 2000. Use of variable remineralization periods to improve the abrasion resistance of previously eroded enamel. *Caries research,* 34**,** 48-52.

ATTIN, T., MEYER, K., HELLWIG, E., BUCHALLA, W. & LENNON, A. 2003. Effect of mineral supplements to citric acid on enamel erosion. *Archives of oral biology,* 48**,** 753-759.

AUSIELLO, P., APICELLA, A., DAVIDSON, C. L. & RENGO, S. 2001. 3D-finite element analyses of cusp movements in a human upper premolar, restored with adhesive resin-based composites. *Journal of Biomechanics,* 34**,** 1269-1277.

AUSIELLO, P., CIARAMELLA, S., MARTORELLI, M., LANZOTTI, A., ZARONE, F., WATTS, D. C. & GLORIA, A. 2017. Mechanical behavior of endodontically restored canine teeth: Effects of ferrule, post material and shape. *Dental Materials,* 33**,** 1466-1472.

AUSIELLO, P., RENGO, S., DAVIDSON, C. L. & WATTS, D. C. 2004. Stress distributions in adhesively cemented ceramic and resin-composite Class II inlay restorations: a 3D-FEA study. *Dental Materials,* 20**,** 862-872.

AUSTIN, R., GIUSCA, C., MACAULAY, G., MOAZZEZ, R. & BARTLETT, D. 2016. Confocal laser scanning microscopy and area-scale analysis used to quantify enamel surface textural changes from citric acid demineralization and salivary remineralization in vitro. *Dental Materials,* 32**,** 278-284.

AYKUT-YETKINER, A., WIEGAND, A. & ATTIN, T. 2014. The effect of saliva substitutes on enamel erosion in vitro. *Journal of Dentistry,* 42**,** 720-725.

BAEK, J. H., NA, J., LEE, B. H., CHOI, E. & SON, W. S. 2009. Optical approach to the periodontal ligament under orthodontic tooth movement: a preliminary study with optical coherence tomography. *American Journal of Orthodontics and Dentofacial Orthopedics,* 135**,** 252-259.

BANDLISH, R. B., MCDONALD, A. V. & SETCHELL, D. J. 2006. Assessment of the amount of remaining coronal dentine in root-treated teeth. *Journal of Dentistry,* 34**,** 699-708.

BANERJEE, A., PABARI, H., PAOLINELIS, G., THOMPSON, I. D. & WATSON, T. F. 2011. An in vitro evaluation of selective demineralised enamel removal using bio-active glass air abrasion. *Clinical oral investigations,* 15**,** 895-900.

BARBOUR, M., FINKE, M., PARKER, D., HUGHES, J., ALLEN, G. & ADDY, M. 2006. The relationship between enamel softening and erosion caused by soft drinks at a range of temperatures. *Journal of dentistry,* 34**,** 207-213.

BARBOUR, M. & REES, J. 2004. The laboratory assessment of enamel erosion: a review. *Journal of Dentistry,* 32**,** 591-602.

BARCELOS, L., BICALHO, A., VERÍSSIMO, C., RODRIGUES, M. & SOARES, C. 2017. Stress distribution, tooth remaining strain, and fracture resistance of endodontically treated molars restored without or with one or two fiberglass posts and direct composite resin. *Operative dentistry,* 42**,** 646-657.

BARDSLEY, P. 2008. The evolution of tooth wear indices. *Clinical Oral Investigations,* 12**,** 15-19.

BARNES, D., BLANK, L., THOMPSON, V. & GINELL, J. 1991. Clinical investigation of a posterior composite materials after 5 and 8 years. *Die Quintessenz,* 42**,** 1067-1080.

BARON, P. 1999. The development of dentistry, 1000–2000. *The Lancet,* 354**,** SIV11.

BARONE, A., DERCHI, G., ROSSI, A., MARCONCINI, S. & COVANI, U. 2008. Longitudinal clinical evaluation of bonded composite inlays: A 3-year study. *Quintessence International,* 39.

BARTLETT, D. & DUGMORE, C. 2008. Pathological or physiological erosion—is there a relationship to age? *Clinical oral investigations,* 12**,** 27-31.

BARTLETT, D., GANSS, C. & LUSSI, A. 2008. Basic Erosive Wear Examination (BEWE): a new scoring system for scientific and clinical needs. *Clinical oral investigations,* 12**,** 65-68.

BARTLETT, D. & SHAH, P. 2006. A critical review of non-carious cervical (wear) lesions and the role of abfraction, erosion, and abrasion. *Journal of dental research,* 85**,** 306-312.

BARTLETT, D. W., LUSSI, A., WEST, N., BOUCHARD, P., SANZ, M. & BOURGEOIS, D. 2013. Prevalence of tooth wear on buccal and lingual surfaces and possible risk factors in young European adults. *Journal of dentistry,* 41**,** 1007-1013.

BASSETT, R. W., INGRAHAM, R. & KOSER, J. R. 1964. *An atlas of cast gold procedures*, Department of Operative Dentistry, University of Southern California, School of Dentistry.

BASSIR, M. M., LABIBZADEH, A. & MOLLAVERDI, F. 2013a. The effect of amount of lost tooth structure and restorative technique on fracture resistance of endodontically treated premolars. *J Conserv Dent,* 16**,** 413-7.

BASSIR, M. M., LABIBZADEH, A. & MOLLAVERDI, F. 2013b. The effect of amount of lost tooth structure and restorative technique on fracture resistance of endodontically treated premolars. *Journal of Conservative Dentistry,* 16**,** 413-417.

BATISTA, G. R., TORRES, C. R. G., SENER, B., ATTIN, T. & WIEGAND, A. 2016. Artificial saliva formulations versus human saliva pretreatment in dental erosion experiments. *Caries research,* 50**,** 78-86.

BENAZZI, S., KULLMER, O., GROSSE, I. R. & WEBER, G. W. 2011. Using occlusal wear information and finite element analysis to investigate stress distributions in human molars. *Journal of Anatomy,* 219**,** 259-272.

BERNARDON, J. K., MAIA, E. A. V., CARDOSO, A. C., DE ARAÚJO JR, E. M. & MONTEIRO JR, S. 2002. Diagnosis and management of maxillary incisors affected by incisal wear: an interdisciplinary case report. *Journal of Esthetic and Restorative Dentistry,* 14**,** 331-339.

BERTASSONI, L. E., HABELITZ, S., PUGACH, M., SOARES, P. C., MARSHALL, S. J. & MARSHALL, G. W. 2010. Evaluation of surface structural and mechanical changes following remineralization of dentin. *Scanning,* 32**,** 312-319.

BEVENIUS, J., L'ESTRANGE, P., KARLSSON, S. & CARLSSON, G. 1993. Idiopathic cervical lesions: in vivo investigation by oral microendoscopy and scanning electron microscopy. A pilot study. *Journal of oral rehabilitation,* 20**,** 1-9.

BHARTI, R., WADHWANI, K., TIKKU, A. & CHANDRA, A. 2010. Dental amalgam: An update. *Journal of Conservative Dentistry,* 13**,** 204-208.

BLACK, S. & AMOORE, J. 1993. Measurement of forces applied during the clinical cementation of dental crowns. *Physiological measurement,* 14**,** 387.

BLASER, P. K., LUND, M. R., COCHRAN, M. & POTTER, R. H. 1983. Effect of designs of Class 2 preparations on resistance of teeth to fracture. *Operative dentistry,* 8**,** 6.

BOARO, L. C. C., XAVIER, T. A., BRANDT, W. C. & BRAGA, R. R. 2013. How cavity dimension influences in the composite deformation during polymerization shrinkage. *Journal of Research in Dentistry,* 1**,** 127-133.

BORCIC, J., ANIC, I., SMOJVER, I., CATIC, A., MILETIC, I. & RIBARIC, S. P. 2005. 3D finite element model and cervical lesion formation in normal occlusion and in malocclusion. *Journal of oral rehabilitation,* 32**,** 504-510.

BORJIAN, A., FERRARI, C. C., ANOUF, A. & TOUYZ, L. Z. 2010. Pop-cola acids and tooth erosion: an in vitro, in vivo, electron-microscopic, and clinical report. *International journal of dentistry,* 2010.

BRESCHI, L., MAZZONI, A., RUGGERI, A., CADENARO, M., DI LENARDA, R. & DE STEFANO DORIGO, E. 2008. Dental adhesion review: aging and stability of the bonded interface. *Dental materials,* 24**,** 90-101.

BROCA, P. 1879. Instructions relatives à l'étude anthropologique du système dentaire. *Bulletins de la Société d'anthropologie de Paris,* 2**,** 128-163.

BRUDEVOLD, F., GARDNER, D. E. & SMITH, F. A. 1956. The distribution of fluoride in human enamel. *Journal of Dental Research,* 35**,** 420-429.

BRUNTON, P. A., CATTELL, P., BURKE, F. T. & WILSON, N. H. 1999. Fracture resistance of teeth restored with onlays of three contemporary tooth-colored resin-bonded restorative materials. *The Journal of prosthetic dentistry,* 82**,** 167-171.

BUZALAF, M. A. R., HANNAS, A. R. & KATO, M. T. 2012. Saliva and dental erosion. *Journal of Applied Oral Science,* 20**,** 493-502.

CAIRNS, A., WATSON, M., CREANOR, S. & FOYE, R. 2002. The pH and titratable acidity of a range of diluting drinks and their potential effect on dental erosion. *Journal of Dentistry,* 30**,** 313-317.

CALATAYUD, J. 2003. History of the development and evolution of local anesthesia since the coca leaf. *Anesthesiology,* 98**,** 1503.

CALVO-GUIRADO, J., MATÉ-SÁNCHEZ DE VAL, J., RAMOS-OLTRA, M., PÉREZ-ALBACETE MARTÍNEZ, C., RAMÍREZ-FERNÁNDEZ, M., MAIQUEZ-GOSÁLVEZ, M., GEHRKE, S., FERNÁNDEZ-DOMÍNGUEZ, M., ROMANOS, G. & DELGADO-RUIZ, R. 2018. The Use of Tooth Particles as a Biomaterial in Post-Extraction Sockets. Experimental Study in Dogs. *Dentistry journal,* 6**,** 12.

CAMPOS, L., PARRA, D., VASCONCELOS, M., VAZ, M. & MONTEIRO, J. 2014. DH and ESPI laser interferometry applied to the restoration shrinkage assessment. *Radiation Physics and Chemistry,* 94**,** 190-193.

CANEPPELE, T. M. F., JERONYMO, R. D. I., DI NICOLÓ, R., ARAÚJO, M. A. M. D. & SOARES, L. E. S. 2012. In Vitro assessment of dentin erosion after immersion in acidic beverages: surface profile analysis and energy-

dispersive X-ray fluorescence spectrometry study. *Brazilian dental journal,* 23**,** 373-378.

CARVALHO, T. S. & LUSSI, A. 2015. Susceptibility of enamel to initial erosion in relation to tooth type, tooth surface and enamel depth. *Caries research,* 49**,** 109-115.

CARVALHO, T. S. & LUSSI, A. 2020. Acidic Beverages and Foods Associated with Dental Erosion and Erosive Tooth Wear. *The Impact of Nutrition and Diet on Oral Health.* Karger Publishers.

CASSIMIRO-SILVA, P. F., MAIA, A. M. A., DE MELO MONTEIRO, G. Q. & GOMES, A. S. Mitigation of enamel erosion using commercial toothpastes evaluated with optical coherence tomography. Sixth International Conference on Lasers in Medicine, 2016. International Society for Optics and Photonics, 96700Y-96700Y-7.

CATE, H. T. B. 1968. Dental erosion in industry. *Occupational and Environmental Medicine,* 25**,** 249-266.

CAVADINI, C., SIEGA-RIZ, A. M. & POPKIN, B. M. 2000. US adolescent food intake trends from 1965 to 1996. *Archives of disease in childhood,* 83**,** 18-24.

CHABOUIS, H. F., FRON CHABOUIS, H., SMAIL FAUGERON, V. & ATTAL, J.-P. 2013. Clinical efficacy of composite versus ceramic inlays and onlays: A systematic review. *Dental materials,* 29**,** 1209-1218.

CHADWICK, R. G. 2019. *Dental erosion*, Quintessence publishing.

CHEAIB, Z. & LUSSI, A. 2011. Impact of acquired enamel pellicle modification on initial dental erosion. *Caries research,* 45**,** 107-112.

CHENG, R., YANG, H., SHAO, M.-Y., HU, T. & ZHOU, X.-D. 2009a. Dental erosion and severe tooth decay related to soft drinks: a case report and literature review. *Journal of Zhejiang University Science B,* 10**,** 395-399.

CHENG, Z.-J., WANG, X.-M., CUI, F.-Z., GE, J. & YAN, J.-X. 2009b. The enamel softening and loss during early erosion studied by AFM, SEM and nanoindentation. *Biomedical Materials,* 4**,** 015020.

CHEW, H., ZAKIAN, C., PRETTY, I. & ELLWOOD, R. 2014. Measuring initial enamel erosion with quantitative light-induced fluorescence and optical coherence tomography: an in vitro validation study. *Caries research,* 48**,** 254-262.

CHRISTENSEN, G. J. 2008. Considering tooth-colored inlays and onlays versus crowns. *The Journal of the American Dental Association,* 139**,** 617-620.

CHRISTENSEN, G. J. 2017. Crown, onlay, or direct restoration? *Dental Economics*.

CHUN-TE KO, A., HEWKO, M. D., LEONARDI, L., SOWA, M. G., DONG, C. C., WILLIAMS, P. & CLEGHORN, B. 2005. Ex vivo detection and characterization of early dental caries by optical coherence tomography and Raman spectroscopy. *Journal of biomedical optics,* 10**,** 031118.

CHUN, K. J., CHOI, H. & LEE, J. 2014. Comparison of mechanical property and role between enamel and dentin in the human teeth. *Journal of dental biomechanics,* 5.

CIANCONI, L., CONTE, G. & MANCINI, M. 2011. Shear bond strength, failure modes, and confocal microscopy of bonded amalgam restorations. *Dental Materials Journal,* 30**,** 216-21.

COLSTON, B. W., SATHYAM, U. S., DASILVA, L. B., EVERETT, M. J., STROEVE, P. & OTIS, L. 1998. Dental oct. *Optics express,* 3**,** 230-238.

ÇÖTERT, H. S., ŞEN, B. H. & BALKAN, M. 2001. In vitro comparison of cuspal fracture resistances of posterior teeth restored with various adhesive restorations. *International Journal of Prosthodontics,* 14.

CRAIG, R. & PEYTON, F. 1958. Elastic and mechanical properties of human dentin. *Journal of Dental Research,* 37**,** 710-718.

CRAIG, R. G., PEYTON, F. A. & JOHNSON, D. W. 1961. Compressive Properties of Enamel, Dental Cements, and Gold. *Journal of Dental Research,* 40**,** 936-945.

CREATH, K., ROBINSON, D. & REID, G. 1993. Interferogram Analysis. *DW Robinson and GT Reid (In-stitute of Physics Publishing Bristol and Philadelphia, 1993) p,* 94.

CUY, J. L., MANN, A. B., LIVI, K. J., TEAFORD, M. F. & WEIHS, T. P. 2002. Nanoindentation mapping of the mechanical properties of human molar tooth enamel. *Archives of oral biology,* 47**,** 281-291.

DA VEIGA, A. M. A., CUNHA, A. C., FERREIRA, D. M. T. P., DA SILVA FIDALGO, T. K., CHIANCA, T. K., REIS, K. R. & MAIA, L. C. 2016. Longevity of direct and indirect resin composite restorations in permanent posterior teeth: A systematic review and meta-analysis. *Journal of dentistry,* 54**,** 1-12.

DALPINO, P., FRANCISCHONE, C., ISHIKIRIAMA, A. & FRANCO, E. 2002. Fracture resistance of teeth directly and indirectly restored with composite resin and indirectly restored with ceramic materials. *American Journal of Dentistry,* 15**,** 389-394.

DANELON, M., PESSAN, J. P., SANTOS, V. R. D., CHIBA, E. K., GARCIA, L. S. G., DE CAMARGO, E. R. & DELBEM, A. C. B. 2018. Fluoride toothpastes containing micrometric or nano-sized sodium trimetaphosphate reduce enamel erosion in vitro. *Acta Odontologica Scandinavica,* 76**,** 119-124.

DARBY, E. 1892. Dental erosion and the gouty diathesis: Are they usually associated. *Dent Cosmos,* 34**,** 629-640.

DAVIDSON, C. 2000. Handling of polymerization stresses in resin-based restorative materials. *Dental News,* 7**,** 9-13.

DAVIS, G. R., TAYEB, R. A., SEYMOUR, K. G. & CHERUKARA, G. P. 2012. Quantification of residual dentine thickness following crown preparation. *Journal of dentistry,* 40**,** 571-576.

DAWES, C. 1969. The effects of flow rate and duration of stimulation on the concentrations of protein and the main electrolytes in human parotid saliva. *Archives of Oral Biology,* 14**,** 277-294.

DAWES, C. 1987. Physiological factors affecting salivary flow rate, oral sugar clearance, and the sensation of dry mouth in man. *Journal of dental research,* 66**,** 648-653.

DAWES, C. 2003. What is the critical pH and why does a tooth dissolve in acid?

DE ALENCAR, C. R. B., DE ALENCAR, A., MAGALHÃES, M., DE ANDRADE MOREIRA MACHADO, T. M., DE OLIVEIRA, H., HONÓRIO, D. & RIOS 2014. In situ effect of a commercial CPP-ACP chewing gum on the human enamel initial erosion. *Journal of Dentistry,* 42**,** 1502-1507.

DE MEDEIROS, R.-A., DOS SANTOS, D.-M., PESQUEIRA, A.-A., CAMPANER, M. & BITENCOURT, S.-B. 2019. Stress distribution in fixed mandibular prostheses fabricated by CAD/CAM and conventional techniques: Photoelastic and strain gauge analyses. *Journal of clinical and experimental dentistry,* 11**,** e807.

DE MUNCK, J., VAN LANDUYT, K., PEUMANS, M., POITEVIN, A., LAMBRECHTS, P., BRAEM, M. & VAN MEERBEEK, B. 2005. A Critical Review of the Durability of Adhesion to Tooth Tissue: Methods and Results. *Journal of Dental Research,* 84**,** 118-132.

DE SOUZA, G. D., PEREIRA, G., DIAS, C. & PAULILLO, L. 2002. Fracture resistance of premolars with bonded class II amalgams. *Operative Dentistry,* 27**,** 349-353.

DEJAK, B. & MLOTKOWSKI, A. 2008. Three-dimensional finite element analysis of strength and adhesion of composite resin versus ceramic inlays in molars. *Journal of Prosthetic Dentistry,* 99**,** 131-40.

DEJAK, B. & MŁOTKOWSKI, A. 2013. The influence of ferrule effect and length of cast and FRC posts on the stresses in anterior teeth. *Dental Materials,* 29**,** e227-e237.

DELLA BONA, A., MECHOLSKY JR, J. J. & ANUSAVICE, K. J. 2004. Fracture behavior of lithia disilicate-and leucite-based ceramics. *Dental Materials,* 20**,** 956-962.

DENG, J. M., YU, X., DAVIS, E. L. & JOYNT, R. B. 1995. Effect of restorative materials on cuspal flexure. *Quintessence International,* 26.

DETOLLA, D. H., ANDREANA, S., PATRA, A., BUHITE, R. & COMELLA, B. 2000. The role of the finite element model in dental implants. *Journal of Oral Implantology,* 26**,** 77-81.

DEVLIN, H., BASSIOUNY, M. & BOSTON, D. 2006. Hardness of enamel exposed to Coca-Cola® and artificial saliva. *Journal of Oral Rehabilitation,* 33**,** 26-30.

DIRXEN, C., BLUNCK, U. & PREISSNER, S. 2013. Clinical performance of a new biomimetic double network material. *The open dentistry journal,* 7**,** 118.

DOUGLAS, W. Methods of improve fracture resistance of teeth. International symposium on posterior composite resin dental materials, 1985, 1985. Peter Szulc Publishing Co.

DOWKER, S. E. P., ELLIOTT, J. C., DAVIS, G. R. & WASSIF, H. S. 2003. Longitudinal study of the three-dimensional development of subsurface enamel lesions during in vitro demineralisation. *Caries Research,* 37**,** 237-245.

DOYLE, S. L., HODGES, J. S., PESUN, I. J., LAW, A. S. & BOWLES, W. R. 2006. Retrospective cross sectional comparison of initial nonsurgical endodontic treatment and single-tooth implants. *Journal of endodontics,* 32**,** 822-827.

DUANGTHIP, D., MAN, A., POON, P. H., LO, E. C. M. & CHU, C.-H. 2017. Occlusal stress is involved in the formation of non-carious cervical lesions. A systematic review of abfraction. *Am J Dent,* 30**,** 212-20.

DUGMORE, C. & ROCK, W. 2003. The progression of tooth erosion in a cohort of adolescents of mixed ethnicity. *International Journal of Paediatric Dentistry,* 13**,** 295-303.

DUGMORE, C. & ROCK, W. 2004. The prevalence of tooth erosion in 12-year-old children. *British Dental Journal,* 196**,** 279-282.

DUQUIA, R., OSINAGA, P., DEMARCO, F., HABEKOST, L. & CONCEIÇÃO, E. 2006. Cervical microleakage in MOD restorations: in vitro comparison of indirect and direct composite. *Operative dentistry,* 31**,** 682-687.

DUSCHNER, H. 1995. A new application of confocal laser scanning microscopy with the Leica CLSM: Histomorphological studies of sound and carious dental tissues. *Sci Tech Inf,* 9**,** 20-24.

DUSCHNER, H., GÖTZ, H., WALKER, R. & LUSSI, A. 2000. Erosion of dental enamel visualized by confocal laser scanning microscopy. *Tooth Wear and Sensitivity. London, Martin Dunitz***,** 67-73.

EAKLE, W. S., MAXWELL, E. H. & BRALY, B. V. 1986. Fractures of posterior teeth in adults. *Journal of the American Dental Association,* 112**,** 215-218.

EDGAR, W. M., HIGHAM, S. M. & MANNING, R. H. 1994. Saliva Stimulation and Caries Prevention. *Advances in dental research,* 8**,** 239-245.

EHLEN, L., MARSHALL, T., QIAN, F., WEFEL, J. & WARREN, J. 2008. Acidic beverages increase the risk of in vitro tooth erosion. *Nutrition research (New York, N.Y.),* 28**,** 299-303.

EISENBURGER, M. & ADDY, M. 2003. Influence of liquid temperature and flow rate on enamel erosion and surface softening. *Journal of oral rehabilitation,* 30**,** 1076-1080.

EISENBURGER, M., ADDY, M., HUGHES, J. A. & SHELLIS, R. P. 2001a. Effect of time on the remineralisation of enamel by synthetic saliva after citric acid erosion. *Caries Research,* 35**,** 211-5.

EISENBURGER, M., HUGHES, J., WEST, N., SHELLIS, R. & ADDY, M. 2001b. The use of ultrasonication to study remineralisation of eroded enamel. *Caries research,* 35**,** 61-66.

EISENBURGER, M., SHELLIS, R. P. & ADDY, M. 2004. Scanning electron microscopy of softened enamel. *Caries Research,* 38**,** 67-74.

EL WAZANI, B., DODD, M. & MILOSEVIC, A. 2012. The signs and symptoms of tooth wear in a referred group of patients. *British dental journal,* 213**,** E10-E10.

ELDIWANY, M., POWERS, J. & GEORGE, L. 1993. Mechanical properties of direct and post-cured composites. *American journal of dentistry,* 6**,** 222-224.

ERF, R. 2012. *Speckle metrology*, Elsevier.

FABIANELLI, A., GORACCI, C., BERTELLI, E., DAVIDSON, C. L. & FERRARI, M. 2006. A clinical trial of Empress II porcelain inlays luted to vital teeth with a dual-curing adhesive system and a self-curing resin cement. *Journal of Adhesive Dentistry,* 8.

FALLER, R. V., EVERSOLE, S. L. & TZEGHAI, G. E. 2011. Enamel protection: a comparison of marketed dentifrice performance against dental erosion. *American Journal of Dentistry,* 24**,** 205.

FARAH, J. & CRAIG, R. 1975. Distribution of stresses in porcelain-fused-to-metal and porcelain jacket crowns. *Journal of Dental Research,* 54**,** 255-261.

FARAH, J. W., CRAIG, R. G. & MEROUEH, K. A. 1989. Finite element analysis of three- and four-unit bridges. *Journal of Oral Rehabilitation,* 16**,** 603-611.

FARAH, J. W., DENNISON, J. B. & POWERS, J. M. 1977. Effects of design on stress distribution of intracoronal gold restorations. *The Journal of the American Dental Association,* 94**,** 1151-1154.

FARES, J., SHIRODARIA, S., CHIU, K., AHMAD, N., SHERRIFF, M. & BARTLETT, D. 2009. A new index of tooth wear. Reproducibility and application to a sample of 18- to 30-year-old university students. *Caries Research,* 43**,** 119-125.

FASBINDER, D. J., DENNISON, J. B., HEYS, D. R. & LAMPE, K. 2005. The clinical performance of CAD/CAM-generated composite inlays. *The Journal of the American Dental Association,* 136**,** 1714-1723.

FEATHERSTONE, J. D. & LUSSI, A. 2006. Understanding the chemistry of dental erosion. *Monogr Oral Sci,* 20**,** 66-76.

FEHRENBACH, M. J. & POPOWICS, T. 2015. *Illustrated dental embryology, histology, and anatomy*, Elsevier Health Sciences.

FEILZER, A., DE GEE, A. & DAVIDSON, C. 1987. Setting stress in composite resin in relation to configuration of the restoration. *Journal of Dental Research,* 66**,** 1636-1639.

FENNIS, W. M., KUIJS, R. H., KREULEN, C. M., VERDONSCHOT, N. & CREUGERS, N. H. 2004. Fatigue resistance of teeth restored with cuspal-coverage composite restorations. *International Journal of Prosthodontics,* 17**,** 313-317.

FERLA JDE, O., RODRIGUES, J. A., ARRAIS, C. A., ARANHA, A. C. & CASSONI, A. 2013. Influence of photo-activation source on enamel demineralization around restorative materials. *Pesquisa Odontologica Brasileira = Brazilian Oral Research,* 27**,** 286-92.

FERNANDES, L. O., GRAÇA, N. D., MELO, L. S., SILVA, C. H. & GOMES, A. S. Monitoring the gingival regeneration after aesthetic surgery with optical coherence tomography. Lasers in Dentistry XXII, 2016. International Society for Optics and Photonics, 96920Q.

FERRARI, M., VICHI, A., MANNOCCI, F. & MASON, P. N. 2000. Retrospective study of the clinical performance of fiber posts. *American journal of dentistry,* 13**,** 9B-13B.

FIELD, J., WATERHOUSE, P. & GERMAN, M. 2010. Quantifying and qualifying surface changes on dental hard tissues in vitro. *Journal of dentistry,* 38**,** 182-190.

FRANKENBERGER, R., SINDEL, J., KRAMER, N. & PETSCHELT, A. 1999. Dentin bond strength and marginal adaptation: direct composite resins vs ceramic inlays. *OPE TIVE DENTISTRY,* 24**,** 147-155.

FRASSETTO, A., BRESCHI, L., TURCO, G., MARCHESI, G., DI LENARDA, R., TAY, F., PASHLEY, D. & CADENARO, M. 2016. Mechanisms of degradation of the hybrid layer in adhesive dentistry and therapeutic agents to improve bond durability--A literature review. *Dental materials,* 32**,** e41-e53.

FRIED, D., XIE, J., SHAFI, S., FEATHERSTONE, J. D., BREUNIG, T. & LE, C. Q. 2002. Imaging caries lesions and lesion progression with polarization sensitive optical coherence tomography. *Journal of biomedical optics,* 7**,** 618-628.

GANSS, C., KLIMEK, J. & SCHWARZ, N. 2000. A comparative profilometric in vitro study of the susceptibility of polished and natural human enamel and dentine surfaces to erosive demineralization. *Archives of oral biology,* 45**,** 897-902.

GANSS, C., SCHLUETER, N. & KLIMEK, J. J. A. O. O. B. 2007. Retention of KOH-soluble fluoride on enamel and dentine under erosive conditions—a comparison of in vitro and in situ results. 52**,** 9-14.

GAŠPERŠIČ, D. 1995. Micromorphometric analysis of cervical enamel structure of human upper third molars. *Archives of oral biology,* 40**,** 453-457.

GEHRT M, T. J., SCHLEY J, WOLF ART S. 2012. Heat-pressed veneered zirconia crowns: 4 years of clinical performance. *IADR Abstract #150, Helsinki*.

GEHRT, M., WOLFART, S., RAFAI, N., REICH, S. & EDELHOFF, D. 2013. Clinical results of lithium-disilicate crowns after up to 9 years of service. *Clinical oral investigations,* 17**,** 275-284.

GENG, J.-P., TAN, K. B. & LIU, G.-R. 2001. Application of finite element analysis in implant dentistry: a review of the literature. *The Journal of prosthetic dentistry,* 85**,** 585-598.

GHER, M. E., DUNLAP, R. M., ANDERSON, M. H. & KUHL, L. V. 1987. Clinical survey of fractured teeth. *The Journal of the American Dental Association,* 114**,** 174-177.

GOODACRE, C. J., CAMPAGNI, W. V. & AQUILINO, S. A. 2001. Tooth preparations for complete crowns: An art form based on scientific principles. *The Journal of Prosthetic Dentistry,* 85**,** 363-376.

GOPAKUMAR, A. & GOPAKUMAR, V. 2011. Stanley L Drummond-Jackson. Pioneer of intravenous anaesthesia in dentistry. *SAAD digest,* 27**,** 61-65.

GRENBY, T., PHILLIPS, A., DESAI, T. & MISTRY, M. 1989. Laboratory studies of the dental properties of soft drinks. *British Journal of Nutrition,* 62**,** 451-464.

GRIPPO, J. O. 1991. Abfractions: a new classification of hard tissue lesions of teeth. *Journal of Esthetic and Restorative Dentistry,* 3**,** 14-19.

GRIPPO, J. O., SIMRING, M. & COLEMAN, T. A. 2012. Abfraction, abrasion, biocorrosion, and the enigma of noncarious cervical lesions: a 20-year perspective. *Journal of Esthetic and Restorative Dentistry,* 24**,** 10-23.

GROBLER, S. & VAN DER HORST, G. 1982. Biochemical analysis of various cool drinks with regard to enamel erosion, de-and remineralization. *The Journal of the Dental Association of South Africa= Die Tydskrif van die Tandheelkundige Vereniging van Suid-Afrika,* 37**,** 681.

GROSSMAN, D. 1989. Photoelastic examination of bonded crown interfaces. *J Dent Res,* 68**,** 271.

GUESS, P. C., SELZ, C. F., STEINHART, Y.-N., STAMPF, S. & STRUB, J. R. 2013. Prospective clinical split-mouth study of pressed and CAD/CAM all-ceramic partial-coverage restorations: 7-year results. *International Journal of Prosthodontics,* 26.

GUIMARÃES, J. C., SOELLA, G. G., DURAND, L. B., HORN, F., BARATIERI, L. N., MONTEIRO JR, S. & BELLI, R. 2014. Stress amplifications in dental non-carious cervical lesions. *Journal of biomechanics,* 47**,** 410-416.

GÜRSOY, M., KÖNÖNEN, E., TERVAHARTIALA, T., GÜRSOY, U. K., PAJUKANTA, R. & SORSA, T. 2010. Longitudinal study of salivary proteinases during pregnancy and postpartum. *Journal of Periodontal Research,* 45**,** 496.

GURUNATHAN, D., SOMASUNDARAM, S. & KUMAR, S. 2012. Casein phosphopeptide-amorphous calcium phosphate: a remineralizing agent of enamel. *Australian dental journal,* 57**,** 404-408.

HALL, A. F., BUCHANAN, C. A., MILLETT, D. T., CREANOR, S. L., STRANG, R. & FOYE, R. H. 1999. The effect of saliva on enamel and dentine erosion. *Journal of dentistry,* 27**,** 333-339.

HALLSWORTH, A. & WEATHERELL, J. 1969. The microdistribution, uptake and loss of fluoride in human enamel. *Caries research,* 3**,** 109-118.

HAMBA, H., NIKAIDO, T., INOUE, G., SADR, A. & TAGAMI, J. 2011. Effects of CPP-ACP with sodium fluoride on inhibition of bovine enamel demineralization: a quantitative assessment using micro-computed tomography. *Journal of dentistry,* 39**,** 405-413.

HANNIG, M. 2002. The protective nature of the salivary pellicle. *International Dental Journal,* 52**,** 417-423.

HANNIG, M., FIEBIGER, M., GUNTZER, M., DOBERT, A., ZIMEHL, R. & NEKRASHEVYCH, Y. 2004. Protective effect of the in situ formed short-term salivary pellicle. *Arch Oral Biol,* 49**,** 903-10.

HANNIG, M. & HANNIG, C. 2014. The pellicle and erosion.

HARA, A., ANDO, M., GONZALEZ-CABEZAS, C., CURY, J., SERRA, M. & ZERO, D. 2006. Protective effect of the dental pellicle against erosive challenges in situ. *Journal of Dental Research,* 85**,** 612-616.

HARA, A. T., GONZÁLEZ-CABEZAS, C., CREETH, J. & ZERO, D. T. 2008. The effect of human saliva substitutes in an erosion–abrasion cycling model. *European journal of oral sciences,* 116**,** 552-556.

HARA, A. T. & ZERO, D. T. 2008. Analysis of the erosive potential of calcium-containing acidic beverages. *European journal of oral sciences,* 116**,** 60-65.

HARA, A. T. & ZERO, D. T. 2014. The potential of saliva in protecting against dental erosion.

HARIRI, I., SADR, A., SHIMADA, Y., TAGAMI, J. & SUMI, Y. 2012. Effects of structural orientation of enamel and dentine on light attenuation and local refractive index: an optical coherence tomography study. *Journal of dentistry,* 40**,** 387-396.

HARLEY, K. 1999. Tooth surface loss: Tooth wear in the child and the youth. *British Dental Journal,* 186**,** 492-496.

HEAD, J. 1912. A STUDY OF SALIVA AND ITS ACTION ON TOOTH ENAMEL IN REFERENCE TO ITS HARDENING AND SOFTENING. *Journal of the American Medical Association,* 59**,** 2118.

HEALTH, U. D. O. & SERVICES, H. 2004. Guidance for industry, sterile drug products produced by aseptic processing-current good manufacturing practice. *http://www.fda.gov/CbER/gdlns/steraseptic.pdf*.

HEINTZE, S. D., ALBRECHT, T., CAVALLERI, A. & STEINER, M. 2011. A new method to test the fracture probability of all-ceramic crowns with a dual-axis chewing simulator. *Dental Materials,* 27**,** e10-e19.

HELLSTRÖM, I. 1977. Oral complications in anorexia nervosa. *European Journal of Oral Sciences,* 85**,** 71-86.

HEMINGWAY, C., PARKER, D., ADDY, M. & BARBOUR, M. 2006. Erosion of enamel by non-carbonated soft drinks with and without toothbrushing abrasion. *British Dental Journal,* 201**,** 447-450.

HEMINGWAY, C. A. 2008. *The interaction of food-approved proteins and salivary pellicle on tooth surfaces and their impact on tooth demineralisation*. University of Bristol.

HEURICH, E., BEYER, M., JANDT, K. D., REICHERT, J., HEROLD, V., SCHNABELRAUCH, M. & SIGUSCH, B. W. 2010. Quantification of dental erosion—A comparison of stylus profilometry and confocal laser scanning microscopy (CLSM). *Dental Materials,* 26**,** 326-336.

HEYMANN, H. O., BAYNE, S. C., STURDEVANT, J. R., WILDER, A. D. & ROBERSON, T. M. 1996. The clinical performance of CAD-CAM–generated ceramic inlays: a four-year study. *The Journal of the American Dental Association,* 127**,** 1171-1175.

HEYMANN, H. O., STURDEVANT, J. R., BRUNSON, W. D., WILDER, A. D., SLUDER, T. B. & BAYNE, S. C. 1988. Twelve-month clinical study of dentinal adhesives in class V cervical lesions. *The Journal of the American Dental Association,* 116**,** 179-183.

HOLLISTER, S. J., LIN, C., SAITO, E., LIN, C., SCHEK, R., TABOAS, J., WILLIAMS, J., PARTEE, B., FLANAGAN, C. & DIGGS, A. 2005. Engineering craniofacial scaffolds. *Orthodontics & craniofacial research,* 8**,** 162-173.

HOLMES, J. R., SULIK, W. D., HOLLAND, G. A. & BAYNE, S. C. 1992. Marginal fit of castable ceramic crowns. *The Journal of prosthetic dentistry,* 67**,** 594-599.

HORNBY, K., RICKETTS, S. R., PHILPOTTS, C. J., JOINER, A., SCHEMEHORN, B. & WILLSON, R. 2014. Enhanced enamel benefits from a novel toothpaste and dual phase gel containing calcium silicate and sodium phosphate salts. *Journal of Dentistry,* 42**,** S39-S45.

HOUNSFIELD, G. N. 1973. Computerized transverse axial scanning (tomography): Part 1. Description of system. *The British journal of radiology,* 46**,** 1016-1022.

HSIEH, Y.-S., HO, Y.-C., LEE, S.-Y., CHUANG, C.-C., TSAI, J.-C., LIN, K.-F. & SUN, C.-W. 2013. Dental optical coherence tomography. *Sensors,* 13**,** 8928-8949.

HUANG, D., SWANSON, E. A., LIN, C. P., SCHUMAN, J. S., STINSON, W. G., CHANG, W., HEE, M. R., FLOTTE, T., GREGORY, K. & PULIAFITO, C. A. 1991. Optical coherence tomography. *science,* 254**,** 1178-1181.

HUI, J. 2013. Conserving Tooth Structure: Onlay vs. Crown? *Allentxdentist*.

HUNTLEY, J. M. 1998. Automated fringe pattern analysis in experimental mechanics: a review. *The Journal of Strain Analysis for Engineering Design,* 33**,** 105-125.

HUR, B., KIM, H. C., PARK, J. K. & VERSLUIS, A. 2011. Characteristics of non-carious cervical lesions–an ex vivo study using micro computed tomography. *Journal of oral rehabilitation,* 38**,** 469-474.

HUYSMANS, M. C. D. N. J. M., CHEW, H. P. & ELLWOOD, R. P. 2011. Clinical studies of dental erosion and erosive wear. *Caries Research,* 45 Suppl 1**,** 60-8.

ICHIM, I., SCHMIDLIN, P., KIESER, J. & SWAIN, M. 2007. Mechanical evaluation of cervical glass-ionomer restorations: 3D finite element study. *Journal of dentistry,* 35**,** 28-35.

IMFELD, T. 1996a. Dental erosion. Definition, classification and links. *European Journal of Oral Sciences,* 104**,** 151-155.

IMFELD, T. 1996b. Prevention of progression of dental erosion by professional and individual prophylactic measures. *European Journal of Oral Sciences,* 104**,** 215-220.

IONTA, F. Q., MENDONÇA, F. L., DE OLIVEIRA, G. C., DE ALENCAR, C. R. B., HONORIO, H. M., MAGALHAES, A. C. & RIOS, D. 2014. In vitro assessment of artificial saliva formulations on initial enamel erosion remineralization. *Journal of dentistry,* 42**,** 175-179.

İPLIKÇIOĞLU, H., AKCA, K., ÇEHRELI, M. C. & ŞAHIN, S. 2003. Comparison of non-linear finite element stress analysis with in vitro strain gauge measurements on a Morse taper implant. *International Journal of Oral & Maxillofacial Implants,* 18.

IRELAND, A. J., MCGUINNESS, N. & SHERRIFF, M. 1995. An investigation into the ability of soft drinks to adhere to enamel. *Caries Research,* 29**,** 470-6.

ISAACS, M. 1987. The porcelain inlay re-examined. *CDS review,* 80**,** 52-53.

ISO5436-1 2000. ISO 5436-1: 2000- Geometrical Product Specifications (GPS) – Surface Texture: Profile method; Measurement Standards -Part 1: Material Measures, International Organization for Standardization, Geneva.

ISO/TR14569-1 2007. ISO/TR 14569-1: 2007- Dental materials – Guidance on testing of wear – Part 1: Wear by toothbrushing.

ISOKAWA, S., TODA, Y. & KUBOTA, K. 1970. A scanning electron microscopic observation of etched human peritubular dentine. *Archives of oral biology,* 15**,** 1303-IN30.

JAEGGI, T. & LUSSI, A. 1999. Toothbrush abrasion of erosively altered enamel after intraoral exposure to saliva: an in situ study. *Caries Research,* 33**,** 455-461.

JAEGGI, T. & LUSSI, A. 2006. Prevalence, incidence and distribution of erosion. *Dental Erosion,* 20**,** 44-65.

JAEGGI, T. & LUSSI, A. 2014. Prevalence, incidence and distribution of erosion. *Erosive Tooth Wear.* Karger Publishers.

JANTARAT, J., PANITVISAI, P., PALAMARA, J. E. & MESSER, H. H. 2001. Comparison of methods for measuring cuspal deformation in teeth. *J Dent,* 29**,** 75-82.

JÄRVINEN, V., MEURMAN, J., HYVÄRINEN, H., RYTÖMAA, I. & MURTOMAA, H. 1988. Dental erosion and upper gastrointestinal disorders. *Oral surgery, oral medicine, oral pathology,* 65**,** 298-303.

JAYARAJ, D. & GANESAN, S. 2015. Salivary pH and buffering capacity as risk markers for early childhood caries: A clinical study. *International journal of clinical pediatric dentistry,* 8**,** 167.

JIANG, H., DU, M., HUANG, W., PENG, B., BIAN, Z. & TAI, B. 2011. The prevalence of and risk factors for non-carious cervical lesions in adults in Hubei Province, China. *Community dental health,* 28**,** 22-28.

JIANG, W., BO, H., YONGCHUN, G. & LONGXING, N. 2010. Stress distribution in molars restored with inlays or onlays with or without endodontic treatment: A three-dimensional finite element analysis. *The Journal of Prosthetic Dentistry,* 103**,** 6-12.

JOHANSSON, A.-K., OMAR, R., CARLSSON, G. E. & JOHANSSON, A. 2012. Dental erosion and its growing importance in clinical practice: from past to present. *International journal of dentistry,* 2012.

JOHANSSON, A. K., LINGSTRÖM, P., IMFELD, T. & BIRKHED, D. 2004. Influence of drinking method on tooth-surface pH in relation to dental erosion. *European journal of oral sciences,* 112**,** 484-489.

JOHNSTON, J. F., PHILLIPS, R. W. & DYKEMA, R. W. 1965. *Modern practice in crown and bridge prosthodontics*, WB Saunders Co.

JOTKOWITZ, A. & SAMET, N. 2010. Rethinking ferrule–a new approach to an old dilemma. *British dental journal,* 209**,** 25-33.

KANG, H., DARLING, C. L. & FRIED, D. 2012. Nondestructive monitoring of the repair of enamel artificial lesions by an acidic remineralization model using polarization-sensitive optical coherence tomography. *Dental Materials,* 28**,** 488-494.

KANG, H., JIAO, J. J., LEE, C., LE, M. H., DARLING, C. L. & FRIED, D. 2010. Nondestructive assessment of early tooth demineralization using cross-polarization optical coherence tomography. *IEEE journal of selected topics in quantum electronics,* 16**,** 870-876.

KARL, M., DICKINSON, A., HOLST, S. & HOLST, A. 2009. Biomechanical methods applied in dentistry: a comparative overview of photoelastic examinations, strain gauge measurements, finite element analysis and three-dimensional deformation analysis. *The European journal of prosthodontics and restorative dentistry,* 17**,** 50-57.

KATO, M. T. & BUZALAF, M. A. R. 2012. Iron supplementation reduces the erosive potential of a cola drink on enamel and dentin in situ. *Journal of Applied Oral Science,* 20**,** 318-322.

KATO, M. T., LANCIA, M., SALES-PERES, S. H. C. & BUZALAF, M. A. R. 2010. Preventive effect of commercial desensitizing toothpastes on bovine enamel erosion in vitro. *Caries Research,* 44**,** 85-89.

KERN, M., SASSE, M. & WOLFART, S. 2012. Ten-year outcome of three-unit fixed dental prostheses made from monolithic lithium disilicate ceramic. *The Journal of the American Dental Association,* 143**,** 234-240.

KHAN, F., YOUNG, W., SHAHABI, S. & DALEY, T. 1999. Dental cervical lesions associated with occlusal erosion and attrition. *Australian Dental Journal,* 44**,** 176-186.

KHERA, S., ASKARIEH, Z. & JAKOBSEN, J. 1990. Adaptability of two amalgams to finished cavity walls in Class II cavity preparations. *Dental Materials,* 6**,** 5-9.

KILIARIDIS, S., JOHANSSON, A., HARALDSON, T., OMAR, R. & CARLSSON, G. 1995. Craniofacial morphology, occlusal traits, and bite force in persons with advanced occlusal tooth wear. *American journal of orthodontics and dentofacial orthopedics,* 107**,** 286-292.

KIM, E.-J. & JIN, B.-H. 2019. Effects of Titratable Acidity and Organic Acids on Enamel Erosion In Vitro. *Journal of Dental Hygiene Science,* 19**,** 1-8.

KIM, S., LEE, K., SEONG, S., LEE, M., LEE, I., SON, H., KIM, H., OH, M. & CHO, B. 2009. Two-year clinical effectiveness of adhesives and retention form on resin composite restorations of non-carious cervical lesions. *Operative dentistry,* 34**,** 507-515.

KING, R. 2017. *The Making of the Dentiste, c. 1650-1760*.

KINNEY, J., BALOOCH, M., MARSHALL, S., MARSHALL JR, G. & WEIHS, T. 1996. Hardness and Young's modulus of human peritubular and intertubular dentine. *Archives of Oral Biology,* 41**,** 9-13.

KINNEY, J., MARSHALL, S. & MARSHALL, G. 2003. The mechanical properties of human dentin: a critical review and re-evaluation of the dental literature. *Critical Reviews in Oral Biology & Medicine,* 14**,** 13-29.

KITCHENS, M. & OWENS, B. 2007. Effect of Carbonated Beverages, Coffee, Sports and High Energy Drinks, and Bottled Water on thein vitroErosion Characteristics of Dental Enamel. *The journal of clinical pediatric dentistry,* 31**,** 153-159.

KLIMEK, J., HELLWIG, E. & AHRENS, G. 1982. Effect of plaque on fluoride stability in the enamel after amine fluoride application in the artificial mouth. *Deutsche Zahnarztliche Zeitschrift,* 37**,** 836.

KORIOTH, T. & VERSLUIS, A. 1997. Modeling the mechanical behavior of the jaws and their related structures by finite element (FE) analysis. *Critical Reviews in Oral Biology & Medicine,* 8**,** 90-104.

KOSHOJI, N. H., BUSSADORI, S. K., BORTOLETTO, C. C., PRATES, R. A., OLIVEIRA, M. T. & DEANA, A. M. 2015. Laser speckle imaging: a novel method for detecting dental erosion. *PloS one,* 10**,** e0118429.

KOVACIC, I., DIVJAK, A., MODRIC, D., CATIC, A., FILIPOVIC-ZORE, I. & CELEBIC, A. 2019. Short mini-dental implants as denture retainers-digital image correlation and 2-year cohort study. *Clinical Oral Implants Research,* 30**,** 236-236.

KUHN, J., GOLDSTEIN, S., FELDKAMP, L., GOULET, R. & JESION, G. 1990. Evaluation of a microcomputed tomography system to study trabecular bone structure. *Journal of Orthopaedic Research,* 8**,** 833-842.

KURER, H. 1991. The classification of single-rooted, pulpless teeth. *Quintessence International,* 22.

LAGERWEIJ, M., BUCHALLA, W., KOHNKE, S., BECKER, K., LENNON, A. & ATTIN, T. 2006. Prevention of erosion and abrasion by a high fluoride concentration gel applied at high frequencies. *Caries Research,* 40**,** 148-153.

LAMBRECHTS, P. 1987. Evaluation of clinical performance for posterior composite resins and dentin adhesives. *Operative dentistry,* 12**,** 53.

LAMBRECHTS, P., VAN MEERBEEK, B., PERDIGAO, J., GLADYS, S., BRAEM, M. & VANHERLE, G. 1996. Restorative therapy for erosive lesions. *European journal of oral sciences,* 104**,** 229-240.

LAMBROU, D., LARSEN, M. J., FEJERSKOV, O. & TACHOS, B. 1981. The Effect of Fluoride in Saliva on Remineralization of Dental Enamel in Humans. *Caries Research,* 15**,** 341-345.

LANGE, R. & PFEIFFER, P. 2009. Clinical evaluation of ceramic inlays compared to composite restorations. *Operative dentistry,* 34**,** 263-272.

LARSEN, M. 2001. Prevention by means of fluoride of enamel erosion as caused by soft drinks and orange juice. *Caries Research,* 35**,** 229-234.

LARSEN, M. & RICHARDS, A. 2002. Fluoride is unable to reduce dental erosion from soft drinks. *Caries Research,* 36**,** 75-80.

LARSEN, M. J. 1973. Dissolution of enamel. *European Journal of Oral Sciences,* 81**,** 518-522.

LAURANCE-YOUNG, P. 2012. *Comparative physicochemical changes of human and bovine enamel following a short duration acid exposure*. UCL (University College London).

LEE, H.-E., LIN, C.-L., WANG, C.-H., CHENG, C. & CHANG, C.-H. 2002. Stresses at the cervical lesion of maxillary premolar—a finite element investigation. *Journal of Dentistry,* 30**,** 283-290.

LEE, S.-H., LEE, J.-J., CHUNG, H.-J., PARK, J.-T. & KIM, H.-J. 2016. Dental optical coherence tomography: new potential diagnostic system for cracked-tooth syndrome. *Surgical and Radiologic Anatomy,* 38**,** 49-54.

LEE, W. C. & EAKLE, W. S. 1984. Possible role of tensile stress in the etiology of cervical erosive lesions of teeth. *Journal of Prosthetic Dentistry,* 52**,** 374-380.

LEINFELDER, K. 2005. Indirect posterior composite resins. *Compendium of continuing education in dentistry (Jamesburg, NJ: 1995),* 26**,** 495-503; quiz 504, 527.

LERTCHIRAKARN, V., PALAMARA, J. E. & MESSER, H. H. 2003. Finite element analysis and strain-gauge studies of vertical root fracture. *Journal of endodontics,* 29**,** 529-534.

LEUNG, V.-H. & DARVELL, B. 1997. Artificial salivas for in vitro studies of dental materials. *Journal of dentistry,* 25**,** 475-484.

LEVINE, M., AGUIRRE, A., HATTON, M. & TABAK, L. 1987. Artificial salivas: present and future. *Journal of dental research,* 66**,** 693-698.

LEVINE, R. 1973. Fruit juice erosion—an increasing danger? *Journal of dentistry,* 2**,** 85-88.

LEVITCH, L., BADER, J., SHUGARS, D. & HEYMANN, H. 1994. Non-carious cervical lesions. *Journal of dentistry,* 22**,** 195-207.

LI, J.-Y., LAU, A. & FOK, A. S. L. 2013. Application of digital image correlation to full-field measurement of shrinkage strain of dental composites. *Journal of Zhejiang University SCIENCE A,* 14**,** 1-10.

LI, J., FOK, A. S. L., SATTERTHWAITE, J. & WATTS, D. 2009. Measurement of the full-field polymerization shrinkage and depth of cure of dental composites using digital image correlation. *Dental materials,* 25**,** 582-588.

LI, M. H. & BERNABÉ, E. 2016. Tooth wear and quality of life among adults in the United Kingdom. *Journal of dentistry,* 55**,** 48-53.

LI, X., MA, C., XIE, X., SUN, H. & LIU, X. 2016. Pulp regeneration in a full-length human tooth root using a hierarchical nanofibrous microsphere system. *Acta biomaterialia,* 35**,** 57-67.

LI, X., WANG, J., JOINER, A. & CHANG, J. 2014. The remineralisation of enamel: a review of the literature. *Journal of dentistry,* 42**,** S12-S20.

LIBMAN, W. J. & NICHOLLS, J. I. 1995. Load fatigue of teeth restored with cast posts and cores and complete crowns. *International Journal of Prosthodontics,* 8.

LIMA, A. F. D., SPAZZIN, A. O., GALAFASSI, D., CORRER-SOBRINHO, L. & CARLINI-JÚNIOR, B. 2010. Influence of ferrule preparation with or without glass fiber post on fracture resistance of endodontically treated teeth. *Journal of Applied Oral Science,* 18**,** 360-363.

LIN, W. T., KITASAKO, Y., NAKASHIMA, S. & TAGAMI, J. 2017. A comparative study of the susceptibility of cut and uncut enamel to erosive demineralization. *Dental materials journal,* 36**,** 48-53.

LINKOSALO, E. & MARKKANEN, H. 1985. Dental erosions in relation to lactovegetarian diet. *European Journal of Oral Sciences,* 93**,** 436-441.

LITONJUA, L., BUSH, P., ANDREANA, S., TOBIAS, T. & COHEN, R. 2004. Effects of occlusal load on cervical lesions. *Journal of oral rehabilitation,* 31**,** 225-232.

LIU, W., ZHANG, Q. C., WU, X. J. & ZHU, H. 2010. Tooth wear and dental pathology of the Bronze–Iron Age people in Xinjiang, Northwest China: Implications for their diet and lifestyle. *Homo,* 61**,** 102-116.

LIU, Y., TJÄDERHANE, L., BRESCHI, L., MAZZONI, A., LI, N., MAO, J., PASHLEY, D. H. & TAY, F. R. 2011. Limitations in Bonding to Dentin and Experimental Strategies to Prevent Bond Degradation. *Journal of Dental Research,* 90**,** 953-968.

LLOYD, P. M. & PALIK, J. F. 1993. The philosophies of dowel diameter preparation: a literature review. *The Journal of prosthetic dentistry,* 69**,** 32-36.

LOPES, G. C. 2011. Effect of dentin age and acid etching time on dentin bonding. *Journal of adhesive dentistry,* 13**,** 139.

LOPES, L. M., LEITAO, J. G. & DOUGLAS, W. H. 1991. Effect of a new resin inlay/onlay restorative material on cuspal reinforcement. *Quintessence International,* 22.

LUSSI, A. 2006. *Erosive tooth wear - a multifactorial condition of growing concern and increasing knowledge of Dental Erosion*.

LUSSI, A. 2009. Dental erosion--novel remineralizing agents in prevention or repair. *Advances in Dental Research,* 21**,** 13-16.

LUSSI, A., BOSSEN, A., HÖSCHELE, C., BEYELER, B., MEGERT, B., MEIER, C. & RAKHMATULLINA, E. 2012a. Effects of enamel abrasion, salivary

pellicle, and measurement angle on the optical assessment of dental erosion. *Journal of biomedical optics,* 17**,** 0970091-09700913.

LUSSI, A. & CARVALHO, T. S. 2015. Analyses of the erosive effect of dietary substances and medications on deciduous teeth. *PloS one,* 10**,** e0143957.

LUSSI, A. & HELLWIG, E. 2001. Erosive potential of oral care products. *Caries research,* 35**,** 52-56.

LUSSI, A. & HELLWIG, E. 2014. Risk assessment and causal preventive measures. *Erosive Tooth Wear*. Karger Publishers.

LUSSI, A., JAEGGI, T., GERBER, C. & MEGERT, B. 2004a. Effect of amine/sodium fluoride rinsing on toothbrush abrasion of softened enamel in situ. *Caries research,* 38**,** 567-571.

LUSSI, A., JAEGGI, T. & SCHÄRER, S. 1993. The influence of different factors on in vitro enamel erosion. *Caries Research,* 27**,** 387-393.

LUSSI, A., JAEGGI, T. & ZERO, D. 2004b. The role of diet in the aetiology of dental erosion. *Caries Research,* 38 Suppl 1**,** 34-44.

LUSSI, A., LUSSI, J., CARVALHO, T. & CVIKL, B. 2014. Toothbrushing after an erosive attack: will waiting avoid tooth wear? *European Journal of Oral Sciences,* 122**,** 353-359.

LUSSI, A., MEGERT, B., EGGENBERGER, D. & JAEGGI, T. 2008. Impact of different toothpastes on the prevention of erosion. *Caries Research,* 42**,** 62-67.

LUSSI, A., MEGERT, B., SHELLIS, R. P. & WANG, X. 2012b. Analysis of the erosive effect of different dietary substances and medications. *British journal of nutrition,* 107**,** 252-262.

LUSSI, A. & SCHAFFNER, M. 2000. Progression of and risk factors for dental erosion and wedge-shaped defects over a 6-year period. *Caries Research,* 34**,** 182-187.

LUSSI, A., SCHAFFNER, M., HOTZ, P. & SUTER, P. 1991. Dental erosion in a population of Swiss adults. *Community dentistry and oral epidemiology,* 19**,** 286-290.

LUSSI, A., SCHLÜTER, N., RAKHMATULLINA, E. & GANSS, C. J. C. R. 2011. Dental erosion–an overview with emphasis on chemical and histopathological aspects. 45**,** 2-12.

LYNCH, C. D., O'SULLIVAN, V. R. & MCGILLYCUDDY, C. T. 2006. Pierre Fauchard: the 'Father of Modern Dentistry'. *British dental journal,* 201**,** 779-781.

MACHADO, A., SOARES, C., REIS, B., BICALHO, A., RAPOSO, L. & SOARES, P. 2017. Stress-strain Analysis of Premolars With Non-carious Cervical Lesions: Influence of Restorative Material, Loading Direction and Mechanical Fatigue. *Operative dentistry,* 42**,** 253-265.

MACHOY, M., SEELIGER, J., SZYSZKA-SOMMERFELD, L., KOPROWSKI, R., GEDRANGE, T. & WOŹNIAK, K. 2017. The use of optical coherence tomography in dental diagnostics: a state-of-the-art review. *Journal of healthcare engineering,* 2017.

MAGNE, P. 2006. Composite resins and bonded porcelain: the postamalgam era. *CDA Journal,* 34**,** 135-147.

MAGNE, P. 2007. Efficient 3D finite element analysis of dental restorative procedures using micro-CT data. *Dental Materials,* 23**,** 539-548.

MAGNE, P. & BELSER, U. C. 2002. Rationalization of shape and related stress distribution in posterior teeth: a finite element study using nonlinear contact analysis. *International Journal of Periodontics & Restorative Dentistry,* 22.

MAGNE, P. & BELSER, U. C. 2003. Porcelain Versus Composite Inlays/Onlays: Effects of Mechanical Loads on Stress Distribution, Adhesion, and Crown Flexure. *International Journal of Periodontics & Restorative Dentistry,* 23**,** 542-555.

MAGNE, P. & DOUGLAS, W. H. 1999. Optimization of resilience and stress distribution in porcelain veneers for the treatment of crown-fractured incisors. *International Journal of Periodontics & Restorative Dentistry,* 19.

MAGNE, P. & DOUGLAS, W. H. 2000. Cumulative effects of successive restorative procedures on anterior crown flexure: Intact versus veneered incisors. *Quintessence International,* 31.

MAGNE, P. & KNEZEVIC, A. 2009. Influence of overlay restorative materials and load cusps on the fatigue resistance of endodontically treated molars. *Quintessence International,* 40.

MAGNE, P. & OGANESYAN, T. 2009. CT scan-based finite element analysis of premolar cuspal deflection following operative procedures. *Int J Periodontics Restorative Dent,* 29**,** 361-369.

MAGNE, P., STANLEY, K. & SCHLICHTING, L. H. 2012. Modeling of ultrathin occlusal veneers. *Dental materials,* 28**,** 777-782.

MAGNE, P. & TAN, D. T. 2008. Incisor compliance following operative procedures: a rapid 3-D finite element analysis using micro-CT data. *Journal of Adhesive Dentistry,* 10.

MAGNE, P., VERSLUIS, A. & DOUGLAS, W. H. 1999. Rationalization of incisor shape: experimental-numerical analysis. *The Journal of prosthetic dentistry,* 81**,** 345-355.

MAHONEY, E. & KILPATRICK, N. M. 2003. Dental erosion: part 1. Aetiology and prevalence of dental erosion. *NZ Dent J,* 99**,** 33-41.

MAHONEY, E. K., ROHANIZADEH, R., ISMAIL, F., KILPATRICK, N. & SWAIN, M. 2004. Mechanical properties and microstructure of hypomineralised enamel of permanent teeth. *Biomaterials,* 25**,** 5091-5100.

MAIDA, C. A., MARCUS, M., SPOLSKY, V. W., WANG, Y. & LIU, H. 2013. Socio-behavioral predictors of self-reported oral health-related quality of life. *Quality of Life Research,* 22**,** 559-566.

MAIR, L. 1992. Wear in dentistry—current terminology. *Journal of Dentistry,* 20**,** 140-144.

MANESH, S. K., DARLING, C. L. & FRIED, D. 2009. Nondestructive assessment of dentin demineralization using polarization-sensitive optical coherence tomography after exposure to fluoride and laser irradiation. *Journal of Biomedical Materials Research Part B: Applied Biomaterials: An Official Journal of The Society for Biomaterials, The Japanese Society for Biomaterials, and The Australian Society for Biomaterials and the Korean Society for Biomaterials,* 90**,** 802-812.

MANHART, J., CHEN, H., NEUERER, P., SCHEIBENBOGEN-FUCHSBRUNNER, A. & HICKEL, R. 2001. Three-year clinical evaluation of composite and ceramic inlays. *American journal of dentistry,* 14**,** 95-99.

MANHART, J., MEHL, A., OBERMEIER, T., HICKEL, R. & KUNZELMANN, K. Finite element study on stress distribution in dependence on cavity width and materials properties. Academy of dental materials: proceedings of conference on clinically appropriate alternatives to amalgam: biophysical factors in restorative decision-making, 1996.

MANN, C., RANJITKAR, S., LEKKAS, D., HALL, C., KAIDONIS, J., TOWNSEND, G. & BROOK, A. 2014. Three-dimensional profilometric assessment of early enamel erosion simulating gastric regurgitation. *Journal of dentistry,* 42**,** 1411-1421.

MANSO, A. P. & CARVALHO, R. M. 2017. Dental cements for luting and bonding restorations: self-adhesive resin cements. *Dental Clinics,* 61**,** 821-834.

MANTON, D. J., MANTON, F., CAI, Y., YUAN, G. D., WALKER, N. J., COCHRANE, C., REYNOLDS, L. J., BREARLEY MESSER, E. C. & REYNOLDS 2010. Effect of casein phosphopeptide-amorphous calcium phosphate added to acidic beverages on enamel erosion in vitro. *Australian Dental Journal,* 55**,** 275-279.

MARCHESI, G., FRASSETTO, A., MAZZONI, A., APOLONIO, F., DIOLOSÀ, M., CADENARO, M., DI LENARDA, R., PASHLEY, D., TAY, F. & BRESCHI, L. 2014. Adhesive performance of a multi-mode adhesive system: 1-year in vitro study. *Journal of Dentistry,* 42**,** 603-612.

MARCHESI, G., FRASSETTO, A., VISINTINI, E., DIOLOSÀ, M., TURCO, G., SALGARELLO, S., DI LENARDA, R., CADENARO, M. & BRESCHI, L. 2013. Influence of ageing on self-etch adhesives: one-step vs. two-step systems. *European journal of oral sciences,* 121**,** 43-49.

MARCHI, G., MITSUI, F. & CAVALCANTI, A. 2008. Effect of remaining dentine structure and thermal-mechanical aging on the fracture resistance of bovine roots with different post and core systems. *International endodontic journal,* 41**,** 969-976.

MARSHALL JR, G. W., MARSHALL, S. J., KINNEY, J. H. & BALOOCH, M. 1997. The dentin substrate: structure and properties related to bonding. *Journal of Dentistry,* 25**,** 441-458.

MAUPOMÉ, G., AGUILAR-AVILA, M., MEDRANO-UGALDE, H. & BORGES-YANEZ, A. 1999. In vitro quantitative microhardness assessment of enamel with early salivary pellicles after exposure to an eroding cola drink. *Caries Research,* 33**,** 140-147.

MAUPOME, G., MAUPOMÉ, G., DÍEZ-DE-BONILLA, J., TORRES VILLASEÑOR, G., ANDRADE-DELGADO, L. D. C. & CASTAÑO, V. 1998. In vitro Quantitative Assessment of Enamel Microhardness after Exposure to Eroding Immersion in a Cola Drink. *Caries Research,* 32**,** 148-153.

MCCORMICK, N. & LORD, J. 2010. Digital Image Correlation. *Materials Today,* 13**,** 52-54.

MCCOY, G. 1982. The etiology of gingival erosion. *J Oral Implantol,* 10**,** 361-362.

MCDONALD, A. & SETCHELL, D. 2005. Developing a tooth restorability index. *Dental update,* 32**,** 343-348.

MCGUINNESS, N. J. P., WILSON, A. N., JONES, M. L. & MIDDLETON, J. 1991. A stress analysis of the periodontal ligament under various orthodontic loadings. *European journal of orthodontics,* 13**,** 231-242.

MCKNIGHT HANES, C. & WHITFORD, G. M. 1992. Fluoride Release from Three Glass Ionomer Materials and the Effects of Varnishing with or without Finishing. *Caries Research,* 26**,** 345-350.

MCLAREN, E. & WHITEMAN, Y. 2010. Ceramics: rationale for material selection. *Compendium of continuing education in dentistry,* 31**,** 666-8, 670, 672 passim; quiz 680, 700.

MCLAREN, E. A. & CAO, P. T. 2009. Ceramics in dentistry—part I: classes of materials. *Inside dentistry,* 5**,** 94-103.

MCLEAN, J. 1971. The estimation of cement film thickness by an in vivo technique. *Br dent j,* 131**,** 107-111.

MCLEAN, J. W. 1980. Long-term aesthetic dentistry. *Quintessence international*

20**,** 701.

MELCHER, A. H., HOLOWKA, S., PHAROAH, M. & LEWIN, P. K. 1997. Non-invasive computed tomography and three-dimensional reconstruction of the dentition of a 2,800-year-old Egyptian mummy exhibiting extensive dental disease. *American journal of physical anthropology,* 103**,** 329-340.

MENG, Y., ZHANG, H.-Q., PAN, F., HE, Z.-D., SHAO, J.-L. & DING, Y. 2011. Prevalence of dental caries and tooth wear in a Neolithic population (6700–5600 years BP) from northern China. *Archives of oral biology,* 56**,** 1424-1435.

MERDJI, A., MOOTANAH, R., BOUIADJRA, B. A. B., BENAISSA, A., AMINALLAH, L. & MUKDADI, S. 2013. Stress analysis in single molar tooth. *Materials Science and Engineering: C,* 33**,** 691-698.

MEREDITH, N. & SETCHELL, D. J. 1997. In vitro measurement of cuspal strain and displacement in composite restored teeth. *Journal of Dentistry,* 25**,** 331-337.

MEROUEH, K. 1987. Finite element analysis of partially edenturous mandible rehabilitated with an osseointegrated cylindrical implant. *J Oral Implantol,* 13**,** 215-238.

MESQUITA, R. V., AXMANN, D. & GEIS-GERSTORFER, J. 2006. Dynamic visco-elastic properties of dental composite resins. *Dental Materials,* 22**,** 258-267.

MEURMAN, J., DRYSDALE, T. & FRANK, R. 1991. Experimental erosion of dentin. *European journal of oral sciences,* 99**,** 457-462.

MEURMAN, J. & FRANK, R. 1991a. Progression and surface ultrastructure of in vitro caused erosive lesions in human and bovine enamel. *Caries research,* 25**,** 81-87.

MEURMAN, J., RYTÖMAA, I., KARI, K., LAAKSO, T. & MURTOMAA, H. J. C. R. 1987. Salivary pH and glucose after consuming various beverages, including sugar-containing drinks. 21**,** 353-359.

MEURMAN, J. & TEN GATE, J. 1996. Pathogenesis and modifying factors of dental erosion. *European Journal of Oral Sciences,* 104**,** 199-206.

MEURMAN, J. H. & FRANK, R. M. 1991b. Scanning Electron Microscopic Study of the Effect of Salivary Pellicle on Enamel Erosion. *Caries Research,* 25**,** 1-6.

MEYER-LUECKEL, H., UMLAND, N., HOPFENMULLER, W. & KIELBASSA, A. 2004. Effect of mucin alone and in combination with various dentifrices on in vitro remineralization. *Caries research,* 38**,** 478-483.

MICHAEL, J., TOWNSEND, G., GREENWOOD, L. & KAIDONIS, J. 2009. Abfraction: separating fact from fiction. *Australian dental journal,* 54**,** 2-8.

MILLER, W. 1907. Experiments and observations on the wasting of tooth tissue variously designated as erosion, abrasion, chemical abrasion, denudation, etc. *Dent Cosmos,* 49**,** 1-23,109-124,225-147.

MILLWARD, A., SHAW, L., HARRINGTON, E. & SMITH, A. J. C. R. 1997. Continuous monitoring of salivary flow rate and pH at the surface of the dentition following consumption of acidic beverages. 31**,** 44-49.

MILOSEVIC, A., YOUNG, P. & LENNON, M. 1994. The prevalence of tooth wear in 14-year-old school children in Liverpool. *Community dental health,* 11**,** 83-86.

MIN, J., KWON, H. & KIM, B. 2011. The addition of nano-sized hydroxyapatite to a sports drink to inhibit dental erosion—in vitro study using bovine enamel. *Journal of dentistry,* 39**,** 629-635.

MISTRY, M., ZHU, S., MOAZZEZ, R., DONALDSON, N. & BARTLETT, D. W. 2015. Effect of model variables on in vitro erosion. *Caries research,* 49**,** 508-514.

MITROVIĆ, A., ANTONOVIĆ, D., TANASIĆ, I., MITROVIĆ, N., BAKIĆ, G., POPOVIĆ, D. & MILOŠEVIĆ, M. 2019. 3D Digital Image Correlation Analysis of the Shrinkage Strain in Four Dual Cure Composite Cements. *BioMed Research International,* 2019.

MJOR, I., JOKSTAD, A. & QVIST, V. 1990. Longevity of posterior restorations. *Int Dent J,* 40**,** 11-7.

MOAZZEZ, R. V., AUSTIN, R. S., ROJAS SERRANO, M., CARPENTER, G., COTRONEO, E., PROCTOR, G., ZAIDEL, L. & BARTLETT, D. W. 2014. Comparison of the possible protective effect of the salivary pellicle of individuals with and without erosion. *Caries Research,* 48**,** 57-62.

MONDELLI, J., SENE, F., RAMOS, R. P. & BENETTI, A. R. 2007. Tooth structure and fracture strength of cavities. *Brazilian Dental Journal,* 18**,** 134-8.

MONDELLI, J., STEAGALL, L., ISHIKIRIAMA, A., DE LIMA NAVARRO, M. F. & SOARES, F. B. 1980. Fracture strength of human teeth with cavity preparations. *The Journal of Prosthetic Dentistry,* 43**,** 419-422.

MONTAGNER, A. F., SANDE, F. H. V. D., MÜLLER, C., CENCI, M. S. & SUSIN, A. H. 2018. Survival, Reasons for Failure and Clinical Characteristics of Anterior/Posterior Composites: 8-Year Findings. *Brazilian dental journal,* 29**,** 547-554.

MONTEIRO, J., LOPES, H., VAZ, M. & CAMPOS, J. 2010. Mechanical behaviour of dental composite filling materials using digital holography.

MOORE, A. & TYRER, J. 1995. Phase-stepped ESPI and moiré interferometry for measuring stress-intensity factor andJ integral. *Experimental mechanics,* 35**,** 306-314.

MOORE, A. J. & TYRER, J. R. 1996. Two-dimensional strain measurement with ESPI. *Optics and lasers in engineering,* 24**,** 381-402.

MORETTO, M., MAGALHÃES, A., SASSAKI, K., DELBEM, A. C. B. & MARTINHON, C. 2010. Effect of different fluoride concentrations of experimental dentifrices on enamel erosion and abrasion. *Caries Research,* 44**,** 135-140.

MORGANO, S. M. & BRACKETT, S. E. 1999. Foundation restorations in fixed prosthodontics: current knowledge and future needs. *The Journal of prosthetic dentistry,* 82**,** 643-657.

MORIN, D., DOUGLAS, W., CROSS, M. & DELONG, R. 1988a. Biophysical stress analysis of restored teeth: experimental strain measurement. *Dental Materials,* 4**,** 41-48.

MORIN, D. L., CROSS, M., VOLLER, V. R., DOUGLAS, W. H. & DELONG, R. 1988b. Biophysical stress analysis of restored teeth: modelling and analysis. *Dental Materials,* 4**,** 77-84.

MORITA, Y., UCHINO, M., TODO, M., MATSUSHITA, Y., ARAKAWA, K. & KOYANO, K. 2007. Visualizing displacement and deformation behavior of the periodontium under dental occlusion using a digital image correlation method. *Journal of biomechanical science and engineering,* 2**,** 105-114.

MOTTA, A. B., PEREIRA, L. C. *&* DA CUNHA, A. Finite element analysis in 2D and 3D models for sound and restored teeth. ABAQUS Users' conference, 2006. Citeseer, 329-343.

MULLAN, F., MYLONAS, P., PARKINSON, C., BARTLETT, D. & AUSTIN, R. 2018. Precision of 655 nm Confocal Laser Profilometry for 3D surface texture characterisation of natural human enamel undergoing dietary acid mediated erosive wear. *Dental Materials,* 34**,** 531-537.

MURPHY, F., MCDONALD, A., PETRIE, A., PALMER, G. & SETCHELL, D. 2009. Coronal tooth structure in root-treated teeth prepared for complete and partial coverage restorations. *Journal of oral rehabilitation,* 36**,** 451-461.

MURRAY, P., ABOUT, I., LUMLEY, P., FRANQUIN, J.-C., WINDSOR, L. & SMITH, A. 2003. Odontoblast morphology and dental repair. *Journal of dentistry,* 31**,** 75-82.

MUSANI, I. & PRABHAKAR, A. 2010. Biomechanical stress analysis of mandibular first permanent molar; restored with amalgam and composite resin: a computerized finite element study. *International journal of clinical pediatric dentistry,* 3**,** 5.

MYLONAS, P., AUSTIN, R., MOAZZEZ, R., JOINER, A. & BARTLETT, D. 2018. In vitro evaluation of the early erosive lesion in polished and natural human enamel. *Dental Materials,* 34**,** 1391-1400.

NADAL, F. 1962. Amalgam restorations: cavity preparation, condensing and finishing. *Journal of the American Dental Association (1939),* 65**,** 66.

NAKAGAKI, H., KOYAMA, Y., SAKAKIBARA, Y., WEATHERELL, J. & ROBINSON, C. 1987. Distribution of fluoride across human dental enamel, dentine and cementum. *Archives of oral biology,* 32**,** 651-654.

NAKAJIMA, Y., SHIMADA, Y., MIYASHIN, M., TAKAGI, Y., TAGAMI, J. & SUMI, Y. 2012. Noninvasive cross-sectional imaging of incomplete crown fractures (cracks) using swept-source optical coherence tomography. *International endodontic journal,* 45**,** 933-941.

NAKAYAMA, W. T., HALL, D. R., GRENOBLE, D. E. & KATZ, J. L. 1974. Elastic properties of dental resin restorative materials. *Journal of dental research,* 53**,** 1121-1126.

NG, C. C., DUMBRIGUE, H. B., AL-BAYAT, M. I., GRIGGS, J. A. & WAKEFIELD, C. W. 2006. Influence of remaining coronal tooth structure location on the fracture resistance of restored endodontically treated anterior teeth. *The Journal of prosthetic dentistry,* 95**,** 290-296.

NICKLISCH, N., GANSLMEIER, R., SIEBERT, A., FRIEDERICH, S., MELLER, H. & ALT, K. 2016. Holes in teeth – Dental caries in Neolithic and Early Bronze Age populations in Central Germany. *Annals of anatomy,* 203**,** 90-99.

NIU, L.-N., ZHANG, W., PASHLEY, D., BRESCHI, L., MAO, J., CHEN, J.-H. & TAY, F. 2014. Biomimetic remineralization of dentin. *Dental materials,* 30**,** 77-96.

NIU, X., IFJU, P. G., BIANCHI, J. R. & WALLACE, B. 2000. A DIFFRACTION GRATING FOR COMPLIANT AND POROUS MATERIALS. *Experimental Techniques,* 24**,** 27-30.

NUNN, J., GORDON, P., MORRIS, A., PINE, C. & WALKER, A. 2003. Dental erosion–changing prevalence? A review of British National childrens' surveys. *International Journal of Paediatric Dentistry,* 13**,** 98-105.

O'TOOLE, S., BARTLETT, D. & MOAZZEZ, R. 2016. Efficacy of sodium and stannous fluoride mouthrinses when used before single and multiple erosive challenges. *Australian dental journal,* 61**,** 497-501.

O'TOOLE, S., MISTRY, M., MUTAHAR, M., MOAZZEZ, R. & BARTLETT, D. 2015. Sequence of stannous and sodium fluoride solutions to prevent enamel erosion. *Journal of dentistry,* 43**,** 1498-1503.

ØGAARD, B., DUSCHNER, H., RUBEN, J. & ARENDS, J. 1996. Microradiography and confocal laser scanning microscopy applied to enamel lesions formed in vivo with and without fluoride varnish treatment. *European journal of oral sciences,* 104**,** 378-383.

ØGAARD, B., SEPPÄ, L. & ROLLA, G. 1994. Professional topical fluoride applications—clinical efficacy and mechanism of action. *Advances in Dental Research,* 8**,** 190-201.

OLESZEK-LISTOPAD, J., SARNA-BOS, K., SZABELSKA, A., CZELEJ-PISZCZ, E., BOROWICZ, J. & SZYMANSKA, J. 2015. The use of gold and gold alloys in prosthetic dentistry–a literature review. *Current Issues in Pharmacy and Medical Sciences,* 28**,** 192-195.

OLLEY, R. C., MOAZZEZ, R. & BARTLETT, D. 2015. The relationship between incisal/occlusal wear, dentine hypersensitivity and time after the last acid exposure in vivo. *Journal of dentistry,* 43**,** 248-252.

OPDAM, N. J. M., BRONKHORST, E. M., LOOMANS, B. A. C. & HUYSMANS, M.-C. D. N. J. M. 2010. 12-year Survival of Composite vs. Amalgam Restorations. *Journal of Dental Research,* 89**,** 1063-1067.

OSBORNE, J., HOFFMAN, R. & FERGUSON, G. 1972. Conservation of tooth structure. *Journal-Alabama Dental Association,* 56**,** 24-26.

OSHIRO, M., YAMAGUCHI, K., TAKAMIZAWA, T., INAGE, H., WATANABE, T., IROKAWA, A., ANDO, S. & MIYAZAKI, M. 2007. Effect of CPP-ACP paste on tooth mineralization: an FE-SEM study. *Journal of oral science,* 49**,** 115-120.

OTIS, L. L., EVERETT, M. J., SATHYAM, U. S. & COLSTON JR, B. W. 2000. Optical coherence tomography: a new imaging: technology for dentistry. *The Journal of the American Dental Association,* 131**,** 511-514.

OWENS, B. & KITCHENS, M. 2007. The Erosive Potential of Soft Drinks on Enamel Surface Substrate: An. *Scanning Electron Microscopy Investigation. J Contemp Dent Pract***,** 011-020.

OZEN, J., CAGLAR, A., BEYDEMIR, B., AYDIN, C. & DALKIZ, M. 2007. Three-dimensional finite element stress analysis of different core materials in maxillary implant-supported fixed partial dentures. *Quintessence International,* 38.

PAEPEGAEY, A.-M., BARKER, M. L., BARTLETT, D. W., MISTRY, M., WEST, N. X., HELLIN, N., BROWN, L. J. & BELLAMY, P. G. 2013. Measuring enamel erosion: a comparative study of contact profilometry, non-contact profilometry and confocal laser scanning microscopy. *Dental Materials,* 29**,** 1265-1272.

PALAMARA, D., PALAMARA, J., TYAS, M. & MESSER, H. 2000. Strain patterns in cervical enamel of teeth subjected to occlusal loading. *Dental materials,* 16**,** 412-419.

PALAMARA, J., PALAMARA, D. & MESSER, H. 2002. Strains in the marginal ridge during occlusal loading. *Australian dental journal,* 47**,** 218-222.

PALAMARA, J., PALAMARA, D., MESSER, H. & TYAS, M. 2006. Tooth morphology and characteristics of non-carious cervical lesions. *Journal of dentistry,* 34**,** 185-194.

PAN, Y., XU, X., SUN, F. & MENG, X. 2019. Surface morphology and mechanical properties of conventional and self-adhesive resin cements after aqueous aging. *Journal of Applied Oral Science,* 27.

PANICH, M. & POOLTHONG, S. 2009. The effect of casein phosphopeptide–amorphous calcium phosphate and a cola soft drink on in vitro enamel hardness. *The Journal of the American Dental Association,* 140**,** 455-460.

PANITVISAI, P. & MESSER, H. H. 1995. Cuspal deflection in molars in relation to endodontic and restorative procedures. *J Endod,* 21**,** 57-61.

PAPAGIANNI, C., VAN DER MEULEN, M., NAEIJE, M. & LOBBEZOO, F. 2013. Oral health-related quality of life in patients with tooth wear. *Journal of oral rehabilitation,* 40**,** 185-190.

PARK, K.-J., SCHNEIDER, H. & HAAK, R. 2013. Assessment of interfacial defects at composite restorations by swept source optical coherence tomography. *Journal of biomedical optics,* 18**,** 076018.

PEREIRA, J., PEREIRA, A., MCDONALD, A., PETRIE, J. & KNOWLES 2013. Effect of cavity design on tooth surface strain. *The Journal of prosthetic dentistry,* 110**,** 369-375.

PEREIRA, J. R., DE ORNELAS, F., RODRIGUES CONTI, P. C. & LINS DO VALLE, A. 2006. Effect of a crown ferrule on the fracture resistance of endodontically treated teeth restored with prefabricated posts. *The Journal of Prosthetic Dentistry,* 95**,** 50-54.

PEREZ, C. 2010. Alternative technique for class V resin composite restorations with minimum finishing/polishing procedures. *Operative dentistry,* 35**,** 375-379.

PETERS, W. H. & RANSON, W. F. 1982. Digital Imaging Techniques In Experimental Stress Analysis. *Optical Engineering,* 21**,** 213427.

PHILLIPS, R. W. 1991. Science of dental material. *WB Saunders Company. P,* 23**,** 177-213.

PIEGER, S., SALMAN, A. & BIDRA, A. S. 2014. Clinical outcomes of lithium disilicate single crowns and partial fixed dental prostheses: a systematic review. *The Journal of prosthetic dentistry,* 112**,** 22-30.

PIOTROWSKI, B. T., GILLETTE, W. B. & HANCOCK, E. B. 2001. Examining the prevalence and characteristics of abfractionlike cervical lesions in a population of US veterans. *The Journal of the American Dental Association,* 132**,** 1694-1701.

PIWOWARCZYK, A., LAUER, H.-C. & SORENSEN, J. A. 2004. In vitro shear bond strength of cementing agents to fixed prosthodontic restorative materials. *The Journal of prosthetic dentistry,* 92**,** 265-273.

PIWOWARCZYK, A., OTTL, P., LAUER, H. C. & KURETZKY, T. 2005. A Clinical Report and Overview of Scientific Studies and Clinical Procedures Conducted on the 3M ESPE Lava™ All-Ceramic System. *Journal of Prosthodontics: Implant, Esthetic and Reconstructive Dentistry,* 14**,** 39-45.

POGGIO, C., CECI, M., BELTRAMI, R., LOMBARDINI, M. & COLOMBO, M. 2014a. Atomic force microscopy study of enamel remineralization. *Annali di Stomatologia,* 5**,** 98-102.

POGGIO, C., GULINO, C., MIRANDO, M., COLOMBO, M. & PIETROCOLA, G. 2017. Preventive effects of different protective agents on dentin erosion: An in vitro investigation. *Journal of clinical and experimental dentistry,* 9**,** e7.

POGGIO, C., LOMBARDINI, M., COLOMBO, M. & BIANCHI, S. 2010. Impact of two toothpastes on repairing enamel erosion produced by a soft drink: An AFM in vitro study. *Journal of Dentistry,* 38**,** 868-874.

POGGIO, C., LOMBARDINI, M., VIGORELLI, P. & CECI, M. 2013. Analysis of dentin/enamel remineralization by a CPP-ACP paste: AFM and SEM study. *Scanning: The Journal of Scanning Microscopies,* 35**,** 366-374.

POGGIO, C., LOMBARDINI, M., VIGORELLI, P., COLOMBO, M. & CHIESA, M. 2014b. The role of different toothpastes on preventing dentin erosion: An sem and afm study®. *Scanning: The Journal of Scanning Microscopies,* 36**,** 301-310.

POLANSKY, R., ARNETZL, G., HAAS, M., KEIL, C., WIMMER, G. & LORENZONI, M. 2000. Residual dentin thickness after 1.2-mm shoulder preparation for Cerec crowns. *International journal of computerized dentistry,* 3**,** 243-258.

POLITANO, G., FABIANELLI, A., PAPACCHINI, F. & CERUTTI, A. 2016. The use of bonded partial ceramic restorations to recover heavily compromised teeth. *Int. J. Esthet. Dent,* 11**,** 314-336.

POPESCU, D. P., SOWA, M. G. & HEWKO, M. D. 2008. Assessment of early demineralization in teeth using the signal attenuation in optical coherence tomography images. *Journal of biomedical optics,* 13**,** 054053.

POWERS, N. 2006. Archaeological evidence for dental innovation: an eighteenth century porcelain dental prosthesis belonging to Archbishop Arthur Richard Dillon. *British dental journal,* 201**,** 459-463.

PRATI, C., CHERSONI, S., MONGIORGI, R., MONTANARI, G. & PASHLEY, D. H. 1999. Thickness and morphology of resin-infiltrated dentin layer in young, old, and sclerotic dentin. *Operative Dentistry,* 24**,** 66-72.

QASIM, T., BUSH, M., HU, X. & LAWN, B. 2005. Contact damage in brittle coating layers: Influence of surface curvature. *Journal of Biomedical Materials Research Part B: Applied Biomaterials,* 73**,** 179-185.

RAKHMATULLINA, E., BEYELER, B. & LUSSI, A. 2013. Inhibition of enamel erosion by stannous fluoride containing rinsing solutions. *Schweizer Monatsschrift für Zahnmedizin= Revue mensuelle suisse d'odonto-stomatologie= Rivista mensile svizzera di odontologia e stomatologia,* 123**,** 192-198.

RAKHMATULLINA, E., RAKHMATULLINA, A., BOSSEN, C., WANG, B., BEYELER, C., MEIER, A. & LUSSI 2011. Application of the specular and diffuse reflection analysis for in vitro diagnostics of dental erosion: correlation with enamel softening, roughness, and calcium release. *Journal of biomedical optics,* 16**,** 107002.

RAMAKRISHNAIAH, R., ALAQEEL, S. M., ALKHERAIF, A. A., DIVAKAR, D. D., ELSHARAWY, M., MATINLINNA, J. P. & VALLITTU, P. K. 2018. Micro and nano structural analysis of dental ceramic and luting resin interface and the effect of water exposure on integrity of cement interface. *Journal of Biomaterials and Tissue Engineering,* 8**,** 136-143.

RANJITKAR, S., KAIDONIS, J. A., TOWNSEND, G. C., VU, A. M. & RICHARDS, L. C. 2008. An in vitro assessment of the effect of load and pH on wear between opposing enamel and dentine surfaces. *Archives of oral biology,* 53**,** 1011-1016.

RANJITKAR, S., RODRIGUEZ, J. M., KAIDONIS, J. A., RICHARDS, L. C., TOWNSEND, G. C. & BARTLETT, D. W. 2009. The effect of casein phosphopeptide–amorphous calcium phosphate on erosive enamel and dentine wear by toothbrush abrasion. *Journal of Dentistry,* 37**,** 250-254.

RAO, R., JAIN, A., VERMA, M., LANGADE, D. & PATIL, A. 2017. Comparative evaluation of remineralizing potential of Fluoride using three different remineralizing protocols: An in vitro study. *Journal of Conservative Dentistry,* 20**,** 463.

RAO, S. 1986. The finite element method in engineering.

RASTOGI, P. 1993. Speckle Metrology, edited by RS Sirohi. New York: Marcel Dekker.

REEH, E. S., DOUGLAS, W. H. & MESSER, H. H. 1989a. Stiffness of Endodontically-treated Teeth Related to Restoration Technique. *Journal of Dental Research,* 68**,** 1540-1544.

REEH, E. S., MESSER, H. H. & DOUGLAS, W. H. 1989b. Reduction in tooth stiffness as a result of endodontic and restorative procedures. *Journal of Endodontics,* 15**,** 512-516.

REES, J., HAMMADEH, M. & JAGGER, D. 2003. Abfraction lesion formation in maxillary incisors, canines and premolars: a finite element study. *European journal of oral sciences,* 111**,** 149-154.

REES, J., JACOBSEN, P. & HICKMAN, J. 1994. The elastic modulus of dentine determined by static and dynamic methods. *Clinical materials,* 17**,** 11-15.

REES, J., LOYN, T. & CHADWICK, B. 2007. Pronamel and tooth mousse: An initial assessment of erosion prevention in vitro. *Journal of Dentistry,* 35**,** 355-357.

REES, J. S. 1998. The role of cuspal flexure in the development of abfraction lesions: a finite element study. *Eur J Oral Sci,* 106**,** 1028-32.

REES, J. S. 2002. The effect of variation in occlusal loading on the development of abfraction lesions: a finite element study. *Journal of oral rehabilitation,* 29**,** 188-193.

REES, J. S. & HAMMADEH, M. 2004. Undermining of enamel as a mechanism of abfraction lesion formation: a finite element study. *European journal of oral sciences,* 112**,** 347-352.

REICH, S., UHLEN, S., GOZDOWSKI, S. & LOHBAUER, U. 2011. Measurement of cement thickness under lithium disilicate crowns using an impression material technique. *Clinical oral investigations,* 15**,** 521-526.

REN, Y.-F., ZHAO, Q., MALMSTROM, H., BARNES, V. & XU, T. 2009. Assessing fluoride treatment and resistance of dental enamel to soft drink erosion in vitro: applications of focus variation 3D scanning microscopy and stylus profilometry. *journal of dentistry,* 37**,** 167-176.

RESTARSKI, J., GORTNER JR, R. & MCCAY, C. 1945. Effect of acid beverages containing fluorides upon the teeth of rats and puppies. *Journal of the American Dental Association,* 32**,** 668-675.

RIOS, D., HONÓRIO, H. M., MAGALHÃES, A., DELBEM, A., MACHADO, M. A. A. M., SILVA, S. M. B. D. & BUZALAF, M. A. R. 2006. Effect of salivary stimulation on erosion of human and bovine enamel subjected or not to subsequent abrasion: an in situ/ex vivo study. *Caries research,* 40**,** 218.

RIOS, D., HONÓRIO, H. M., MAGALHÃES, A. C., WIEGAND, A., MACHADO, M. A. D. A. M. & BUZALAF, M. A. R. 2009. Light cola drink is less erosive than the regular one: an in situ/ex vivo study. *journal of dentistry,* 37**,** 163-166.

ROBERSON, T. M., HEYMANN, H. & SWIFT JR, E. 2002. Introduction to operative dentistry. *Roberson TM, Heymann HO, Swift EJ: Student art and science of operative dentistry. 4th Ed. St. Louis: The CV Mosby Co*, 1-3.

ROBINSON, C., WEATHERELL, J. & HALLSWORTH, A. 1971. Variation in composition of dental enamel within thin ground tooth sections. *Caries research,* 5, 44-57.

ROBINSON, D., AGUILAR, L., GATTI, A., ABDUO, J., LEE, P. V. S. & ACKLAND, D. 2019. Load response of the natural tooth and dental implant: A comparative biomechanics study. *The journal of advanced prosthodontics,* 11, 169-178.

ROMANINI-JUNIOR, J. C., KUMAGAI, R. Y., ORTEGA, L. F., RODRIGUES, J. A., CASSONI, A., HIRATA, R. & REIS, A. F. 2018. Adhesive/silane application effects on bond strength durability to a lithium disilicate ceramic. *Journal of Esthetic & Restorative Dentistry: Official Publication of the American Academy of Esthetic Dentistry,* 30, 346-351.

ROMEED, S. A., FOK, S. L. & WILSON, N. H. F. 2006. A comparison of 2D and 3D finite element analysis of a restored tooth. *Journal of Oral Rehabilitation,* 33, 209-215.

ROMEED, S. A., MALIK, R. & DUNNE, S. M. 2012. Stress analysis of occlusal forces in canine teeth and their role in the development of non-carious cervical lesions: abfraction. *International journal of dentistry,* 2012.

ROPERTO, R., SOUSA, Y. T., DIAS, T., MACHADO, R., PERREIRA, R. D., LEONI, G. B., PALMA-DIBB, R. G., RODRIGUES, M. P., SOARES, C. J. & TEICH, S. 2019. Biomechanical behavior of maxillary premolars with conservative and traditional endodontic cavities. *Quintessence international (Berlin, Germany: 1985),* 50, 350-356.

ROSELLA, D., ROSELLA, G., BRAUNER, E., PAPI, P., PICCOLI, L. & POMPA, G. 2015. A tooth preparation technique in fixed prosthodontics for students and neophyte dentists. *Annali di Stomatologia,* 6, 104-109.

ROUX, S., RÉTHORÉ, J. & HILD, F. 2009. Digital image correlation and fracture: an advanced technique for estimating stress intensity factors of 2D and 3D cracks. *Journal of physics. D, Applied physics,* 42, 214004.

RUBIN, C., KRISHNAMURTHY, N., CAPILOUTO, E. & YI, H. 1983. Clinical Science Stress Analysis of the Human Tooth Using a Three-dimensional Finite Element Model. *Journal of Dental Research,* 62, 82-86.

RÜEGSEGGER, P., KOLLER, B. & MÜLLER, R. 1996. A microtomographic system for the nondestructive evaluation of bone architecture. *Calcified tissue international,* 58, 24-29.

RUIZ, J.-L. 2017. *Supra-gingival Minimally Invasive Dentistry: A Healthier Approach to Esthetic Restorations*, John Wiley & Sons.

RUIZ JL, C. G. 2011. Myths vs. realities, State of the art indirect posterior restorations. *Journal of Cosmetic Dentistry,* 27**,** 63-72.

SADOWSKY, S. J. 2006. An overview of treatment considerations for esthetic restorations: a review of the literature. *The Journal of prosthetic dentistry,* 96**,** 433-442.

SAGSEN, B. & ASLAN, B. 2006. Effect of bonded restorations on the fracture resistance of root filled teeth. *International Endodontic Journal,* 39**,** 900-904.

SALEEM, Q., WILDMAN, R., HUNTLEY, J. & WHITWORTH, M. 2003. A novel application of speckle interferometry for the measurement of strain distributions in semi-sweet biscuits. *Measurement Science and Technology,* 14**,** 2027.

SANDERS, A. E., SLADE, G. D., JOHN, M. T., STEELE, J. G., SUOMINEN-TAIPALE, A. L., LAHTI, S., NUTTALL, N. M. & ALLEN, P. F. 2009. A cross-national comparison of income gradients in oral health quality of life in four welfare states: application of the Korpi and Palme typology. *Journal of Epidemiology & Community Health,* 63**,** 569-574.

SANO, H. 2006. Microtensile Testing, Nanoleakage, and Biodegradation of Resin-Dentin Bonds. *Journal of Dental Research,* 85**,** 11-14.

SANTANA, F., CASTRO, C., SIMAMOTO-JÚNIOR, P., SOARES, P., QUAGLIATTO, P., ESTRELA, C. & SOARES, C. 2011. Influence of post system and remaining coronal tooth tissue on biomechanical behaviour of root filled molar teeth. *International endodontic journal,* 44**,** 386-394.

SANTOS-FILHO, P. C. F., VERÍSSIMO, C., SOARES, P. V., SALTARELO, R. C., SOARES, C. J. & MARCONDES MARTINS, L. R. 2014. Influence of Ferrule, Post System, and Length on Biomechanical Behavior of Endodontically Treated Anterior Teeth. *Journal of Endodontics,* 40**,** 119-123.

SANTOS, N. M., JORDÃO, M. C., IONTA, F. Q., MENDONÇA, F. L., DI LEONE, C. C. L., BUZALAF, M. A. R., OLIVEIRA, T. M., HONÓRIO, H. M., CRUVINEL, T. & RIOS, D. 2018. Impact of a simplified in situ protocol on enamel loss after erosive challenge. *PloS one,* 13**,** e0196557.

SANTOS, V. R., LUCCHESI, J. A., CORTELLI, S. C., AMARAL, C. M., FERES, M. & DUARTE, P. M. 2007. Effects of glass ionomer and microfilled composite subgingival restorations on periodontal tissue and subgingival biofilm: A 6-month evaluation. *Journal of periodontology,* 78**,** 1522-1528.

SAURO, S., MANNOCCI, F., PIEMONTESE, M. & MONGIORGI, R. 2008. In situenamel morphology evaluation after acidic soft drink consumption: protection factor of contemporary toothpaste. *International journal of dental hygiene,* 6**,** 188-192.

SAURO, S., THOMPSON, I. & WATSON, T. 2011. Effects of common dental materials used in preventive or operative dentistry on dentin permeability and remineralization. *Operative dentistry,* 36**,** 222-230.

SCHIPPER, R. G., SILLETTI, E. & VINGERHOEDS, M. H. 2007. Saliva as research material: biochemical, physicochemical and practical aspects. *Archives of oral biology,* 52**,** 1114-1135.

SCHLICHTING, L. H., MAIA, H. P., BARATIERI, L. N. & MAGNE, P. 2011. Novel-design ultra-thin CAD/CAM composite resin and ceramic occlusal veneers for the treatment of severe dental erosion. *The Journal of prosthetic dentistry,* 105**,** 217-226.

SCHLICHTING, L. H., RESENDE, T. H., REIS, K. R. & MAGNE, P. 2016. Simplified treatment of severe dental erosion with ultrathin CAD-CAM composite occlusal veneers and anterior bilaminar veneers. *The Journal of prosthetic dentistry,* 116**,** 474-482.

SCHLUETER, N., HARA, A., SHELLIS, R. P. & GANSS, C. 2011. Methods for the measurement and characterization of erosion in enamel and dentine. *Caries Research,* 45 Suppl 1**,** 13-23.

SCIAMMARELLA, C. A. & SCIAMMARELLA, F. M. 2012. *Experimental Mechanics of Solids*.

SEOW, L., TOH, C. & WILSON, N. 2005. Remaining tooth structure associated with various preparation designs for the endodontically treated maxillary second premolar. *The European journal of prosthodontics and restorative dentistry,* 13**,** 57-64.

SEOW, L. L., TOH, C. G. & WILSON, N. H. 2015. Strain measurements and fracture resistance of endodontically treated premolars restored with all-ceramic restorations. *Journal of dentistry,* 43**,** 126-132.

SETHI, S. 2016. A clinical case involving severe erosion of the maxillary anterior teeth restored with direct composite resin restorations. *Int J Esthet Dent,* 11**,** 281-6.

SHAHRBAF, S., MIRZAKOUCHAKI, B., OSKOUI, S. S. & KAHNAMOUI, M. A. 2007. The Effect of Marginal Ridge Thickness on the Fracture Resistance of Endodontically-treated, Composite Restored Maxillary Premolars. *Operative dentistry,* 32**,** 285-290.

SHELLIS, R. P., FEATHERSTONE, J. D. & LUSSI, A. 2014. Understanding the chemistry of dental erosion. *Erosive Tooth Wear*. Karger Publishers.

SHELLIS, R. P., GANSS, C., REN, Y., ZERO, D. T. & LUSSI, A. 2011. Methodology and models in erosion research: discussion and conclusions. *Caries Research,* 45 Suppl 1**,** 69-77.

SHEN, J., WILDMAN, J. & STEELE, J. 2013. Measuring and decomposing oral health inequalities in an UK population. *Community dentistry and oral epidemiology,* 41**,** 481-489.

SHERFUDHIN, H., SHERFUDHIN, J., HOBEICH, C., CARVALHO, M., ABOUSHELIB, W., SADIG, Z. & SALAMEH 2011. Effect of different ferrule designs on the fracture resistance and failure pattern of endodontically treated teeth restored with fiber posts and all-ceramic crowns. *Journal of Applied Oral Science,* 19**,** 28-33.

SHILLINGBURG, H. T., HOBO, S., WHITSETT, L. D. & BRACKETT, S. E. 1997. *Fundamentals of Fixed Prosthodontics, 3rd ed, 1997*, Quintessence Publishing.

SHIMIZU, Y., USUI, K., ARAKI, K., KUROSAKI, N., TAKANOBU, H. & TAKANISHI, A. 2005. Study of finite element modeling from CT images. *Dental materials journal,* 24**,** 447-455.

SHOR, A., NICHOLLS, J. I., PHILLIPS, K. M. & LIBMAN, W. J. 2003. Fatigue load of teeth restored with bonded direct composite and indirect ceramic inlays in MOD class II cavity preparations. *International Journal of Prosthodontics,* 16.

SHORTALL, A., UCTASLI, S. & MARQUIS, P. 2001. Fracture resistance of anterior, posterior and universal light activated composite restoratives. *Operative dentistry,* 26**,** 87-96.

SIDHU, S. & WATSON, T. 1998. Interfacial characteristics of resin-modified glass-ionomer materials: a study on fluid permeability using confocal fluorescence microscopy. *Journal of dental research,* 77**,** 1749-1759.

SIEGELE, D. & SOLTESZ, U. 1989. Numerical investigations of the influence of implant shape on stress distribution in the jaw bone. *International Journal of Oral & Maxillofacial Implants,* 4.

SILVERSTONE, L., SAXTON, C., DOGON, I. & FEJERSKOV, O. 1975. Variation in the pattern of acid etching of human dental enamel examined by scanning electron microscopy. *Caries research,* 9**,** 373-387.

SIM, T., KNOWLES, J., NG, Y. L., SHELTON, J. & GULABIVALA, K. 2001. Effect of sodium hypochlorite on mechanical properties of dentine and tooth surface strain. *International Endodontic Journal,* 34**,** 120-132.

SINESCU, C., NEGRUTIU, M., TOPALA, F., IONITA, C., NEGRU, R., FABRIKY, M., MARCAUTEANU, C., BRADU, A., DOBRE, G. & MARSAVINA, L. Ceramic and polymeric dental onlays evaluated by photo-elasticity, optical coherence tomography, and micro-computed tomography. Optical Complex Systems: OCS11, 2011. International Society for Optics and Photonics, 817208.

SINESCU, C. G., NEGRUTIU, M.-L. V., TODEA, C. C., BALABUC, C. I., FILIP, L. M., ROMINU, R., BRADU, A., HUGHES, M. R. & PODOLEANU, A. G. 2008. Quality assessment of dental treatments using en-face optical coherence tomography. *Journal of Biomedical Optics,* 13**,** 054065.

SIVASITHAMPARAM, K., HARBROW, D., VINCZER, E. & YOUNG, W. G. 2003. Endodontic sequelae of dental erosion. *Australian Dental Journal,* 48**,** 97-101.

SMALL, B. 2006. Material choice for restorative dentistry: inlays, onlays, crowns, and bridges. *General dentistry,* 54**,** 310-312.

SMITH, B. G. & KNIGHT, J. K. 1984. An index for measuring the wear of teeth. *British Dental Journal,* 156**,** 435-438.

SMITH, W., MARCHAN, S. & RAFEEK, R. 2008. The prevalence and severity of non-carious cervical lesions in a group of patients attending a university hospital in Trinidad. *Journal of oral rehabilitation,* 35**,** 128-134.

SOARES, C. J., MARTINS, L. R. M., FONSECA, R. B., CORRER-SOBRINHO, L. & FERNANDES NETO, A. J. 2006. Influence of cavity preparation design on fracture resistance of posterior Leucite-reinforced ceramic restorations. *The Journal of prosthetic dentistry,* 95**,** 421-429.

SOARES, L. E. S., DE OLIVEIRA, R. & NAHÓRNY, S. 2016. The effects of acid erosion and remineralization on enamel and three different dental materials: FT-Raman spectroscopy and scanning electron microscopy analysis. *Microscopy research and technique,* 79**,** 646-656.

SOARES, P., MACHADO, A., ZEOLA, L., SOUZA, P., GALVÃO, A., MONTES, T., PEREIRA, A., REIS, B., COLEMAN, T. & GRIPPO, J. 2015. Loading and composite restoration assessment of various non-carious cervical lesions morphologies–3D finite element analysis. *Australian dental journal,* 60**,** 309-316.

SOARES, P., SANTOS-FILHO, P., SOARES, C., FARIA, V., NAVES, M., MICHAEL, J., KAIDONIS, J., RANJITKAR, S. & TOWNSEND, G. 2013a.

Non-carious cervical lesions: influence of morphology and load type on biomechanical behaviour of maxillary incisors. *Australian dental journal,* 58**,** 306-314.

SOARES, P. V., DE ALMEIDA MILITO, G., PEREIRA, F. A., ZÉOLA, L. F., DE LIMA NAVES, M. F., FARIA, V. L. G., MACHADO, A. C., SOUZA, P. G. & REIS, B. R. 2013b. Influence of geometrical configuration of the cavity in the stress distribution of restored premolars with composite resin. *Journal of Research in Dentistry,* 1**,** p. 72-82.

SOARES, P. V., SANTOS-FILHO, P. C., GOMIDE, H. A., ARAUJO, C. A., MARTINS, L. R. & SOARES, C. J. 2008a. Influence of restorative technique on the biomechanical behavior of endodontically treated maxillary premolars. Part II: strain measurement and stress distribution. *J Prosthet Dent,* 99**,** 114-122.

SOARES, P. V., SANTOS-FILHO, P. C., MARTINS, L. R. & SOARES, C. J. 2008b. Influence of restorative technique on the biomechanical behavior of endodontically treated maxillary premolars. Part I: fracture resistance and fracture mode. *J Prosthet Dent,* 99**,** 30-37.

SOARES, P. V., SANTOS-FILHO, P. C. F., MARTINS, L. R. M. & SOARES, C. J. 2008c. Influence of restorative technique on the biomechanical behavior of endodontically treated maxillary premolars. Part I: fracture resistance and fracture mode. *The Journal of prosthetic dentistry,* 99**,** 30-37.

SOGNNAES, R. F., WOLCOTT, R. B. & XHONGA, F. A. 1972. Dental Erosion: I. Erosion-like patterns occurring in association with other dental conditions. *The Journal of the American Dental Association,* 84**,** 571-576.

SORENSEN, J. A. & ENGELMAN, M. J. 1990. Ferrule design and fracture resistance of endodontically treated teeth. *The Journal of prosthetic dentistry,* 63**,** 529-536.

SORENSEN, J. A. & MARTINOFF, J. T. 1984. Intracoronal reinforcement and coronal coverage: a study of endodontically treated teeth. *The Journal of prosthetic dentistry,* 51**,** 780-784.

SOUZA, B., LIMA, L., COMAR, L., BUZALAF, M. & MAGALHÃES, A. 2014. Effect of experimental mouthrinses containing the combination of NaF and TiF4 on enamel erosive wear in vitro. *Archives of oral biology,* 59**,** 621-624.

SPENCER, P., YE, Q., PARK, J., TOPP, E. M., MISRA, A., MARANGOS, O., WANG, Y., BOHATY, B. S., SINGH, V., SENE, F., ESLICK, J., CAMARDA, K. & KATZ, J. L. 2010. Adhesive/Dentin Interface: The Weak Link in the Composite Restoration. *Annals of Biomedical Engineering,* 38**,** 1989-2003.

SPIELMAN, A. 2007. The Birth of the Most Important 18th Century Dental Text: Pierre Fauchardâ□™sLe Chirurgien Dentist. *Journal of Dental Research,* 86**,** 922-926.

SPIJKER, A. V. T., RODRIGUEZ, J. M., KREULEN, C. M., BRONKHORST, E. M., BARTLETT, D. W. & CREUGERS, N. H. 2009. Prevalence of tooth wear in adults. *International Journal of Prosthodontics,* 22.

SPREAFICO, R. C., KREJCI, I. & DIETSCHI, D. 2005. Clinical performance and marginal adaptation of class II direct and semidirect composite restorations over 3.5 years in vivo. *Journal of dentistry,* 33**,** 499-507.

SRIREKHA, A. & BASHETTY, K. 2010. Infinite to finite: an overview of finite element analysis. *Indian Journal of Dental Research,* 21**,** 425.

STAINES, M., ROBINSON, W. & HOOD, J. 1981. Spherical indentation of tooth enamel. *Journal of materials science,* 16**,** 2551-2556.

STANINEC, M., NALLA, R. K., HILTON, J. F., RITCHIE, R. O., WATANABE, L. G., NONOMURA, G., MARSHALL, G. W. & MARSHALL, S. J. 2005. Dentin erosion simulation by cantilever beam fatigue and pH change. *Journal of dental research,* 84**,** 371-375.

STEIN, P. S., SULLIVAN, J., HAUBENREICH, J. E. & OSBORNE, P. B. 2005. Composite resin in medicine and dentistry. *Journal of long-term effects of medical implants,* 15.

SULLIVAN, H. 1954. The solubility of enamel surfaces. *Journal of dental research,* 33**,** 504-510.

SUMI, Y., OZAWA, N., NAGAOSA, S., MINAKUCHI, S. & UMEMURA, O. 2011. Application of optical coherence tomography (OCT) to nondestructive inspection of dentures. *Archives of gerontology and geriatrics,* 53**,** 237-241.

SUTTON, M., MCNEILL, S., HELM, J., CHAO, Y. & RASTOGI, P. K. 2000. *Advances in Two-Dimensional and Three-Dimensional Computer Vision Photomechanics*.

SUTTON, M., MCNEILL, S., JANG, J. & BABAI, M. 1988. Effects Of Subpixel Image Restoration On Digital Correlation Error Estimates. *Optical Engineering,* 27**,** 271070.

SWAIN, M. V. & XUE, J. 2009. State of the art of Micro-CT applications in dental research. *Int J Oral Sci,* 1**,** 177-88.

TAHA, N. A., PALAMARA, J. E. & MESSER, H. H. 2011. Fracture strength and fracture patterns of root filled teeth restored with direct resin restorations. *Journal of Dentistry,* 39**,** 527-535.

TAN, P. L., AQUILINO, S. A., GRATTON, D. G., STANFORD, C. M., TAN, S. C., JOHNSON, W. T. & DAWSON, D. 2005. In vitro fracture resistance of endodontically treated central incisors with varying ferrule heights and configurations. *The Journal of prosthetic dentistry,* 93**,** 331-336.

TANASIC, I. 2017. Visualizing Strain Behavior of Mandibles with Gradually Reducing of the Permanent Teeth Using Digital Image Correlation Method. *EC Dental Science,* 11**,** 216-221.

TANASIC, I., MILIC LEMIC, A., TIHACEK SOJIC, L., STANCIC, I. & MITROVIC, N. 2012. Analysis of the compressive strain below the removable and fixed prosthesis in the posterior mandible using a digital image correlation method. *Biomechanics and Modeling in Mechanobiology,* 11**,** 751-758.

TANG, X., TANG, C., SU, H., LUO, H., NAKAMURA, T. & YATANI, H. 2014. The effects of repeated heat-pressing on the mechanical properties and microstructure of IPS e. max Press. *Journal of the mechanical behavior of biomedical materials,* 40**,** 390-396.

TANTBIROJN, D., HUANG, A., ERICSON, M. & POOLTHONG, S. 2008. Change in surface hardness of enamel by a cola drink and a CPP–ACP paste. *Journal of Dentistry,* 36**,** 74-79.

TANTBIROJN, D., VERSLUIS, A., PINTADO, M. R., DELONG, R. & DOUGLAS, W. H. 2004. Tooth deformation patterns in molars after composite restoration. *Dental Materials,* 20**,** 535-542.

TEN, C. A. 1998. Oral Histology: development, structure, and function. Mosby St Louis.

TEN CATE, J. M., BUIJS, M. J., MILLER, C. C. & EXTERKATE, R. A. M. 2008. Elevated Fluoride Products Enhance Remineralization of Advanced Enamel Lesions. *Journal of Dental Research,* 87**,** 943-947.

TEN CATE, J. M. & FEATHERSTONE, J. D. B. 1991. Mechanistic Aspects of the Interactions Between Fluoride and Dental Enamel. *Critical Reviews in Oral Biology and Medicine,* 2**,** 283-296.

THOMAS, S., MALLIA, R., JOSE, M. & SUBHASH, N. 2008. Investigation of in vitro dental erosion by optical techniques. *Lasers in Medical Science,* 23**,** 319-329.

THORDRUP, M., ISIDOR, F. & HÖRSTED-BINDSLEV, P. 2006. A prospective clinical study of indirect and direct composite and ceramic inlays: ten-year results. *Quintessence international (Berlin, Germany: 1985),* 37**,** 139-144.

THRESHER, R. W. & SAITO, G. E. 1973. The stress analysis of human teeth. *Journal of Biomechanics,* 6**,** 443-449.

TILLBERG, A., JÄRVHOLM, B. & BERGLUND, A. 2008. Risks with dental materials. *Dental Materials,* 24**,** 940-943.

TIOSSI, R., LIN, L., CONRAD, H. J., RODRIGUES, R. C. S., HEO, Y. C., DE MATTOS, M. D. G. C., FOK, A. S.-L. & RIBEIRO, R. F. 2012. A digital image correlation analysis on the influence of crown material in implant-supported prostheses on bone strain distribution. *Journal of Prosthodontic Research,* 56**,** 25-31.

TJAN, A. H. & WHANG, S. B. 1985. Resistance to root fracture of dowel channels with various thicknesses of buccal dentin walls. *The Journal of prosthetic dentistry,* 53**,** 496-500.

TOLEDANO, M., OSORIO, E., CABELLO, I. & OSORIO, R. 2014. Early dentine remineralisation: Morpho-mechanical assessment. *Journal of Dentistry,* 42**,** 384-394.

TOOLE, S., PENNINGTON, M., VARMA, S. & BARTLETT, D. 2018. VERIFIABLE CPD PAPER The treatment need and associated cost of erosive tooth wear rehabilitation–a service evaluation within an NHS dental hospital.

TORRES, C., CHINELATTI, M., GOMES SILVA, J., RIZÓLI, F., OLIVEIRA, M. A. H. D. M., PALMA DIBB, R. & BORSATTO, M. 2010. Surface and subsurface erosion of primary enamel by acid beverages over time. *Brazilian dental journal,* 21**,** 337-345.

TRAMINI, P., PÉLISSIER, B., VALCARCEL, J., BONNET, B. & MAURY, L. 2000. A Raman spectroscopic investigation of dentin and enamel structures modified by lactic acid. *Caries Research,* 34**,** 233-240.

TUCKER, K., ADAMS, M., SHAW, L. & SMITH, A. 1998. Human enamel as a substrate for in vitro acid dissolution studies: influence of tooth surface and morphology. *Caries research,* 32**,** 135-140.

TURNER, M. 1956. Stiffness and deflection analysis of complex structures. *journal of the Aeronautical Sciences,* 23**,** 805-823.

TURSSI, C. P., MAEDA, F. A., MESSIAS, D. C., NETO, F., SERRA, M. & GALAFASSI, D. 2011. Effect of potential remineralizing agents on acid softened enamel. *American Journal of Dentistry,* 24**,** 165.

TYSON, J. 2000. Noncontact full-field strain measurement with 3D ESPI. *Sensors,* 17**,** 62-70.

VADERHOBLI, R. M. 2011. Advances in dental materials. *Dental Clinics,* 55**,** 619-625.

VALDIVIA, A. D. C. M., RAPOSO, P., SIMAMOTO JÚNIOR, V., NOVAIS, C. & SOARES 2012. The effect of fiber post presence and restorative technique on the biomechanical behavior of endodontically treated maxillary incisors: An in vitro study. *The Journal of prosthetic dentistry,* 108**,** 147-157.

VAN DIJKEN, J. W. 1999. All-ceramic restorations: classification and clinical evaluations. *Compendium of continuing education in dentistry,* 20**,** 1115-24, 1126 passim; quiz 1136.

VAN DIJKEN, J. W. 2000. Clinical evaluation of three adhesive systems in class V non-carious lesions. *Dental materials,* 16**,** 285-291.

VAN MEERBEEK, B. 2003. Adhesion to enamel and dentin: current status and future challenges. *Operative dentistry,* 28**,** 215-235.

VANNONI, M. & MOLESINI, G. 2004. Speckle interferometry experiments with a digital photocamera. *American Journal of Physics,* 72**,** 906-909.

VANNONI, M. & MOLESINI, G. In-plane, out-of-plane, and time-average speckle interferometry experiments with a digital photocamera. OPTO-Ireland, 2005. International Society for Optics and Photonics, 617-626.

VARANASI, S., MEYERS, I. A. & SYMONS, A. L. 2014. The Effect of Remineralisation Treatments on Demineralised Dentine, an In Vitro Study. *Open Journal of Dentistry and Oral Medicine,* 2**,** 1-8.

VARGAS-FERREIRA, F., PIOVESAN, C., PRAETZEL, J., MENDES, F., ALLISON, P. & ARDENGHI, T. 2010. Tooth erosion with low severity does not impact child oral health-related quality of life. *Caries research,* 44**,** 531-539.

VARVARA, G., PERINETTI, G., DI IORIO, D., MURMURA, G. & CAPUTI, S. 2007. In vitro evaluation of fracture resistance and failure mode of internally restored endodontically treated maxillary incisors with differing heights of residual dentin. *The Journal of prosthetic dentistry,* 98**,** 365-372.

VENABLES, M. C., SHAW, L., JEUKENDRUP, A. E., ROEDIG-PENMAN, A., FINKE, M., NEWCOMBE, R., PARRY, J. & SMITH, A. J. 2005. Erosive effect of a new sports drink on dental enamel during exercise. *Medicine and science in sports and exercise,* 37**,** 39-44.

VERÍSSIMO, C., SIMAMOTO JÚNIOR, P. C., SOARES, C. J., NORITOMI, P. Y. & SANTOS-FILHO, P. C. F. 2014. Effect of the crown, post, and remaining coronal dentin on the biomechanical behavior of endodontically treated maxillary central incisors. *The Journal of Prosthetic Dentistry,* 111**,** 234-246.

VERSLUIS, A., DOUGLAS, W. H. & SAKAGUCHI, R. L. 1996. Thermal expansion coefficient of dental composites measured with strain gauges. *Dental materials,* 12**,** 290-294.

VIANNA, A. L. S. D. V., PRADO, C. J. D., BICALHO, A. A., PEREIRA, R. A. D. S., NEVES, F. D. D. & SOARES, C. J. 2018. Effect of cavity preparation design and ceramic type on the stress distribution, strain and fracture resistance of CAD/CAM onlays in molars. *Journal of Applied Oral Science,* 26.

VON FRAUNHOFER, J. A. & ROGERS, M. M. 2004. Dissolution of dental enamel in soft drinks. *General dentistry,* 52**,** 308-312.

VORONETS, J., JAEGGI, T., BUERGIN, W. & LUSSI, A. 2008. Controlled toothbrush abrasion of softened human enamel. *Caries research,* 42**,** 286-290.

VORONETS, J. & LUSSI, A. 2010. Thickness of softened human enamel removed by toothbrush abrasion: an in vitro study. *Clinical oral investigations,* 14**,** 251-256.

WADA, I., SHIMADA, Y., IKEDA, M., SADR, A., NAKASHIMA, S., TAGAMI, J. & SUMI, Y. 2015. Clinical assessment of non carious cervical lesion using swept-source optical coherence tomography. *Journal of biophotonics,* 8**,** 846-854.

WALSH, L. J. 2009. Contemporary technologies for remineralization therapies: A review. *Int Dent SA,* 11**,** 6-16.

WANG, C. P., WANG, S. B., HUANG, Y., LIU, J. Y., LI, H. Y. & YU 2014. The CPP-ACP relieved enamel erosion from a carbonated soft beverage: An in vitro AFM and XRD study. *Archives of Oral Biology,* 59**,** 277-282.

WANG, X., MEGERT, B., HELLWIG, E., NEUHAUS, K. W. & LUSSI, A. 2011. Preventing erosion with novel agents. *Journal of Dentistry,* 39**,** 163-170.

WASSELL, R., WALLS, A. & MCCABE, J. 1995. Direct composite inlays versus conventional composite restorations: three-year clinical results. *British dental journal,* 179**,** 343.

WATSON, T. 1990a. A confocal microscopic study of some factors affecting the adaptation of a light-cured glass ionomer to tooth tissue. *Journal of dental research,* 69**,** 1531-1538.

WATSON, T. 1991. Applications of confocal scanning optical microscopy to dentistry. *British dental journal,* 171**,** 287.

WATSON, T. & BOYDE, A. 1991. Confocal light microscopic techniques for examining dental operative procedures and dental materials. A status report for the American Journal of Dentistry. *American journal of dentistry,* 4**,** 193-200.

WATSON, T., PILECKI, P., COOK, R., AZZOPARDI, A., PAOLINELIS, G., BANERJEE, A., THOMPSON, I. & BOYDE, A. 2008. Operative dentistry and the abuse of dental hard tissues: confocal microscopical imaging of cutting. *Operative dentistry,* 33**,** 215-224.

WATSON, T. F. 1990b. The application of real-time confocal microscopy to the study of high-speed dental-bur-tooth-cutting interactions. *Journal of microscopy,* 157**,** 51-60.

WATSON, T. F. 1994. Applications of high-speed confocal imaging techniques in operative dentistry. *Scanning,* 16**,** 168-173.

WATSON, T. F. 1997. Fact and artefact in confocal microscopy. *Advances in dental research,* 11**,** 433-441.

WATSON, T. F., ATMEH, A. R., SAJINI, S., COOK, R. J. & FESTY, F. 2014. Present and future of glass-ionomers and calcium-silicate cements as bioactive materials in dentistry: biophotonics-based interfacial analyses in health and disease. *Dental Materials,* 30**,** 50-61.

WATTRISSE, B., CHRYSOCHOOS, A., MURACCIOLE, J. M. & NÉMOZ GAILLARD, M. 2001. Analysis of strain localization during tensile tests by digital image correlation. *Experimental mechanics,* 41**,** 29-39.

WAYNE, J. S., CHANDE, R., PORTER, H. C. & JANUS, C. 2014. Effect of restoration volume on stresses in a mandibular molar: A finite element study. *The Journal of prosthetic dentistry,* 112**,** 925-931.

WEATHERELL, J., ROBINSON, C. & HALLSWORTH, A. 1974. Variations in the chemical composition of human enamel. *Journal of dental research,* 53**,** 180-192.

WEGEHAUPT, F., TAUBCK, T., STILLHARD, A., SCHMIDLIN, P. & ATTIN, T. 2012. Influence of extra- and intra-oral application of CPP-ACP and fluoride on re-hardening of eroded enamel. *Acta odontologica scandinavica,* 70**,** 177-183.

WEISER, F. & BEHR, M. 2015. Self-adhesive resin cements: a clinical review. *Journal of Prosthodontics,* 24**,** 100-108.

WENDT JR, S., HARRIS, B. & HUNT, T. 1987. Resistance to cusp fracture in endodontically treated teeth. *Dental Materials,* 3**,** 232-235.

WEST, N. 2006. Dentine hypersensitivity.

WEST, N., HUGHES, J. & ADDY, M. 2000. Erosion of dentine and enamel in vitro by dietary acids: the effect of temperature, acid character, concentration and exposure time. *Journal of Oral Rehabilitation,* 27**,** 875-880.

WEST, N. X., HUGHES, J. A., PARKER, D. M., MOOHAN, M. & ADDY, M. 2003. Development of low erosive carbonated fruit drinks 2. Evaluation of an experimental carbonated blackcurrant drink compared to a conventional carbonated drink. *Journal of dentistry,* 31**,** 361-365.

WHITE, A. J., YORATH, C., TEN HENGEL, V., LEARY, S. D., HUYSMANS, M. C. D. & BARBOUR, M. E. 2010. Human and bovine enamel erosion under 'single-drink'conditions. *European Journal of Oral Sciences,* 118**,** 604-609.

WHITE, D., KOZAK, K., ZOLADZ, J., DUSCHNER, H. & GÖTZ, H. 2002. Peroxide interactions with hard tissues: effects on surface hardness and surface/subsurface ultrastructural properties. *Compendium of continuing education in dentistry (Jamesburg, NJ: 1995),* 23**,** 42-8; quiz 50.

WIEGAND, A., BLIGGENSTORFER, S., MAGALHAES, A. C., SENER, B. & ATTIN, T. 2008. Impact of the in situ formed salivary pellicle on enamel and dentine erosion induced by different acids. *Acta Odontol Scand,* 66**,** 225-30.

WIEGAND, A., KÖWING, L. & ATTIN, T. 2007a. Impact of brushing force on abrasion of acid-softened and sound enamel. *Archives of oral biology,* 52**,** 1043-1047.

WIEGAND, A., WEGEHAUPT, F., WERNER, C. & ATTIN, T. 2007b. Susceptibility of acid-softened enamel to mechanical wear–ultrasonication versus toothbrushing abrasion. *Caries research,* 41**,** 56-60.

WILDER-SMITH, C. H., WILDER-SMITH, P., KAWAKAMI-WONG, H., VORONETS, J., OSANN, K. & LUSSI, A. 2009. Quantification of dental erosions in patients with GERD using optical coherence tomography before and after double-blind, randomized treatment with esomeprazole or placebo. *The American journal of gastroenterology,* 104**,** 2788-2795.

WILLIAM, K., WATSON, C., MURPHY, W., SCOTTT, J., GREGORY, M. & SINOBAD, D. 1990. Finite element analysis of fixed prostheses attached to osseointegrated implants. *Quintessence International,* 21.

WOLFART, S., ESCHBACH, S., SCHERRER, S. & KERN, M. 2009. Clinical outcome of three-unit lithium-disilicate glass–ceramic fixed dental prostheses: Up to 8 years results. *Dental Materials,* 25**,** e63-e71.

WONGKHANTEE, S., PATANAPIRADEJ, V., MANEENUT, C. & TANTBIROJN, D. 2006. Effect of acidic food and drinks on surface hardness of enamel, dentine, and tooth-coloured filling materials. *Journal of Dentistry,* 34**,** 214-220.

XHONGA, F. & VALDMANIS, S. 1983. Geographic comparisons of the incidence of dental erosion: a two centre study. *Journal of Oral Rehabilitation,* 10**,** 269-277.

YAMANEL, K., YAMANEL, K., CCEDIL, CCEDIL, AGLAR, A., UUML, LSAHI, K., OUML & ZDEN, U. A. 2009. Effects of different ceramic and composite materials on stress distribution in inlay and onlay cavities: 3-D finite element analysis. *Dental Materials Journal,* 28**,** 661-670.

YANG, P., BRUGGEMANN, G. & RITTWEGER, J. 2011. What do we currently know from in vivo bone strain measurements in humans. *J Musculoskelet Neuronal Interact,* 11**,** 8-20.

YETTRAM, A., WRIGHT, K. & PICKARD, H. 1976. Finite element stress analysis of the crowns of normal and restored teeth. *Journal of Dental Research,* 55**,** 1004-1011.

YI, Y.-J. & KELLY, J. R. 2008. Effect of occlusal contact size on interfacial stresses and failure of a bonded ceramic: FEA and monotonic loading analyses. *Dental materials,* 24**,** 403-409.

YOUNG, W. & KHAN, F. 2002. Sites of dental erosion are saliva-dependent. *Journal of oral rehabilitation,* 29**,** 35-43.

ZAHRADNIK, R., PROPAS, D. & MORENO, E. 1977. In vitro enamel demineralization by Streptococcus mutans in the presence of salivary pellicles. *Journal of dental research,* 56**,** 1107-1110.

ZAHRADNIK, R. T., PROPAS, D. & MORENO, E. C. 1978. Effect of Salivary Pellicle Formation Time on In Vitro Attachment and Demineralization by Streptococcus mutans. *Journal of Dental Research,* 57**,** 1036-1042.

ZAYTSEV, D. & PANFILOV, P. 2014. Deformation behavior of human enamel and dentin–enamel junction under compression. *Materials Science and Engineering: C,* 34**,** 15-21.

ZENTNER, A. & DUSCHNER, H. 1996. Structural changes of acid etched enamel examined under confocal laser scanning microscope. *Journal of orofacial orthopedics= Fortschritte der Kieferorthopadie: Organ/official journal Deutsche Gesellschaft fur Kieferorthopadie,* 57**,** 202-209.

ZEOLA, L. F., PEREIRA, F. A., DA MATA GALVÃO, A., MONTES, T. C., DE SOUSA, S. C., TEIXEIRA, D. N. R., REIS, B. R. & SOARES, P. V. 2015.

Influence of non carious cervical lesions depth, loading point application and restoration on stress distribution pattern in lower premolars: a 2D finite element analysis= Influência da profundidade da lesão cervical não cariosa, ponto de aplicação. *Bioscience Journal,* 31.

ZHAN, Z., ZHANG, X., GUO, W. & XIE, S. 2013. Assessment of composition changes in demineralization and remineralization of human dentin using Raman spectroscopy/Beurteilung der Veränderungen in der Zusammensetzung von humanem Dentin durch Demineralisation und Remineralisation mittels Raman-Spektroskopie. *Photonics & Lasers in Medicine,* 2**,** 45-50.

ZHANG, D. & AROLA, D. D. 2004. Applications of digital image correlation to biological tissues. *Journal of Biomedical Optics,* 9**,** 691-699.

ZHANG, Y., SAILER, I. & LAWN, B. R. 2013. Fatigue of dental ceramics. *Journal of dentistry,* 41**,** 1135-1147.

ZHOU, S.-M., HU, H.-P. & WANG, Y.-F. 1989. Analysis of stresses and breaking loads for Class I cavity preparations in mandibular first molars. *Quintessence international (Berlin, Germany: 1985),* 20**,** 205.

ZHU, J., RONG, Q., WANG, X. & GAO, X. 2017. Influence of remaining tooth structure and restorative material type on stress distribution in endodontically treated maxillary premolars: A finite element analysis. *The Journal of Prosthetic Dentistry,* 117**,** 646-655.

ZI YUN, L., QING HUI, Z., YAN, Z. & HUAN CAI, L. 2015. Prevalence of non-carious cervical lesions and associated risk indicators in middle-aged and elderly populations in Southern China. *Chin J Dent Res,* 18**,** 41-50.

ZIENKIEWICZ, O. C., TAYLOR, R. L., ZIENKIEWICZ, O. C. & TAYLOR, R. L. 1977. *The finite element method*, McGraw-hill London.

ZIPKIN, I. & MCCLURE, F. 1949. Salivary citrate and dental erosion: procedure for determining citric acid in saliva-dental erosion and citric acid in saliva. *Journal of Dental Research,* 28**,** 613-626.

ZORTUK, M., BOLPACA, P., KILIC, K., OZDEMIR, E. & AGULOGLU, S. 2010. Effects of finger pressure applied by dentists during cementation of all-ceramic crowns. *European journal of dentistry,* 4**,** 383.

APPENDIX A- PATIENT CONSENT FORM

NHS REC Form 11/LO/0939

Title of project: Biomechanical aspects of enamel and dentine

Please initial box

I confirm that I have read and understood the information sheet dated 5/8/11 (version 2) for the above study and have had the opportunity to ask questions.	☐
I confirm that I have had sufficient time to consider whether or not I want to be included in the study	☐
I understand that my participation is voluntary and that I am free to withdraw at any time without giving a reason without my dental care & legal rights being affected.	☐
I gift this tooth/teeth for research and understand that it /they may be used in future ethically approved research	☐

APPENDIX B- WORK SUBMITTED FOR PUBLICATION OR PRESENTED AT CONFERENCES

Published Papers:

Alhamdan, M.M., Knowles, J.C. and McDonald, A., 2019. Digital Image Correlation and Strain Gauges to Map and Compare Strain in Teeth with Different Quantity and Quality of Remaining Tooth Structure. *The International journal of prosthodontics*, *32*(1), pp.82-90.

Papers Submitted for Publication:

-Comparison of the Remineralisation Potential of Five Toothpastes on Eroded Human Enamel and Dentine Produced by a Soft Drink.

-Analysis of Restored Erosion Lesion Strain with Strain Gauges and 3D-FEA.

Titles of posters presented:

“Comparison of the Remineralisation Potential of Five Toothpastes on Eroded human Enamel Produced by a Soft Drink” – UCL Research Away Day 2017.

“Digital Image Correlation and Strain Gauges to Map and Compare Strain in Teeth with Different Quantity and Quality of Remaining Tooth Structure” – IADR 2018.